K. REED
853-9914

THE INSTITUTE OF PAPER SCIENCE AND TECHNOLOGY, ATLANTA, GEORGIA

PULPING PROCESSES

PROJECT ADVISORY COMMITTEE MEETING

March 20-21, 1990

The Institute of Paper Science and Technology

Atlanta, Georgia

THE INSTITUTE OF PAPER SCIENCE AND TECHNOLOGY, ATLANTA, GEORGIA

PULPING PROCESSES

PROJECT ADVISORY COMMITTEE MEETING

March 20-21, 1990

The Institute of Paper Science and Technology

Atlanta, Georgia

STATUS REPORT

TO THE

PULPING PROCESSES PROJECT ADVISORY COMMITTEE

March 20-21, 1990

The Institute of Paper Science and Technology

Atlanta, Georgia

TABLE OF CONTENTS

PROJECT SUMMARY FORM

DATE: March 20, 1990

PROJECT NO. 3473-1: FUNDAMENTAL PROCESS IN ALKALI RECOVERY

PROJECT LEADERS: H. L. Empie, K. M. Nichols

IPST GOAL:

Increase capacity of existing systems.

OBJECTIVE:

A quantitative description of all key processes in the burning of alkaline process black liquor is to be developed, encompassing reaction paths and rate equations for drying, pyrolysis, gaseous combustion, char oxidation, sulfide formation and fume formation. The overall goal is a comprehensive understanding of black liquor combustion and applicaton of that knowledge to improve recovery boiler performance.

CURRENT FISCAL YEAR BUDGET: $250,000

PRIOR RESULTS:

Sulfur Release

A model was developed that predicts the amount of sulfur volatilized from a black liquor drop during pyrolysis. Equations were developed to predict the amount of sulfur released from thiosulfate and sulfide as a function of pyrolysis time and temperature. The effects that changing a drop's physical parameters had on the transfer of heat to and through a pyrolyzing black liquor drop were determined. The kinetic and heat transfer models were combined to produce a model that predicts the amount of sulfur that will be released from a pyrolyzing black liquor drop as a function of the drop's physical characteristics, its sulfur composition, and the heating environment to which it is exposed. Predictions from the model were compared with sulfur releases obtained from pyrolysis tests of actual black liquor drops.

Single-Particle Burning

Models for each of the first three burning stages of a black liquor droplet have been developed. Drying was modeled as an external heat transfer limited process. The drop temperature and mass were predicted by simultaneous mass and energy balances around the drop. Volatiles burning was also modeled as an external heat transfer limited process. Volatiles burning ends when the particle has swollen to its maximum size, and this diameter can be empirically predicted from the initial dry mass. As the break point between drying and volatiles burning is impossible to measure experimentally, the two models

(drying and volatiles burning) were combined to predict the time to maximum volume. The rate of volatilization was accurately predicted by the model, fitting the data over the entire oxygen range tested (0% - 21%). Char burning was modeled as limited by oxygen mass transfer to the char surface. The presence of the sulfate/sulfide cycle in char burning was established through tests with pure soda liquor and soda liquor loaded with sodium sulfate. The char burning model accurately predicted the time for char burn (from maximum volume to smelt coalescence) for both kraft and soda liquors.

Char Gasification

An experimental apparatus was constructed for determination of the rate of reaction of black liquor char carbon with CO2. Sufficient char was obtained by pyrolyzing black liquor in the DOE flow-reactor. Initial demonstration tests were performed and showed that reaction temperature could be controlled and CO/CO2 concentration data could be collected continuously during the char gasification period.

FT-IR Measurements

Absorption spectra were obtained at several temperature levels between 300 K and 1000 K, by passing the IR beam through an electrically heated cell containing prepared mixtures of CO and N2 gas. Procedures and computer algorithms were developed for quantitative temperature determination from the CO spectra. Considerable effort was expended reducing errors which were due to instrument distortion.

Fume Formation

Performance evaluation of the gas heater and droplet reactor to be used in fume formation measurements was completed. A considerable body of temperature and gas flow data was compiled for the range of operating conditions and equipment configurations. Several trials of black liquor droplet combustion were conducted at gas flow conditions of 600-900°C and 2-6 ft/s. Video tapes clearly showed distinct phases of droplet combustion. Particulate matter was successfully captured on a vacuum-assisted glass fiber-filter.

SUMMARY OF RESULTS SINCE LAST REPORT:

Char Gasification

The rate of gasification of a specific black liquor char with CO2 has been experimentally measured for a 5% CO2 concentration in N2. Twelve gasification tests were performed at four operating conditions, giving triplicate date for each condition. The four operating conditions were the four possible combinations of two gas flow rates (5 slpm, 10 slpm) and two temperatures (700°C and 800°C). These data are currently being analyzed.

FT-IR Measurements

The objective of this project is to develop the techniques which will permit the quantification of CO and CO2 concentrations as well as gas phase temperature from a Fourier transform infrared spectroscopy (FT-IR) spectrum of the gas above a burning black liquor char bed. FT-IR measurements to date have taken place by passing the IR beam through an electrically heated cell containing prepared mixtures of CO and N2 gas.

During this past 6 month period a detailed temperature profiling of the electrically heated cell was performed. The FT-IR method is a line-of-sight method and thus yields an averaged temperature across the width of the cell. The temperature profiling with the thermocouples was performed to determine what temperature variations if any exist within the cell, in order to more properly evaluate the line-of-sight temperatures determined from absorption spectra. Temperature gradients within the cell were found to be negligible.

Recent efforts have also focused on the development of mathematical techniques needed to determine gas phase temperatures from CO absorption spectra. Results of temperature calculations from low temperature (25-500°C) spectra have yielded accuracies of 1-3%. Results of temperature calculations from higher temperature (500-1000°C) have not been as good. Complications with obtaining high quality CO absorption spectra, as well as an incomplete knowledge of the absorption of infrared radiation by CO at these high temperatures has slowed progress in this area.

Work has been initiated to implement the FT-IR instrumentation to the DOE flow reactor for CO/CO2 and temperature measurements during black liquor combustion. Design and selection of the necessary equipment is being finalized. This includes optical arms which will transmit the IR beam from the optical table to the reactor and from the reactor to the detector, and modifications to the view ports of the flow reactor.

Fume Formation

Results are limited since the Ph.D. (Chris Verrill) student conducting this work has spent most of the time during this reporting period at James River Corporation's Corporate Research and Development facility doing an industrial internship not related to fume formation. Currently the experimental equipment constructed in Appleton is being reassembled. Sample black liquors for experimentation are being obtained.

PLANNED ACTIVITY THROUGH FISCAL YEAR 1990:

Char Gasification

Analysis of the present data on the rate of CO_2 gasification should indicate whether the rate of CO_2 gasification is controlled by mass transfer or by kinetics at these temperatures (700°C and 800°C). Interpretation of this data should also assist IPST in conducting additional gasification testing. It is planned that future testing will include determination of the CO_2 gasification rate at a wider set of operating conditions, as well as determination of the H_2O gasification rate.

FT-IR Measurement

Efforts will continue on improving the accuracy of temperatures obtained from CO absorption spectra, particularly at temperatures greater than 500°C. The focus will then shift to interpretation of spectra for the quantification of gas species concentrations. While this is going on, work will continue to implement the FT-IR instrumentation onto the DOE flow reactor. Following completion of the design, equipment will be purchased and modifications to the view ports of the flow reactor will be made. Initial FT-IR measurements during combustion of black liquor in the DOE flow reactor are scheduled to begin in the Fall of 1990.

Fume Formation

The first experimental objective of this project will be the determination of the time period(s) during combustion when the fume is formed. A method will be used which coordinates timed observation of combustion with a sample of the generated particulate captured on a moving filter tape. Any morphological and chemical information obtained during this phase of experimentation may suggest specific experiments to investigate formation mechanisms in later phases of the project.

Initial experiments at IPST will be to optimize the method of capturing fume samples from burning droplets and devise the best analytical procedure for identifying the presence of fume studying its composition and morphology. The first analysis of fume coordinated with droplet combustion progress can be expected in early Summer 1990.

STUDENT RESEARCH:

P. Miller, Ph.D.-1986; K. Goerg, M.S.-1986, Ph.D.-1989; K. Kulas, M.S.-1986, Ph.D.-1989; D. Sumnicht, M.S.-1986, Ph.D.-1989; G. Aiken, Ph.D.-1987; C. Verrill, M.S.-1987, Ph.D.-1991; M. Robinson, Ph.D.-1987; F. Harper, Ph.D.-1989; G. Kulas, Ph.D-1989; G. Maule, M.S.-1988; P. Medvecz, Ph.D.-1990; D. Miller, M.S.-1991; S. Lee, M.S.-1990; D. Miller, M.S.-1991.

Project 3473-1 Status Report

FT-IR MEASUREMENTS FOR BLACK LIQUOR COMBUSTION DIAGNOSTICS

(P. Medvecz, IPST Ph.D. candidate; K. Nichols, Thesis advisor)

The principal reaction region within the recovery boiler is the lower furnace, i.e., below the point of black liquor entry. Although significant reactions occur in and on the surface of the char bed, characterization of the gas phase immediately above the bed may contain information important for enhancing lower furnace performance. A study of this region may also provide data useful in the evaluation of alternate burning related chemical recovery processes, e.g., cyclone gasification.

Non-intrusive spectroscopic instrumentation has been used to characterize the gas phase region within burning systems. These techniques have been used in relatively clean combustion environments to measure gas temperature, gas species concentration, soot particle size, turbulence patterns, and velocity.

In 1987 it was decided that the Institute's efforts in black liquor char combustion research might benefit from applying a spectroscopic technique to the study of the gas phase above a burning black liquor char bed. It was thought that an accurate knowledge of the gas phase composition directly above the bed surface would be particularly beneficial in understanding the mechanism of char combustion as well as determining char burning rates. In addition, it was thought that research directed towards other problems related to black liquor combustion, such as sulfur releaser or NO_x formation, might benefit from the development of a non-intrusive, in situ, spectroscopic technique.

Therefore, a project was begun in 1987 by Pat Medvecz, Ph.D. candidate, which would focus on the implementation of some existing spectroscopic technique to the black liquor combustion environment for the analysis of gas concentrations and temperatures. The technique selected should be versatile enough to be used in both a small bench-top black liquor reactor as well as in the Institute's large DOE funded in-flight reactor.

After a thorough review of the literature, Fourier transform infrared spectroscopy (FT-IR) appeared to be particularly well suited for the analysis of the gas phase immediately above a burning black liquor char bed. This assumption was based upon a consideration of the composition of the gases present above a burning black liquor char bed, as well as a consideration of the effect of interferences (fume, IR emission) upon the transmission of an infrared beam through this hostile combustion environment. Furthermore, FT-IR has been successfully used in two similar coal burning applications for obtaining qualitative and quantitative gas phase information.

The use of FT-IR in combustion diagnostics is accomplished by directing the infrared beam from the instrument's interferometer through a combustion chamber and to a detector. The partial absorption of the infrared beam by the gases present in the combustion chamber results in a Fourier transform infrared absorption spectrum which is a plot of absorbance on the vertical axis and frequency (cm^{-1}) on the horizontal axis. The position of the peaks in the absorption spectrum are characteristic for each different gaseous species, which makes qualitatively identifying the components in the gas phase relatively easy. In addition, the spectrum can be interpreted to determine both gas concentrations and temperatures, although this is a non-trivial task.

The Institute's efforts in applying FT-IR spectroscopic techniques to a black liquor combustion environment have lead to the completion of several key steps. First, a Fourier transform infrared spectrometry (Laser Precision Analytical RFX-75) has been selected, tested, purchased and set up in-house to be used for this study. Second, a reactor which is suitable for the combustion of black liquor char and which will provide optical accessibility to the gaseous phase immediately above the char bed surface has been designed, constructed, and successfully tested. A schematic diagram of this reactor is provided in Figure 1.

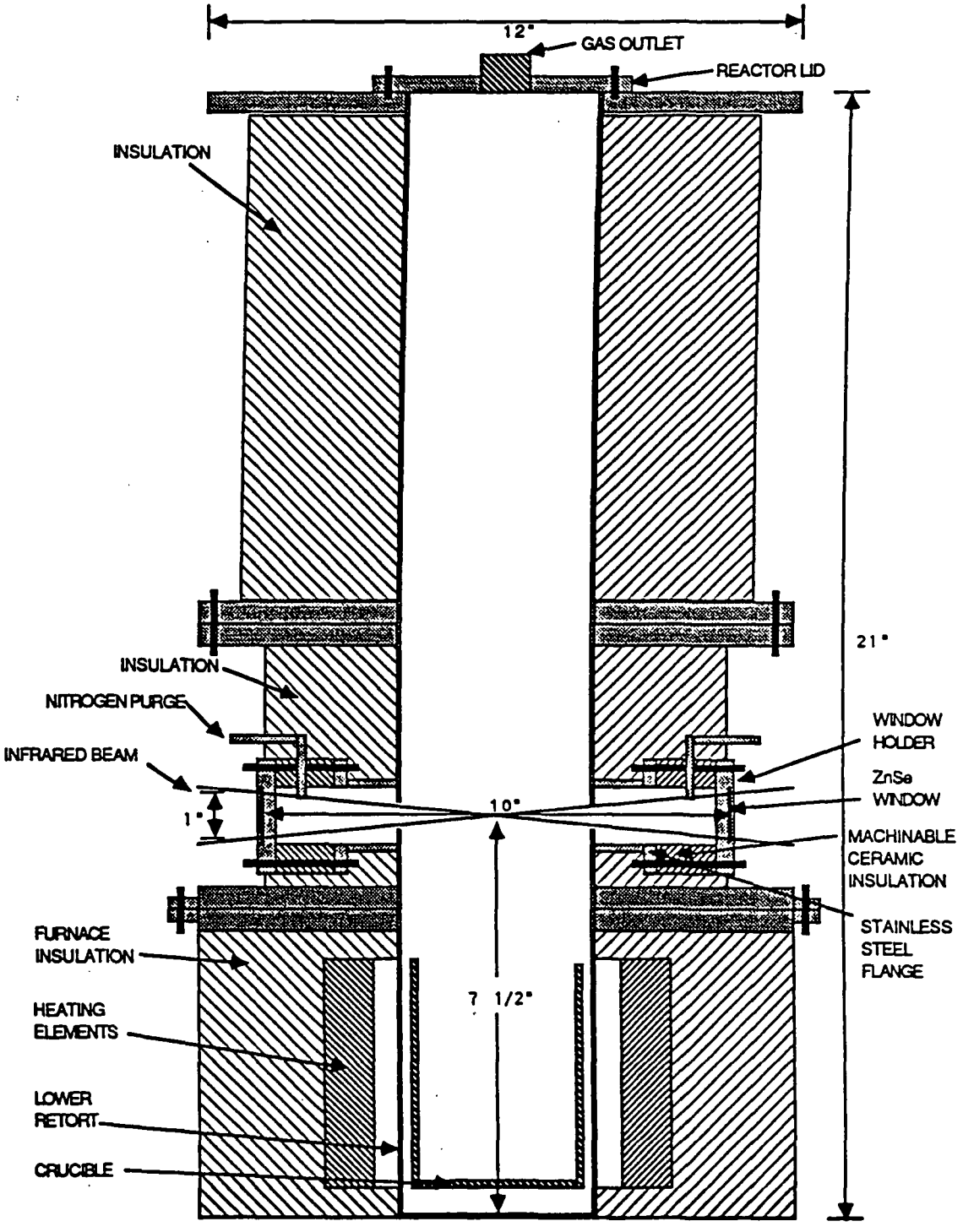

Fig. 1 Schematic Diagram of Black Liquor Char Combustion Reactor

The completion of these two steps enables us to make qualitative measurements of the gas phase above a burning, bench-top scale, char bed. These spectra have made it possible to identify the gaseous components present above the char bed during both pyrolysis and char combustion, at temperatures as high as 1000°C. A typical infrared absorption spectrum during char combustion is provided in Figure 2. While the identification of the gaseous components can be readily accomplished, it is much more difficult to interpret these spectra to obtain concentration and temperature information. This difficulty results from an incomplete knowledge of how CO and CO_2 absorb infrared radiation at high temperatures.

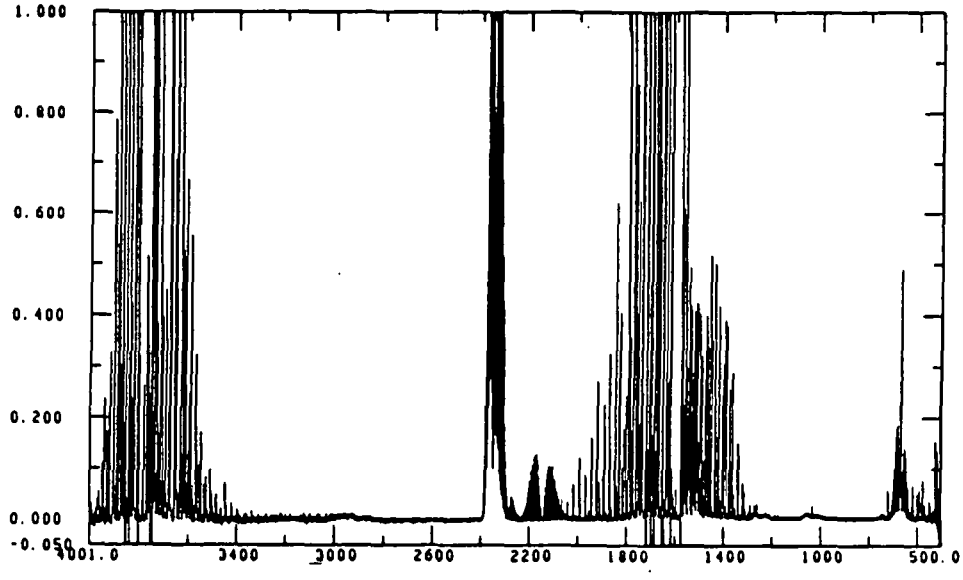

Fig. 2 Infrared Absorption Spectrum of the Gaseous Phase Above a Burning Black Liquor Char Bed at 700°C

The literature regarding the absorption of infrared radiation by CO and CO_2 is incomplete at high temperatures. In order to make concentration and temperature measurements of gases using infrared absorption spectroscopy, the rotational fine structure of the rotational-vibrational absorption lines must be considered. In Figure 3 an absorption spectrum of CO at room temperature is given. The individual lines shown in this spectrum are referred to as the rotational fine structure of the absorption band. The group of peaks on the right side of this absorption band are known as the P-Branch lines and the group of lines on the left are referred to as the R-Branch lines. The shape and height of these lines are the spectral information which is needed to make concentration and temperature determinations. Unfortunately, an accurate theoretical or experimental knowledge of the spectral parameters which affect the shape of these lines is not known at high temperatures. Therefore, before concentration and temperature information can be obtained from the spectra obtained during char combustion, an understanding of infrared absorption of CO and CO_2 under controlled conditions, i.e. known gas temperatures and concentrations, must first be developed.

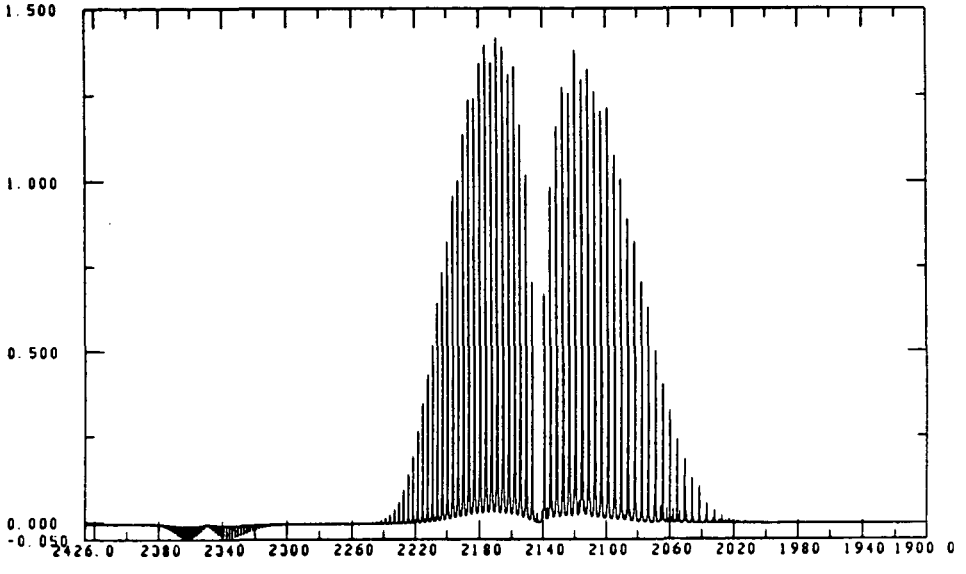

Fig. 3 Room Temperature CO Absorption Spectrum

In order to provide an environment which will facilitate the acquisition of infrared absorption spectra of gas mixtures at high temperatures, up to 1000°C, a specialized gas cell had to be designed and constructed. The desired characteristics of the cell include the following; first, it must provide optical accessibility for the infrared beam; second, it should provide a uniform gas temperature profile across the beam path through the cell; and finally, the temperature of the gas must be controllable and reproducible at temperatures between 25-1000°C. A schematic diagram of the gas cell which has been designed for this thesis is provided in Figure 4.

The gas cell, shown in Figure 4, is made entirely of stainless steel, with the exception of the windows. It is heated by placing it in an electrical tube furnace. The tube furnace provides a uniform radiation heat flux to the outer wall of the cell. The gas inside the cell is heated by conduction with the cell wall, natural convection induced from temperature gradients which exist in the cell, and finally by radiation from the walls. The heat flux from the furnace is controlled by a digital temperature controller which has a control precision of $\pm$ 1°C.

No attempt has been made to seal the gas cell. The cell is maintained at atmospheric pressure by continuously allowing a small part of the gas volume to flow out of the cell through an outlet stream replenishing this gas with a supply from a gas inlet stream. FT-IR is a line-of-sight technique, and therefore an average temperature spectrum is obtained if temperature gradients exist along the beam path. Therefore, the room temperature gas which enters the cell must first be preheated in a coil which is wound on the interior of the cell. Heat transfer calculations have been performed to determine the length of coil needed to bring the entering gas up to the furnace temperature before it is released into the bulk volume of the cell. This technique ensures that the temperature profile within the cell will not be affected by the use of the inlet gas stream.

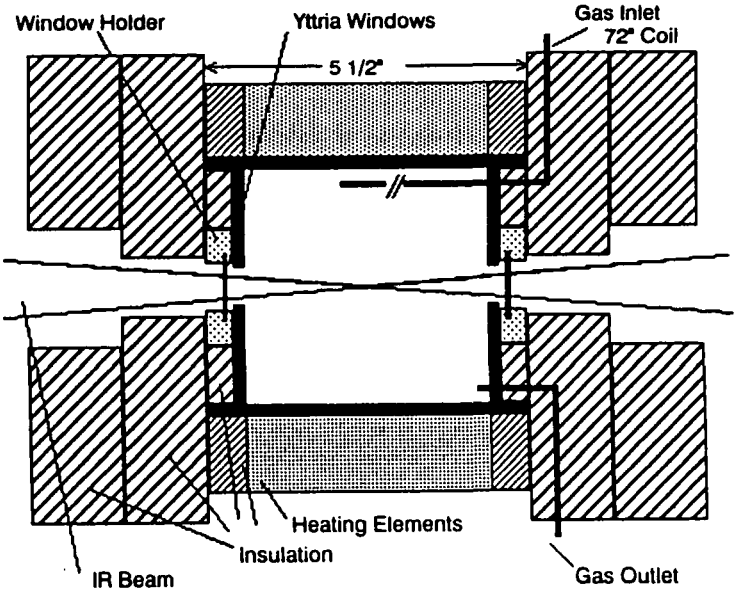

Fig. 4 Schematic Diagram of High Temperature Gas Cell

To verify that a near uniform temperature distribution exists within the cell, temperature profiles within the gas cell along the IR beam's path have been performed at temperatures of 100, 300, 500, 700, 800, 900, and 1000°C. A typical temperature profile is shown in Figure 5. The profile shown in this figure was obtained using an unshielded thermocouple. Consideration has been given to

account for thermocouple errors resulting from radiation, convection, and conduction. The profiling work has revealed that a temperature gradient does exist along the infrared beam's path. However, the gradient is not very significant, 1-1.5%, and with proper averaging its effect on absorption spectra can be readily taken into account.

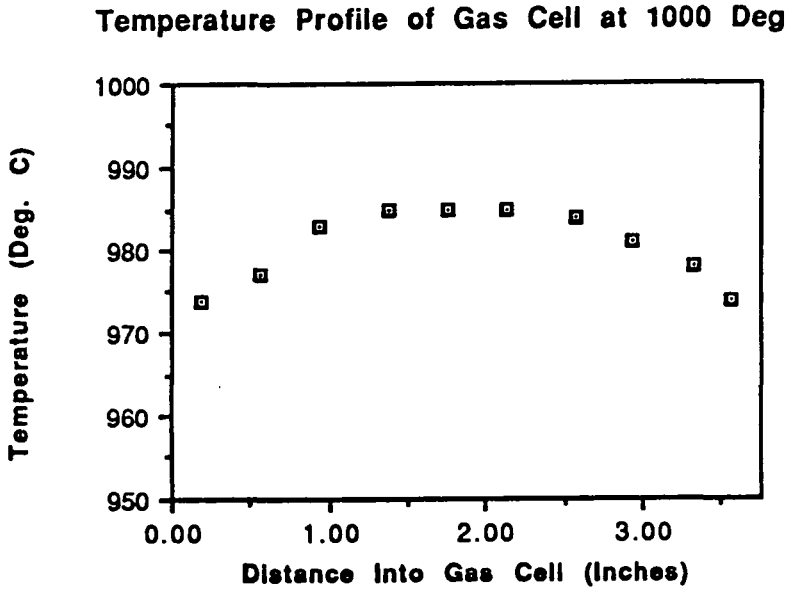

Fig. 5 Temperature Profile in Gas Cell at 1000°C

The windows which have been selected for use in the gas cell are made of either yttrium oxide (Y_2O_3) or sapphire. These materials have been selected based upon their infrared transmission properties and thermal stability. Few materials have been found which possess the characteristics required for this application. Even these materials have poor transmission of infrared radiation at high temperatures, which reduces the signal to noise ratio obtained from spectra recorded at high temperatures.

The construction of the gas cell has provided the necessary environment in which to record reference spectra. Furthermore, the determination of temperature profiles within the cell gives an accurate knowledge of the temperature of the gas within the cell at various furnace set point temperatures. The acquisition of either CO or CO_2 spectra recorded at these temperatures has provided a set of reference spectra of known gas concentration, pressure, and temperature. In Figures 6-12 CO absorption spectra are shown at various temperatures up to 1000°C. In each of these figures only the P-Branch of the absorption band is shown. The R-Branch is often convoluted with CO_2 lines, particularly at high temperatures. This set of data will provide the information needed to evaluate the changes which occur in line shapes and heights as a result of temperature changes. This set of spectra will also provide the references which can be used to evaluate the mathematical techniques which are developed to make temperature and concentration measurements from absorption spectra.

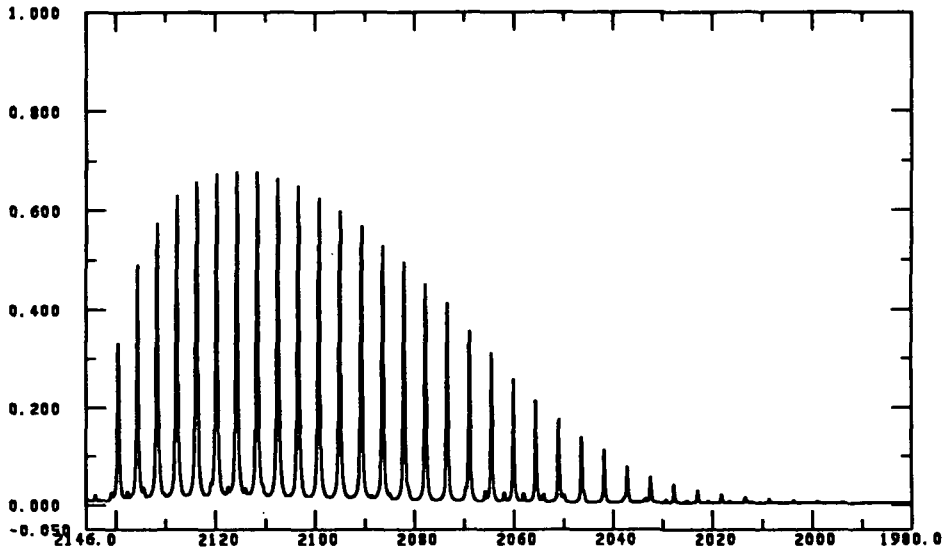

Fig. 6 P-Branch of CO Absorption Spectrum at 100°C

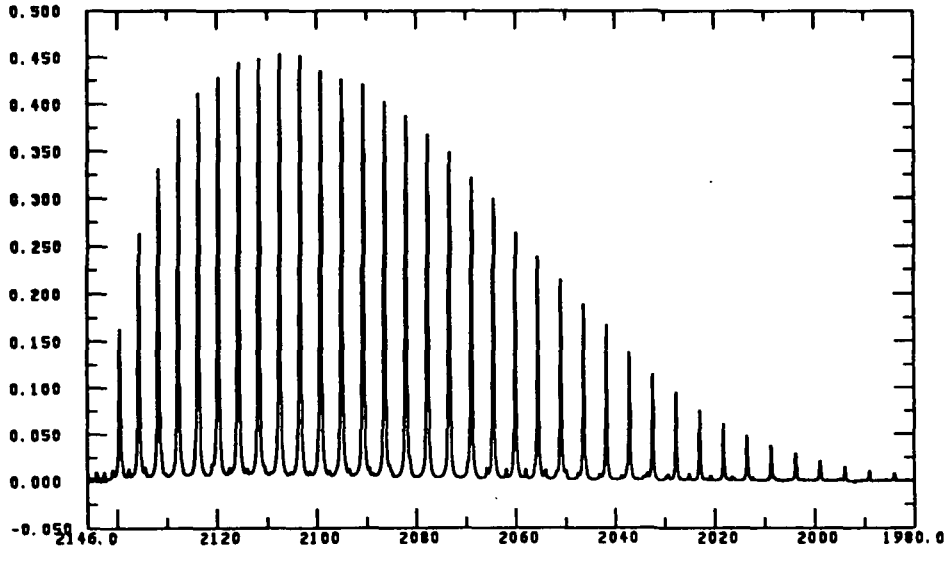

Fig. 7 P-Branch of CO Absorption Spectrum at 300°C

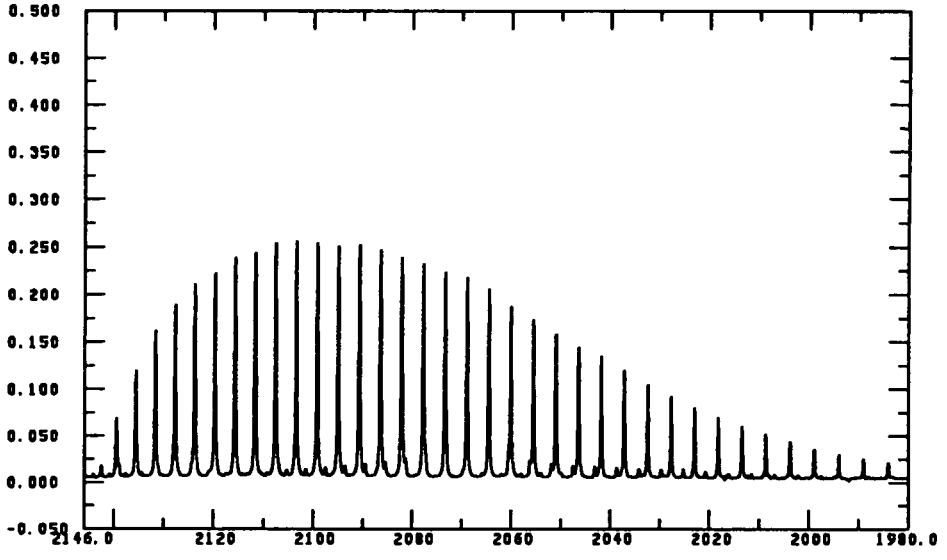

Fig. 8 P-Branch of CO Absorption Spectrum at 500°C

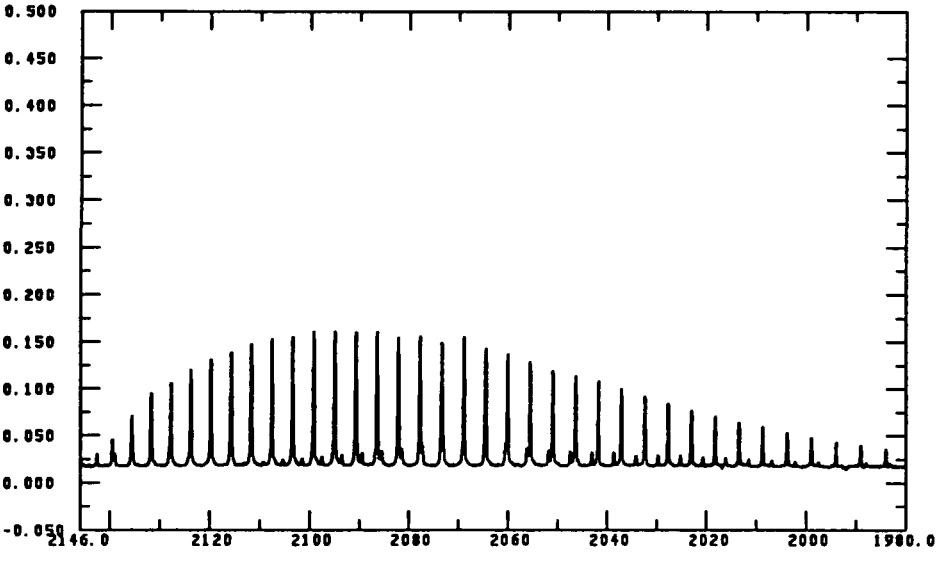

Fig. 9 P-Branch of CO Absorption Spectrum at 700°C

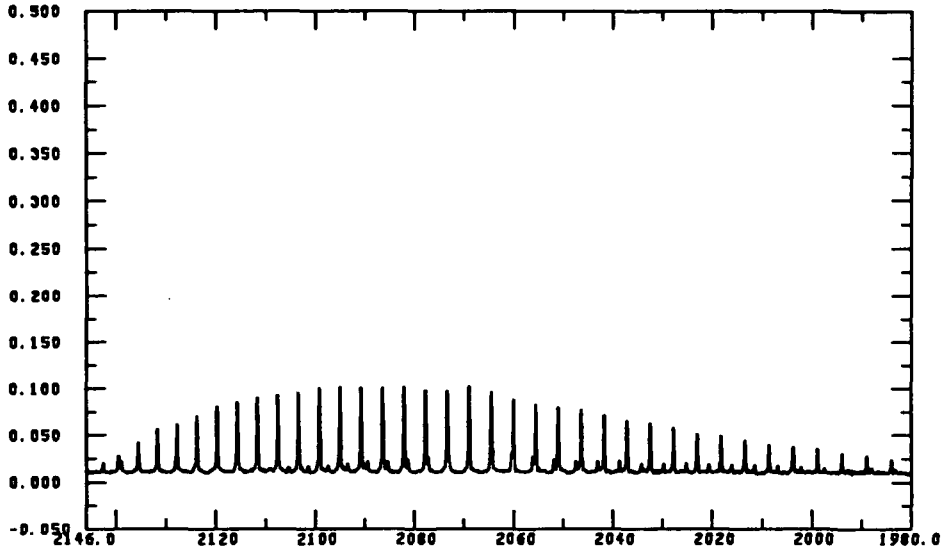

Fig. 10 P-Branch of CO Absorption Spectrum at 800°C

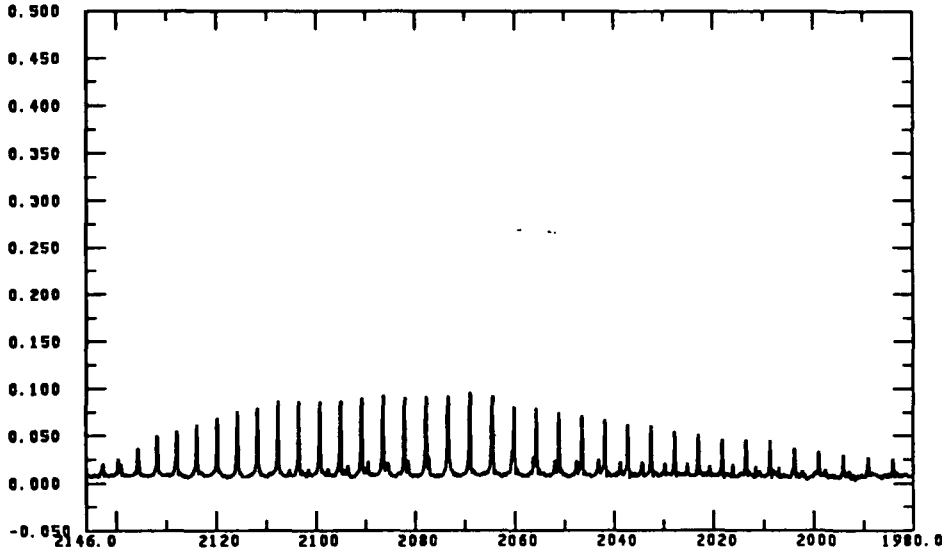

Fig. 11 P-Branch of CO Absorption Spectrum at 900°C

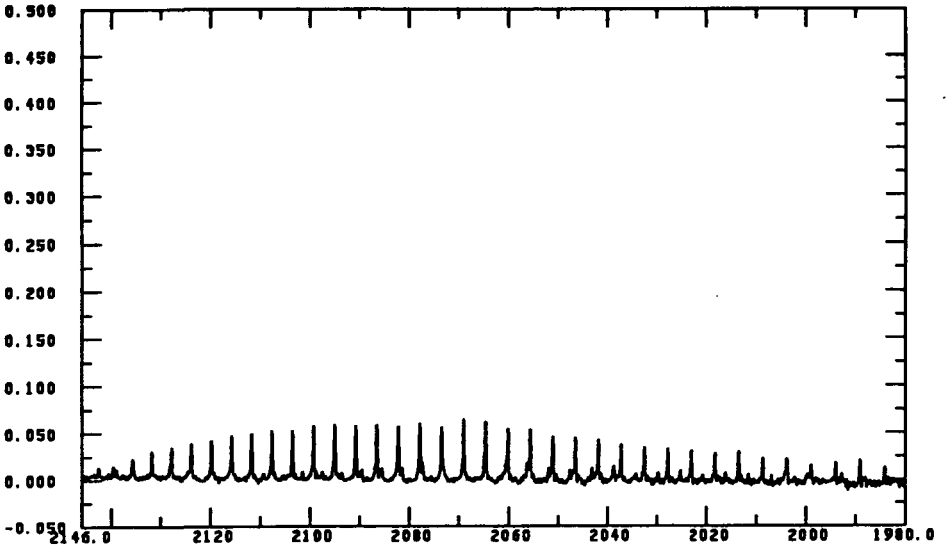

Fig. 12 P-Branch of CO Absorption Spectrum at 1000°C

All of the spectra shown in Figures 6-12 were recorded at the same concentration, 3% CO in nitrogen, yet the shape of the spectra are dramatically different. At high temperatures, two main spectral changes are observed; first, the peak heights become less intense and second, more CO lines are observed. It is the observation of the changing peak height distribution among the lines which is used to calculate temperatures. A mathematical relationship between the intensity of an absorption line and the energy of the transition producing the line has been developed in classical spectroscopy texts. If the relationship between peak height and transition energy is plotted for each absorption line, a straight line should result with the slope of the line equal to -1/Temperature.

Although this development is straight forward, the determination of temperatures from CO absorption spectra is complicated by three factors; first, the peak heights recorded by a FT-IR instrument are severely distorted by the limited resolution of the instrument, second, fundamental line broadening data needed in the calculations is not available, and finally, the spectra used for the calculations must be of very high quality.

Efforts have been made during the past year to overcome these difficulties. The problem of instrument distortion has been handled by developing a mathematical description of the distortion and then correcting the spectra accordingly. The problem of limited high temperature spectral data has not yet been fully resolved. However, thorough review of the literature has recently led to several possible solutions to the problem. Finally, the difficulty of obtaining quality spectra has been resolved by changing the window material used in the gas cell and by precisely aligning the FT-IR instrument.

Overcoming some of the complications in the temperature determination analysis has significantly improved the results. Figures 13-16 are plots of Peak Intensity vs. Energy for CO absorption spectra recorded at temperatures of 295, 362, 1048, and 1149K. The temperature calculated from the slope of the lines in these plots are 294.8, 354, 1073, and 1153K respectively. The errors associated with these calculations are 0.07, 2.2, 2.4, and 0.3% respectively. The results of these calculations are very encouraging. The accuracy obtained from these plots meet all expectations of the technique. However, these values represent the best results to date. Much work is still needed to be able to get these results routinely and at all temperatures.

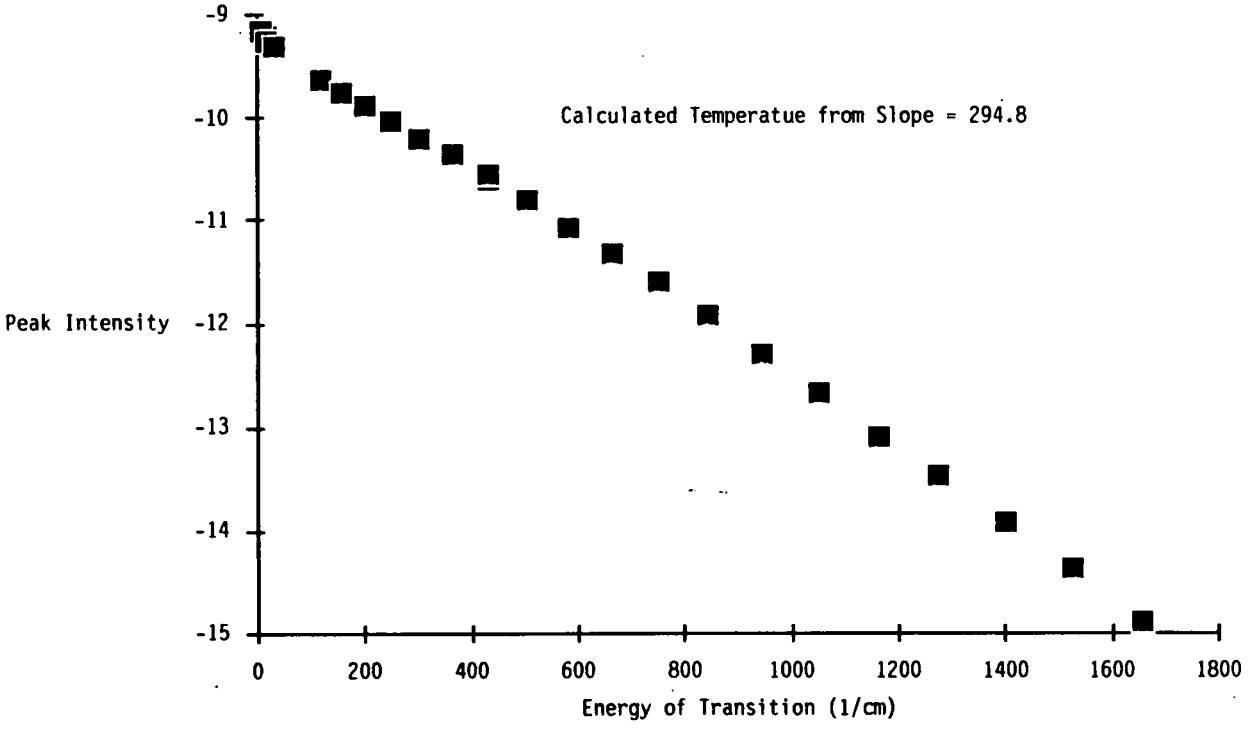

Fig. 13 Calculation of Gas Temperature from 295K CO Absorption Spectrum

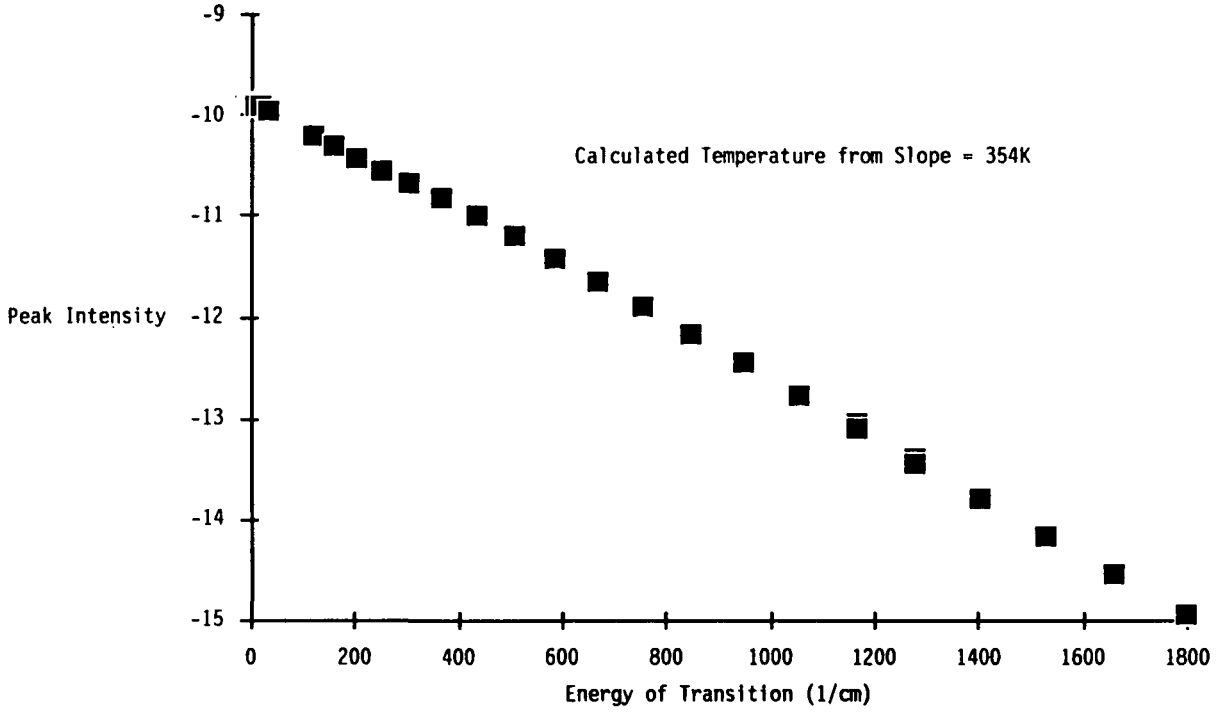

Fig. 14 Calculation of Gas Temperature from 362K CO Absorption Spectrum

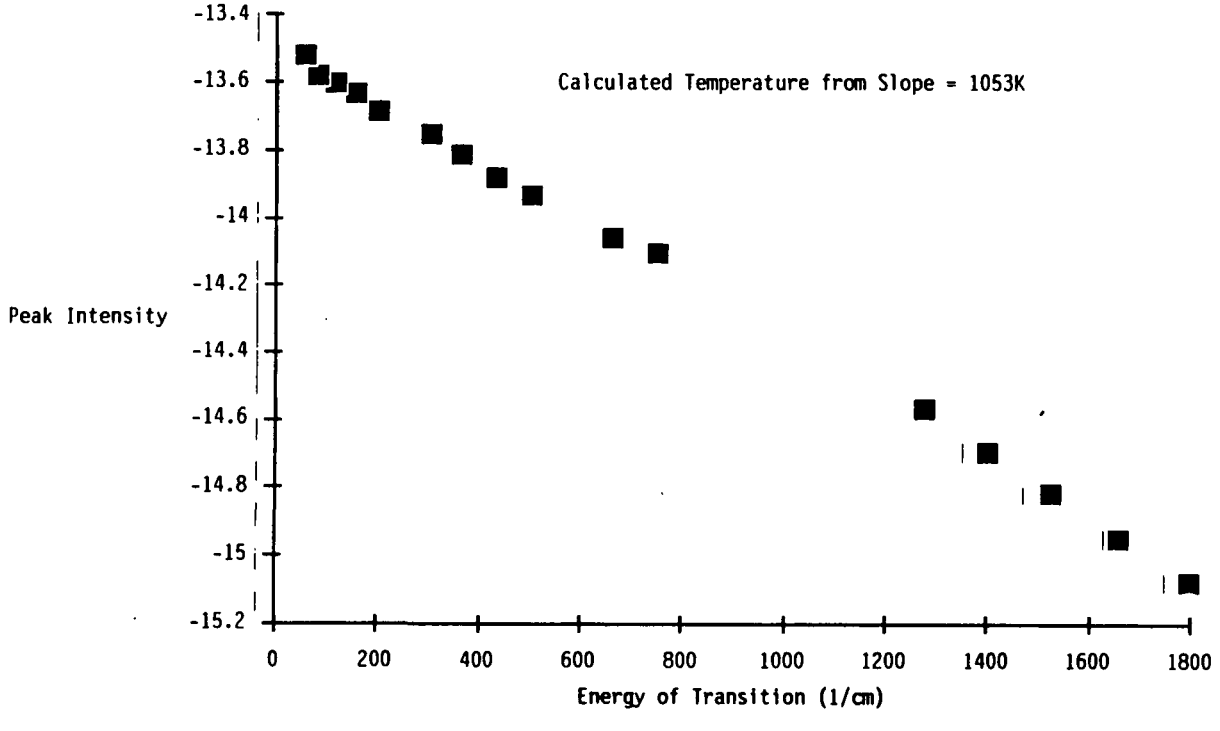

Fig. 15 Calculation of Gas Temperature from 1048K CO Absorption Spectrum

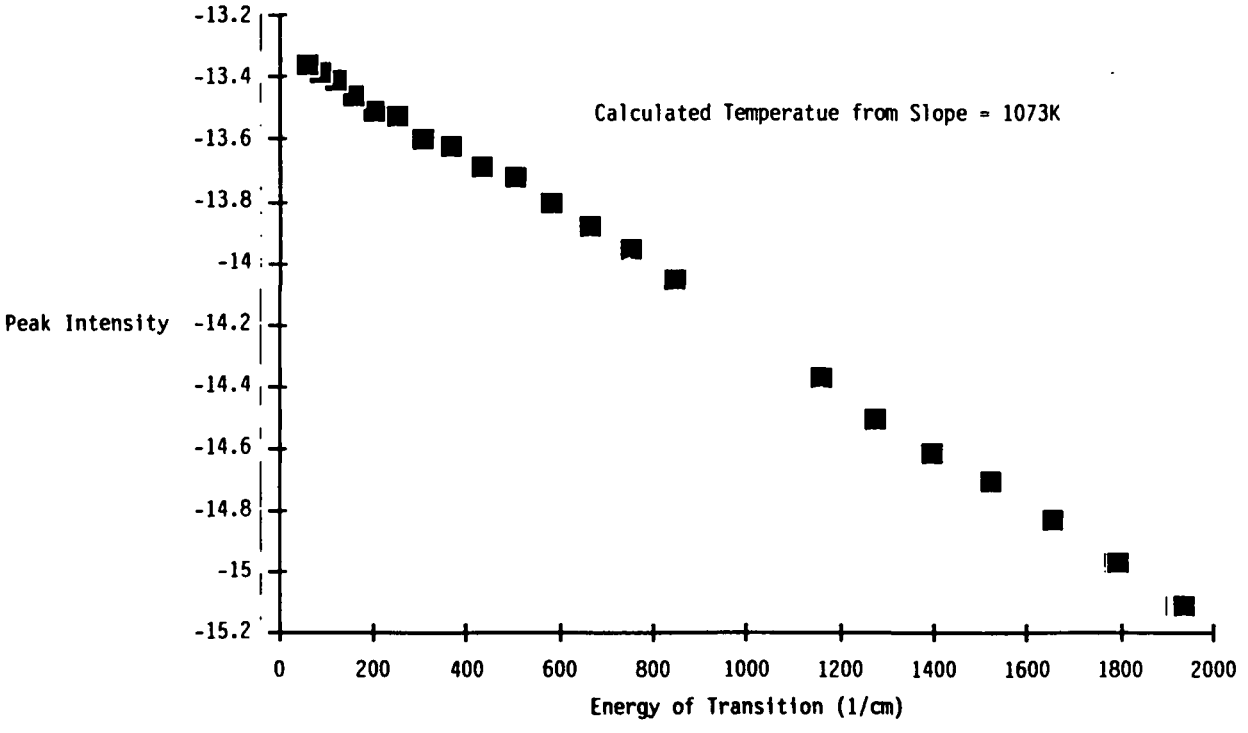

Fig. 16 Calculation of Gas Temperature from 1149K CO Absorption Spectrum

Future work on this project will consist of the completion of temperature determinations from CO absorption spectra. With the success of recent procedures it is expected that temperatures will be accurately determined at temperatures at least as high as 900°C. Following the completion of this work, the determination of gas concentrations from CO and CO_2 spectra will be started. It is believed that the work which has been completed for temperature analyses will be helpful in making concentration measurements as well. Finally, the spectra recorded above burning black liquor char beds will be analyzed, and the concentration of CO and CO_2, as well as the gas phase temperature, will be measured.

The Institute's efforts in this area has been enchanced by the recent commitment of a Masters student, Denise Martin, to join the project. She will use the FT-IR for the analysis of the gas phase above a burning char bed in the Institute's large DOE funded in flight reactor. The objective of her project is to obtain high quality absorption spectra of the gases directly above the char bed in this reactor. This will require modifying the DOE reactor and developing a means to transfer the infrared beam through the reactor to a detector. The completion date of this project will be the Spring of 1991.

PROJECT SUMMARY FORM

DATE: March 20, 1990

PROJECT NO. 3473-6: FUNDAMENTAL STUDIES OF BLACK LIQUOR COMBUSTION
(Supported bu the Office of Industrial Programs -
U.S. Department of Energy)

PROJECT LEADERS: H. L. Empie,
NIST Subcontractor - Dr. A. Macek

IPST GOAL:

Develop fundamental data on black liquor combustion which can be used to enhance energy efficiency and productivity of recovery boilers.

OBJECTIVE:

The three main objectives are:

1. To develop laboratory scale flow reactor systems which will enable the study of both state-of-the-art and advanced recovery systems.

2. To study gas phase and char bed mechanistic processes under realistic and controlled environments with advanced optical and spectroscopic techniques.

3. To develop a data base which will bridge the gap between ongoing fundamental research and commercial application of the resultant findings, culminating in increased thermal efficiency, productivity, and capital effectiveness.

CURRENT FISCAL YEAR BUDGET: $254,000

PRIOR RESULTS:

The project was divided into 4 phases: Phase 1 - in-flight processes; Phase 2 - char bed processes; Phase 3 - inorganic fume formation processes; Phase 4 - recovery furnace simulation. Progress Reports One, Two, and Three have been issued by the Department of Energy. These reports cover all of the work on the project through December, 1987.

In-flight studies were completed with the high solids tests and particle drag measurements.

Data were obtained on drying rates as a function of key variables (drop size, gas velocity, and gas and reactor temperature). Test data were also obained on in-flight pyrolysis and rates of carbon fixation. These data were more difficult to interpret, since differences in swelling and drag resulted in variable residence times in the reactor's in-flight zone. Complementary work on single-drop burning at NIST and elsewhere (primarily at Abo Akademi in Finland) has been of considerable value in clarifying in-flight behavior.

The bed burning studies determined mass transfer coefficients and the boundaries where chemical kinetics becomes important. During the course of the work, modeling studies suggested that char gasification by CO_2 and H_2O might be very important in bed burning in recovery furnace. A limited number of experiments to test this possibility were carried out.

The fume monitoring effort was directed toward simultaneous measurement of fume concentration and particle size distribution, since both would be important variables in fume-gas reactions and in dust depostion. A laser polorization-ratio technique was selected. There have been difficulties in getting this system to work properly, especially for getting measurements inside a closed combustion environment. At the same time, the importance of CO/CO_2 ratio in the product gas from char burning was recognized. As a result, the gas phase measurement task was shifted to CO/CO_2 measurement. This is being done using FTIR spectroscopy.

In Phase 4 a 3-dimensional model of a recovery furnace has been developed by three IPST Ph.D. students. Based upon data from black liquor burning in a single particle reactor, sequential models of the burning stages-drying, volatiles burning, and char burning were written. This burning model was then integrated with a computational fluid dynamics model (called FLUENT as marketed by Creare, Inc. of Hanover, NH) to fully characterize the physical and chemical unit processes occurring in the recovery furnace. One typical mill example was simulated resulting in a final, converged solution. A major drawback that was identified from this exercise was the large computational time requirement, namely over three months on a Micro VAX II.

SUMMARY OF RESULTS SINCE LAST REPORT:

Information on the rate of droplet drying has been collected at high temperature conditions for feed solids concentrations up to 75% solids. Based on the limited data collected, it appears that the drying rate of black liquor droplets reaches a maximum at about 71% and begins to fall off if the initial solids concentration is raised above 71%. The results clearly show that for a given solids concentration, the drying rate of black liquor droplets increases as the liquor feed temperature is increased. The pyrolysis or volatiles evolution stage of black liquor combustion begins when the droplets have dried to at least 80% solids; it proceeds rapidly above the 90% solids.

Results from the experimental study of entrainment characteristics of pyrolyzed black liquor particles (completed at NIST) have contributed to the recovery boiler modeling effort. Drag coefficients from entrained pyrolyzed particles have been found not to vary greatly with particle size and shape. Hence the standard drag coefficient curve for spherical particles can be used for determining entrainment characteristics of liquor particles in recovery boilers.

The char bed reactor has generated quantitative data on char bed burning under controlled conditions representative of a typical recovery furnace. The burning rate data are completely consistent with bed burning being a mass transfer rate limited process. Burning rates are first order in oxygen concentration and increase with air jet velocity, as would be expected for oxygen mass transfer rates. Measured mass transfer coefficients are consistent with results calculated from common mass transfer correlations for turbulent flow in a horizontal slit. The slit width corresponds to the thickness of the air jet over the bed. Char bed temperature profiles were also measured and showed a rapid decrease in temperature within the bed. The thickness of the active burning layer was estimated to be between 3 and 7 cm thick.

In experiments with no water present the ratio of $CO/(CO+CO_2)$ in the product gas was inversely proportional to the inlet oxygen concentration. For 7% O_2, the ratio was 0.4-0.6; for 21% O_2, it was less than 0.25. When water vapor was present, this ratio was generally less than 0.01, regardless of the oxygen content. This was not surprising, since water vapor is known to catalyze the gas phase oxidation of CO to CO_2. Determination of the $CO/(CCO+CO_2)$ ratio just above the char surface has not yet been possible. Work has been under way to develop an optical technique for measuring concentrations and temperatures in black liquor combustion environments based upon FT-IR spectrometry. Results of temperature determinations by this method have yielded accuracies of 1-3% for temperatures under 500°C. Results of temperature measurements in the 500°-1000°C range have not been as good, however work is ongoing to improve the method.

Simulations with the recovery furnace model have provided extraordinary insight into the nature of the black liquor combustion process. The model shows that the main mode of combustion is particle burning. Carryover is not simply determined by liquor spray size, but rather by a complex relationship between drop size, gas flow patterns, and oxygen concentrations. Gas flow patterns are determined primarily by the air inlet geometry and are not greatly modified by liquor sprays and in-flight combustion. Bed shape can have a strong effect on gas flow patterns.

Several issues pertaining to model implementation remain to be resolved. Included are decreasing the computational convergence time by two orders of magnitude, removal of the plane of symmetry in order to permit rotational furnace gas flows, inclusion of recently obtained laboratory data dealing with sodium and sulfur chemistry, and model validation. Comparison of model predictions with actual operating data must be done before the model's credibility can be proved and its usefulness established.

PLANNED ACTIVITY:

The four phases of this program have been completed and the funding has been terminated by the DOE. Since we do not have, at this point, a recovery furnace model that has been validated by actual operating data, a three-year, fifth phase has recently been proposed to DOE for funding. Specific tasks will include:

1. Incorporate recent laboratory data on black liquor properties, char burning, fume formation and deposition, and droplet formation. Remove symmetry constraint.

2. Compare temperature and velocity measurements from the validation study with the model and reconcile any substantive differences.

3. Present the model in a convenient format that will be readily understandable to a broad range of users in the industry. Prepare training materials to facilitate usage of the model.

A newly-hired faculty member, Dr. Robert Horton, will assume responsibility for model refinement; Adjunct Professor T. M. Grace will serve as a consultant.

INTRODUCTION

Several portions of this project have been brought to a conclusion. Two areas reported on at the October, 1989 Black Liquor Research Program review sponsored by OIP-DOE covered in-flight characteristics of high solids black liquor and entrainment of pyrolyzed black liquor particles. Slightly modified versions on these reports are given below.

IN-FLIGHT DROPLET PROCESSES WITH HIGH SOLIDS BLACK LIQUOR

(T. Grace, S. Lien)

Introduction

Previous work on in-flight processes was carried out with feed liquor solids below 70%. The data indicated that the drying rate for black liquor drops falling through a hot environment was influenced by the initial liquor viscosity (at the conditions where the drop is formed). Drying rates were found to increase as initial liquor viscosity decreased. Initial tests were carried out with liquor drops falling countercurrently to upward flowing gas. Another set of tests was performed with the gas flow downward, concurrent with the black liquor drops.

Modern recovery boiler firing practice is now starting to use black liquors in the 70-80% range. One of the questions arising from these new practices is the effect of the very high solids levels on burning behavior. Accordingly, a decision was made to carry out tests with very high solids feed liquor in the flow reactor.

Test Plan and Experimental Procedure

A series of tests was planned to study the in-flight processes of black liquor droplets injected at high % solids. The liquor was to be adjusted to 3 different solids concentrations (70, 75, and 80%). At each solids concentration the liquor would be injected at three temperatures. The temperatures were selected to span the range which will produce uniform droplet formation. The different % solids and temperatures at which the liquor was fed gave different initial viscosities.

The DOE black liquor flow reactor consists of a series of high temperature electric heaters surrounding 4-inch ceramic tubes. A continuous stream of black liquor droplets is injected at the top of the reactor and falls about 200 inches through the entire heated reactor space. A gas stream flows upward through the reactor at a nominal velocity of 5 ft/sec. The average temperature of the reac-

tor is 900° C so that changes in the free-falling droplets can be studied in an environment similar to the recovery boiler.

The feed system consists of a heated stainless steel vessel with a capacity of 2.5 gallons, a gear pump to accurately meter the black liquor flow, a heat exchanger system to adjust the temperature of the liquor, and an injector assembly. The injector causes the continuous stream of liquor to be broken into individual drops as they enter the furnace environment. The drops produced for these tests all haddiameters in the range from 2.0 to 2.2 mm.

Samples of the partially dried droplets can be collected at various points along the length of the in-flight reactor. The samples were collected in a small metal boat which was filled with liquid nitrogen. The liquor samples were immediately quenched as they landed in the liquid N_2 and no further drying or devolatilization occurred. These samples were then analyzed for moisture and fixed carbon.

Several problems occurred in carrying out these tests. In addition to the difficulty of concentrating the liquor up to the desired concentrations, we encountered problems operating the feed system at high solids levels. Because of the limited capacity of the heat exchanger system, the high solids liquor had a very strong tendency to plug the feed line and the droplet formation was very poor. The highest solids concentration which we were able to reach successfully was 78.6%, and only a single test could be performed at this condition. Three complete tests were performed at each of three lower solids concentrations: 66.8%, 71.0%, and 74.9%.

Some plugging occurred in the lower part of the in-flight reactor at all test conditions. It is difficult to judge how much effect this had on the drying in the upper part of the reactor.

Results Obtained

Data were collected at three different feed temperatures for three different solids levels. The solids concentrations measured at the sampling locations are shown in Figures 1 and 3. It is obvious that the apparent drying rate slows significantly as the particles approach 90% solids. This same result was observed in earlier tests. As the liquor drops approach dryness and heat up, pyrolysis occurs simultaneously with drying. Water is produced by pyrolysis as well as being evaporated. The net result is that the apparent drying rate slows down at very high % solids.

The most important variations in the drying rate occur in the first and second sections of the reactor (the first 86 inches). Looking at this part of the drying curves, it is clear that, for a given initial solids level, the drying rate increases with increasing feed temperature. In order to compare initial drying rates on an equivalent basis, only the drying in the first section of the reactor was used to calculate the mass of water evaporated per unit initial drop surface area (mg H_2O/mm^2).

Effect of Solids, Temperature, and Viscosity

Initial drying was analyzed as a function of three feed liquor variables: solids, temperature, and viscosity. Since a single liquor supply was used for all of these tests, only two of the three variables can be considered independent. The initial drop size is the same (within 5%) for all of the tests, so this is not a variable.

Initial drying is plotted against feed liquor temperature in Figure 4. The drying levels out at higher feed temperatures for Tests 135 and 166. This occurs because the liquor solids at the end of the first section of the evaporator is in the 90% range.

An unexpected result was the finding that the maximum amount of drying occurred with feed liquor solids contents in an intermediate region (about 71% solids in these tests). This is shown more clearly in Figure 5 where initial drying is plotted against feed solids.

Using measured viscosities and previously determined viscosity correlations, the liquor viscosity for each inlet liquor condition could be calculated. The initial drying is plotted against viscosity in Figure 6. It is evident that viscosity alone cannot account for differences in evaporation rates.

Insight into what is occurring in these experiments can be gained from the following simplified analysis. The assumptions are:

1. Drying is controlled by external heat transfer and the rate of heat transfer is independent of drop temperature.

2. Swelling occurs and increases the effective heat transfer area during drying.

3. Evaporation of water takes place at the local boiling temperature, determined by the liquor's boiling point rise.

4. Sensible heat changes in the liquor are small compared to the heat of vaporization and can be handled by using an effective heat of vaporization.

5. Residence times for a drop in a given segment of the reactor increase as the drop swells.

6. Liquor solids content changes are not a valid indication of the extent of drying once simultaneous pyrolysis starts to occur.

The drying rate is given by

$$\frac{dmw}{dt} = \frac{Q}{\lambda eff} = \frac{\pi d^2}{4\lambda eff} f^2 Tr^x$$

where

mw = mass of water in the drop

t = time

Q = heat transfer rate

λeff = effective heat of vaporization (including sensible heat effect)

d_i = initial drop diameter

f = swelling factor = $\frac{\text{d swollen}}{\text{d original}}$

T_R = reactor temperature

x = exponent between 1 and 4

Assuming a constant evaporation rate within a given reactor segment, the amount of water evaporated per unit initial surface is given by

$$\frac{4\Delta mw}{\pi d^2} = \frac{f^2}{\lambda eff} TR^x t_R$$

where t_R = residence time in the initial reactor section. Since t_R increases as f increases, it is evident that swelling almost totally dominates the behavior and that all that is being observed is the effect of initial liquor conditions on swelling.

Fixed Carbon Analysis

In addition to measuring the moisture in the droplets, the amount of fixed carbon was also measured. Fixed carbon is an analytical procedure which measures the amount of the carbon in the sample that has been converted to char carbon. It provides a measure of the extent to which pyrolysis has occurred. A completely pyrolyzed char from this liquor will contain about 25% fixed carbon by weight.

The amount of fixed carbon measured was plotted against the solids concentration of the black liquor samples in Figure 7. It is apparent that there is some overlap of the drying and pyrolysis processes. The pyrolysis process begins to occur at about 80% solids and it proceeds rapidly at solids contents about 90%.

Conclusions

Information on the rate of droplet drying has been collected at high temperature conditions for feed solids concentrations up to 75% solids. Based on the limited data collected, it appears that the drying rate of black liquor droplets reaches a maximum at about 71% and begins to fall off if the initial solids concentration is raised above 71%.

The pyrolysis or volatiles evolution stage of black liquor combustion begins when the droplets have dried to at least 80% solids; it proceeds rapidly above 90% solids.

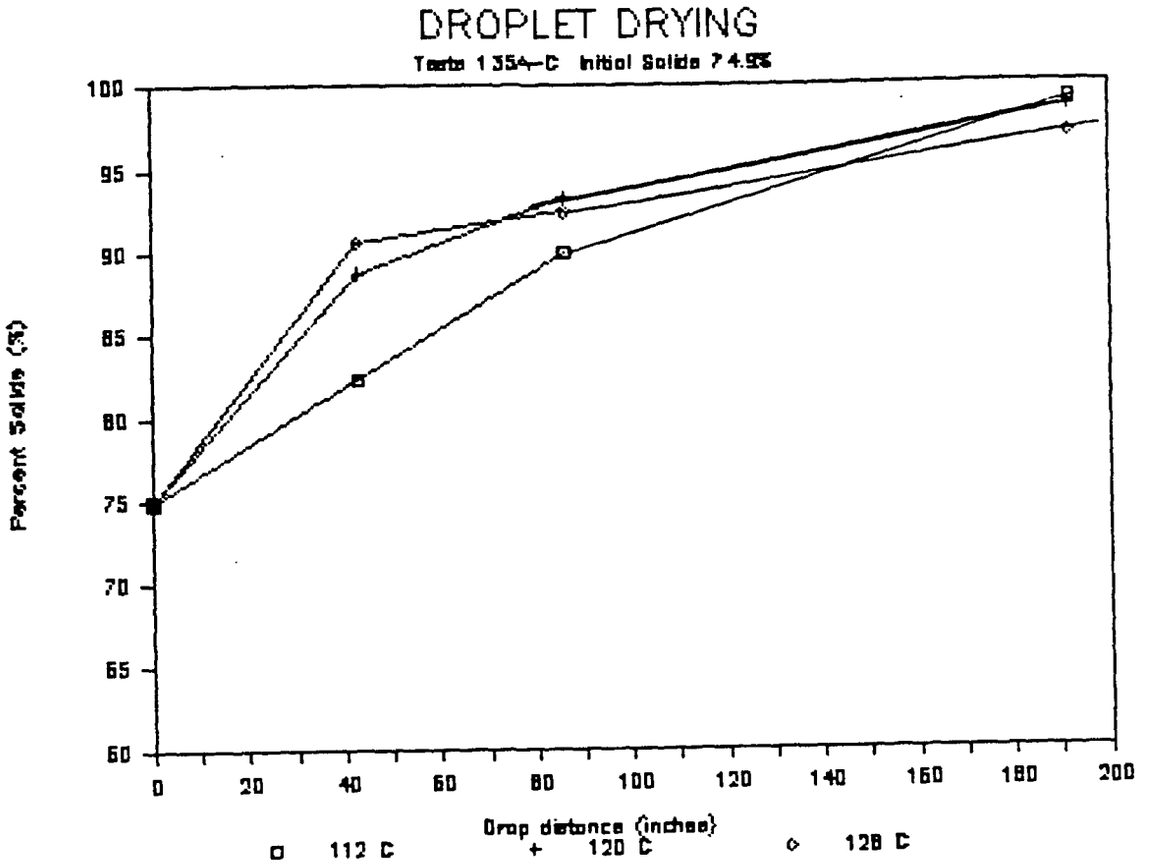

Figure 1: Tests 135A, B, and C

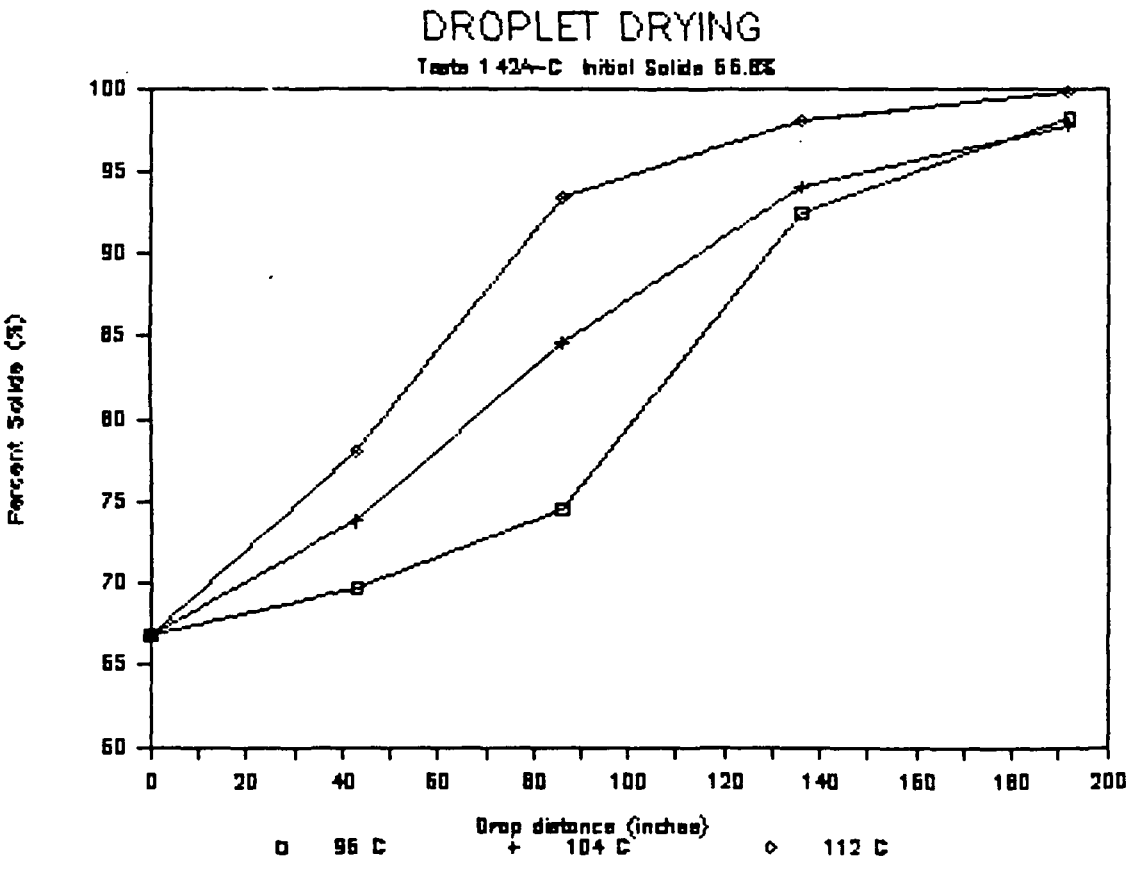

Figure 2: Tests 142 A, B, and C

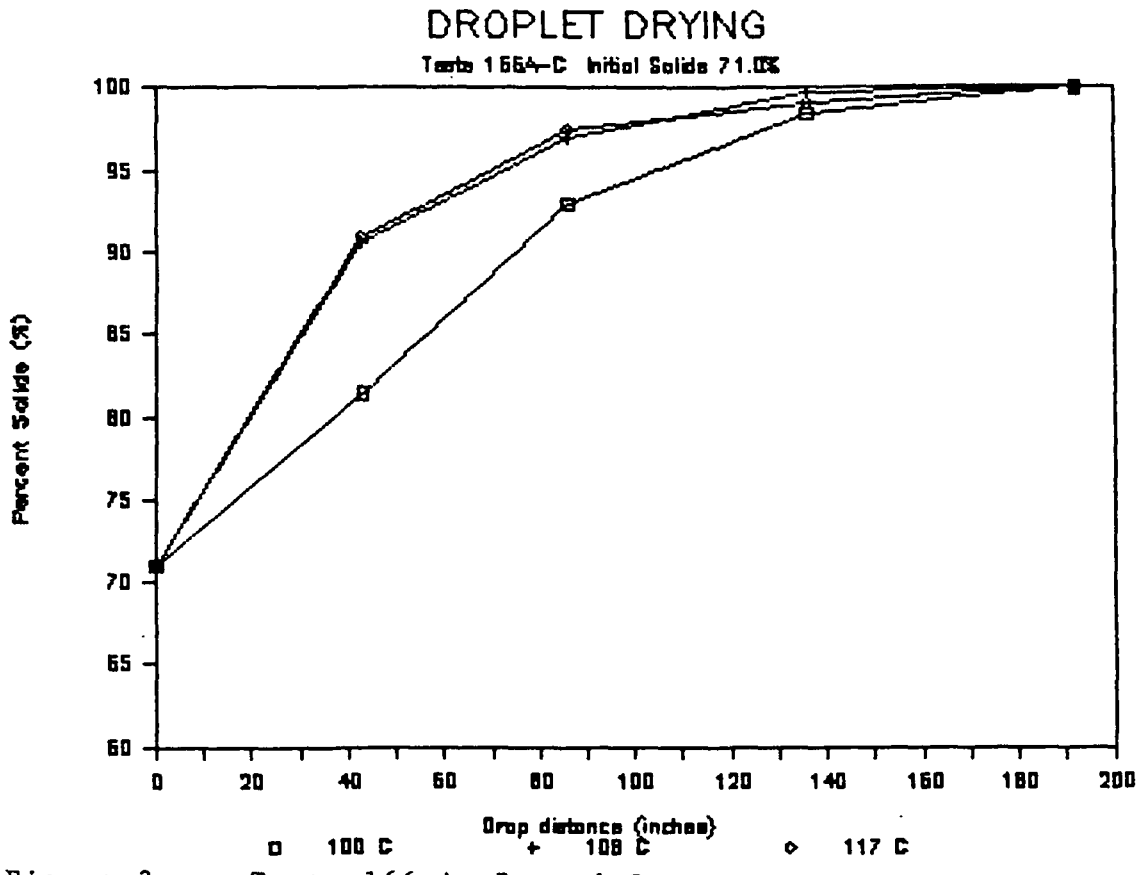

Figure 3: Tests 166 A, B, and C

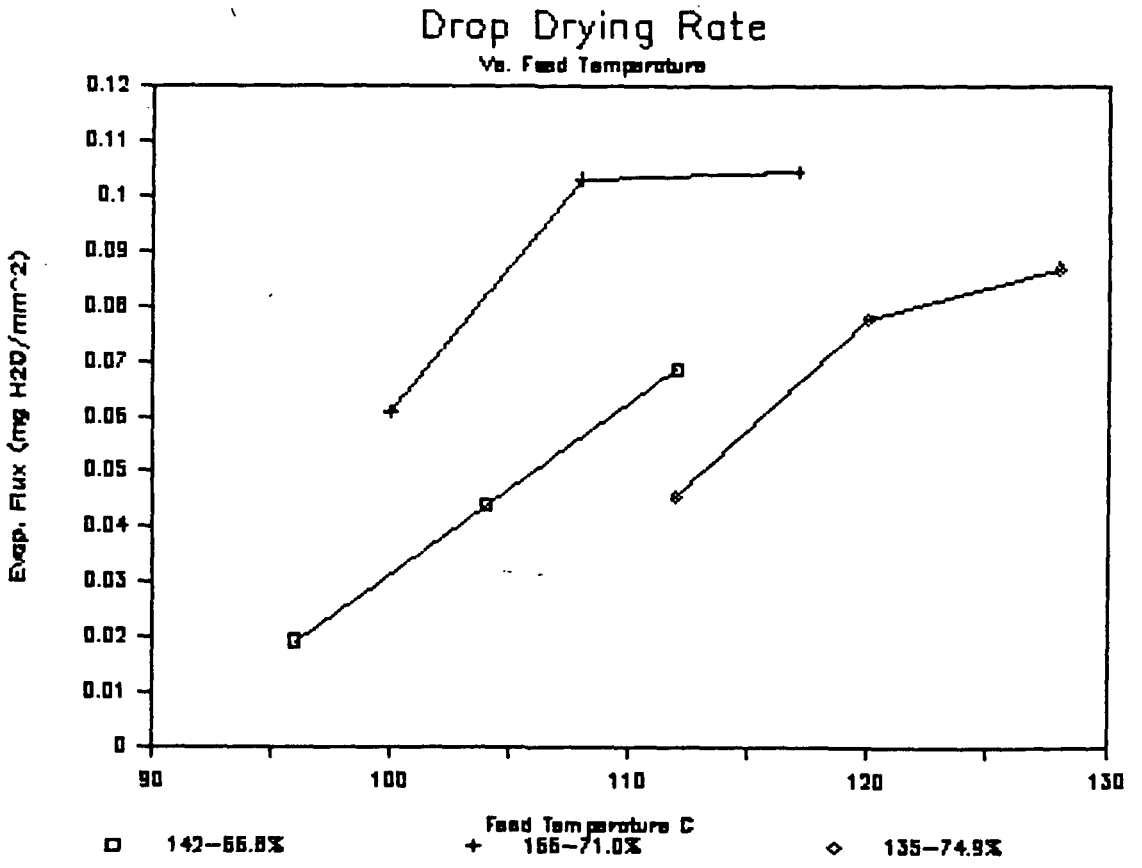

Figure 4: Drop Drying vs. Feed Temperature

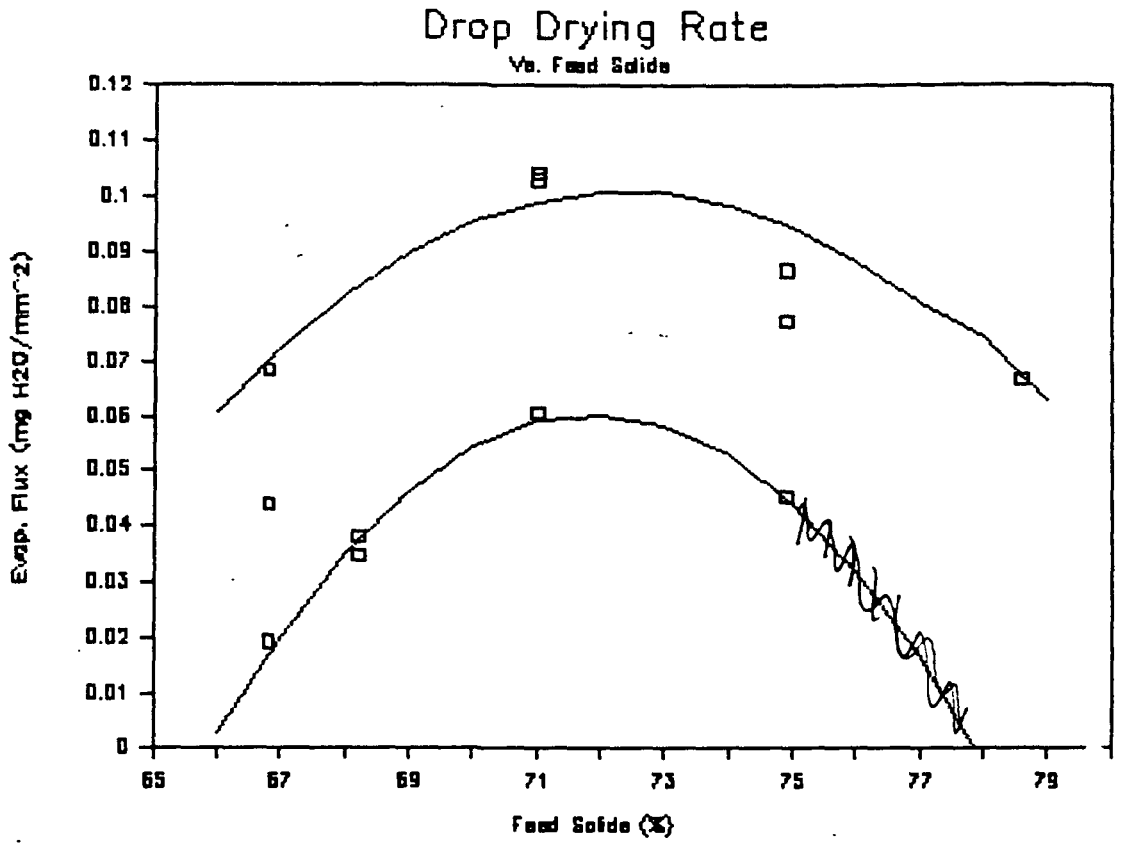

Figure 5

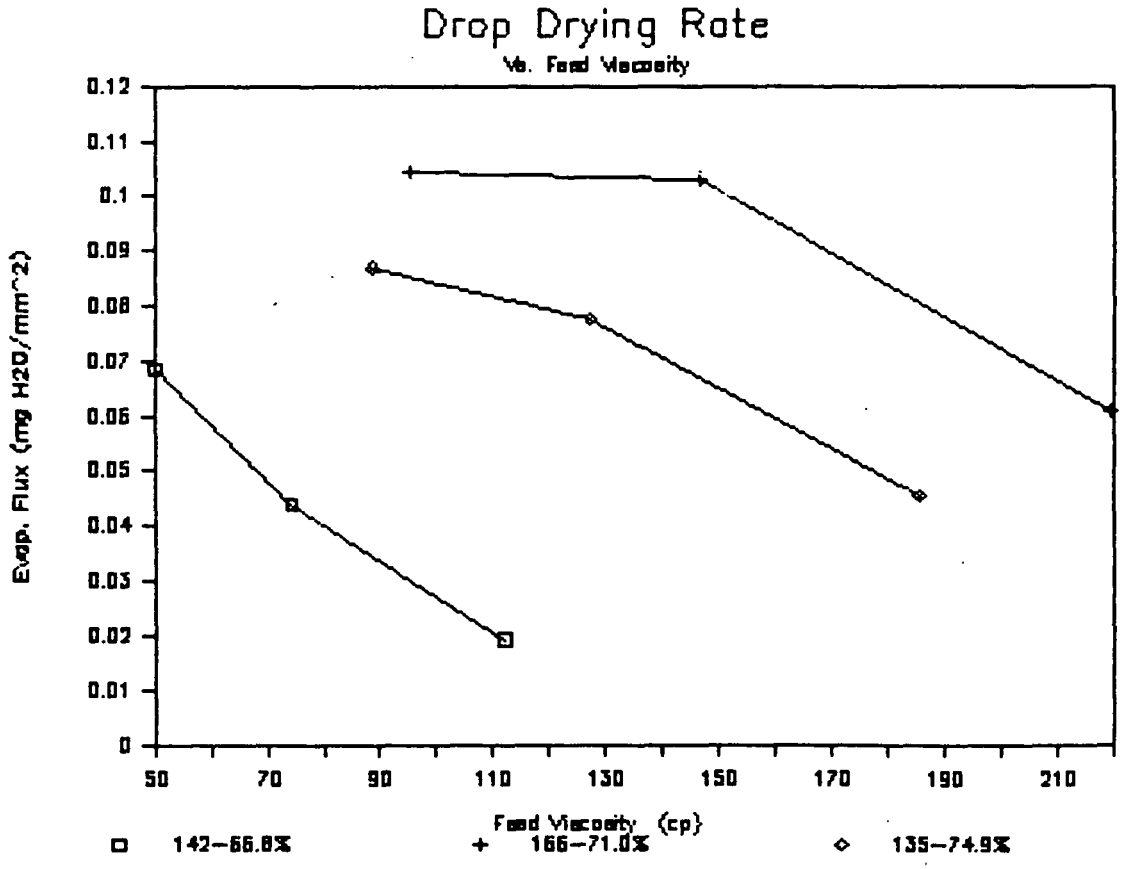

Figure 6

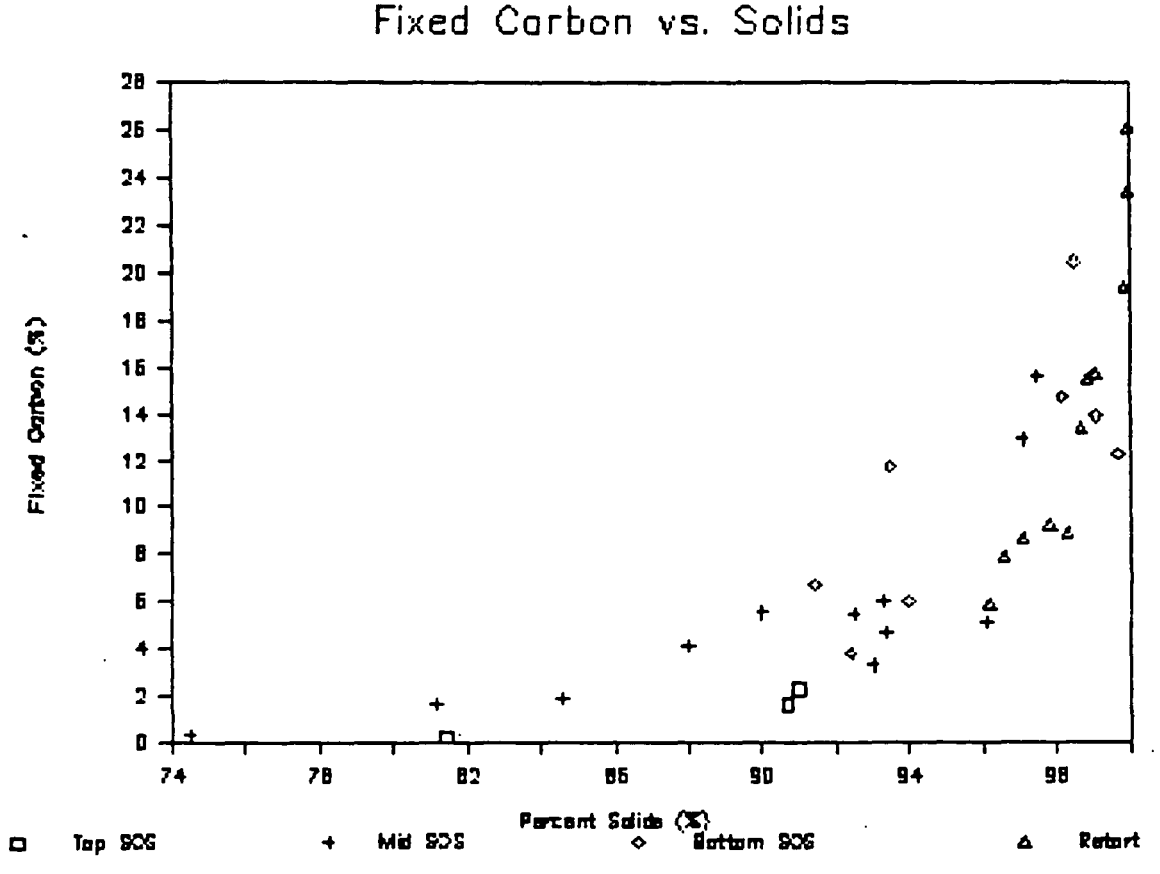

Figure 7: Fixed Carbon Analysis

Project 3473-6 Status Report

ENTRAINMENT OF PYROLYZED BLACK LIQUOR PARTICLES

(Dr. A. Macek - National Institute of Science and Technology - NIST)

This report describes an experimental study of entrainment characteristics of pyrolyzed black-liquor (BL) particles. The objective of the research was to obtain data which would allow estimates of sizes, densities, and drag coefficients of particles entrained upward from char beds in recovery boilers. The experiments were performed in the NIST dilute-phast plug-flow reactor (DPFR). BL drops were injected into the reactor at its top and allowed to travel at elevated temperatures over the entire height of the reactor to its bottom. The key experimental parameter was the upward gas velocity necessary to lift the BL particles with given sizes and densities from the bottom of the reactor. This study was done under subcontract to IPST as part of the DOE-funded project on Fundamentals of Black Liquor Combustion.

EXPERIMENTAL PROCEDURE

Details of the modular construction of the DPFR were described in earlier reports on this project (Ref. 1,2, and 3). The reactor configuration used for entrainment studies is shown in Fig. 1 and the details of the entrainment section at the bottom of the reactor in Fig. 2. BL drops were injected into the reactor at the top Sampling and Observation section, 11.5 ft. (350 cm) above the bottom of the entrainment section. The drop injection and measurement techniques are described in Ref. 2.

As shown in Fig. 2, the reactor gases entered the entrainment section at its bottom, where the temperature was maintained at 1790°F (975°C), i.e., near values above the char bed in a recovery boiler. It is important to note that gas temperatures, hence also gas velocities, decreased with increasing height in the unheated entrainment section to 1560° F (850° C) and then remained near this value over the entire heated part of the reactor to the point of drop injection. The reactor gases were generated underneath the reactor by means of a gas burner, as in earlier combustion experiments. However, most entrainment experiments were conducted under pyrolysis conditions. For these studies the burner was run slightly fuel-rich and its product gases were diluted by nitrogen. Thus, the reactor gases consisted of N_2, CO_2, H_2O, and CO, with virtually no free oxygen. Indeed, all the results reported below were obtained under pyrolysis conditions. All experiments were run with a BL sample containing 65% solids, with initial drop diameters of 2.5 mm.

Several experimental techniques were tried until a satisfactorily controllable procedure was adopted, wherein BL drops were injected at the top of the reactor and the resulting particles were observed and counted visually as they settled at the bottom of the entrainment section. The reactor gas velocity, U_g, was increased continuously to the maximum value which still allowed the settling of all particles to the bottom, as determined by counts of drops injected at the top and of particles seen falling in the entrainment section. For drops with do = 2.5 mm, this value was empirically determined to be 8.2 ft/sec (250 cm/sec) at the bottom, decreasing to 7.3 ft/sec (225 cm/sec) inside the heated section of the reactor. Once this velocity was determined, it was kept constant in actual entrainment tests. In all tests reported below, the particles were observed to settle to the bottom while still in the process of expansion. They remained on the bottom until they expanded to the point where they were lifted by upward flowing gases. As a result of this critical-velocity choice, the residence times of particles at the bottom were short, usually a fraction of a second.

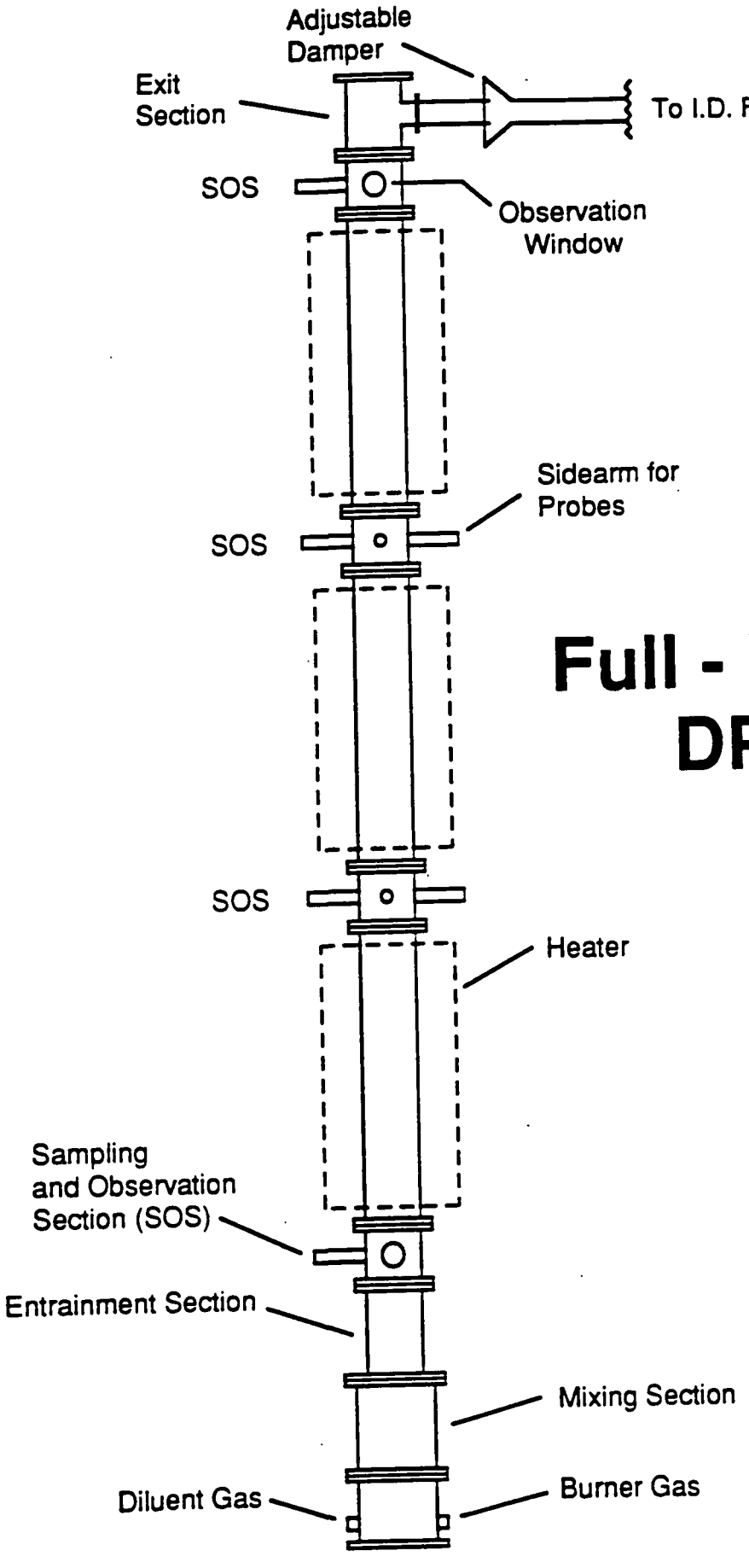

FIGURE 1

Full - Height DPFR

FIGURE 2

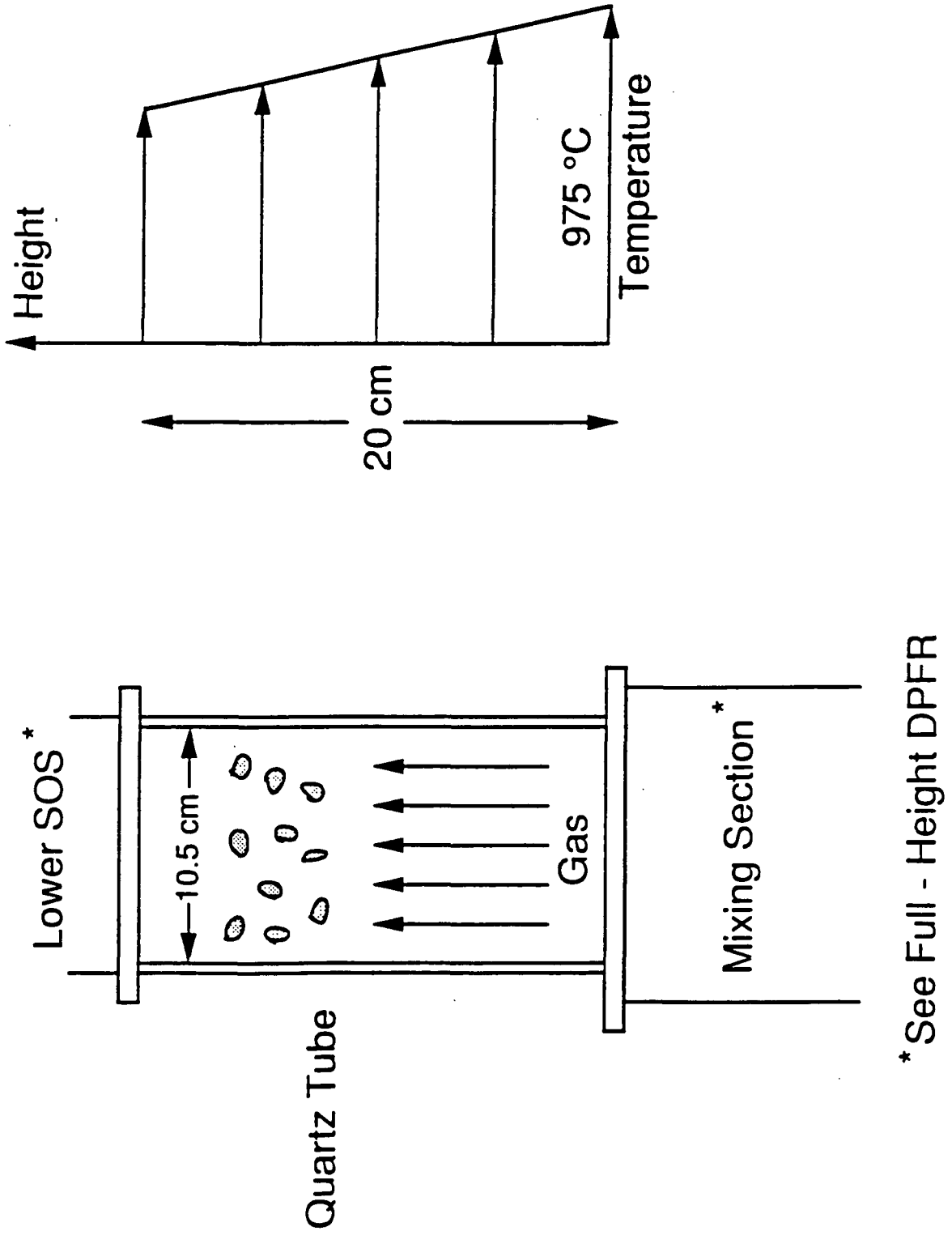
Entrainment Section
Height
975 °C
Temperature
20 cm
Lower SOS*
10.5 cm
Gas
Quartz Tube
Mixing Section*
*See Full - Height DPFR

Table 1 Properties of BL Drops at Injection

	d_o (cm)	m_o (mg)	m_{os} (mg)
Test 1	0.235	8.83	5.74
Test 2	0.260	11.95	7.77

The fact that the gas velocity was decreasing in the entrainment section was convenient for measurement purposes. Because of decreasing U_g, having lifted from the bottom, the particles were not continuously entrained upward, but remained suspended in the transparent section, often for several seconds, moving slowly up and down. During that time, they were photographed with a framing camera for subsequent size measurement. Since the particles, at the point where they were photographed, were almost motionless relative to the outside observer, this procedure provided the direct determination of their terminal settling velocity, U_t, which at the point of suspension is, by definition, equal in magnitude to the upward gas velocity, U_g. Specifically, the information obtained was the size of dried pyrolyzed particles entrainable at the upward gas velocity of 8.2 ft/sec at temperatures of about 1800° F. As will be shown in Section 4.2.4, these data can be used for determination of drag coefficients and particle densities at the point of entrainment.

EXPERIMENTAL DATA

Numerous particles were observed and photographed in suspension, as described in the preceding Section. The data from two tests, presented and discussed below, were chosen, because these particles were measured near the center of the reactor where there is minimum optical distortion due to the curvature of the quartz tube. The sizes and shapes of these are representative of most entrained particles. The two tests differed only in the initial drop diameters. Properties of initial drops are given in Table 1. As discussed above, these drops were exposed to upward flowing gases with T = 850° C and U_g = 225 cm/sec through most of their inflight residence times. They continued to expand over a brief residence time while on the bottom at T = 975° C, whereupon they were entrained upward at U_g = 250 cm/sec.

The data from Test 1 (particles 101 through 110) and Test 2 particles 201 through 206) are presented in Table 2. The values d_A and d_B are the larger and the smaller of the two diameters measured from the framing-camera records. The volume of the equivalent sphere (fourth column) is assumed to be

$$V = \frac{\pi (d_A\, d_B)^{3/2}}{6} \qquad (1)$$

This means that the two measured diameters are given equal weights in the calculation of the third, unseen, dimension. The swollen volume, SV, is defined as volume per unit mass of original solids, V/m_{os}. Alternative geometric assumptions will give somewhat different numerical results, in particular if d_B is much smaller than d_A. For example, assumption of a spheroidal shape, which gives a greater weight to the smaller of the two measured diameters, results in virtually same volumes as those in Table 2 for the nearly-spherical particles 102, 103, 107, and 108, but up to 40% lower in cases of extreme eccentricity (e.g., particle 105). However, it is seen that swollen volumes of both quasi-spherical and oblong particles are scattered over the same range, mostly between 10 and 30 cc per gram of original solids. It will also be seen in subsequent discussion that drag coefficients of oblong particles, calculated from Equation 1, are in good agreement with those obtained from quasi-spherical particles.

RESIDENCE TIME ESTIMATES

Estimates of residence times of drops and particles in flight from the point of injection into reactor gases to a specified point in the reactor were discussed at some length in Ref. 3. Briefly, the computer program written and used for that purpose allows various assumptions about the expansion history, and it computes residence times on the basis of balance of forces due to gravity and to upward drag of the reactor gases. A fortunate conclusion from the results of these computations is that (for drop sizes and reactor dimensions used in this project) the calculated residence times are insensitive to assumption of specific times and locations over which expansions occur.

In view of information obtained previously in this project, it is assumed here that BL drops expanded in the middle of the upper heated section of the DPFR (see Fig. 1) by a linear ratio of 2, and that the expanded diameter and the mass of the particle remained unchanged for the remainder of the time in flight to the bottom of the reactor. The resulting times are about 1.0 sec for d_o = 0.235 cm and 0.9 sec for d_o = 0.260 cm. Estimates were also made of corrections to these residence times caused by two effects. First, the particle masses decrease with time due to drying. Second, the particle diameters decrease somewhat during drying (Ref. 3). Further calculations with the existing computer program show that these two corrections amount only to about 0.1 sec, but in opposite directions, so the combined effect is too small to be estimated. Thus, the above values of about 1 sec are realistic.

As described previously, after the in-flight stage at 850°C, the particles continue to expand for another fraction of a second while on the bottom of the reactor at 975° C. On the basis of all the data obtained at NIST and IPST, it appears likely that most of the drying occurred in flight, and the major part of pyrolysis and expansion to final entrainable volumes took place (Table 2) on the bottom of the reactor.

INTERPRETATION OF EXPERIMENTAL DATA

The data presented in Table 2 can be used further to obtain additional information about properties which the particles must have in order to be entrained upward at temperatures and gas velocities representative of char-bed surfaces. One approach is to rely on prior experience in several laboratories which indicates that dried, devolatilized particles, typically contain 60 to 65% of the weight of original solids in the liquor. This allows estimates of densities, hence also of drag forces necessary to entrain the particles. A second possibility is to use the established drag-coefficient data from the literature and calculate densities and masses which the particles had at the point of entrainment. In this Section we use the data in Table 2 for interpretation of particle characteristics by both approaches.

Table 2 Diameters and Volumes of Pyrolyzed Particles at the Point of Entrainment

Particle No.	d_A (cm)	d_B (cm)	V_s (cm^3)	SV(cm^3/g)
101	0.88	0.51	0.157	27.4
102	0.76	0.63	0.173	30.2
103	0.63	0.59	0.119	20.6
104	0.63	0.42	0.071	12.4
105	1.00	0.46	0.163	28.4
106	0.84	0.59	0.182	31.8
107	0.67	0.55	0.117	20.4
108	0.53	0.46	0.063	11.0
109	0.55	0.29	0.033	5.8
110	0.55	0.29	0.033	5.8
201	0.93	0.51	0.171	22.0
202	0.93	0.55	0.191	24.6
203	0.72	0.51	0.116	15.0
204	1.09	0.46	0.187	23.9
205	1.05	0.46	0.176	22.6
206	0.93	0.42	0.128	16.4

DRAG COEFFICIENTS FROM ASSUMED RESIDUAL MASSES

First, we calculate drag coefficients on the basis of assumed densities. If the residual solids in pyrolized particles constitute 65% of the original mass, the original density of the liquor containing 65% solids was 1.3 gm/cc, the density of pyrolyzed particle is

$$\rho_s = 1.3 \times 0.65 \times 0.65 \times \frac{V_o}{V_s} \qquad (2)$$

The values of V_0 are 0.00680 cc for d_0 = 0.235 cm and 0.00920 cc for d_0 = 0.260 cm. Experimental data for V_S are listed in Table 2.

The drag coefficient for a particle suspended in the gravitational field by a gas stream moving upward at velocity $U_T = U_g$ is

$$C_D = \frac{2F}{\rho_g A U_t^2} \qquad (3)$$

where F is the drag force

$$F = V_s (\rho_s - \rho_g) g \qquad (4)$$

and A the projected area of the particle normal to the direction of the flow. Using the concept of an equivalent sphere from measured particle diameters, the combination of Equations (3) and (4) yields an explicit expression for the drag coefficient:

$$C_D = \frac{2g}{U_t^2}\left[\frac{2}{3}\sqrt{d_A \cdot d_B}\left[\frac{\rho_s}{\rho_g} - 1\right]\right] \qquad (5)$$

Table 3 Densities and Drag Coefficients from Assumed Residual Masses

Particle No.	ρ_s (gm/cc)	C_D
101	0.0237	1.22
102	0.0215	1.14
103	0.0315	1.47
104	0.0524	2.07
105	0.0229	1.19
106	0.0204	1.10
107	0.0319	1.48
108	0.0592	2.24
109	(0.1120)	(3.43)
110	(0.1120)	(3.43)
	Mean and St. Dev., Test 1:	1.49 ± 0.41
201	0.0296	1.56
202	0.0264	1.45
203	0.0435	2.02
204	0.0273	1.48
205	0.0288	1.53
206	0.0396	1.90
	Mean and St. Dev., Test 2:	1.66 ± 0.22
	Overall Mean and St. Dev.:	1.56 ± 0.35

The gas density used in calculations was that of nitrogen, 2.75×10^{-4} g/cc at 975° C, because the reactor gases contained 80 to 85% of N_2.

Particle densities from Equation (2) and the resulting drag coefficients from Equation (5) are given in Table 3. It should be emphasized that the crucial assumption in generating the results in Table 3 from the experimental data in Table 2 concerns particle masses. Specifically, it is assumed a priori that all masses are 3.73 mg for particles No. 101 through 110 (d_o = 0.235 cm) and 5.06 mg for particles No. 201 through 206 (d_o = 0.260 cm).

The mean values and standard deviations in Table 3 do not include particles No. 109 and 110. It can be seen at a glance that sizes of these two particles in Table 2, as well as densities and drag coefficients in Table 3, deviate markedly from the rest of the data. In addition, there are physical reasons for excluding these. It can also be seen by inspection of Table 3 that the mean values of drag coefficients for individual Tests 1 and 2 are well within the standard-deviation bands of each other, so the combining of all the data to obtain the overall mean value is appropriate.

Particle Mass Determinations from Standard Drag Coefficients

The alternative approach to obtaining additional information about entrained particles involves the use of drag coefficients from standard aerodynamics literature (e.g., Ref. 4). The procedure consists of four steps: (a) Reynolds Numbers are calculated from experimental particle diameters and the measured terminal velocity; (b) the drag coefficient corresponding to the Reynolds Number is read from the standard drag curve; (c) the C_D value so determined is substituted into Equation (5) which is then solved for ρ_s; and (d) the actual particle mass, m_s, is obtained from the volume and ρ_s.

In calculation of the Reynolds Numbers,

$$Re = \frac{U \rho_g d}{\mu} \qquad (6)$$

the values of $U = U_T$, the density of nitrogen at 975° C, and $d = \sqrt{d_A \cdot d_B}$ where the same as earlier in this report. The value used for viscosity of nitrogen at 975° C was $\mu = 4.56 \times 10^{-4}$ poise. The value of particle volume V_s in step (d) was taken from Table 2. Thus all geometric and physical assumptions are the same as elsewhere in the report.

The results are given in Table 4. The Table includes the data on all individual particles, but the mean value of mass eprcentages for Test 1 does not inlcude particles 109 and 110. The reasons for the omission are discussed in the next Section.

Table 4 Masses of Entrained Particles from Standard Drag Coefficients

Particle No.	Re	C_D	ρ_s (gm/cc)	m_s (mg)	m_s/m_{os}
101	100.5	1.12	0.0232	3.65	0.64
102	103.8	1.18	0.0221	3.83	0.67
103	91.5	1.26	0.0268	3.17	0.55
104	77.2	1.37	0.0345	2.46	0.43
105	101.7	1.19	0.0228	3.72	0.65
106	105.6	1.17	0.0216	3.93	0.69
107	91.1	1.26	0.0269	3.15	0.55
108	74.1	1.39	0.0367	2.31	0.40
109	59.9	1.55	0.0505	1.68	(0.29)
110	59.9	1.55	0.0505	1.68	(0.29)
Mean and St. Dev.		1.31 ± 0.14			0.57 ± 0.10
201	103.3	1.18	0.0223	3.81	0.49
202	107.3	1.16	0.0211	4.03	0.52
203	90.9	1.26	0.0270	3.14	0.40
204	106.2	1.16	0.0214	3.97	0.51
205	104.2	1.18	0.0220	3.86	0.50
206	93.7	1.24	0.0258	3.29	0.42
Mean and St. Dev.		1.20 ± 0.04			0.47 ± 0.050
Overall Mean and St. Dev.		1.27 ± 0.13			0.53 ± 0.010

DISCUSSION

The two sets of results given in Tables 3 and 4 are derived from the same set of experimental data and they both contain, as the most important output, two properties of particles at the point of entrainment: density (ρ_s) and drag coefficient (C_D). Inasmuch as the results in these two tables were obtained on the basis of two different physical assumptions, it is natural that there should be differences in the results. Equally interesting, however, are the similarities resulting from the two different interpretations. These similarities and differences will be discussed below.

It must be pointed out at the outset that all numerical values in Tables 3 and 4, as well as the volumes in Table 2, are based on the concept of reduction of actual irregularly shaped particles to equivalent spheres. Since this is an approximation, one could expect the confidence in the resulting values to be good for particles where d_A and d_B values are close to each other, but diminishing with increasing eccentricity. While this may be true as far as the exact numerical values are concerned, it is important to show that the geometric aspects are not the causes of differences in trends seen in Tables 3 and 4. Particles No. 102, 103, 107, and 108 are all nearly spherical, but a comparison of the resulting drag coefficients obtained by the two data-interpretation procedures shows excellent agreement for No. 102, reasonable agreement (better than 20%) for No. 103 and No. 107, but divergence in excess of 60% for No. 108. Conversely, the two calculated drag coefficients are identical for the highly eccentric particle No. 105, but widely different for particles No. 109 and 110, even though they are somewhat less eccentric. Thus, reasons for differences in the results obtained by the two interpretation procedures lie elsewhere.

Perhaps the clearest way to see the similarities and differences of the two sets of results is by inspection of the last column in Table 4. There is no equivalent column in Table 3, because that Table was generated on the assumption that all m_s/m_{os} values were equal to 0.65. A major point of agreement between the two data-interpretation procedures is that, for Test 1, most m_s/m_{os} values in Table 4 are fairly close to 0.65. Indeed, this value is within the indicated standard deviation band; moreover, it remains within the wider band of 0.516 ± 0.151 which results when the widely discrepant data from particles No. 109 and 110 are included in the statistics. This basic agreement, albeit rough, is important, because the underlying assumptions for the two sets of calculations are not only different, but also independent of each other.

It was noted earlier in connection with Table 3 that data from particles No. 109 and 110 are at variance with other results of Test 1. Parallel inspection of Tables 3 and 4 both gives a justification for excluding these data from averages in Table 3 and suggests reasons for the discrepancies. It can be seen that the basic assumption of the first data-interpretation alternative -- namely, the forcing of 65% of the mass of original solids into small volumes of these particles -- leads to densities about 3.5 times larger than the average of all other values in Table 3. The immediate consequence is that the calculated drag coefficients are about twice the average of other values in Table 3 and almost three times larger than the corresponding values in Table 4. Consideration of m_s/m_{os} data in Table 4 sheds further light on this matter. To wit, the masses of these two small particles are barely half the amounts expected for even fully dried and devolatilized particles, suggesting the possibility that these were fragments. If so, they should not be related to the total solids in the origi-

nal drop. To be sure, the good agreement between the numbers of injected BL droplets and the particles seen falling to the bottom indicates that most particles did not fragment during their flight down the length of the reactor. However, occasional fragmentation may well have occurred, either in flight or, more likely, upon impact at the bottom.

An additional note on anomalous particles No. 109 and 110 is in order here. Even if these particles were indeed fragments, it should be made clear that the values of m_s are not suspect, so this is not the reason for rejecting the two m_s/m_{os} values. Indeed, there are no valid grounds, either physical or statistical, to reject any vealues in Table 4. The only reason why the mean value of m_s/m_{os} for Test 1 does not include particles 109 and 110 is that it appears physically unrealistic to associate their masses with the original droplets. Thus, while the separate values of both m_s and m_{os} are as valid as the rest of the data, the inclusion of $m_s m_{os}$ values for these two particles would be misleading.

All entries for Test 2 in Table 4 show less scatter, but also lower m_s/m_{os} values than in Test 1. There is no obvious explanation for that difference. One possibility is that, because of larger drop and particle sizes, the particles had to remain on the bottom of the reactor for a longer time until they devolatilized to a greater extent than in Test 1. A simpler possibility is that, despite the relatively small standard deviation in Test 2, the calculated mass-losses are still within the overall range of data scatter. The drag coefficients from both tests, clearly, are statistically the same.

It is crucial to emphasize that the question of mechanism of mass losses, normal pyrolysis or fragmentation, does not affect the determination of drag coefficients in Table 4, which are equally valid in either case. In particular, it should be noted that the mean values given in that Table include particles No. 109 and 110. Even though the two corresponding drag coefficients are in fact significantly higher than any others, their elimination from the statistics would result only in negligible lowering of the overall mean value, from 1.27 ± 0.13 to 1.22 ± 0.08. Thus, no "weeding" of data is necessary. By contrast, if drag coefficients for these two particles had been included in the statistics of Table 3, the overall mean would have increased from 1.56 ± 0.35 to 1.80 ± 0.70. While this increase of the mean is still moderate, the associated standard deviation (rather large even without the addition of the two values) becomes such as to make the data appear quantitatively non-reproducible.

The foregoing discussion shows that the two procedures for determination of drag coefficients at the point of entrainment lead to similar mean values, given in Tables 3 and 4, respectively. It is especially gratifying that, for particles where there is good agreement between drag coefficients from the two procedures, the calculated mass losses are near values one would expect for devolatilized BL char. However, the procedure of obtaining the coefficients from the standard drag curve is clearly preferable to the a priori assumption of masses in particles for two reasons: (a) it eliminates the problem of mechanical mass losses (chipping, fragmentation), and (b) it gives statistically better results without rejection of any data points. This is not surprising. The drag curve from standard aerodynamics literature used in the present study is not only universally accepted for spherical particles, but also has been shown to provide a good approximation for other shapes, as long as all particle dimensions are of the same order of magnitude.

CONCLUSIONS

The results of the present study lead to several conclusions relevant to the understanding and modeling of entrainment and carryover in recovery boilers:

1. A drag force corresponding to C_D values of about 1.2 to 1.3 is required to entrain particles resulting from pyrolysis of BL drops 2.5 mm in diameter. At the actual temperature of 1790° F (975° C) used in the present study, this C_D corresponds to an upward gas velocity of 8.2 ft/sec (250 cm/sec).

2. The velocity required to entrain the same particles at any other temperature can be easily obtained from Eq. (5). In particular, it can be noted that, since ρ_s/ρ_g is much larger than unity, the entrainment velocity is almost exactly proportional to $\sqrt{T}$.

3. Drag coefficients do not vary greatly with shapes and sizes of particles (see Table 4), indicating that the same coefficients may be applicable to other, moderately different, initial drop sizes.

4. In the absence of fragmentation, the use of C_D values from the standard drag curve for spherical particles is compatible with a a priori assumption of 60 to 65% residual solids in the pyrolyzed particles.

In view of the fact that the residual mass of pyrolyzed particles cannot be grossly different than 60% of the original solids, the last conclusion lends confidence to the use of the standard drag-coefficient curve for spherical particle for determination of entrainment characteristics in recovery boilers. This can be done in several ways. If there is information on either sizes or densities of particles entrained at a given gas velocity and temperature, the C_D values for particles can be obtained from the curve and used to calculate entrainment velocities at any other temperature. This, in effect, is what was done in the present study. Alternatively, if no direct measurement is available, one can make use of the overall mean of drag coefficients determined herein (Table 4) for approximate estimates of sizes and densities of pyrolyzed BL particles entrainable at any velocity and temperature.

LIST OF SYMBOLS

A	area
C_D	drag coefficient
d	diameter of spherical drop or particle
d_A	larger of the two measured particle diameters
d_B	smaller of the two measured particle diameters
F	drag force on particle
g	acceleration due to gravity
m	mass
Re	Reynolds Number
SV	swollen volume
T	temperature
U	velocity
V	volume
μ	gas viscosity
ρ	density

SUBSCRIPTS

f	final
g	gas
o	initial
s	solid
t	terminal (velocity)

References

1. Fundamental Studies of Black Liquor Combustion, Report No. 1

2. Fundamental Studies of Black Liquor Combustion, Report No. 2

3. Fundamental Studies of Black Liquor Combustion, Report No. 3

4. H. Schlichting, Boundary Layer Theory, McGraw-Hill, New York (1962).

PROJECT SUMMARY FORM

DATE: February 26, 1990

PROJECT NO. 3474: ENVIRONMENTALLY COMPATIBLE PRODUCTION OF BLEACHED PULP

PROJECT LEADER: T.J. McDonough

IPST GOAL:

To improve the process of production of bleached chemical pulp to make it more compatible with the environment.

OBJECTIVE:

To define pulping and bleaching technology that will decrease or eliminate the need for chlorine in the bleaching sequence.

CURRENT FISCAL YEAR BUDGET: $250,000

PRIOR RESULTS: 18 months 3 weeks

Results obtained since the inception of this project are summarized in the September 6, 1988 Status Report. They include empirical optimization of kraft and alkaline sulfite-anthraquinone processes for pulping to low kappa numbers, and studies of methods for reducing chlorine use by making oxygen delignification more selective or by applying hydrogen peroxide. Several pretreatments for improving oxygen stage selectivity have been studied. These include nitrogen dioxide, chlorine and bromine. Nitrogen dioxide pretreatment, in particular, has been studied from a mechanistic point of view, with the aim of finding better alternative pretreatments.

Formation of dioxins and AOX (ABSORBABLE ORGANIC HALOGEN) during bleaching were studied and a particular combination of control measures was shown to be effective. Analytical procedures for AOX were implemented, effects of method parameters were briefly studied and the precision of the method was determined.

SUMMARY OF RESULTS SINCE LAST REPORT:

The major part of the results obtained since the last report consists of a study of nitrogen dioxide pretreatment mechanisms by Dr. H. Ohi, whose report is attached. Experiments with model compounds showed that lignin units containing free phenolic hydroxyl groups react readily with nitrogen dioxide by

substitution and side chain displacement to give nitro compounds and ring degradation products, but that fully etherified units are not nitrated or degraded. Nitric acid does not react under pretreatment conditions, but it does accelerate the reactions of nitrogen dioxide with lignin models.

Nitrogen dioxide oxidizes aliphatic hydroxyls in the alpha position to carbonyl groups. A dimeric beta-aryl ether model containing no free phenolic hydroxyl groups underwent this reaction and, to a lesser extent, cleavage in the side chain to give veratraldehyde. This oxidation of a benzyl alcohol group to an alpha carbonyl group is significant because it enhances reactivity of the interunit ether linkage to oxygen and alkali. Similarly, ring nitration with side chain displacement can lead to cleavage of carbon-carbon bonds in condensed lignin units. Both observations suggest pathways for lignin depolymerization by nitrogen dioxide, which would account for acceleration of a subsequent oxygen delignification stage. Accordingly, gel filtration chromatography showed that the pretreatment decreased the average molecular size of lignin removed by oxygen delignification.

Conversely, the model studies make it unlikely that the mechanism proposed by Lindeberg and Walding is correct. These authors suggested that nitration of nonphenolic lignin units accelerates their cleavage in an alkaline oxygen stage. Our results, however, show that nitration of these groups is unlikely to occur. To clarify this, kraft pulp was methylated and then nitrogen dioxide treated and oxygen delignified. The effect of the pretreatment was strongly attenuated by the pulp having been methylated before the pretreatment, showing that nitrogroup assisted cleavage of ether linkages is not an important component of the pretreatment mechanism. The slight acceleration observed is probably due to the introduction of alpha carbonyl groups.

PLANNED ACTIVITY THROUGH FISCAL YEAR 1990:

(1) Conclude studies of mechanism of oxygen bleaching selectivity improvement by nitrogen dioxide pretreatment.

(2) Select and examine alternative pretreatments leading to an improved, oxygen-based, prebleaching stage.

(3) Continue studies of effects of chlorination stage variables on formation of dioxins and AOX.

(4) Initiate Ph.D. thesis research on effects of bleaching process variables on amounts, nature, and treatability of chlorinated organic compounds formed during bleaching.

(5) Conclude Ph.D. thesis research on medium consistency chlorination kinetics.

1. INTRODUCTION

Pretreatment of kraft pulp with nitrogen dioxide has been shown to be an effective method for both improvement of delignification and protection of carbohydrate degradation in oxygen bleaching. However, the mechanism of its action is not clear. The objective of this research is to learn more about the mechanism.

Abrahamsson et al. [1] have determined methanol in spent liquor obtained after the pretreatment of kraft pulp with NO_2 and O_2, and supposed that the demethylation of lignin leads to formation of hydrophilic groups and that this will contribute to the enhanced delignification. Lindeberg and Walding [2] have proposed a mechanism of action of NO_2 whereby nitro groups introduced into the aromatic rings of non phenolic lignin units promote ether cleavage in alkali, which in turn creates new phenolic hydroxyl groups to serve as oxygen delignification initiation sites. However, they do not show any experimental results supporting the introduction of nitro groups into the non phenolic lignin units.

Oxygen delignification is known to be initiated at free phenolic hydroxyl groups. If methoxyl groups of non phenolic lignin units could be demethylated, oxygen delignification would be enhanced. Therefore, it is important to clarify the reaction of non phenolic lignin units in the pretreatment with NO_2 as well as that of free phenolic lignin units. Furthermore, there is no clear evidence of nitro groups or nitroso groups introduced into lignin although nitrogen-containing groups are found to be introduced into lignin in the pretreatment [1,3].

Abrahamsson et al.[1] have pointed out that the pretreatment leads to a modification of lignin and the formation of species which attack carbohydrates is suppressed. Byrd and Gratzl [4] have speculated that the formation of catechol groups results in improved protection of carbohydrates. Lindeberg and Walding [2] have reported that the presence of nitrated lignin in oxygen bleaching of kraft pulp leads to a decrease in carbohydrate depolymerization and retards delignification.

$$NO + H_2O \rightleftharpoons HNO_2 + H^+$$

2. RESULTS AND DISCUSSION

2.1 Reactivity of free phenolic lignin units and non phenolic lignin units

The reactivity of free phenolic lignin units should be higher than that of non phenolic lignin units in the pretreatment with NO_2. To clarify this, experiments were carried out using vanillyl alcohol and veratryl alcohol as lignin model compounds on a linter cellulose substrate. As shown in Table 1, vanillyl alcohol was easily decomposed by the pretreatment, even when the molar ratio of NO_2 to vanillyl alcohol was 1.3. On the other hand, veratryl alcohol was relatively stable. These results indicate that the demethylation and the oxidation of lignin should occur mainly at free phenolic lignin units.

If a small amount of non phenolic lignin units could be demethylated and oxidized in the pretreatment, the reactivity of lignin in oxygen bleaching might be improved. Therefore, the results of other experiments are discussed later.

Table 1 Reactivity of vanillyl alcohol and veratryl alcohol on linter cellulose during NO_2 pretreatment.

Molar ratio of NO_2 to model compounds	1.3	3.0	13	25
Vanillyl alcohol recovered, %	0	0	0	0
Veratryl alcohol recovered, %	-	100	-	90.3

Notes: Dosage of each model compound is 150mg on 10g of linter cellulose.
Reaction temperature: 20 C, reaction time: 10min.

As shown in Table 2 and Fig. 1, in the NO_2 pretreatment of vanillyl alcohol, 4-nitroguaiacol (2-methoxy-4-nitrophenol) and 4,6-dinitroguaiacol (2-methoxy-4,6-dinitrophenol) were identified by GC-MS using the authentic compounds. The total yield of the nitrated products increased with increasing NO_2 charge. This implies that the nitration rates of vanillyl alcohol became faster with higher concentration of NO_2, and that the decomposition of vanillyl alcohol was retarded in spite of increasing NO_2 charge. In the case of veratryl alcohol, the yields of 1,2-dimethoxy-4-nitrobenzene were very small in these experiments.

These results indicate that nitro groups should be introduced into free phenolic lignin units, and that the extent of nitration of free phenolic lignin units should be larger than that of non phenolic lignin units.

Table 2 Yields of nitrated products in NO_2 pretreatment of vanillyl alcohol on linter cellulose.

Molar ratio of NO_2 to vanillyl alcohol	1.3	3.0	13	25
4-Nitroguaiacol, mol %	8.7	8.8	9.4	10.3
4,6-Dinitroguaiacol, mol %	0.5	2.8	14.6	15.8

Notes: Dosage of vanillyl alcohol is 150mg on 10g of linter cellulose.
Reaction temperature: 20 C, reaction time: 10min.

(Insert Fig. 1 -Nitration of vanillyl alcohol in NO_2 pretreatment.)

2.2 Mechanism of reaction of free phenolic lignin model compounds with NO_2

It is known that phenolic compounds are nitrated with nitric acid. Compared with the concentrations of nitric acid normally used in this reaction, those of nitric acid in the NO_2 pretreatment should be low, even if most of the NO_2 were to react with water to form HNO_3 and NO. As shown in Table 3, 4-nitroguaiacol and 4,6-dinitroguaiacol were not detected in treating vanillyl alcohol in HNO_3 aqueous solution without NO_2.

Table 3 Reactivity of vanillyl alcohol in HNO_3 aqueous solution without NO_2.

Molar ratio of HNO_3 to vanillyl alcohol	1.6	21
Vanillyl alcohol recovered, %	76	67
4-Nitroguaiacol and 4,6-dinitroguaiacol	0	0

Notes: Vanillyl alcohol (150mg) was treated in 30mL of HNO_3 aqueous solution.
Reaction temperature: 20 C, reaction time: 10min.

Furthermore, the yields of nitro compounds in the reaction of nitrous acid and lignin model compounds are known to be very low [5]. The total yield of nitro compounds in the NO_2 pretreatment of vanillyl alcohol was 9.2-26.1% (Table 2). These facts suggest that the mechanism of nitration by NO_2 should be different from those by nitric acid and nitrous acid.

On the other hand, the addition of HNO_3 to the NO_2 pretreatment has a moderate effect on delignification in oxygen bleaching [6]. Therefore, it is also important to investigate effects of HNO_3 on reactivity of vanillyl alcohol in the NO_2 treatment. As shown in Table 4, in the presence of HNO_3 (No. 1 and No.4), the yields of 4-nitroguaiacol and nitrated vanillyl alcohol which is considered to be 4-hydroxymethyl-6-nitroguaiacol (4-hydroxymethyl-2-methoxy-6-nitrophenol) were significantly higher than those in the absence of HNO_3 (No. 2 and No. 5), and no

vanillyl alcohol was recovered for No. 4 while 55% of vanillyl alcohol was recovered for No. 5. These results indicate that HNO_3 accelerates the nitration and oxidation of vanillyl alcohol by NO_2, and are in accord to the moderate effect of HNO_3 on delignification. That is to say, the residual lignin of kraft pulp should be oxidized and nitrated in the NO_2 pretreatment with HNO_3 more than without HNO_3, and therefore, these reactions should contribute to the degradation of lignin in oxygen bleaching.

Table 4 Effects of HNO_3 on reactivity of vanillyl alcohol during NO_2 treatment.

No.	Solvent	Molar ratio to vanillyl alcohol NO_2	Molar ratio to vanillyl alcohol HNO_3	Vanillyl alcohol yield recovered, mol %	4-Nitroguaiacol yield, mol%	Nitrated Vanillyl alcohol [a] yield, mol%
1	Dioxane/ water	3	6	0	11	17
2	Dioxane/ water	3	0	0	5.4	7.4
3	Dioxane/ water	0	6	81	0	0
4	Ethanol/ water	3	6	0	7.1	12
5	Ethanol/ water	3	0	55	1.8	1.8
6	Ethanol/ water	0	6	79	0	0

Legend: a): Molecular weight is 199.

Notes: Vanillyl alcohol (1mmol) was dissolved in 10mL of dioxane (No. 1-3) or ethanol (No. 4-6), and then 30mL of water or 0.2M HNO_3 was added.

Reaction temperature: 20 C, reaction time: 10min.

"Nitrous fumes" are used in organic chemistry as selective oxidizing agents; the first step is hydrogen abstraction:

$$RH + NO_2 = R\cdot + HONO$$ [7)]

Furthermore, it has been reported that reaction of *o*- and *p*-cresol and xylenols, and 2-naphthol with nitrogen dioxide gives nitrocyclohexadienones and nitrophenols [8)], and that the mechanism for formation of the dienones involves abstraction of the phenolic hydrogen by the nitrogen dioxide followed by combination of the resulting phenoxy radical at ortho or para position with a second molecule of nitrogen dioxide [9)]. Therefore, the nitration of vanillyl alcohol by NO_2 is considered to be initiated at the formation of a phenoxy radical. The possible mechanism is proposed in Fig. 2.

It is well-known that NO_2 easily reacts with water to form HNO_3 and NO according to the following equation:

$$3NO_2 + H_2O = NO_2 + HNO_2 + HNO_3 = NO + 2HNO_3$$

The velocity of NO_2 consumption seems to be retarded in the presence of HNO_3, and therefore, the reaction of NO_2 with vanillyl alcohol could be accelerated.

(Insert Fig. 2 - Possible mechanism of nitration of vanillyl alcohol by NO_2.)

Under these conditions, the yields of 4,6-dinitroguaiacol were trace while nitrated vanillyl alcohol (4-hydroxymethyl-6-nitroguaiacol) was detected. It seems to be important to clarify the various reactivity of vanillyl alcohol on a linter cellulose substrate and in some solvents.

As shown in Table 5, $NaNO_3$ has no significant effect on the nitration of vanillyl alcohol in the NO_2 treatment. Furthermore, acetovanillone was more stable in the NO_2 treatment than vanillyl alcohol (No. 2 in Table 4). These results indicate that the side chain structures of free phenolic lignin units should influence the oxidation and nitration of lignin nuclei.

Engstrom and Samuelson [10] have reported on the role of HNO_3 for the NO_2 pretreatment of kraft pulp at comparatively higher temperature that HNO_3 reacts with lignin and then regenerates NO_2. Under these conditions, HNO_3 has an effect on delignification in oxygen bleaching, but it also causes the depolymerization of carbohydrates [11]. On the other hand, HNO_3 at our mild temperature has no significant effects on viscosity after oxygen bleaching [6]. Therefore, the mechanism at mild temperature was discussed in this study.

Table 5 NO_2 treatment of free phenolic lignin model compounds.

Lignin model compound	Condition (molar ratio to model)	Recovered yield, mol%	4-Nitroguaiacol yield, mol%	Nitrated vanillyl alcohol [a] yield, mol%
Vanillyl alcohol	NO_2: (3) $NaNO_3$: (6)	0	5.8	8.6
Acetovanillone	NO_2 : (3)	93	0.8	---

Legend: a): Molecular weight is 199.

Notes: Each model compound (1mmol) was dissolved in 10mL of dioxane, and then 30mL of water or 0.2M $NaNO_3$ was added.

Reaction temperature: 20 C, reaction time: 10min.

2.3 Oxidation and nitration of non phenolic lignin model compounds by NO_2

As mentioned before, veratryl alcohol was relatively stable in the NO_2 pretreatment. However, it is important to clarify more about reactions of non phenolic lignin model compounds during NO_2 treatment because of an important effect of change of non phenolic lignin units on oxygen bleaching. In this section, veratryl alcohol and 1-(3,4-dimethoxyphenyl)-2-(2-methoxy-4-

methylphenoxy)propan-1-ol were treated under conditions with a higher charge of NO_2 and HNO_3 than that in section 2.2.

As shown in Table 6 and Fig. 3, a major reaction of veratryl alcohol during the NO_2 treatment was the oxidation of a benzyl alcohol group to an α-carbonyl group. On the other hand, the yields of 1,2-dimethoxy-4-nitrobenzene were small, that is to say, the nitration of veratryl alcohol was a minor reaction.

A small decrease of the total yields do not deny that demethylation of veratryl alcohol might occur. However, the demethylation seems to be very small because of no formation of nitrated guaiacol, although determination of methanol was not done here.

Table 6 Oxidation and nitration of veratryl alcohol by NO_2.

Condition	Recovered yield, mol%	Veratraldehyde yield, mol%	1,2-Dimethoxy-4-nitrobenzene yield, mol%
NO_2 : 21mmol	81	11	0.4
NO_2 : 21mmol, and HNO_3 : 12mmol	79	13	1.1

Notes: Veratryl alcohol (1mmol) was dissolved in 10mL of dioxane, and then 30mL of water or 0.4M HNO_3 was added. Reaction temperature: 20 C, reaction time: 10min.

Studies on the reactions of hydroxymethyl radical and methoxy radical with O_2, NO, NO_2 has been reported [12]. However, further studies are needed to clarify the mechanism of oxidation and nitration of non phenolic lignin model compounds with NO_2.

It is well-known that aromatic compounds are nitrated with nitric acid and sulfuric acid, and this reaction is explained by an electrophilic aromatic substitution

by a nitronium ion. Furthermore, Perrin [13] has proposed the electron-transfer mechanism for nitration of aromatic compounds by a nitronium ion. It is not clear that the nitration of veratryl alcohol in our experiments can be explain by these mechanism of nitration by a nitronium ion, or not. It might be explained by another possible mechanism which is an electron-transfer mechanism by NO_2 shown in Fig. 3.

(Insert Fig. 3 -Oxidation and nitration of veratryl alcohol by NO_2.)

A major reaction of 1-(3,4-dimethoxyphenyl)-2-(2-methoxy-4-methylphenoxy)propan-1-ol was also the oxidation of a benzyl alcohol group to an α-carbonyl group, and a small amount of veratraldehyde was formed (Table 7 and Fig. 4). In this case, the yields of 1,2-dimethoxy-4-nitrobenzene were trace.

Table 7 NO_2 treatment of 1-(3,4-dimethoxyphenyl)-2-(2-methoxy-4-methylphenoxy)propan-1-ol.

Condition (molar ratio to model)	Recovered yield, mol %	α-carbonyl cpd.[a] yield, mol %	Veratraldehyde yield, mol %	1,2-Dimethoxy 4-nitrobenzene yield, mol %
NO_2: (21)	67	25	4.7	trace
NO_2 : (21) HNO_3 : (12)	63	25	3.5	trace

Legend: a) 1-(3,4-Dimethoxyphenyl)-2-(2-methoxy-4-methylphenoxy)propan-1-one

Notes: A starting compound (0.5mmol) was dissolved in 5mL of dioxane in a 500mL round flask, and then 15mL of water or 0.4M HNO_3 was added to it.
NO_2 treatment was carried out in the 500mL round flask.
Reaction temperature: 20 C, reaction time: 10min.

It has been reported that β-methine protons of β-ether type lignin model compounds are active toward O_2-alkali when they are adjacent to an α-carbonyl group, and that such compounds degrade via intermediate hydroperoxide to phenols and carboxylic acids [14]. Therefore, the oxidation to an α-carbonyl compound by NO_2 is important. The formation of veratraldehyde might be also important, because it occurred as a results of cleavage of a C_α-C_β bond. However, it is not clear that a C_γ hydroxyl group might affect the cleavage, or not.

(Insert Fig. 4 - Reaction of 1-(3,4-dimethoxyphenyl)-2-(2-methoxy-4-methylphenoxy)propane-1-ol with NO_2.)

Some non phenolic lignin model compounds are known to be nitrated with nitric acid or nitrous acid [15]. However, the results in Table 6 and Table 7 indicate that nitration of non phenolic lignin units should be trace in the NO_2 pretreatment. Therefore, the enhancement of oxygen delignification by NO_2 can not be explained by Lindeberg mechanism [2].

2.4 Degradation of lignin macromolecule

The results mentioned in Table 2 and Table 4 also suggest that side chains of free phenolic lignin units should be substituted by nitro groups, and that the 5-position of condensed free phenolic lignin units might be substituted (Fig. 5a, 5b). These reactions as well as the oxidation by NO_2 should contribute to degradation of the lignin macromolecule.

(Insert Fig. 5a, 5b - A possible reaction of condensed free phenolic lignin units with NO_2.)

In the absence of molecular size data, it was considered possible that the increased hydrophilicity of lignin by demethylation and oxidation might lead to dissolution of larger fragments at an earlier stage of lignin depolymerization and consequently more complete lignin removal. On the other hand, the degradation of lignin by both nitration and oxidation could result in the dissolved lignin from the pretreated pulp consisting of smaller fragments. To resolve this, the molecular weight distributions by gel filtration chromatography of lignins dissolved during oxygen bleaching were determined.

As shown in Fig. 6, the dissolved lignin from kraft pulp NO_2-pretreated and oxygen-bleached had smaller fragments compared with that from pulp oxygen-bleached without the pretreatment. Furthermore, a part of the lignin in NO_2-pretreated kraft pulp was dissolved in alkali without oxygen bleaching. These results indicate that lignin in kraft pulp was degraded by the pretreatment with NO_2. The results of Kappa numbers and viscosities for the pulp samples oxygen bleached were shown in Table 8.

Table 8 Kappa number and viscosity of NO_2-pretreated and oxygen-bleached kraft pulp.

NO_2 dosage,	After alkali extraction [a)]	After oxygen bleaching	
% on pulp	Kappa number	Kappa number	Viscosity, cps
0	35.1	23.2	23.3
1.4	31.8	21.2	27.4
8.0	30.4	17.4	28.8

Legend: a): NO_2-pretreated kraft pulps were extracted with alkali without oxygen bleaching. The alkali was the same as that for oxygen bleaching.

Notes: Oxygen bleaching conditions: pulp consistency: 27%, NaOH charge: 2%, Mg^{2+} charge: 0.1%, reaction time: 20min (from 100 C to 115 C), oxygen pressure: 70psig at 45 C. Kappa number of untreated pulp: 38.7.

(Insert Fig. 6 - Molecular weight distributions by GFC of lignins dissolved during oxygen bleaching.)

2.5 NO_2 pretreatment and oxygen bleaching of methylated kraft pulp

The mechanism of NO_2 enhancement of oxygen delignification may involve only demethylation, oxidation and nitration of lignin at free phenolic lignin units. However, as mentioned before, the reactivity of lignin in oxygen bleaching would be similarly improved if non phenolic lignin units reacted in the pretreatment.

The results of section 2.3 indicate that an α-carbonyl group can be formed at non phenolic lignin units of kraft pulp. Consequently, lignin will be cleaved into two fragments at the unit which has an α-carbonyl group and a β-aryl-ether bond [11]. Therefore, it is expected that the formation of α-carbonyl groups in the NO_2 pretreatment can cause enhancement of oxygen delignification at non phenolic lignin units.

On the other hand, previous work at IPST [16] has cast doubt on the mechanism proposed by Lindeberg and Walding. That is to say, NO_2-pretreated kraft pulp has been methylated with diazomethane and then oxygen-bleached, but contrary to expectations based on the Lindeberg mechanism, its bleaching rate has been severely retarded by the methylation. This result has indicated that the effect of nitro groups in non phenolic lignin units on delignification should be small.

To confirm the above expectation and to further clarify this doubt, kraft pulp was methylated with diazomethane first, and then NO_2-pretreated and oxygen-bleached in this study.

As shown in Table 9, the amounts of nitrogen introduced into methylated kraft pulp by the NO_2 pretreatment were very small, although nitrogen was also introduced by diazomethane and these values are close to the limit of detection.

Table 9 Nitrogen contents of methylated kraft pulp pretreated with NO_2.

NO_2 dosage, % on pulp	Methylated kraft pulp, % in pulp	Un-methylated kraft pulp % in pulp
0	0.16	NA a)
1.4	0.15	0.12
8.0	0.15	0.18

Legend: a): Not analyzed.

The nitrogen content for 0.18% in Table 9 is calculated approximately 0.5mol/200g lignin. According to the results of un-methylated kraft lignin by Andersson and Samuelson [3], the nitrogen contents has been 0.29-1.55% (0.04-0.22mol/200 lignin). These results indicate that nitrogen should be introduced mainly into free phenolic lignin units, and that the this amount should be less than 0.5mol/200g lignin.

When free phenolic lignin units of kraft pulp are methylated, oxygen bleaching is significantly retarded. Therefore, the effect of reactions at non phenolic lignin units on oxygen bleaching are expected to be observed clearly in experiments using methylated kraft pulp. As shown in Table 10, oxygen delignification of methylated kraft pulp was slightly enhanced by the NO_2 pretreatment.

These decrease of lignin contents are small in this experiments. However, these results indicate that the enhancement of oxygen bleaching by the NO_2 pretreatment should be partly explained by the reaction of non phenolic lignin units which have an α-carbonyl group as expected before.

Table 10 NO_2 pretreatment and O_2 bleaching of methylated kraft pulp.

NO_2 dosage, % on pulp	Before oxygen bleaching		After oxygen bleaching	
	Lignin, %	Viscosity, cps	Lignin, %	Viscosity, cps
0	5.0	32.4	4.8	26.2
1.4	5.0	31.9	4.6	25.1
8.0	5.0	31.1	4.5	25.1

Note: Oxygen bleaching conditions: pulp consistency: 27%, NaOH charge: 2%, Mg^{+2} charge: 0.1%, reaction time: 30min (from 100 C to 112 C), oxygen pressure: 70psig at 45 C.

2.6 Carbohydrate protection effect

An attempt has been made at IPST to obtain evidence for a carbohydrate protecting effect of NO_2-modified lignin [6]. This has been tested by adding NO_2-modified kraft lignin to simulated oxygen bleaches of cotton linters, but no protective effect of NO_2-modified lignin has been seen.

As shown in Table 11, a small amount of 4-nitroguaiacol was detected in the NO_2 pretreatment of kraft pulp. These are similar to Andersson and Samuelson's results [17]. It might be a protector against carbohydrate degradation. One hypothesis here concerning the mechanism by which carbohydrate depolymerization is retarded is that a nitrophenol structure scavenges free radicals formed by the reaction of oxygen with lignin. To prove this hypothesis 4-nitroguaiacol was added to oxygen bleaching of kraft pulp.

Contrary to the expectation, 4-nitroguaiacol had no effect on a carbohydrate protection during oxygen bleaching (Table 12).

Table 11 Formation of 4-nitroguaiacol in NO_2 pretreatment of kraft pulp.

NO_2 dosage, % on pulp	1.4	8.0
4-nitroguaiacol formed, ppm on pulp weight	180	100

Note: Pretreated pulp was washed with water, and 4-nitroguaiacol in the water was determined.

Table 12 Effect of 4-nitroguaiacol added to oxygen bleaching of kraft pulp on Kappa number and viscosity.

Dosage of 4-nitroguaiacol, % on pulp	Kappa number	Viscosity, cps
0	25.2	23.7
0.05	24.6	23.7
0.15	25.4	24.2
0.30	24.6	23.8

Note: Oxygen bleaching conditions: pulp consistency: 27%, NaOH charge: 2%, Mg^{+2} charge: 0.1%, reaction time: 20min (from 100 C to 115 C), oxygen pressure: 70psig at 45 C.

3. CONCLUSION

When vanillyl alcohol and veratryl alcohol are treated on a linter cellulose substrate under the NO_2 pretreatment conditions, vanillyl alcohol easily decomposes while veratryl alcohol is relatively stable. From vanillyl alcohol, 4-nitroguaiacol and 4,6-dinitroguaiacol (2-methoxy-4,6-dinitrophenol) are formed.

Vanillyl alcohol is not nitrated in HNO_3 aqueous solution without NO_2. The addition of HNO_3 to the NO_2 treatment accelerates the oxidation and nitration of vanillyl alcohol. The nitration of vanillyl alcohol by NO_2 is considered to be initiated at the formation of a phenoxy radical.

In the NO_2 treatment, a major reaction of veratryl alcohol and 1-(3,4-dimethoxyphenyl)-2-(2-methoxy-4-methylphenoxy)propan-1-ol are the oxidation of a benzyl alcohol group to an α-carbonyl group, and the nitration is a minor reaction.

The dissolved lignin from kraft pulp NO_2-pretreated and oxygen-bleached has smaller fragments compared with that from pulp oxygen-bleached without the pretreatment.

Oxygen delignification of methylated kraft pulp is slightly enhanced by the NO_2 pretreatment.

During the NO_2 pretreatment, the oxidation and nitration of lignin should occur mainly at free phenolic lignin units. Free phenolic lignin units of kraft pulp should be oxidized and nitrated in the NO_2 pretreatment with HNO_3 more than without HNO_3. These reaction should contribute to degradation of lignin macromolecule. The mechanism of NO_2 enhancement of oxygen delignification should involve demethylation, oxidation and nitration of lignin at free phenolic lignin units, and the formation of an α-carbonyl group by NO_2 at non phenolic β-ether type lignin units should partly cause the enhancement of oxygen delignification.

4. EXPERIMENTAL

4.1 Material

Vanillyl alcohol (4-hydroxy-3-methoxybenzyl alcohol), acetovanillone, 4-nitroguaiacol, syringaldehyde, veratryl alcohol (3,4-dimethoxybenzyl alcohol), 3',4'-dimethoxyacetophenone, and 1,2-dimethoxy-4-nitrobenzene were supplied by Aldrich Chemical Company, Inc (Aldrich). Vanillyl alcohol was recrystallized from chloroform/ hexane. 4,6-Dinitroguaiacol was synthesized using 4-nitroguaiacol and NO_2 and identified by a H-NMR spectrum shown in Fig. A1. Veratraldehyde was synthesized using vanilline (Aldrich) and diazomethane. 1-(3,4-Dimethoxyphenyl)-2-(2-methoxy-4-methylphenoxy)propan-1-ol was given by Dr. P. Balousek.

Kraft pulp with Kappa number 38.7 and viscosity 34.8 was prepared from Lobroly pine under the following conditions: effective alkali: 16%, sulfidity: 25%, liquor to wood ratio: 4, H-factor 1600.

4.2 NO_2 pretreatment of lignin model compounds on a linter cellulose substrate

Vanillyl alcohol or veratryl alcohol (150mg) was dissolved in 150mL of ether and added to 10.0g of linter cellulose in a 1L round flask, and the flask was shaken thoroughly. After the ether was removed in an evaporator, water was added to adjust the consistency of the linter cellulose to 25%. NO_2 pretreatment was carried out according to a procedure [18] which may be generally described as follows: The flask was placed on a modified Calab type rotary evaporator and a vacuum of approximately 28 in. of Hg was applied. Then cold N_2O_4 (NO_2) was placed in a chilled special pipette and the pipette was connected to the modified rotary evaporator. By opening the two inside valves, the N_2O_4 was sent, and the evaporator was rotated. Then by adding small amounts of O_2, any NO which might be present was converted to NO_2. After 10min reaction time at 20 C room the flask was taken off the evaporator, and water was poured into the flask.

The linter cellulose was washed with 200mL of water four times. The filtrate was gathered and diluted to 1000mL quantitatively, and 25mL of the filtrate was

extracted with 25mL of ether five times without acidification. The ether fraction was washed with 5mL of water and treated with anhydrous sodium sulfate. Syringaldehyde as an internal standard was added to the ether fraction, which was concentrated to 4mL.

4.3 NO_2 treatment of lignin model compounds in solutions

4.3.1 HNO_3 aqueous solution

HNO_3 aqueous solution (30mL) was added to vanillyl alcohol (150mg) in a 1L round flask, and the flask was shaken for 10min at 20 C. After the reaction, 200mL of water was added to it. The solution was shaken for 5min and then diluted to 1000mL quantitatively. The subsequent procedures were the same as in section 4.2, and gas chromatography of this sample was carried out according to section 4.4.1.

4.3.2 Free phenolic lignin model compounds in organic solvent/ water solutions

Vanillyl alcohol or acetovanillone (1mmol) was dissolved in 10mL of dioxane or ethanol in a 1L round flask, and then 30mL of water, 0.2M HNO_3 or 0.2M $NaNO_3$ was added to it. NO_2 treatment was carried out in the modified Calab type rotary evaporator. After 10min reaction time at 20 C the flask was taken off the evaporator, and the solution was extracted with 50mL of ether four times immediately. The ether fraction was washed with 5mL of water and treated with anhydrous sodium sulfate. Syringaldehyde as an internal standard was added to the ether fraction.

4.3.3 Non phenolic lignin model compounds in dioxane/ water solution

Veratryl alcohol (1mmol) was dissolved in 10mL of dioxane in a 1L round flask, and then 30mL of water or 0.4M HNO_3 was added to it. NO_2 treatment was carried out in the modified Calab type rotary evaporator, and after 10min reaction time at 20 C the solution was extracted with ether in the same way as in section 4.3.2. 3',4'-Dimethoxyacetophenone as an internal standard was added to the ether fraction.

1-(3,4-Dimethoxyphenyl)-2-(2-methoxy-4-methylphenoxy)propan-1-ol (0.5mmol) was dissolved in 5mL of dioxane in a 500mL round flask, and then 15mL

of water or 0.4M HNO_3 was added to it. The subsequent procedures were the same as those for veratryl alcohol.

4.4 Gas chromatography and mass spectrometry

4.4.1 Reaction products from NO_2 pretreatment of lignin model compounds on a linter cellulose substrate

The concentrated sample was subjected to gas chromatography (GC) directly. Conditions of GC are as follows: Column: HP17 Crosslinked 50% Ph Me Silicone, 10m X 0.53mm X 0.002mm film thickness, det. (FID) temp.: 280 C, inj. temp.: 250 C, column temp.: 150 C, 5 C/min, 280 C, 20min. The relative retention times of compounds used are shown in Table A1.

Conditions of gas chromatography-mass spectrometry (GC-MS) are as follows: Hewlett Packard HP5985B GC/MS System, 70eV, column: OV17, 2m X 2mm, column temp.: 100 C, 10 C/min, 300 C. Mass spectra of 4-nitroguaiacol (2-methoxy-4-nitrophenol) and 4,6-dinitroguaiacol (2-methoxy-4,6-dinitrophenol) are shown in Fig. A2 and Fig. A3, respectively. They were compared with the authentic spectra.

4.4.2 Reaction products from NO_2 treatment of free phenolic lignin model compounds and veratryl alcohol in organic solvent/ water solutions

The ether fraction was subjected to GC directly. Conditions of GC are the same as in section 4.4.1. A response factor of the nitrated vanillyl alcohol was assumed to be the same as that of the starting material.

A concentrated sample was subjected to GC-MS. Conditions of GC-MS are as follows: Mass spectrometer: Model VG 70SE, column: DB-5 (30m), column temp.: 160 C, 4 C/min, 200 C (for vanillyl alcohol), and 150 C, 10min, 5 C/min, 200 C (for veratryl alcohol). The results for vanillyl alcohol and veratryl alcohol are shown in Fig. A4(a, b, c,) and Fig. A5(a, b, c, d), respectively. Mass spectra of veratraldehyde and 1,2-dimethoxy-4-nitrobenzene were compared with the authentic spectra.

4.4.3 Reaction products from NO_2 treatment of 1-(3,4-Dimethoxyphenyl)-2-(2-methoxy-4-methylphenoxy)propan-1-ol in dioxane/ water solution

The ether fraction was subjected to GC directly. Conditions of GC are the same as in section 4.4.1 except column temp.: 160 C, 10 C/min, 230 C, 20min. The relative retention times of compounds used are shown in Table A1. A response factor of 1-(3,4-Dimethoxyphenyl)-2-(2-methoxy-4-methylphenoxy)propan-1-one was assumed to be the same as that of the starting material.

A concentrated sample was subjected to GC-MS. Conditions of GC-MS are the same as in section 4.4.2 except column temp.: 170 C, 3 C/min, 240 C. The results are shown in Fig. A6(a, b, c, d).

4.5 NO_2 pretreatment of kraft pulp

Kraft pulp was washed with distilled water several times and dewatered to pulp consistency 40%. The pulp (10g) of was fluffed, and then pulp consistency was adjusted to 25%. NO_2 pretreatment was carried out according to a procedure described in section 4.2. The kraft pulp was washed with 200mL of water four times. The filtrate was gathered and diluted to 1000mL quantitatively. The kraft pulp was washed again and air-dried. The filtrate was extracted with ether, and 4-nitroguaiacol in it was determined by GC.

4.6 Oxygen bleaching of kraft pulp and preparation of dissolved lignin

4.6.1 Oxygen bleaching

Pretreated kraft pulp (3g) was fluffed and an aqueous solution including NaOH, Mg^{2+} was added to it, and then pulp consistency was adjusted to 27%. The fluffed pulp was put into a 60mL polypropylene jar (Nalgene Polypropylene Wide-Mouth Jar) which had 40 small holes (1.0mm). Seven samples in the jars without covers were set in a 2.2L stainless steel autoclave with a Teflon case, and oxygen-bleached. Temperature in the autoclave was monitored. Reaction time was counted from the time when the temperature was at 100 C. Oxygen bleaching was carried out under the following conditions: NaOH charge: 2%, Mg^{2+} charge: 0.1%, oil bath temp. set: 120 C, reaction time: 20min (from 100 C to 115 C), oxygen pressure: 70psig at 45 C.

4-Nitroguaiacol was added to the aqueous solution in the experiments to clarify its effects on carbohydrate protection.

4.6.2 Preparation of dissolved lignin

After oxygen bleaching, pulp was put into a 10mL plastic syringe and pushed to sample about 1mL of black liquor without dilution, and then the pulp was washed with water and air-dried. NO_2-pretreated pulp was also extracted with alkali for oxygen bleaching in the same way before oxygen bleaching.

Kappa number and viscosity of pulp samples were determined by Tappi methods (T236cm-85 and T230om-82, respectively).

4.7 Gel filtration chromatography

The black liquor sample was diluted with 1.0M NaOH and soaked for 4days in order to remove an effect of association of lignin molecules, and then 0.15mL of the sample was subjected to gel filtration chromatography (GFC) [19]. Conditions of GFC are as follows: Column: Sephadex G-50 medium, 50cm X 2.5cm, effluent: 0.5M NaOH, detection: absorbance at 280nm. Chromatograms were calibrated by using the delignification degrees of corresponding bleached pulps.

4.8 NO_2 pretreatment and oxygen bleaching of methylated kraft pulp

Kraft pulp was washed with methanol and air-dried, and then was kept in a desiccator over diphosphorus pentaoxide for a week. The dried kraft pulp (6g) was suspended in 300ml of dried methanol in a 1L flask, and 0.07mol of diazomethane in 250mL of ether was added to it. Diazomethane was added to it again after a day. The methylation was repeated seven times. After the final methylation, it was confirmed that diazomethane remained in the flask for 4 days. The methylated kraft pulp was separated from liquor, and then washed with water sufficiently and air-dried.

The methylated kraft pulp (10g) was fluffed, and then pulp consistency was adjusted to 25%. NO_2 pretreatment was carried out according to a procedure described in section 4.2. The pulp was washed with water and air-dried.

Pretreated pulp (3g) was fluffed, and a aqueous solution including NaOH, Mg^{2+} was added to it. Oxygen bleaching was carried out under the same conditions as in section 4.6.1 except reaction time: 30min (from 100 C to 112 C).

After oxygen bleaching, pulp was washed with water and air-dried. Acid-insoluble lignin content in pulp was determined by a Tappi method (T222om-83). Nitrogen content of pulp was determined by a conventional method at Atlantic Microlab. Inc.

REFERENCES

1) Abrahamsson, K., Lowendahl, L. and Samuelson, O., *Svensk Papperstidn.*, **84**: R152-R158(1981)

2) Lindeberg, O. and Walding, J., *Tappi J.*, **70**(10): 119-123(1987)

3) Andersson, L. and Samuelson, O., *Svensk Papperstidn.*, **87**(9): R59-R60(1984)

4) Byrd, M. and Gratzl, J. S., Tappi 1986 Research and Development Conference, 1986, p. 21-25

5) Bolker, H. I., Kung, F. L. and Kee, M. L., *Tappi*, **50**(4): 199-202(1967)

6) IPST Status report on project 3474, September 6, 1988

7) Cotton, F. A. and Wilkinson, G., Advanced Inorganic Chemistry 3rd Edition, Interscience Publishers, New York, 1972, p. 358

8) Fischer, A. and Mathivanan, N., *Tetrahedron Letters*, **29**(16): 1869-1872(1988)

9) Brunton, G., Cruse, H. W., Riches, K. M., and Whittle, A., *Tetrahedron Letters,* **20**: 1093(1979) [Fischer, A. and Mathivanan, N., *Tetrahedron Letters,* **29**(16): 1869-1872(1988)]

10) Engstrom, T. and Samuelson, O., *Svensk Papperstidn.*, **86**: R173-R177(1983)

11) Samuelson, O. and Sjoberg, L. -A., *Svensk Papperstidn.*, **85**: R69-R72(1982), **87**(6): R30-R35(1984)

12) Pagsberg, P., Munk, J., Anastasi, C., and Simpson, J., *J. Phys. Chem.*, **93**(13): 5162-5165(1989)

13) Perrin, C. L., *J. Am, Chem. Soc.*, **99**: 5516(1977) [Lowry, T. H. and Richardson, K. S., Mechanism and Theory in Organic Chemistry 3rd Edition, Harper & Row, Publishers, New York, 1987, p. 638]

14) Aoyagi, T., Hosoya, S. and Nakano, J., Chemistry of Delignification with Oxygen, Ozone, and Peroxides (Gratzl, J. S., Nakano, J. and Singh, R. P. Eds.), Uni Publishers Co., Ltd., Tokyo, 1980, p. 165-171

15) Dence, C. W., Lignins (Sarkanen, K.V. and Ludwig, C. H. Eds.), Wiley-Interscience, New York, 1971, p. 373-432

16) IPST report on project 3474, February 9, 1989

17) Andersson S.-I., Samuelson, O., *Svensk Papperstidn.*, **88**(9): R102-R104(1985)

18) IPST Pulping and Bleaching Group Procedure No. 307

19) Ohi, H. and Ishizu, A., *Mokuzai Gakkaishi,* **35**(8): 748-753(1989)

APPENDIX

Table A1 Relative retention times of lignin model compounds.

Compound	Column temperature	
	150 C, 5 C/min, 280 C	160 C, 10 C/min, 230 C, 20min
	Relative retention time	Relative retention time
o-Benzoquinone	0.32	
Vanillyl alcohol	0.55	
Acetovanillone	0.63	
4-Nitroguaiacol (2-Methoxy-4-nitrophenol)	0.73	
Syringaldehyde	1.00 (ca. 8.3min)	
4,6-Dinitroguaiacol (2-methoxy-4,6-dinitrophenol)	1.21	
Nitrated syringaldehyde a)	1.32	
Nitrated vanillyl alcohol b)	1.41	
Veratraldehyde	0.61 (0.71*)	0.81
Veratryl alcohol	0.64 (0.76*)	
3',4'-Dimethoxyacetophenone	0.76 (1.00*)	1.00 (ca. 3.8min)
1,2-Dimethoxy-4-nitrobenzene	0.88	
1-(3,4-Dimethoxyphenyl)-2-(2-methoxy-4-methylphenoxy)propan-1-ol		6.37
1-(3,4-Dimethoxyphenyl)-2-(2-methoxy-4-methylphenoxy)propan-1-one		6.63

Legend : a): Considered to be 4-nitrosyringol (2,6-dimethoxy-4-nitrophenol).
b): Considered to be 4-hydroxymethyl-6-nitroguaiacol (4-hydroxymethyl-2-methoxy-6-nitrophenol), Molecular weight: 199.
*: 150 C, 10min, 5 C/min, 280 C.

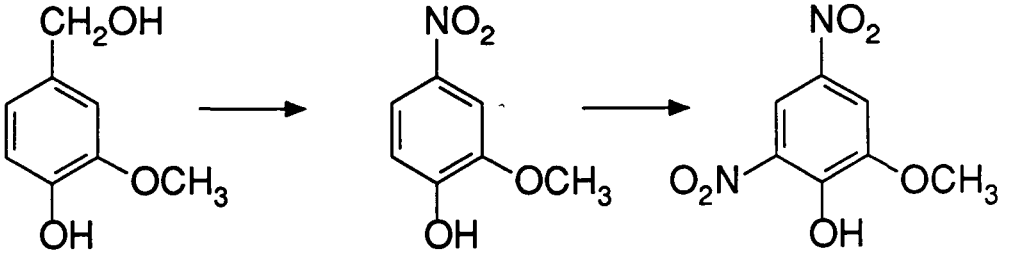

Vanillyl alcohol

4-Nitroguaiacol
(2-Methoxy-4-nitrophenol)

4,6-Dinitroguaiacol
(2-Methoxy-4,6-dinitrophenol)

Fig. 1 Nitration of vanillyl alcohol in NO_2 pretreatment.

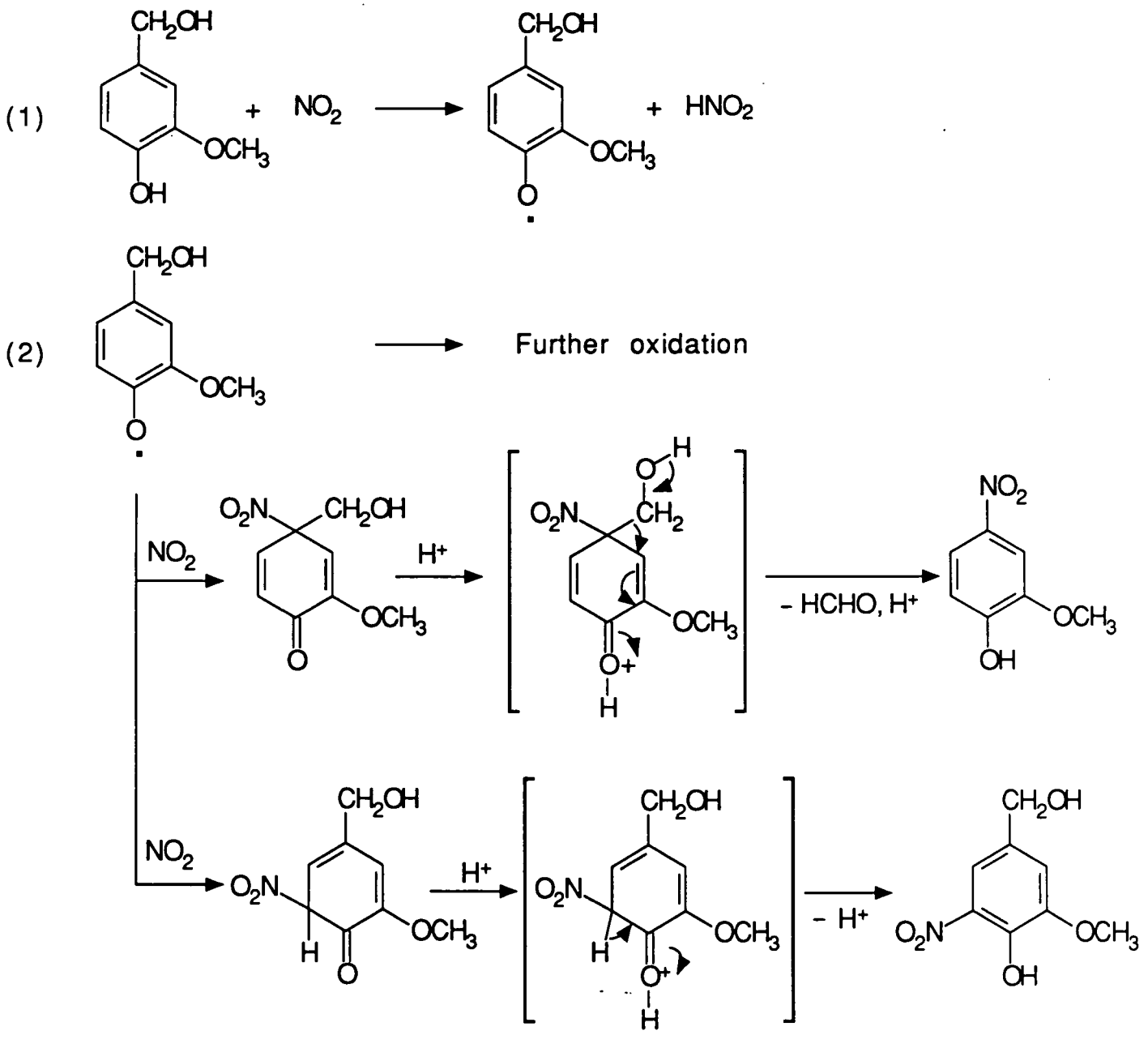

Fig. 2 Possible mechanism of nitration of vanillyl alcohol by NO_2.

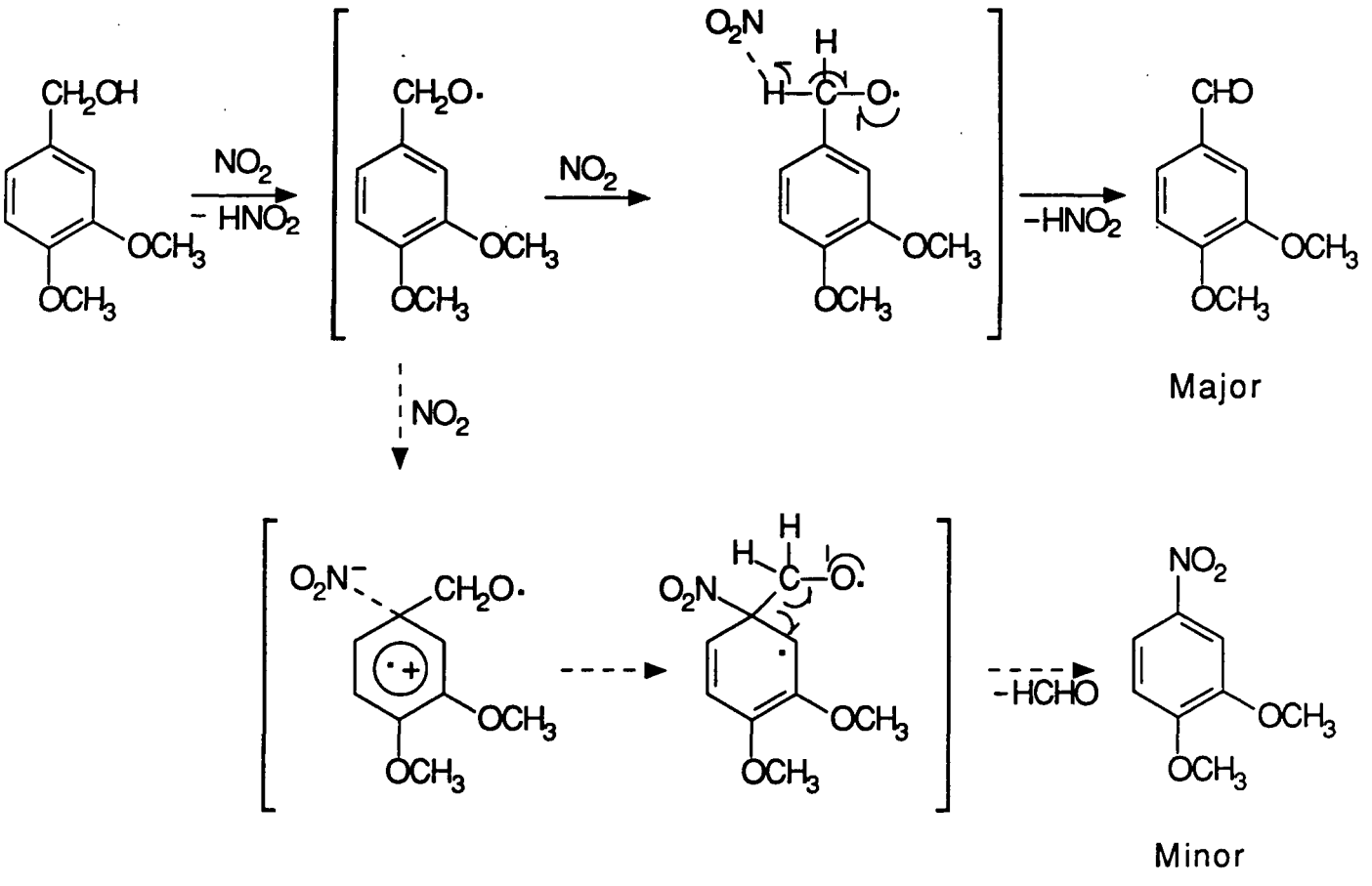

Fig.3 Oxidation and nitration of veratryl alcohol by NO_2 treatment.

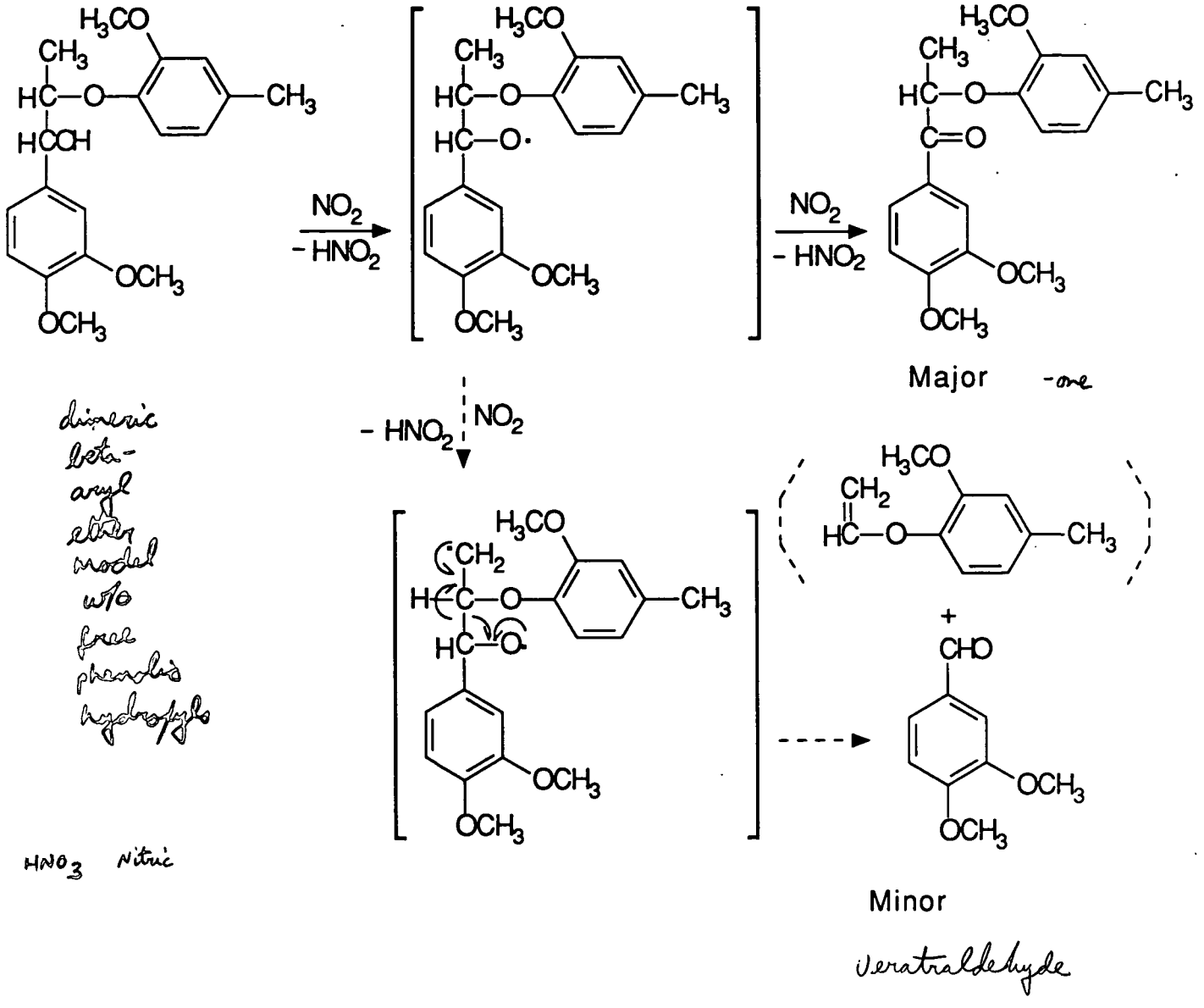

Fig. 4 Reaction of 1-(3,4-dimethoxyphenyl)-2-(2-methoxy-4-methylphenoxy)propan-1-ol with NO_2.

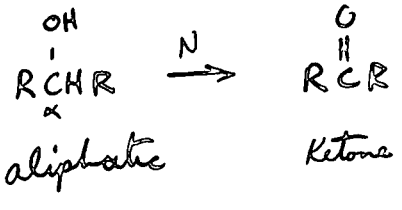

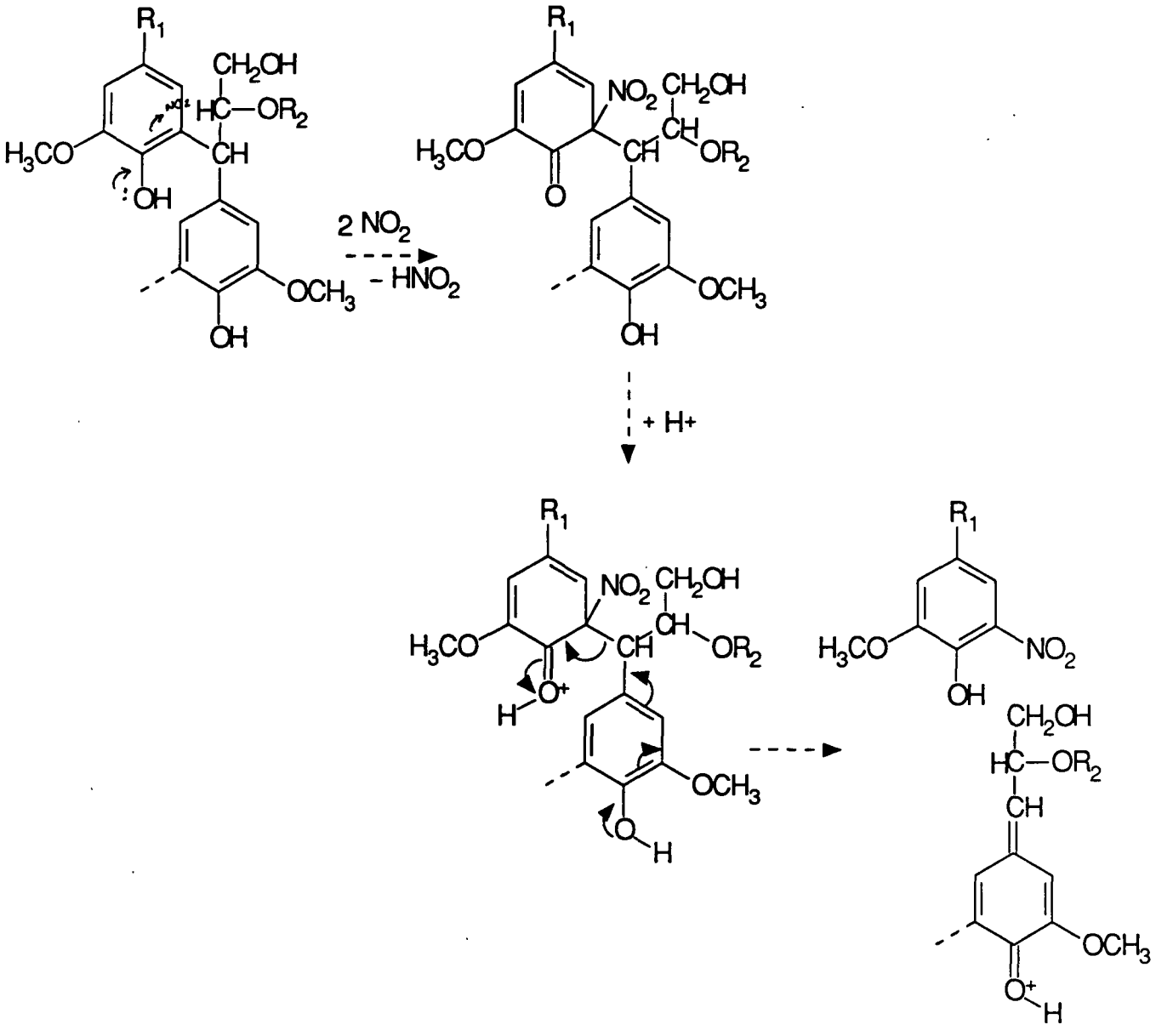

Fig. 5a A possible reaction of a condensed free phenolic lignin unit with NO_2.

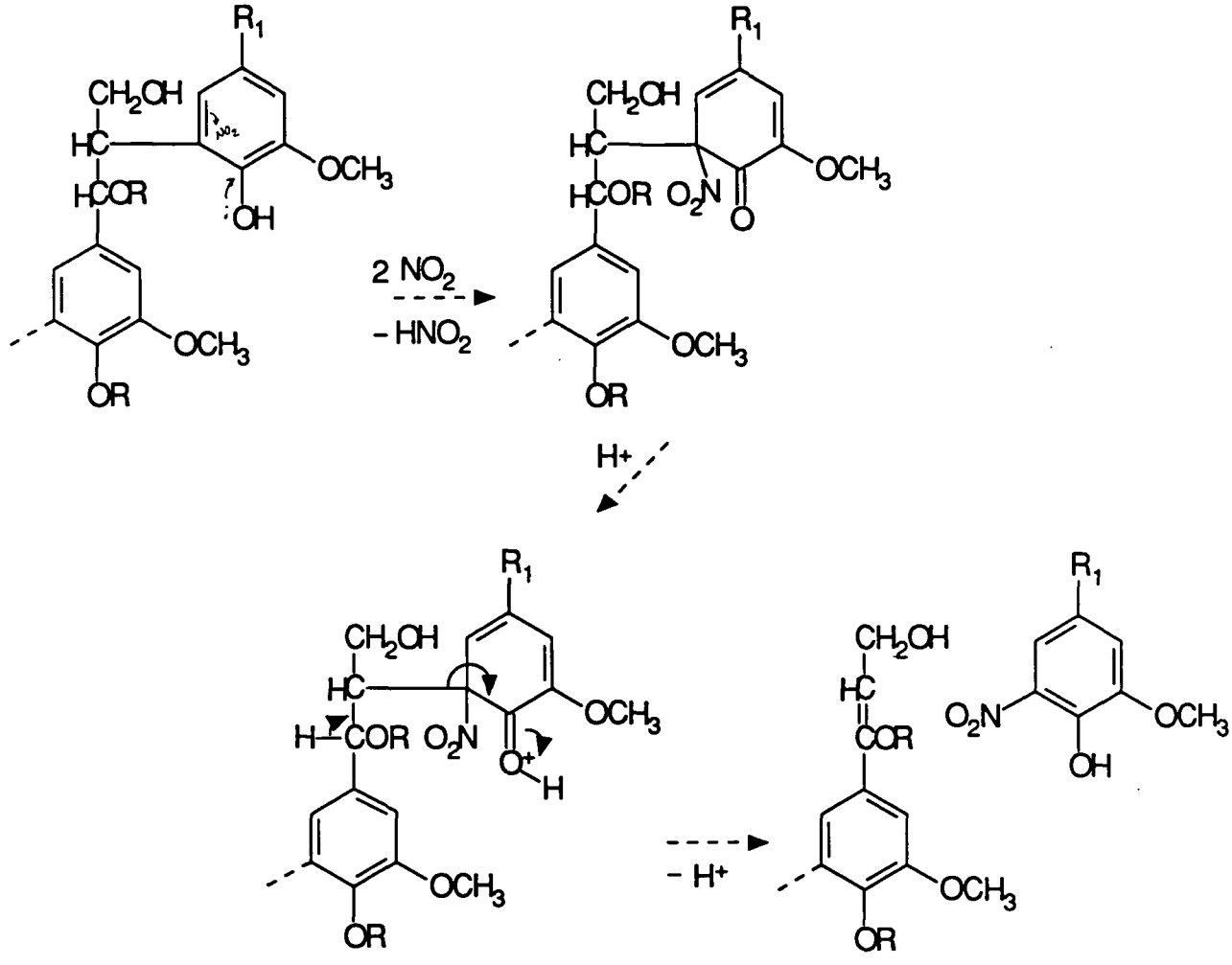

Fig. 5b A possible reaction of a condensed free phenolic lignin unit with NO_2.

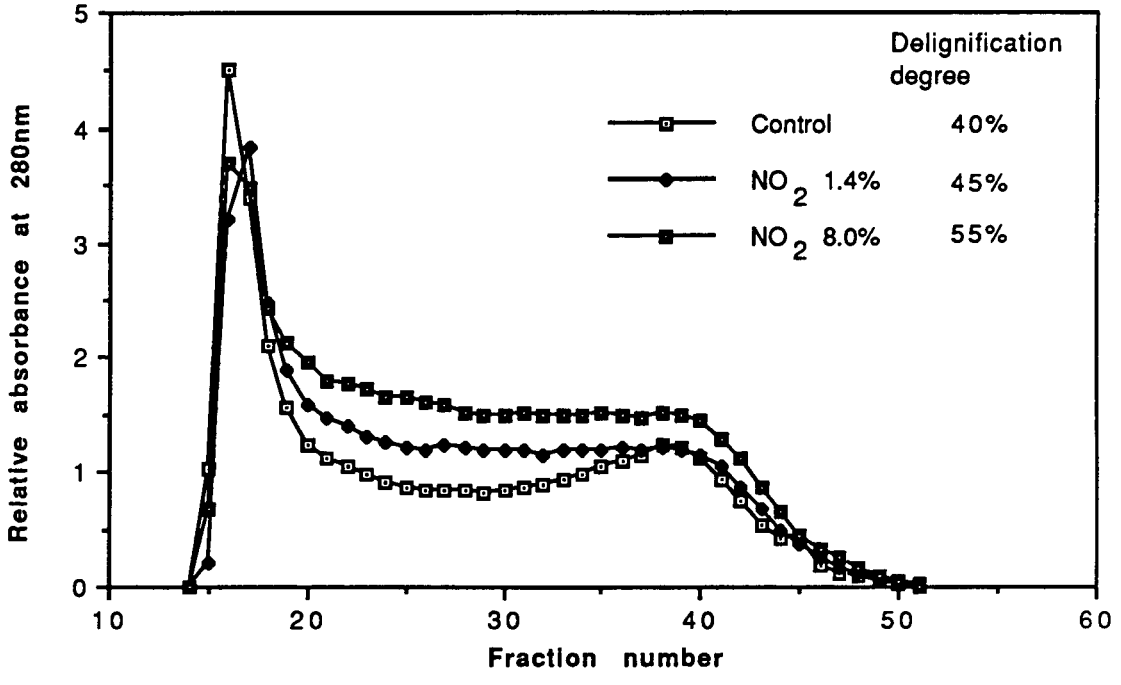

Fig. 6 Molecular weight distributions by GFC of lignins dissolved during oxygen bleaching.

PROJECT SUMMARY FORM

DATE: March 20, 1990

PROJECT NO. 3475: FUNDAMENTALS OF SELECTIVITY IN PULPING AND BLEACHING

PROJECT LEADER: D. R. Dimmel

IPC GOAL:

Improved process for bleached chemical pulps

OBJECTIVE:

Provide a fundamental understanding of the chemical and physical reactions that control both:

(1) the rate of lignin removal, hemicellulose dissolution, and cellulose degradation, and
(2) the structures of the lignin, hemicelluloses and cellulose that remain in the pulp after pulping and bleaching.

CURRENT FISCAL YEAR BUDGET: $90,000

PRIOR RESULTS:

The detailed mechanistic studies of pulping delignification chemistry conducted in this project have led to a greater understanding of the factors which control lignin fragmentation and condensation reactions. A significant portion of the research was directed towards understanding the reactions of anthrahydroquinone (AHQ) with lignin substrates. Our interest here relates to the fact that anthraquinone (AQ) pulping systems show improved selectivites. The research, including related student work has led to over 30 publications in the last 10 years, with several additional articles submitted and in preparation.

The project has also been concerned with understanding the chemistries associated with carbohydrate chain cleavage reactions that occur during alkaline pulping and bleaching. Such reactions cause a lowering of the degree of polymerization (DP) and thus a loss in paper strength properties. Changes in DP are seen by changes in pulp viscosities and molecular weight distributions. Earlier work in this project involved developing a GPC method for obtaining cellulose molecular weights.

Research activity in the past few years has concerned comparing the reactivity difference of amorphous crystalline and cellulose samples; any observed difference should reflect the importance of "physical effects" in carbohydrate chain cleavage reactions. A relatively high viscosity amorphous cellulose sample has been prepared from a cotton linters cellulose. The amorphous sample

was reduced with sodium borohydride ($NaBH_4$) to prevent "pealing" losses in monomer units when heated in alkali. The viscosity losses as a function of time of heating at 150°C in alkali ("pulping") were much greater for the stabilized amorphous cellulose sample than for a corresponding stabilized crystalline cellulose sample. The rate of DP loss was further increased slightly when either amorphous or crystalline cellulose was heated in alkali in the presence of AQ.

The reactivity trends observed for amorphous and crystalline cellulose in the "pulping" experiments were similar in an oxygen-alkali "bleaching" reaction at 100°C. The more reactive sample was the amorphous cellulose. The viscosity losses for amorphous cellulose in oxygen-alkali were inhibited by the presence of magnesium. The addition of cobalt, above a level of 0.162 mole $CoSO_4$/100 g of cellulose greatly accelerated the amorphous cellulose viscosity losses. The combination of Mg and Co was even more harmful to the sample's viscosity. Treatment of cotton linters and amorphous cellulose with SO_2 to remove metals caused no loss of viscosities at pH 2.3; however, at pH values below 2.3, large viscosity losses were observed.

A sample of cotton linters (12% consistency) was treated with 0.2% hydrogen peroxide at 50°C and pH 11 and the viscosity determined as a function of time. In comparison to an amorphous cellulose, the linters displayed a much slower loss of viscosity with time. A combination of added magnesium sulfate and sodium silicate prevented viscosity losses during peroxide reaction with the amorphous cellulose.

Cotton linters were treated with dilute acid for a day to hydrolyze and remove any amorphous cellulose component. A portion of the product was reduced with $NaBH_4$. Samples were then exposed to O_2/NaOH and low levels of cobalt at 100°C for various time periods. The acid-treated linters showed severe viscosity drops with reaction time. The corresponding $NaBH_4$ reduced, acid-treated linters showed only small viscosity losses with time. A kraft pulp showed similar small losses. A detailed oxygen-alkali/cobalt study of viscosity changes with crystalline, amorphous, and kraft celluloses was performed. The results generally confirmed the earlier findings, but left in doubt the magnitude of viscosity losses at early reaction times for the kraft and highly crystalline cellulose.

It is apparent that highly crystalline cellulose samples and kraft pulp degrade much more slowly than amorphous cellulose under pulping and bleaching conditions.

SUMMARY OF RESULTS SINCE LAST REPORT:

A Georgia Tech coop student, Mark Johnson, was added to the research team of Dimmel and VanVreede. New amorphous and crystalline cellulous samples were prepared. Crystalline cellulose and kraft pulp were again subjected to reaction with oxygen-alkali/cobalt and viscosities measured for early reaction times. The results clearly indicate that these two substrates have good stability in the conditions applied.

PLANNED ACTIVITY THROUGH FISCAL YEAR 1990:

The large backlog of results of the project's carbohydrate research has been organized in preparation for internal and external publications. Publication of the research results and performing supporting experiments for the publications will bew the focus of the fiscal year 1990 activities.

POTENTIAL FUTURE ACTIVITY:

The amorphous cellulose bleaching chemistry studies could be expanded to examine (1) additional chemicals (ozone, chlorine dioxide, etc.), (2) process variables, (3) the influence of selected metals and "dead load" salt effects, and (4) more detailed molecular weight distributions. The aim will be to develop a fundamental understanding of bleaching chemistry which may lead to better nonchlorine bleaching systems. Additional activities on delignification reactions will require additional personnel.

Project 3475 Status Report

FUNDAMENTALS OF SELECTIVITY IN PULPING AND BLEACHING

Reporting Period: September, 1989 - March, 1990

OBJECTIVE

The goal of chemical pulping is to liberate, without degradation, carbohydrate fibers from wood through delignification. Unfortunately, alkaline pulping processes are not very selective for lignin removal. For example, in kraft pulping the loss of carbohydrate material may be comparable to, or even exceed, that of the lignin.[1-2] In addition, reduction of the carbohydrate chain length, leading to decreased pulp viscosity and product strength, also occurs.[1-3] The objective of this project is to elucidate the mechanisms of carbohydrate and lignin degradation reactions which occur during pulping and bleaching. A better understanding of the chemistry involved will ultimately facilitate better control of pulping and bleaching selectivities.

GENERAL INFORMATION

This project has been concerned with two principal research areas: carbohydrate pulping and bleaching reactions, and lignin pulping reactions. The research focus in the last two years has been mainly with carbohydrate reactions; this is what will be reported here. The personnel typically associated with lignin fundamental research have been moved temporarily into a more applied lignin project (3661).

INTRODUCTION

Over the past 15 years, the research staff of Project 3475 and several M.S. and Ph.D. students at the Institute have been involved in research directed at understanding the fundamental underlying chemistry associated with carbohydrate chain cleavage reactions. Such reactions significantly affect hemicellulose yield losses and cellulose viscosity losses. Recent project research has focused on determining the extent to which the physical state of the carbohydrate - dissolved, amorphous, or crystalline - influences the degree of chain cleavage occurring during pulping.

Earlier project research demonstrated that the extensive degradation seen with amylose/anthraquinone (AQ) did not apply to cellulose/AQ systems and that the nature of glycosidic linkage (α for amylose, β for cellulose) was not the cause of the reactivity difference.[4] Rather, the high reactivity of amylose appeared to be related to its water solubility. Unlike amylose, most of the glycosidic linkages of crystalline cellulose will be inaccessible to attack by reagents, such as NaOH or AQ. Another factor in explaining the amylose/cellulose reactivity difference is the general low occurrence of significant reaction between two insoluble substrates; both cellulose and AQ will be insoluble in alkali, even at high temperatures.

One way to examine physical effects is to compare the reactivities of 1,5-anhydrocellobiitol (a soluble cellulose model) and 1,5-anhydrocellobiitol which has been attached to a polystyrene network (an insoluble cellulose model), as shown below. The insoluble cellulose model has been prepared and characterized as part of a student Ph.D. thesis[5] and project work. The reactions of the insoluble model are now being studied by M.S. student Todd Schwantes.

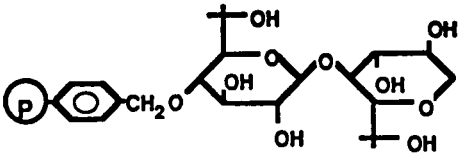

Amorphous cellulose (a random, disordered form) should be more reactive than crystalline cellulose (an ordered form) since the accessibility of reagents to the glycosidic linkages would be much greater. Experiments were devised to test this hypothesis using a crystalline cotton linters sample and an amorphous sample derived from it; both were stabilized against "peeling" reactions by sodium borohydride reduction. After performing several reactions, we learned that the "crystalline" cotton linters contains some amorphous material. Therefore, the linters were treated with dilute acid for a day to hydrolyze and remove the amorphous component. The treated product was reduced with $NaBH_4$ to give what we call "crystalline" cellulose. The preparative scheme is given in Figure 1.

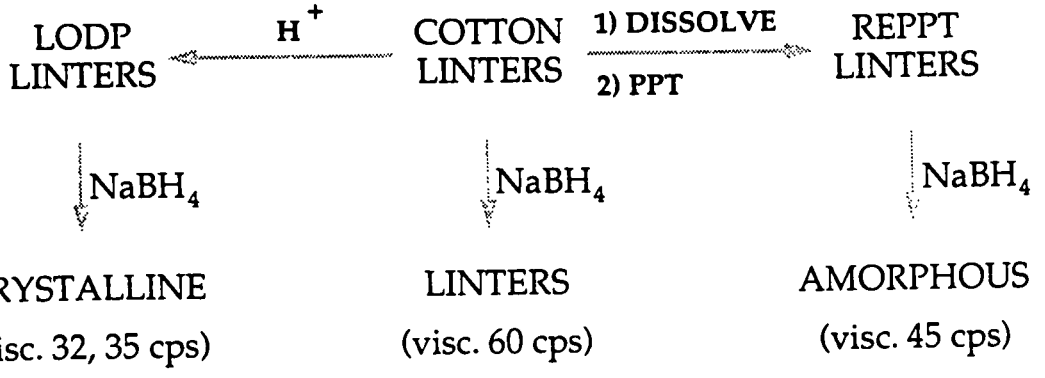

Figure 1. Cellulose sample preparations.

Two procedures are typically used to estimate the extent of carbohydrate chain cleavage reaction. One involves carbonilation of the carbohydrate hydroxyl groups and then determining molecular weight distributions by gel phase chromatography (GPC). The procedure was originally developed several years in this project. While much useful information is obtained by GPC, the method is very

time consuming. The other procedure, measuring the viscosity of a specific concentration of cellulose in a solvent, is fast but less informative with regard to molecular weight distributions. In our case, the two methods correlated well (Figure 2); consequently, the faster method was most often used.

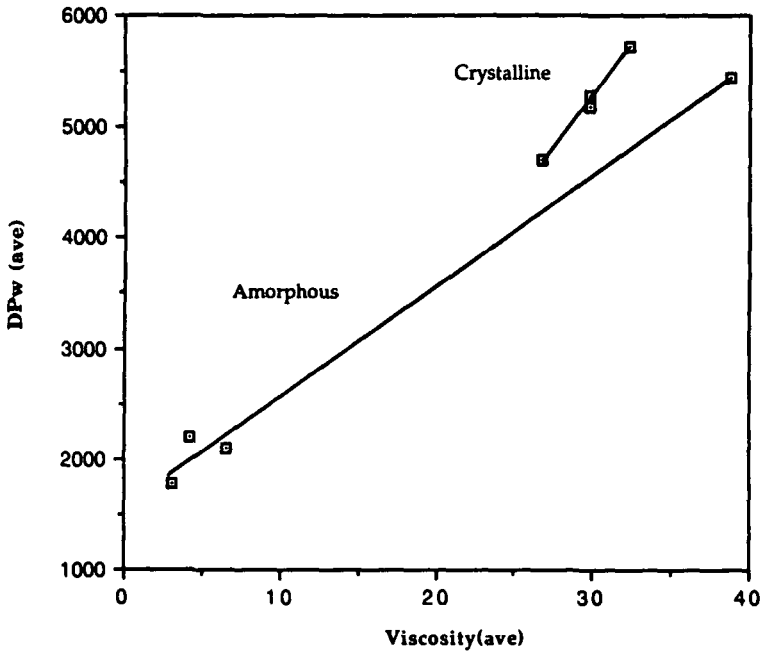

Figure 2. Correlation of DPw and Viscosity for Cellulose Samples which have been degraded in The Presence of Oxygen/Alkali/Cobalt.

CELLULOSE PULPING REACTIONS

A direct comparison of the viscosity changes associated by heating (stabilized) linters and amorphous cellulose in 1M NaOH at 152°C is presented in Figure 3. The viscosity decreases for the highly crystalline cellulose are less than the linters (Figure 4). As can be seen, the amorphous sample is considerably more reactive than the linters or crystalline cellulose. Presumably, the viscosity drops because of alkali-promoted chain cleavage reactions; such reactions are more prominent with the amorphous material because of the accessibility and increased flexibility around the glycosidic bonds, which allows cleavage mechanisms, such as $S_N1cB(2)$, to occur more readily.

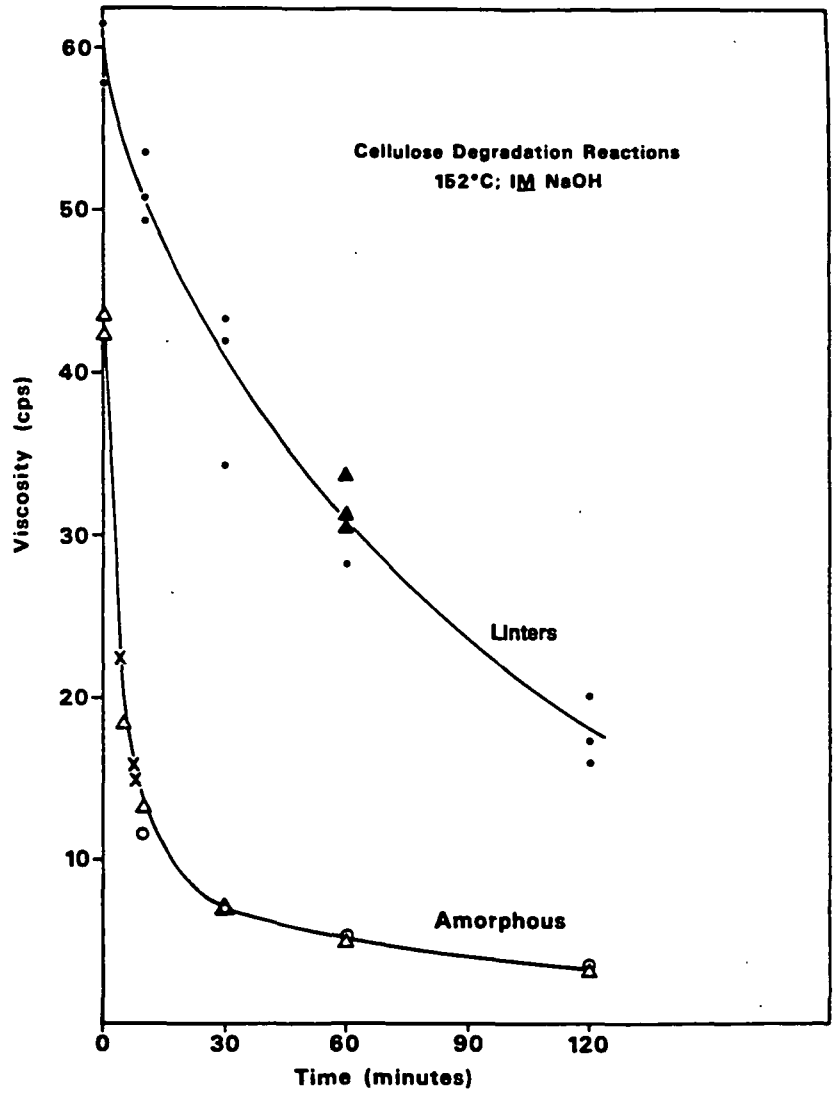

Figure 3. Viscosity changes associated with heating cotton linters and amorphous cellulose at 152°C in 1M NaOH for different time periods. The different symbols for each curve represent determinations done on different days, i.e., duplicate experiments.

Amorphous cellulose would appear to be an ideal substrate for studying the extent of carbohydrate chain cleavage reactions as a function of changes in conditions and reagents. The amorphous material will exaggerate the chemistry over what might be displayed by crystalline cellulose or a wood pulp. [The chemistry displayed by a wood pulp might simply be a result of reactions occurring with the amorphous regions in the pulp.] Thus, a survey of some pulping and bleaching chemistry was initiated with the amorphous cellulose.

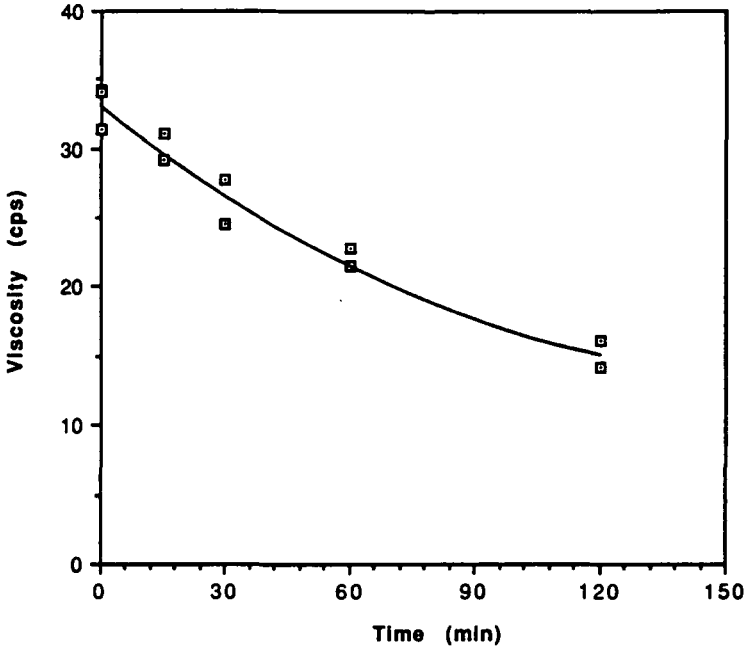

Figure 4. Viscosity changes associated with heating crystalline cellulose at 150°C in 1M NaOH for different time periods.

As mentioned in the Introduction Section, we have been concerned over the possibility that AQ causes carbohydrate chain cleavage reactions during pulping, leading to pulps with somewhat lower tear strength. Therefore, four cellulose samples (2 different linters and 2 different amorphous) were heated in alkali with and without AQ; the two sets were done on different days. In 3 out of 4 samples, the AQ appeared to cause a small viscosity drop (Table 1).

Table 1. Cellulose viscosities (cps) after heating in 1M NaOH.

Linters,[a] 148°C, 60 minutes		Amorphous,[a] 135°C, 10 minutes	
No AQ	AQ[b]	No AQ	AQ[b]
27.5 (27.1-28.0)[c]	29.3 (28.2-30.5)[c]	16.2 (14.0-18.0)[c]	14.6 (13.9-15.5)[c]
35.8 (32.5-38.4)[d]	32.4 (31.3-33.4)[d]	24.9 (21.7-26.8)[d]	22.1 (18.0-24.1)[d]

[a]The two samples had different starting viscosities.
[b]One equiv./glucose equivalent.
[c]Triplicate average (range).
[d]Six sample average (range).

Selected soda and soda/AQ samples, which produced the data in Table 1, were subjected to GPC analysis. There were no major differences in molecular weight distributions observed between the samples; however, the method was less reproducible at the time of measurements than usual and, therefore, firm conclusions are somewhat risky.

Based on the limited data collected, it appears that AQ causes no significant chain cleavage reactions in insoluble carbohydrate substrates. The decreased tear strengths associated with AQ pulping may be better explained by the greater yield, leading to retention of hemicelluloses in the pulp, than by increased chain cleavage reactions.

AMORPHOUS CELLULOSE BLEACHING REACTIONS

Several experiments involving amorphous cellulose and oxygen-alkali-metal and peroxide-metal have been performed. The viscosities observed when heating amorphous cellulose at 100°C for different time periods in 0.1M NaOH under selected conditions are given in Figure 5.

In comparison to the nitrogen control, oxygen leads to a more rapid viscosity loss, especially in the presence of cobalt. The other metal tested, magnesium, had a stabilizing effect when used alone in the oxygen-alkali system. The amorphous cellulose degradation rate (viscosity loss) was not, however, completely retarded in both the oxygen and nitrogen control cases by the presence of Mg. Surprisingly, the combination of Mg and Co caused a greater loss in viscosity than when Co was used alone.

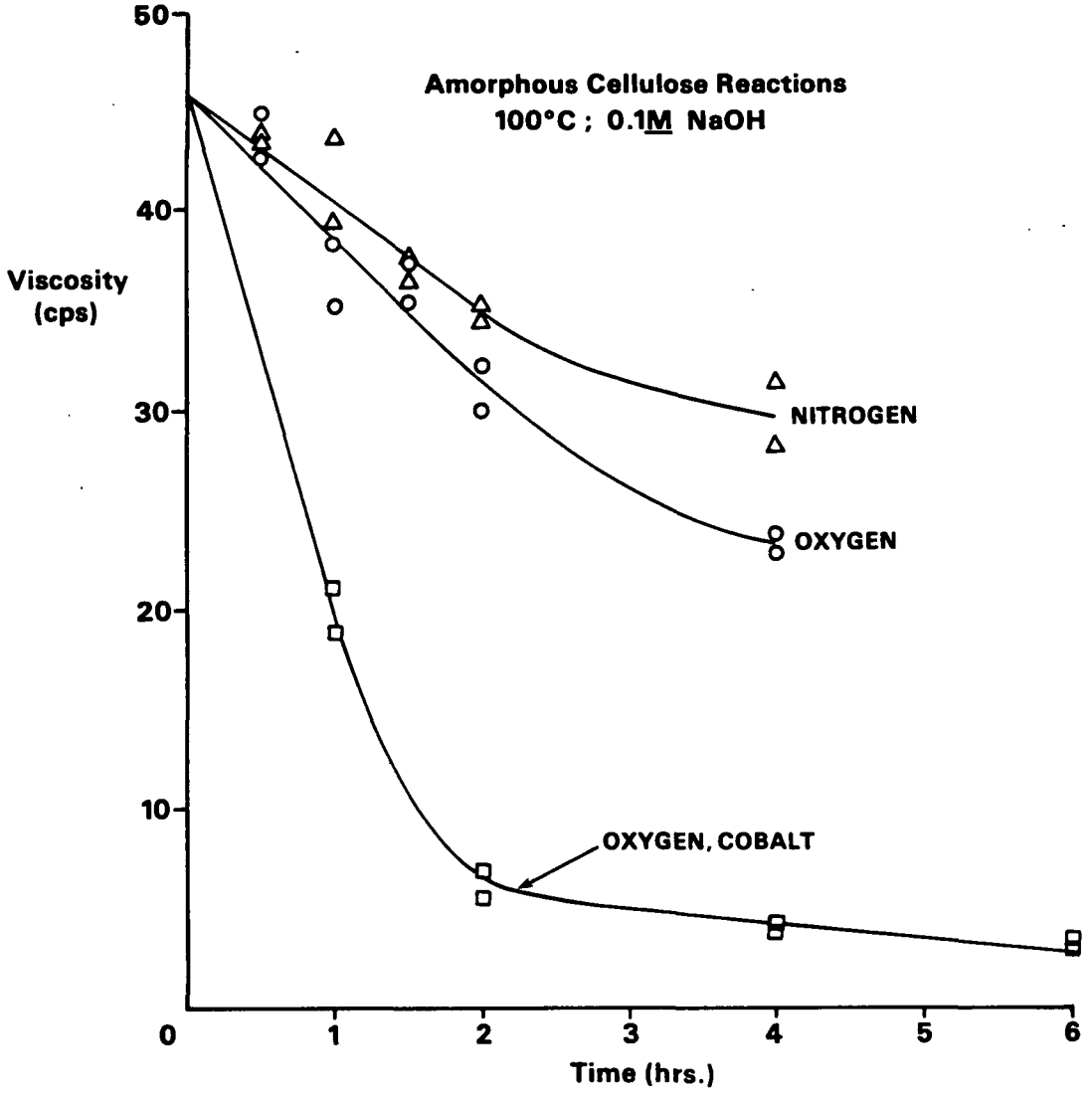

Figure 5. Variations in amorphous cellulose viscosities as a function of time following treatment at 100°C in 0.1M NaOH with the indicated chemicals; the level of $CoSO_4$ used was 0.308 mole/100 g sample x 4 samples = 1.232 moles/2L. Duplicate determinations are shown.

The two metals chosen for study, cobalt and magnesium, are known to cause chain cleavage reactions in models and stabilize pulps toward oxygen-induced degradation, respectively.[5,6] The results observed here parallel these known properties, but are unusual in a few aspects. The data indicate that the magnesium protecting effects are not lasting and apparently not helpful in the presence of cobalt; the latter was an unexpected result.[7] Also, cobalt promoted degradation in the nitrogen control case, possibly indicating that the control case is not completely oxygen-free.

The response of amorphous cellulose-oxygen-alkali system to different levels of cobalt is shown in Figure 6. The cobalt appeared to have little effect below a level of 0.162 mole of $CoSO_4$/100 g of amorphous cellulose. Above this level, there was a rapid drop in viscosity with increasing amounts of cobalt.

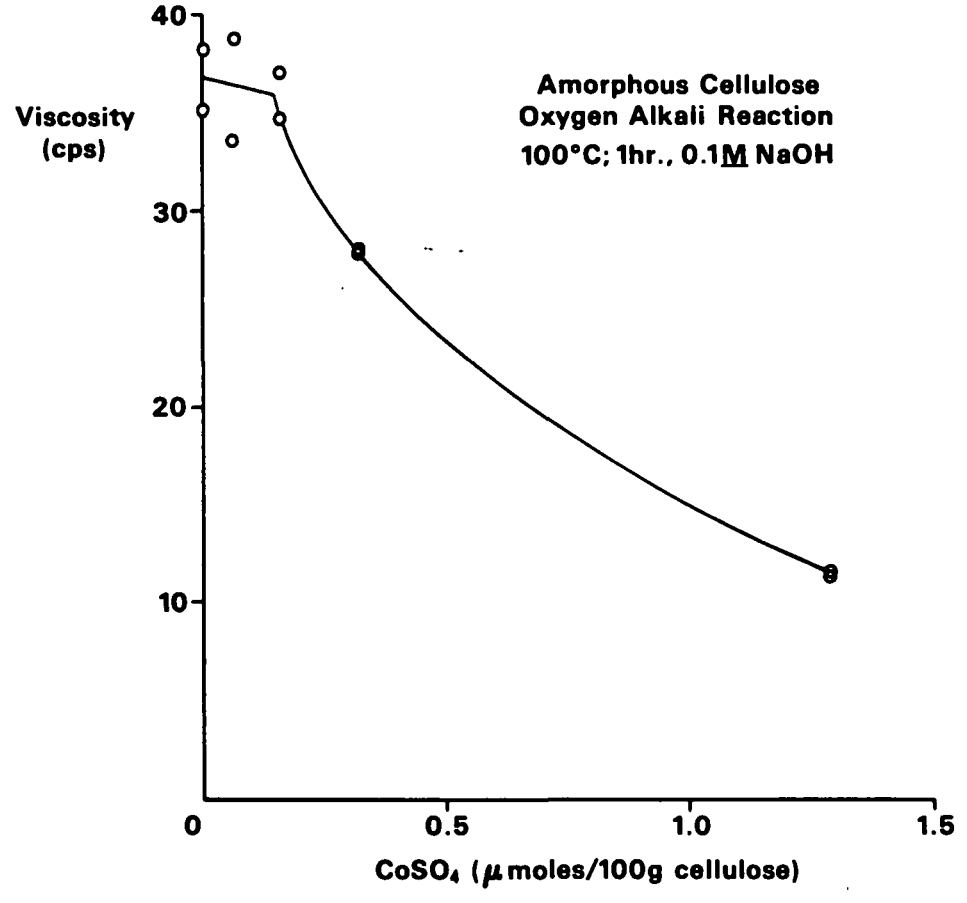

Figure 6. Variations in amorphous cellulose viscosities with different levels of cobalt for samples heated at 100°C for 1 hour in 0.1M NaOH; duplicates were done at each cobalt level.

A comparison of the reactivities of cotton linters and amorphous cellulose samples toward oxygen-alkali containing cobalt at 100°C is shown in Figure 7. Again, as in the pulping experiments, the amorphous sample exhibits a much higher reactivity (loses viscosity faster). After 4 hours, the viscosity of the linters is roughly one-half that of the starting viscosity, while in the amorphous case it is one-tenth.

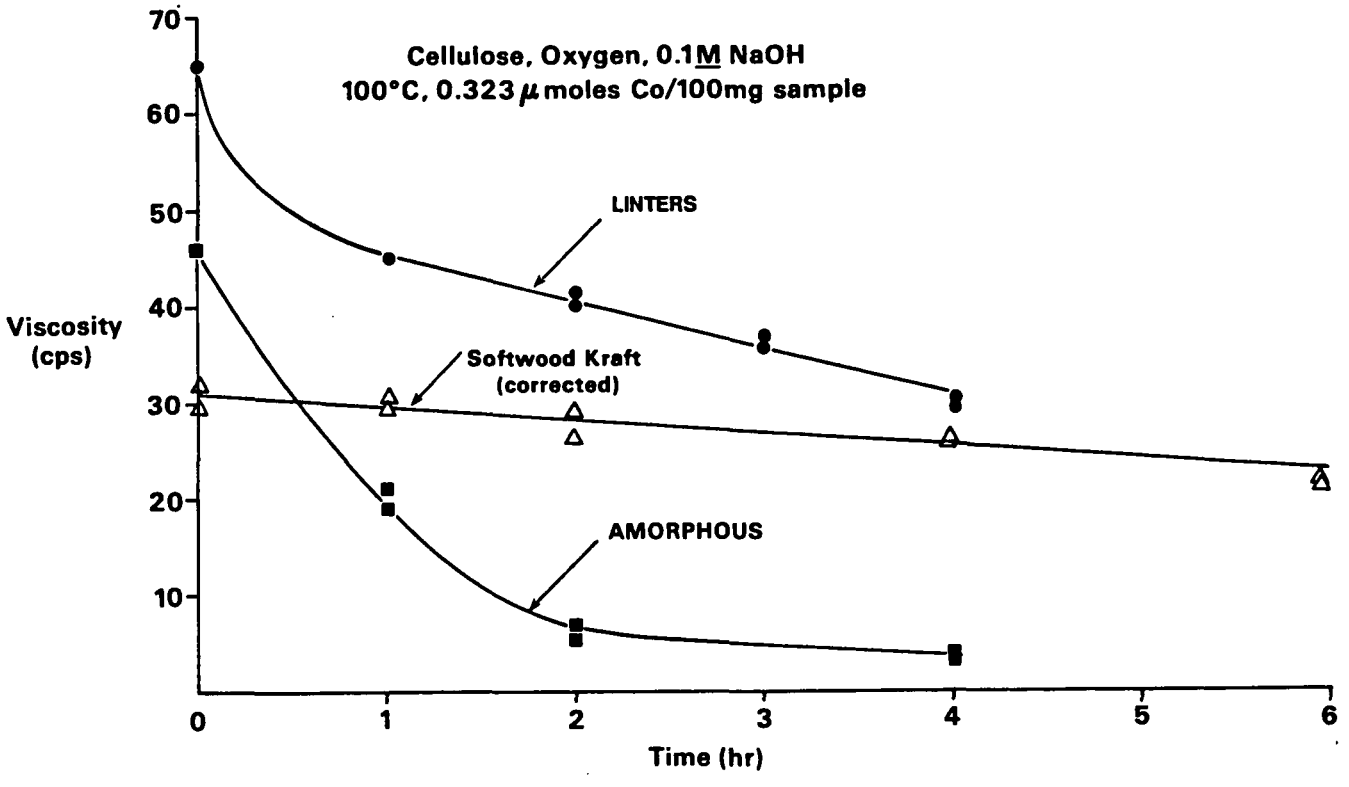

Figure 7. Variation of viscosities as a function of time for linters, kraft pulp, and amorphous cellulose under the conditions stated; duplicates were done in most cases.

The initial rapid drop in viscosity for the linters sample was our first real indication that the linters probably contained some amorphous cellulose. The viscosity losses for the crystalline cellulose sample towards oxygen-alkali-cobalt were slight (Figure 8). As seen in the figure, there is a dramatic difference in reactivity between the crystalline and amorphous cellulose.

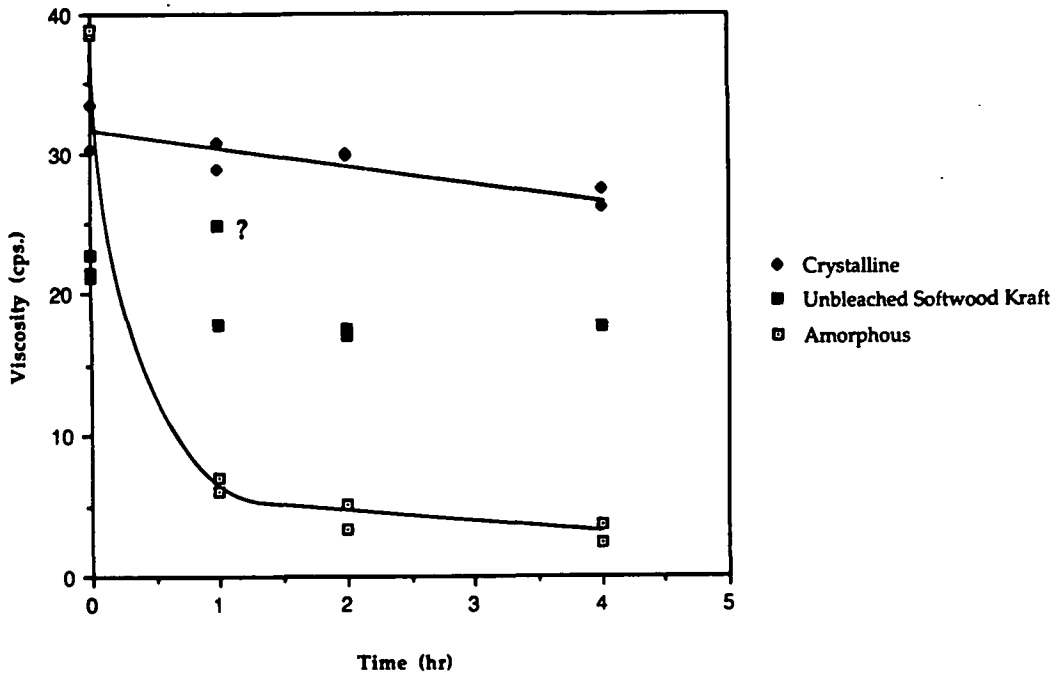

Figure 8. Variation of viscosities as a function of time for crystalline, kraft pulp, and amorphous cellulose under the conditions stated.

The viscosity losses for unbleached kraft pulp under the same conditions are small; however, the data in Figure 8 does not clearly point to a linear drop in viscosity with time. In the earlier study (Figure 7), the kraft pulp showed a straight line response with a slope similar to the crystalline cellulose results; the absolute values of the viscosities determinations were not, however, available in the earlier work due to a wrong (consistent) sample dilution. Recent work has shown that a new unbleached kraft pulp does not lose viscosity over 4 hours of treatment with oxygen-alkali-cobalt. Obviously kraft pulps are relatively stable to the conditions and must be fairly free of amorphous material, which is rapidly degraded.

The cleavage of glycosidic linkages might possibly be linked to radical reactions associated with lignin-oxygen reactions. Therefore, a couple of oxygen-alkali amorphous cellulose reactions were done in the presence of a kraft pulp - a material which contains lignin. No noticeable effects on amorphous cellulose viscosity losses were observed in the kraft vs. control cases.

A sample of amorphous cellulose was pretreated with nitrogen dioxide prior to reaction with oxygen-alkali in the presence of cobalt and magnesium. The NO_2 treatment caused a severe loss of viscosity (45 to 23) and did not protect the cellulose from the oxygen-alkali-cobalt degradation reactions (viscosity dropped from 23 to 6 with a 1 hour treatment).

Several sets of peroxide reactions have been performed. The experiments were done at 50-60°C, 12% consistency, and an initial pH of 11; all reaction samples were still basic at the conclusion of the heating period. As expected, the viscosity drop of an amorphous cellulose sample increased with increasing peroxide application (Table 2). Also, the addition of magnesium and silicate stabilized the amorphous cellulose toward extensive degradation. Copper also seemed to have a small stabilizing effect; however, this was subsequently shown to be related to copper induced decomposition of the peroxide, which lowered the level of peroxide available for reaction.

Table 2. Viscosity values after heating amorphous cellulose[a] at 60°C for 1 hour at 12% consistency with different levels of peroxide and metal salts.

Peroxide (%)	Alkali (%)	Additives	Viscosity (cps) - Duplicates
--	0.033	--	44.5, 43.2
0.2	0.10	--	12.3, 10.7
0.4	0.15	--	7.1, 7.8
1.0	0.39	--	4.4, 4.5
0.4	0.14	0.37 M $CuSO_4 \cdot 5H_2O$	13.8, 10.1
0.4	0.13	0.2% $MgSO_4 \cdot 7H_2O$ 4.5% Na_2SiO_3	39.8, 35.1

[a]Starting viscosity 45 cps.

A time study of amorphous cellulose and of linters with 0.2% peroxide at 50°C produced the data shown in Figure 9. A companion study with crystalline cellulose showed only a few percent drop in viscosity with time (Figure 10). The

initial rapid drop in viscosity observed in the crystalline case was not confirmed in a subsequent study with a new crystalline sample; here the viscosity showed no loss with time over a 0-40 minute period. Again, we have some uncertainty as to which set of data more accurately reflects the true response of crystalline cellulose towards peroxide. Yet, the data obviously shows that, in the absence of stabilizers, peroxide causes severe chain cleavage of amorphous cellulose and little, if any, cleavage of crystalline cellulose.

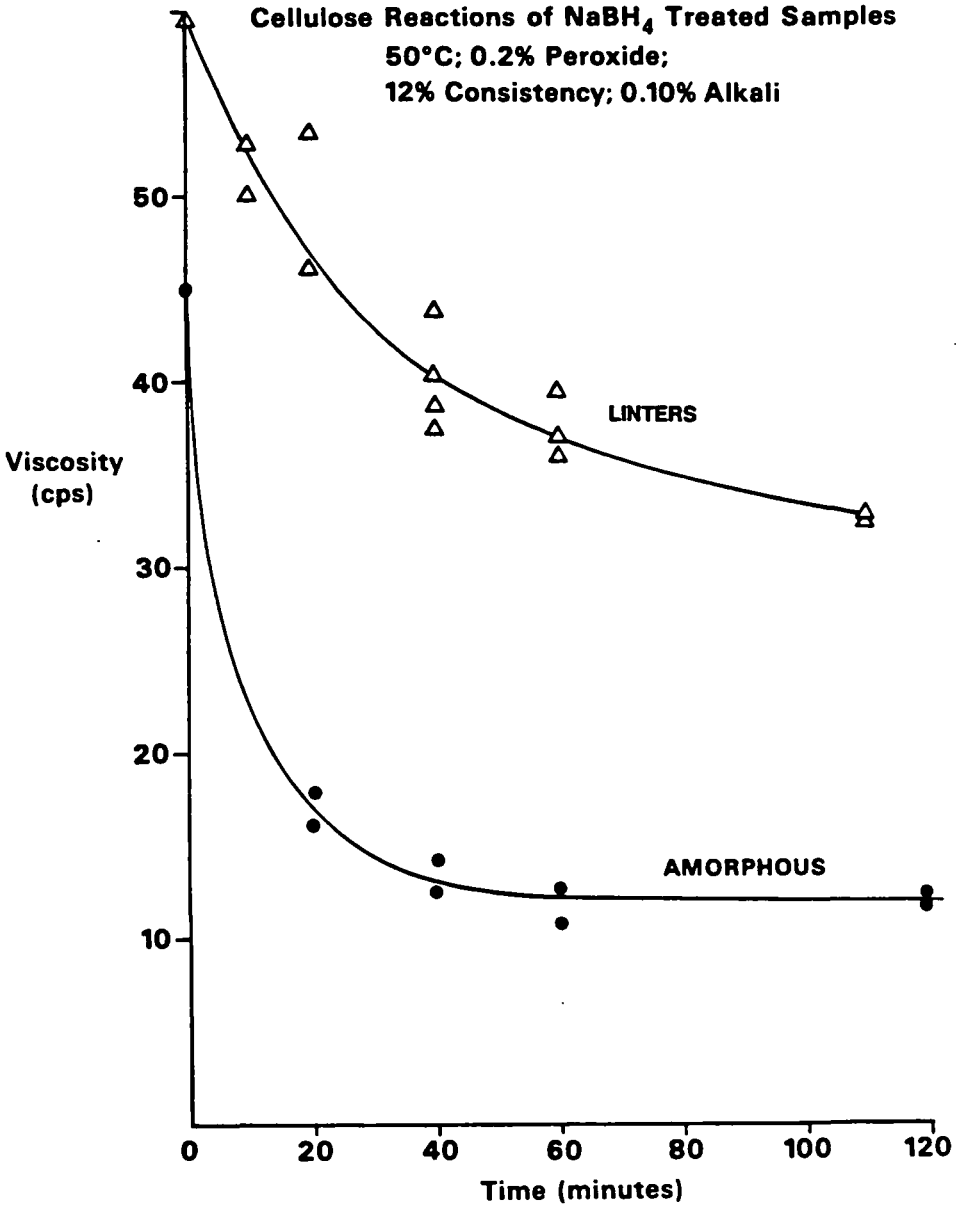

Figure 9. Variations in cellulose viscosities as a function of time under the conditions indicated.

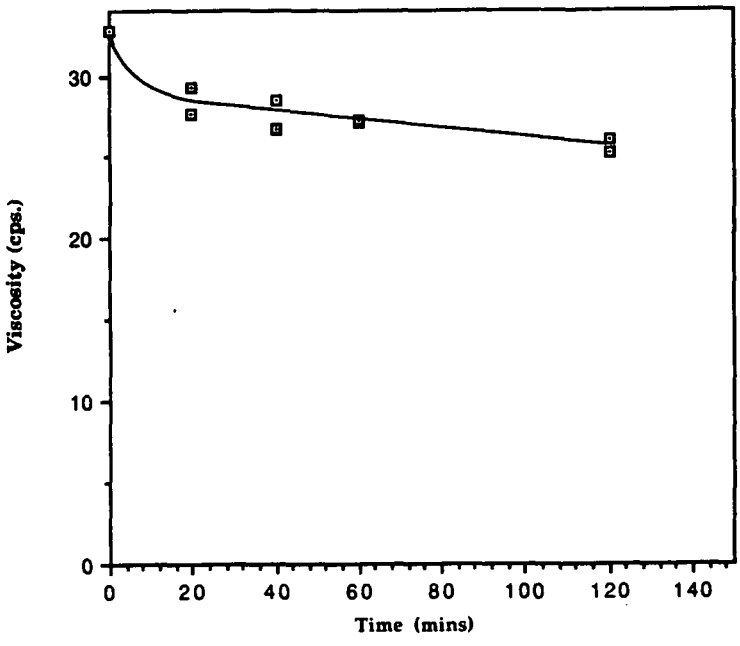

Figure 10. Viscosity variations with time of reaction for crystalline cellulose (12% consistency) with 0.2% Hydrogen peroxide and 0.10% alkali at 50°C.

FUTURE STUDIES

The studies outlined above indicate that there is a great deal which can be learned about carbohydrate degradation reactions from the behavior of amorphous cellulose under selected conditions. Some experiments need to be expanded to more clearly substantiate the findings. The amorphous cellulose bleaching chemistry studies could be expanded to examine (1) additional chemicals [ozone, chlorine dioxide, etc.], (2) process variables, (3) the influence of selected metals and "dead load" salt effects, and (4) more detailed molecular weight distributions. The aim will be to develop a fundamental understanding of bleaching chemistry which may lead to better nonchlorine bleaching systems.

REFERENCES

1. Matthews, C. H., Svensk Papperstid. 77:629(1974).

2. Schroeder, L. R., Project 3284 Interim Report to the Program Committee, March 17, 1986.

3. Schroeder, L. R.; Wabers, B. A., Project 3475-1 Interim Report to the Program Committee, Sept. 10, 1982.

4. Schroeder, L. R.; Lingnowski, H. J., Project 3475-1 Interim Report, Sept. 5, 1985.

5. Graves, D. P., Jr.; Thompson, N. S.; Schroeder, L. R., J. Wood Chem. Technol. 2:115(1982).

6. Croon, I.; Andrews, D. H., Tappi 54(11):1893(1971).

7. Gilbert, A. F.,; Pavlovova, E.; Rapson, W. H., Tappi 56(6):95(1973).

INSTITUTE OF PAPER SCIENCE AND TECHNOLOGY

Donald R. Dimmel
Professor and Principal Research Scientist

PROJECT SUMMARY FORM

DATE: March 20, 1990

PROJECT NO. 3524: Fundamentals of Brightness Stability

PROJECT LEADER: A.J. Ragauskas

IPST GOAL : Increase the usefulness of high yield fibers

OBJECTIVE: Research activities will be directed at investigating the fundamental chemical reactions which are initiated when high yield pulps are photolyzed. As our knowledge of the photooxidation of mechanical pulp increases, methods to stop or significantly retard the yellowing process will follow.

CURRENT FISCAL YEAR BUDGET: $155,000

PRIOR RESULTS:

Previous research efforts at IPST have been successful at designing and building a "Solar Simulator" which simulates the effects of sunlight on mechanical pulp. The kinetic rates of yellowing were determined for an assortment of high yield pulps. The effect of several experimental parameters (i.e. moisture content, singlet oxygen, metal salts, pH, etc) have been examined with respect to their effect on the rate of brightness reversion. Analytical procedures were developed to monitor the rate of photo-yellowing. A variety of spectroscopic procedures were employed to identify some of the chromophoric species which were formed when mechanical pulp was irradiated. The results of these investigations have led to a novel method of detecting and quantifying the levels of ortho-quinones present in mechanical pulps. In addition, the detection of ferulic acid in irradiated mechanical pulp has indicated that more than one chromophoric species may be involved in the yellowing process.

PLANNED ACTIVITY THROUGH FISCAL YEAR 1990:

Installation and calibration of the "Solar Simulator" is currently being pursued. Procedures are being established with Georgia Tech so as to gain access to their high field NMR facilities.

Synthetic methodology will be developed so as to provide an efficient means of preparing a variety of lignin and quinoid model compounds which have been proposed to occur in mechanical pulp.

FUTURE RESEARCH ACTIVITY:

A series of lignin model compounds are to be prepared and photolyzed on a solid support matrix. The products formed from the photolysis experiments will be characterized using several analytical techniques, i.e. IR, NMR, MS,.... For example, a study of the photooxidation of coniferyl alcohol on a solid matrix is to be examined. The results of these studies should provide information on the mechanism of photoformation of ferulic acid.

The photoreactivity of quinones, under the brightness reversion conditions, will also be explored. A careful examination of the literature provides extensive examples of the tendency of quinones to undergo solution phase polymerization and photochemical reactions. The extent to which the solid matrix of mechanical pulp could mediate the chemical reactivity of quinones is currently unknown. However, a general review of solid state chemistry clearly suggests that the matrix can have a profound effect on the reaction profile. The above proposed studies will therefore extend our knowledge of the chemical reactivity of quinones formed in mechanical pulp.

Previous IPST research efforts demonstrated that derivatization of ortho-quinones with trialkyl phosphites could be employed as a means of detecting ortho-quinones in mechanical pulp by means of 31P NMR. This technique will also be employed in this proposed study.

Finally, research efforts will also be directed at further isolating and characterizing the products formed from the photolysis of mechanical pulp.

Collectively, these research investigations will provide information as to what is occurring in the chemically complex structure of mechanical pulp when it is irradiated.

Project 3524 Status Report

FUNDAMENTALS OF BRIGHTNESS STABILITY

Reporting Period: September, 1989 -- March, 1990

OBJECTIVES

The aim of this research is to investigate the fundamental chemical reactions which are initiated when high yield pulps are photolyzed and to apply this knowledge to stop or significantly retard the yellowing process. This goal will be accomplished in three parts. First, a series of lignin model compounds will be synthesized and then photolyzed on a solid support matrix (part I). The photolytic behavior of quinones under the brightness reversion conditions will also be studied (part II). The results of these investigations will provide valuable information about what is occurring in the more chemically complex structure of mechanical pulps. These studies will then be used to design novel methods of photo-stabilizing mechanical pulp (part III).

GENERAL INFORMATION

This Status Report is for general distribution to Institute member companies and summarizes current and future activities for this project. Initial efforts in this area were focused on setting-up laboratory facilities at IPST and establishing working procedures with Georgia Tech, so as to gain access to a variety of their technical facilities. Most of these tasks are now either complete or in the final stages.

An extensive review of the brightness reversion literature was undertaken and this led to a new research proposal. The remainder of this report will highlight the proposed areas of research and discuss the impact of these studies.

Project 3524 Status Report

Research Proposal

FUNDAMENTALS OF BRIGHTNESS STABILITY

BACKGROUND

The use of high yield mechanical pulps has received increasing attention for the last two decades. Several timely reviews have highlighted the current and future demands for these types of pulps[1,2]. Despite the recent interest in high yield pulps, their commercial use is often limited to low value or short life-cycle paper products due to the inherent photo-instability of mechanical pulps. The photochemical initiated reactions result in the yellowing of both bleached and unbleached mechanical pulps and therefore decrease the brightness of these pulps[3]. It is this fundamental problem that has hindered further use of mechanical pulps for a variety of commercial applications. Research efforts directed at examining the photo-yellowing process have been successful in defining some of the important parameters involved in this reaction.

Early investigations by Leary[4a, b] and others[5a, b] clearly determined that the yellowing of high yield pulp is initiated by the absorption of near UV light (k = 300 - 400 nm) by the lignin component of the pulp. Furthermore, the presence of oxygen was shown to be crucial for the photo-yellowing process to occur.

A variety of other factors, such as pH[6], metal salts[7], bleaching procedures[8], moisture and resin content[6, 9] have also been examined to determine their role in the photo-degradation process. To date, these investigations have not been successful in finding manufacturing conditions which would significantly reduce the rate of photo-yellowing.

Although the exact chemical reactions by which mechanical pulp undergoes the photo-yellowing process remains ambiguous, certain important aspects of this process have now been determined. The reaction is initiated by the absorption of a photon of light by chromophoric structures present in lignin, such as a and b carbonyl groups and/or double bonds conjugated with a phenyl ring. It has been proposed that the excited state of these compounds then leads to the formation of radicals either directly by an intramolecular bond cleavage process[10] (Scheme 1, pathway a) or intermolecularly via abstraction of a phenolic hydrogen[4b] (Scheme 1, pathway b). Alternatively it has been suggested that the excited state could lead to the generation of singlet oxygen which could further react with lignin generating radical intermediates[11] (Scheme 1, pathway c). The resulting radicals then undergo a variety of thermal and/or photochemical reactions. Highlights of this proposed photochemical initiated reaction are summarized in Scheme 1. Consistent with these proposed photochemical initiated reactions is the detection of free-radicals in photo-irradiated mechanical pulp by means of electron spin resonance[12].

The formation of quinones or polymeric material derived from quinones is believed to occur during the irradiation of mechanical pulp[4b]. It has been proposed that the resulting quinoid products are the main contributing components in the yellowing of pulp[13]. Several other products have also been detected in photo-yellowed high yield pulp, and their role in the brightness reversion process is under investigation[14].

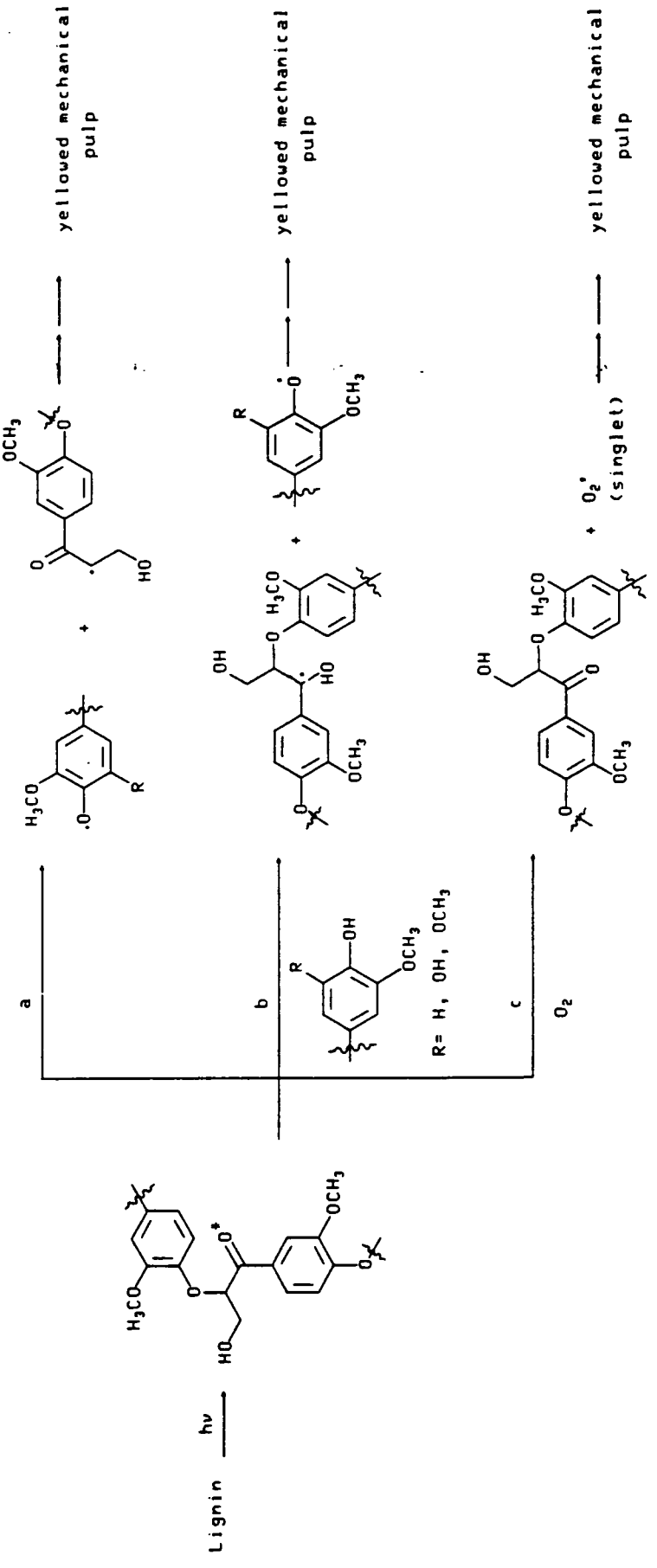
Lignin
hν
a
b
c
R= H, OH, OCH3
O2
yellowed mechanical pulp
yellowed mechanical pulp
yellowed mechanical pulp
+ O2' (singlet)

Scheme 1

Project 3524 Status Report

PROPOSED STUDY

Part I:

The photo-initiatated yellowing reactions of mechanical pulp will be studied using a series of trimer (A, B) and tetramer (C) models of lignin.

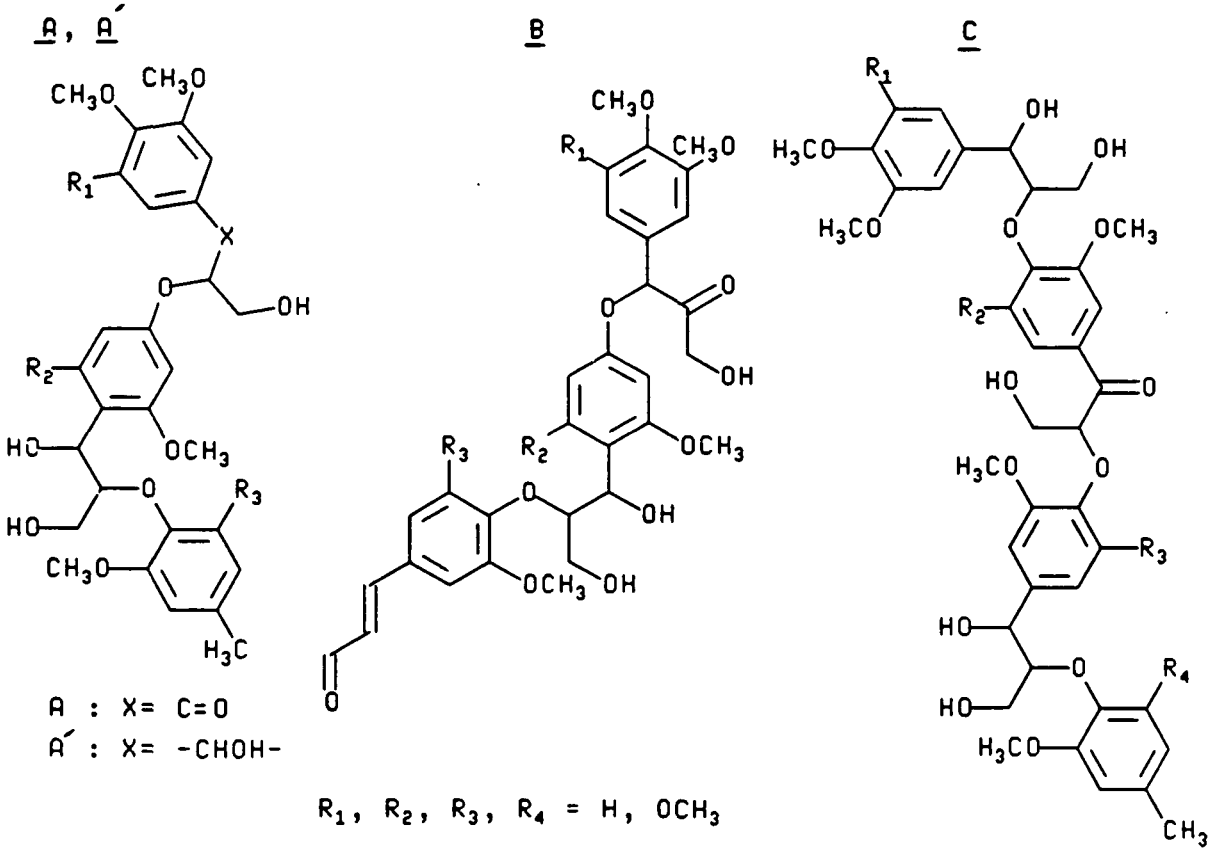

The proposed compounds will be adsorbed onto cotton linters. The resulting mixtures will then be irradiated with the same frequency of light that is responsible for photo-yellowing of mechanical pulp. Several light sources will be employed, such as the Oriel Solar Simulator and commericially available fluorescent lamps. Use of these experimental conditions will, to a first approximation, replicate the circumstances under which brightness reversion occurs.

The photochemical experiments will provide a means of modeling not only the initial photolysis reactions that occur with lignin but also the subsequent reactions that result in the formation of colored material. It is the contention of this proposal that the chemical reactions which occur after the initial photolytic step play an important role in the overall yellowing process. The synthetic methodology needed to prepare these compounds has been developed by several notable research groups in this field[15a, b, c]. The proposed synthetic route to the desired compounds is summarized in Scheme 2.

To date, all model studies of the photo-yellowing process have employed either mono or dimeric models of lignin. These model compounds greatly oversimplify the structure of lignin; yet these investigations have been crucial to our understanding of the photo-yellowing process. For example, studies by Gellerstedt[16] and Castellan[17] have clearly demonstrated the potential of a variety of structural components of lignin to undergo photolytic reactions, as shown in Scheme 3.

After the initial photolytic reactions, the reactive intermediates in these studies most likely do not undergo further reactions typical of lignin. For example, the photolysis of 4-hydroxy-3-methoxy-(2-methoxyphenoxy)acetophenone yielded a variety of products, several of which could be attributed to a radical coupling mechanism and/or the addition of radicals to unreacted starting material[17]. Radical coupling reactions of the type shown below presumably are not favored in a polymeric material such as lignin due to restricted geometric considerations.

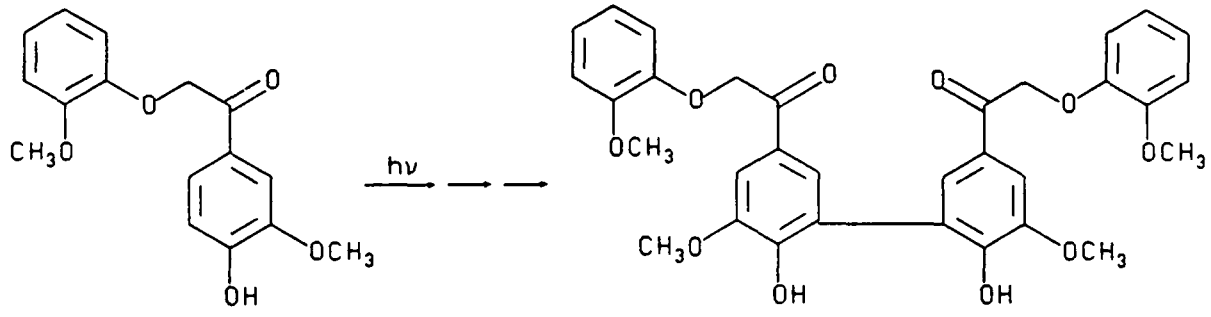

+ several other products

The probability of generating a radical pair adjacent to an a or b carbonyl group or next to another radical intermediate is unlikely. There are approximately 5-15 carbonyl groups per 100 phenyl propane units in high yield pulps[18]. Therefore the "concentration" of carbonyl groups and radicals present in mechanical pulp would be low.

Scheme 2

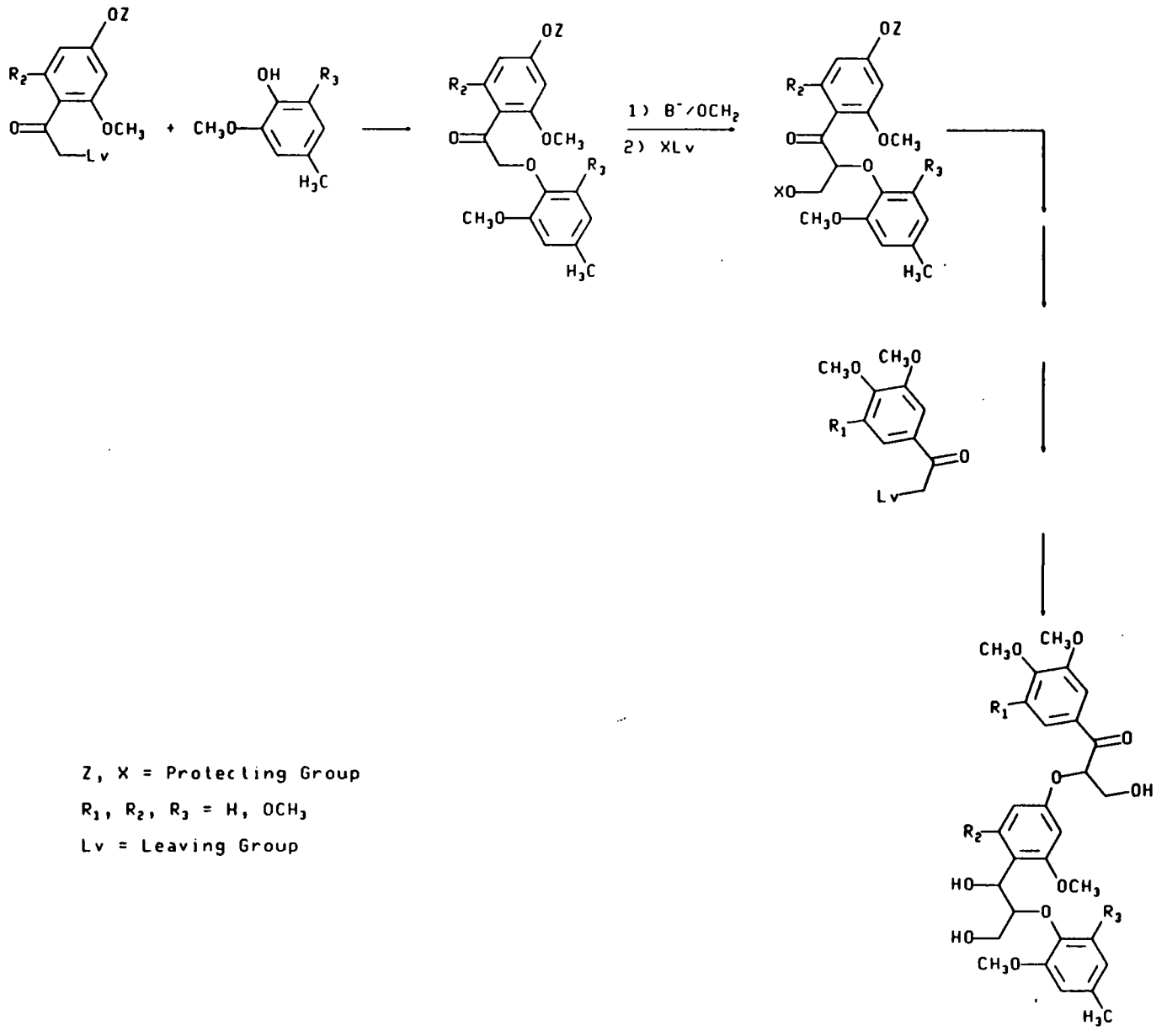

Z, X = Protecting Group

R_1, R_2, R_3 = H, OCH_3

Lv = Leaving Group

Scheme 3

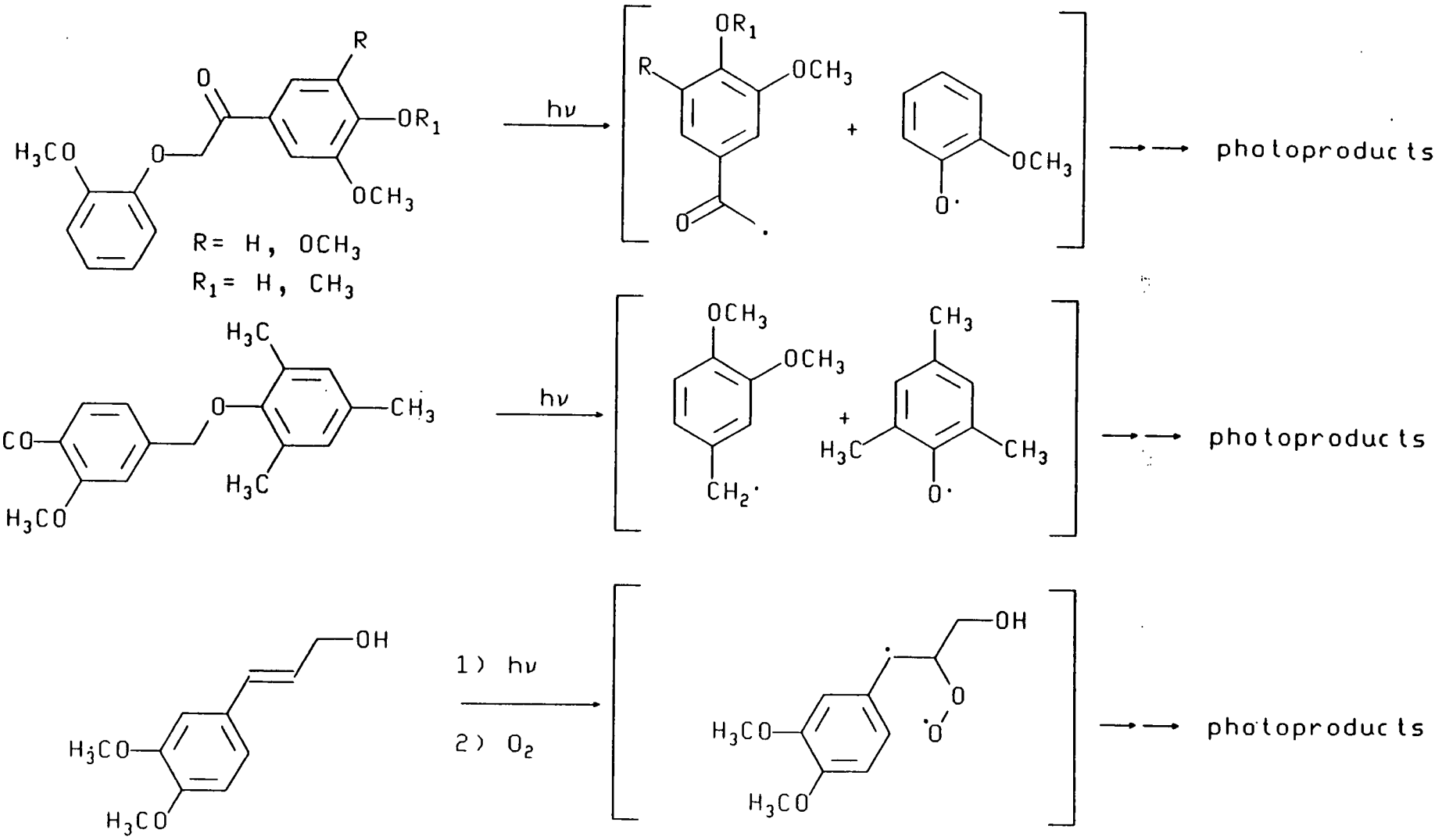
R
O
OR1
H3CO
O
OCH3
R= H, OCH3
R1= H, CH3
hν
OR1
R
OCH3
O
+
OCH3
O·
photoproducts
H3C
CH3
H3CO
O
CH3
H3CO
H3C
hν
OCH3
OCH3
CH2·
+
CH3
H3C
CH3
O·
photoproducts
OH
H3CO
H3CO
1) hν
2) O2
OH
O
O
H3CO
H3CO
photoproducts

Clearly, present model studies do not take proximity effects, nor do they address the formation of quinoid type products, which are known to be formed upon irradiation of mechanical pulp. The difference in the product mixtures formed from model studies and mechanical pulp studies questions the validity of the model studies as they pertain to photo-yellowing. Photolysis of compounds A, B and C should generate radical intermediates which would be closer in structure to those generated in mechanical pulp.

Upon completion of these studies the photochemical reactions will be repeated in the presence of A'. The photolysis of A, B or C on a solid support matrix containing A' will provide a means of modeling the intermolecular reactions which may occur in mechanical pulp after the initial photochemical reaction.

Along with the above considerations, the radicals formed from photolysis of mechanical pulp have the potential to undergo a series of intramolecular reactions, an example of which is illustrated below.

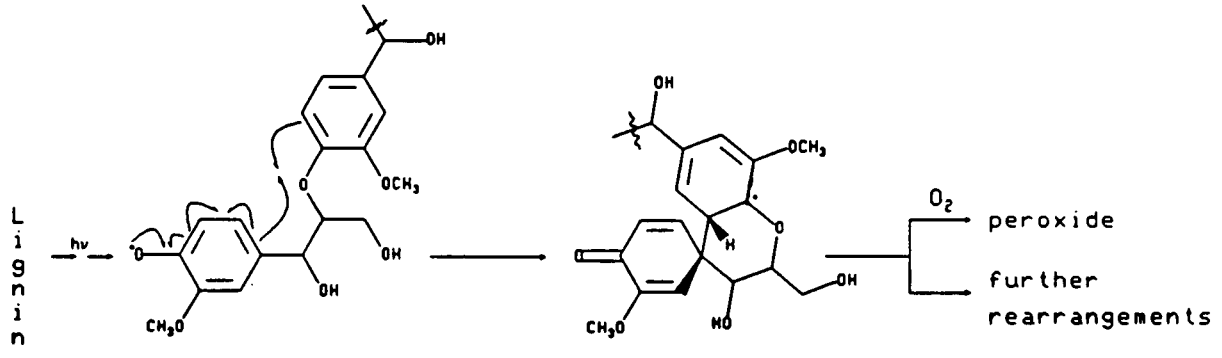

Examination of the literature indicates that these types of reactions have not been considered. The use of the proposed model systems should provide a means of investigating this possibility.

Current model studies assume that the preferred conformation of the lignin does not greatly influence either the photolysis reaction or the subsequent reactions. It is reasonable to expect that the preferred conformation of lignin and that of the monomeric or dimeric model compounds will differ greatly. Indeed, Molecular Minimization calculations (version 2) for the dimeric compound D and the trimeric structure E show conformational differences[19], with the latter compound assuming a much more restricted degree of freedom.

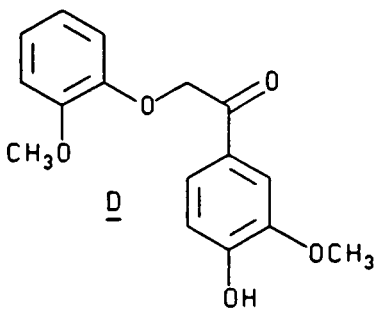

D

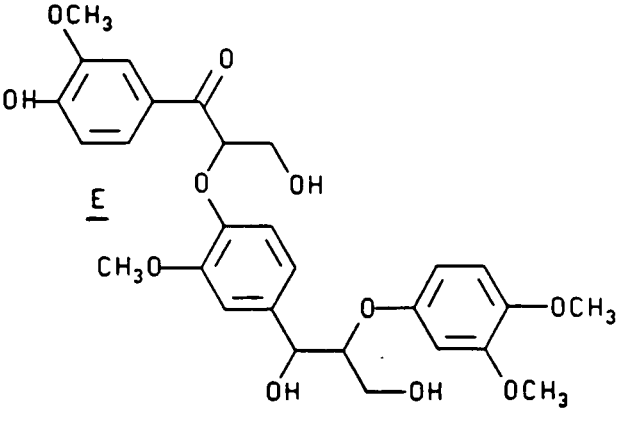

E

Whether such conformational differences influence either the initial photolysis reaction or subsequent steps is currently unknown. The photoreactivity of compounds A, B and C will provide a means of exploring these effects.

Research efforts will also be directed toward grafting mixtures of either A/A' or B/A', or C/A' onto a polymer. The resulting heterogenous polymer supported mixtures will then be irradiated under the photo-yellowing conditions. The use of a polymer support phase will provide a unique means of controlling both the relative distribution and orientation of the lignin model compounds. The advantages of employing these type of lignin model compounds have been demonstrated in the recent research efforts of D.R. Dimmel[15d].

Part II

The reaction profile of quinones under the photo-yellowing conditions is another aspect of the brightness reversion process that will be studied in this project. A variety of spectroscopic studies have clearly implicated the presence of quinones in mechanical pulp[20]. Recent studies by Lonsky[14, 21] were successful in developing a quantitative method of monitoring the in situ formation of ortho-quinones formed during the photolysis of mechanical pulp. On the basis of these latter studies, it was suggested that the photo-autoxidation of lignin yielding ortho-quinones was the predominant reaction responsible for the yellowing of mechanical pulp. By contrast, studies by Kringstad[22] and Forsskahl[23] suggest that yellowing of mechanical pulp is due, at least in part, to the polymerization of quinones or further photolytic reactions of quinones. An examination of the literature provides extensive examples of the tendency for quinones to undergo solution phase polymerization and photochemical reactions[24]. The extent to which the solid matrix of mechanical pulp could mediate the chemical reactivity of quinones is currently unknown, although a general review of solid state chemistry[25] suggests that the matrix can have a profound effect on the reaction profile. It is therefore proposed that the photochemistry of quinones on a solid support should be investigated to determine the nature of the products formed from photolysis.

Initial photochemical studies in this field will be accomplished with readily accessible compounds such as F.

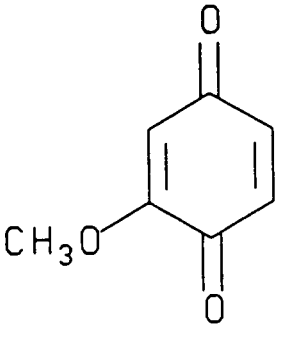

F

The photolytic behavior F, absorbed onto a solid matrix, would be of much interest since the in situ formation of para-quinones is believed to occur by a side chain cleavage mechanism[26] yielding monomeric units such as F.

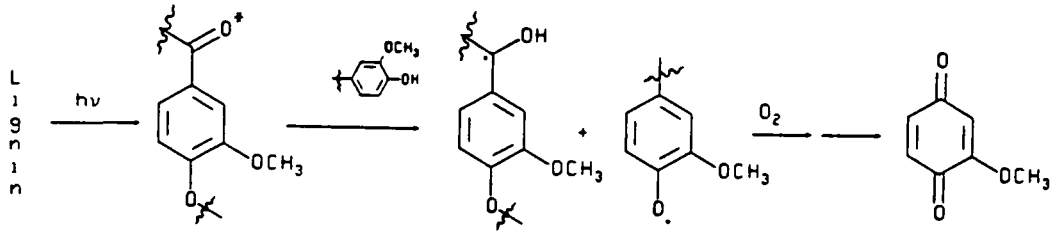

The preliminary studies will employ cotton linters as a solid support phase in an attempt to duplicate, to a first approximation, the chemical environment in which quinones are found in mechanical pulp. The results from the photolysis of F will be especially interesting since the solution phase photochemistry of this compound has already been studied under the photo-yellowing conditions, as shown below[23]. The proposed studies will therefore provide a means of evaluating to what extent the solid matrix can influence the photochemical reactivity of F.

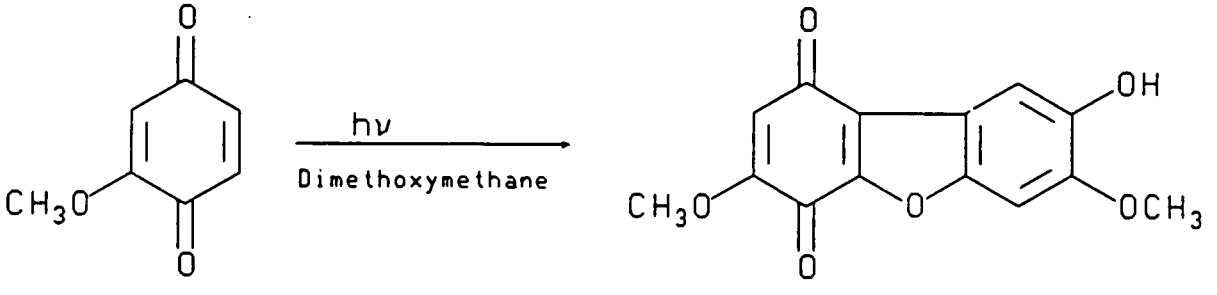

After the initial photolysis experiments are completed the photolysis reactions will be repeated in the presence of A'. These latter experiments will provide a means of investigating the possibility that photolysis of para-quinones in mechanical pulp leads to an intermolecular reaction between lignin and the excited state of the quinone.

The in situ formation of ortho-quinones has been suggested to occur without side chain cleavage from the lignin polymer[26]. To investigate the photoreactivity of these compounds under the photo-yellowing conditions a series of models will be prepared. The first such structures are shown below and a retro synthetic pathway for these compounds is illustrated in Scheme 4. The photolysis experiments will be accomplished in the same manner as described above.

Scheme 4

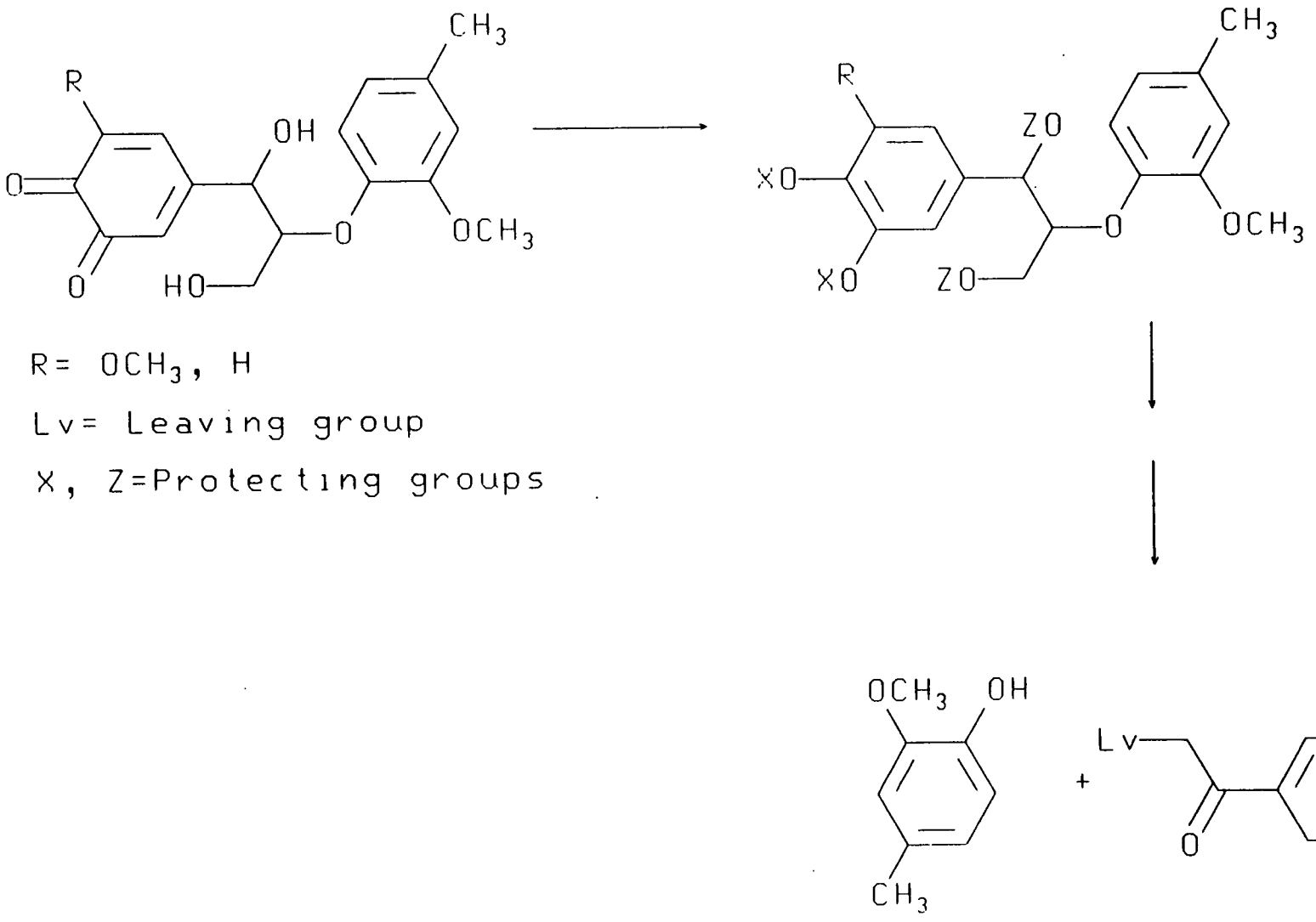

R= OCH_3, H

Lv= Leaving group

X, Z=Protecting groups

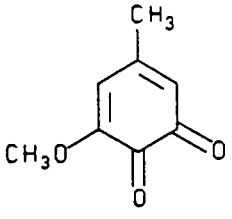

G

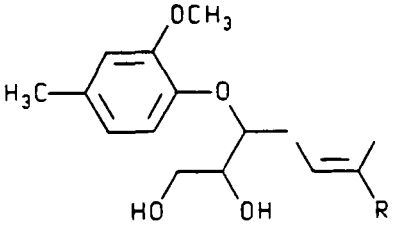

H

R= OCH_3, H

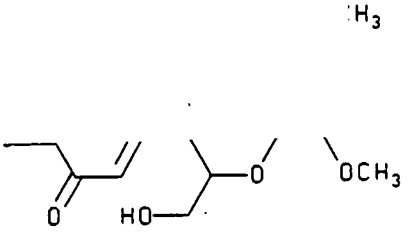

I

The availability of compounds H and I will provide an opportunity to extend the investigative results initiated at IPST[21] into the characterization and formation of ortho-quinones. These studies were dependent upon using trialkyl phosphite derivatives of ortho-quinones and ^{31}P N.M.R. as means of monitoring the presence of ortho-quinones. A series of model compounds were prepared and their ^{31}P chemical shifts were determined, the results of which are shown below.

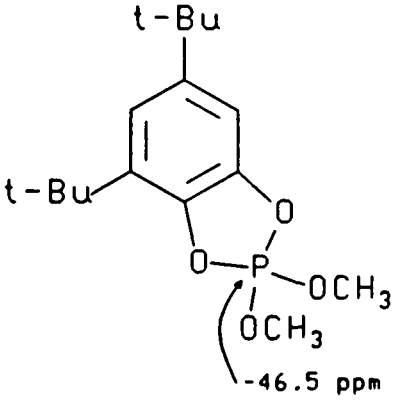

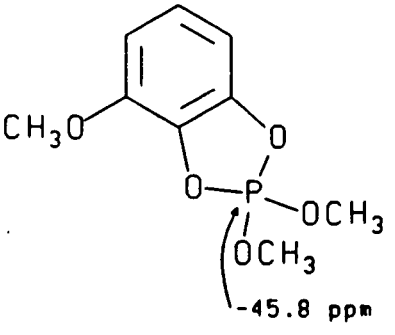

It is proposed that the analogous phosphite derivatives are to be prepared from compounds H and I and that their ^{31}P N.M.R. data will be collected. The results of these studies will provide further needed ^{31}P N.M.R. chemical shift data on the nature of the trialkyl phosphite/ortho-quinone adduct[21]. In addition, the products formed from the irradiation of quinones will also be treated with trialkyl phosphites and their ^{31}P N.M.R. spectral data will be collected. This data will complement the earlier studies performed at IPST and may aid in identifying several unknown chemical shifts which were reported in these studies.

CONCLUSION

This proposal outlines the general methodology that is to be employed in studying brightness reversion of high yield pulp. Investigative efforts will be directed at determining what are the fundamental reactions which yield colored compounds and how can this process be halted. It is anticipated that the use of chemical model studies will provide insight into what is occurring when mechanical pulp is irradiated. In turn, these results will guide our efforts at designing novel methods of retarding the brightness reversion process.

REFERENCES

1. D.H. Breck and G.E. Styan, TAPPI J., 1985(July), 40.

2. G. Goldstein, International Symposium on Wood and Pulping Conference,-1989, 81.

3. G. Gellerstedt, I. Petterson and S. Sundin, Svensk Papperstidn., 1983, R 157.

4. a) G.J. Leary, Tappi, 50(1), 17 (1967).
   b) G.J. Leary, Tappi, 51(6), 257 (1968).

5. a) K.P. Kringstad, Tappi, 52(6), 1070 (1969).
   b) K.P. Kringstad and S.Y. Lin, Norsk Skogindustri, 9, 254 (1971).

6. A. Andbacka, B. Holmborn, and J.S. Gratzl, International Symposium on Wood and Pulping Conference, 1989, 347.

7. J. Janson and I. Forsskahl, International Symposium on Wood and Pulping Conference, 1987, 313.

8. G. Gellerstedt, L.A. Hammar, A. Olsson, I. Petterson and S. Sundin, Svensk Papperstidn., 88(6), R 68(1985).

9. B. Holmbom, A. Akademi, and R. Ekman, International Symposium on Wood and Pulping Conference, 1989, 445.

10. J. Gierer and S.Y. Lin, Svensk Papperstidn., 15(7), 233(1972).

11. I. Forsskahl, H. Tylli and C. Olkkonen, International Symposium on Wood and Pulping Conference, 1989, 431.

12. N.S. Hon, J. Polym. Sci., Poly. Chem. Ed., 13, 2641(1975).

13. S.E. Lebo, Jr., W.F.W. Lonsky, T.J. McDonough and P.J. Medvecz, International Symposium on Wood and Pulping Conference, 1989, 1.

14. U.P. Agarwal, and R.H. Atalla, International Symposium on Wood and Pulping Conference, 1989, 441.

15. a) J.A. Hyatt, Holzforschung, 41(6), 363(1987).
b) J. Ralph, Holzforschung, 41(1), 23(1986).
c) D.R. Dimmel and D. Shepard, J. Wood Chem. Technol., 2(3), 297(1982).
d) P.B. Apfeld and D.R. Dimmel, J. Wood Chem. Technol., 8(4), 461(188).

16. G. Gellerstedt and E.L. Petterson, Acta Chemic. Scand., B 29, 1005(1975).

17. A. Castellan, N. Colombo, C. Cucuphat and P.F. Violet, Holzforschung, 43(3), 179(1989).

18. K.V. Sarkanen, C.H. Ludwig, Lignins, Academic Press, 55(1971).

19. A.J. Ragauskas, unpublished results.

20. A.J. Michell, P.J. Nelson and C.P. Garland, Appl. Spectros., 43(8), 1482(1989).

21. S.E. Lebo, Jr., Doctoral Dissertation, The Institute of Paper Science and Technology, Appleton. Wi, 1988.

22. S.Y. Lin and K.P. Kringstad, Norsk Skogindustri, 9, 252(1971)

23. I. Forsskahl, J. Gustafsson and A. Nybergh, Acta Chem. Scanda., B35, 89(1981).

24. S. Patai, Ed., The Chemistry of Quinoid Compounds, Wiley-Interscience, New York,1974.

25. G.R. Desiraju, Ed., Organic Solid State Chemistry, Elsevier,Amsterdam, 1987.

26. R.W. Johnson, Tappi J., 1989(Dec), 181.

PROJECT SUMMARY FORM

DATE: March 21, 1990

PROJECT NO. 3566: STRONG, INTACT HIGH YIELD FIBERS

PROJECT LEADER: A. W. Rudie, T. J. McDonough

IPST GOAL:

A significant increase in the yield of useful fibers

OBJECTIVE:

Develop wood fiber separation and treatment methods that will allow good control of the strength, physical form and bonding characteristics of the resulting fibers.

CURRENT FISCAL YEAR BUDGET: $150,000

PRIOR RESULTS:

Chemimechanical pulps have been prepared with sheet strength approaching that of kraft and containing fibers having higher breaking load than kraft fibers. Fibers sampled from high yield pulps have been shown to be stronger than corresponding wood sections, indicating that at least some of the fibers in the pulp have retained much or all of their native strength. On the other hand, strong correlations between fiber length, fiber strength and compacted fiber cross-sectional area indicate that the less robust (earlywood) fibers are routinely damaged and broken in refining.

Batch laboratory fiberizations have provided information on the fiber separation mechanism and its implications. Thermal softening was shown to have important effects only at short retention times and only for wood which had not been chemically pretreated. Increasing temperature had a negative effect on the efficiency of fiber separation from chemically treated wood chips.

A series of trials were run in a member company's thermomechanical pulping pilot plant to establish the effects of fiberization temperature on fiber strength retention. The results show that fiberization at 160°C gives stronger fibers than 120°C, and that fiber fragments tend to be weaker than intact fibers. These findings suggest that fiber strength is reduced during fiber separation and that the extent of fiber damage increases with increasing resistance to separation. This confirms that conventional thermomechanical pulping sacrifices strength for surface development by separating fibers at less than optimum temperatures for fiber strength retention.

Efforts to cause strong, intact chemimechanical fibers to form a sheet with kraftlike strength were pursued. Chemical treatment followed by refining gave sheets of tensile strength in excess of 8 km breaking length; hot pressing and artificial bonding were less successful (6 to 5 km respectively). Addition of kraft fines gave promising initial results with unrefined samples.

In related student research, the distribution of bound sulfur in the cell walls of chemically treated wood has been investigated, in view of its implications for chemimechanical pulp properties. A gradient within the S_2 layer was observed under all treatment conditions. The distribution can be manipulated to a limited extent by varying liquor pH and Na_2SO_3 concentration. In addition, a study of prehydrolysis as a pretreatment in chemimechanical pulping has revealed beneficial effects that may lead to a new pulping process.

Recent activity has consisted of support for the development of a consortium to conduct research on chemithermomechanical pulping and thermomechanical pulping. The consortium, combining the research efforts of Georgia Tech, IPST and Herty Foundation, is led by Georgia Tech.

The consortium will make use of a two-stage continuous pilot refining system employing a Sunds Defibrator CD-300 pressurized first stage refiner and a Defibrator ROP-20 atmospheric second stage refiner. It is also equipped with a KMW chip classifier, atmospheric presteaming, atmospheric pre-impregnation, a pressurized second stage of impregnation, pressurized steaming and interstage washing. The system was donated to Georgia Tech by Mead Corporation and has been installed at the Georgia Power Technical Application Center near IPST.

Proposals have been developed for three initial projects to be undertaken by the consortium. They deal with chip size effects, manufacture of CTMP from dense hardwoods, and pulping juvenile wood of southern pines.

SUMMARY OF RESULTS SINCE LAST REPORT:

Activity for the last six months has been confined to shakedown and start-up of the Georgia Institute of Technology CTMP Process Consortium Pilot Plant. Several equipment and operating problems have been resolved and work continues on others. In moving and installing the refiners, problems have arisen in broken steam supply lines, poorly installed seals and worn or damaged bearings. Operating problems have been encountered with blow line and cyclone plugging and poor level and temperature control. Operational success has been achieved in both thermomechanical and open discharge (RMP) operation, but additional experience and fine tuning of procedures is still needed.

PLANNED ACTIVITY THROUGH FISCAL YEAR 1990:

The consortium is committed to pursuing three projects on the influence of raw materials on high yield pulping and pulp quality. These projects investigating the effects of chip size on high yield pulping, the manufacture of CTMP from dense hardwoods, and the pulping of juvenile southern pines, have been approved by a group of prospective consortium member companies, and are outlined in detail in the consortium prospectus. The juvenile pine project will be carried out by IPST. Experimental work on these projects will begin as soon as sufficient funding is secured. A grant proposal has been submitted to the Department of Energy, and if approved, will provide funding for the consortium in July of this year.

An alternative IPST project is planned to make use of the pilot plant until the consortium research begins. The objective is to apply our earlier work on fiber strength and to use the Alkaline Peroxide Mechanical Pulping (APMP) process to maximize both fiber and bond strengths in pulping dense southern hardwoods. Initial efforts will concentrate on optimizing chemical addition for strength and brightness development of typical southern hardwoods, oak and sweet gum. Particular attention will be paid to evaluating and controlling fiber development in the screw compression chip destructuring operations of the process. This work will use the electron microscope to evaluate the locations of fracture in chips impregnated under various conditions, and holopulping with light and electron microscopy to identify the extent of fiber damage in impregnated chips and fully refined samples. The use of chemical pulping procedures to develop bond strength so that fiber strength can be evaluated without resorting to tedious single fiber measurements will also be evaluated.

POTENTIAL FUTURE ACTIVITY:

Future activity will be coordinated with project proposals of the consortium. IPST member funded research will build on both DOE and consortium member-funded projects. Emphasis will be on translation of fiber strength to improved paper properties. The consortium program for 1991 likely will concentrate on the refining process. Likely projects to be considered will be alternative chemical treatment methods to reduce energy demand and/or improve pulp properties, development of refiner plates for production of high yield pulps from dense hardwoods, improvements in process control and on line process optimization with MAPPS, and evaluation and development of new process instrumentation.

PROJECT SUMMARY FORM

DATE: March 20, 1990

PROJECT NO. HIBRT: HIGH BRIGHTNESS, HIGH YIELD PULPS

PROJECT LEADER: A. W. Rudie

IPST GOAL:

A significant increase in brightness and decrease in bleaching cost for high yield pulps.

OBJECTIVE:

Develop a cost effective method to produce high yield pulps of high and stable brightness.

CURRENT FISCAL YEAR BUDGET: NONE ($100,000 for FY-1991)

PRIOR RESULTS:

New Project

PLANNED ACTIVITY THROUGH FISCAL YEAR 1990

Exploratory work will include the following:

1. Evaluate the use of oxygen and oxygen followed by Peroxide for bleaching Southern Pine TMP and CTMP.

2. Evaluate the use of oxygen fortified peroxide bleaching on Southern Pine TMP and CTMP.

3. Evaluate the use of oxygen and oxygen followed by Peroxide for bleaching hardwood TMP and CTMP.

4. Evaluate the use of oxygen fortified peroxided bleaching on hardwood TMP and CTMP.

POTENTIAL FUTURE ACTIVITY:

This project will emphasize development of effective processes for achieving high brightness and stable brightness in high yield pulps. Possible future activities include:

An evaluation of metal and metal complex catalyzed oxygen and/or peroxide bleaching of high yield pulps.

Evaluation of peroxide bleaching at ultra-high pulp consistencies.

RELATED STUDENT RESEARCH:

* Mike Rice. M.S. project entitled "An Evaluation of Quinones and Their Contribution to Brightness Reversion of Southern Pine and Aspen TMP".

Project HIBRT Status Report

HIGH BRIGHTNESS, HIGH YIELD PULPS

Background:

For many years, the rallying cry of high yield pulping research has been 90-90-9; 90 points brightness, 90% yield and 9 km breaking length. Although this remains to be achieved, market aspen CTMP is approaching the most significant properties of bleached kraft pulps from dense hardwoods used in many integrated mills (2). We are now seeing a shift in the R & D emphasis to other characteristics of high yield pulps that still fall far short of chemical pulp performance. For example, brightness reversion of high yield pulps is considered to be the primary characteristic preventing bleached aspen CTMP from making significant inroads into the printing and writing papers market (3).

Although brightness reversion is a significant barrier to market penetration in some paper grades, it has not prevented the acceptance of CTMP in many paper products in Europe (4), or the development of a Market BCTMP industry in Canada (1). The most significant commercial limitation of high yield pulps in the U.S. is a bit more fundamental, it costs too much. If it means handling an additional pulp furnish, market BCTMP purchased at 80 to 90% of the market hardwood kraft price may not be a bargain, particularily for a pulp that is still 10 points short of standard market pulp brightness. In most integrated mills in the U.S., the high energy and bleaching costs of paper grade BCTMP would result in higher unit manufacturing costs than for bleached kraft softwood (5). It is for good reason that, 10 years after the conversion of Rockhammars Bruk to CTMP, there is yet to be a CTMP mill brought on line in the southern U.S.

In order to lower the manufacturing costs of high yield pulps in the U.S. the bleaching costs for the high brightness grades and/or the energy requirements of all grades must be reduced. This project will concentrate on investigating alternative bleaching processes with potential to reduce bleaching costs and/or increase bleached brightness in high yield pulps.

Most work on achieving high brightness has concentrated on the development of multi-stage bleach sequences using conventional bleaching chemicals (6 - 10). Although these sequences have achieved higher brightness and some reduction in chemical requirements, overall peroxide and hydrosulfite charges are still quite high and at $0.60 per pound (9) for both chemicals, the bleaching costs are prohibitive.

In reviewing low cost oxidizing and reducing agents capable of bleaching pulp, one alternative is oxygen. The similarities in reactivity of hydrogen peroxide and oxygen in kraft pulp bleaching (11) suggest that oxygen alone or with hydrogen peroxide might also work in bleaching mechanical pulps.

It is recognized that there are conditions under which oxygen cannot be used to bleach high yield pulps. Thermal reversion studies indicate that oxygen will not work as a bleaching agent at pH 5 to 7 and low oxygen pressures (15). Under the alkaline conditions and high oxygen pressures typical of oxygen pulping and bleaching, high yield pulps also lose brightness (16). The presence of oxygen is implicated in both thermal (12,13) and light (13,14) induced brightness reversion. From another point of view, this provides an incentive for pursuing an oxygen bleaching process. Oxygen is clearly reactive with lignin structures that lead to color formation and may, therefore, be capable of imparting brightness and brightness stability to the resulting pulps if it can be employed without significant loss in yield.

For many years, the stabilized peroxide bleaching of mechanical pulps has generally been thought to proceed by different mechanisms (17) than are peroxide bleaching of kraft pulps, avoiding the radical intermediates implicated in chemical pulp bleaching and oxygen delignification (14,18). Recent evidence of an induction period in stabilized peroxide bleaching and accelerated bleaching by gamma-ray induced hydroxyl radicals (19) demonstrate that radical reaction pathways are important in peroxide bleaching of mechanical pulps. In fact, with completely stabilized peroxide and in the absence of oxygen, the product of peroxide reactions with phenolic α-carbonyl structures are hydroquinones and catechols (20 - 22), precursors to the quinones generally accepted as instrumental in brightness reversion (23). Given the presence and activity of oxygen in peroxide bleaching of kraft pulps (14), oxygen is a logical consideration for bleaching high yield pulps. With a chemical cost around $0.05 per pound oxygen can certainly reduce bleaching costs, if it can be used effectively.

The primary chromophores in mechanical pulps, α-carbonyls and ring conjugated olefins on free phenolic lignin units, are the most acidic of the phenolic groups and should undergo alkaline activation at near neutral pH where the majority of the lignin phenolic structures are still in their acid form. For example, the α-carbonyl acetoguiacone, reacts with oxygen at a pH of 7.5 (24) and milled wood samples are still very reactive to oxygen delignification in bicarbonate buffers (25). The quinones created under mild conditions (15) should be readily degraded at higher temperatures and oxygen pressures or by addition of hydrogen peroxide to the bleaching process. It will be critical to prevent the condensation reactions prevalent in low alkali and acidic oxygen delignification processes (24,26).

Under acidic conditions, oxygen may also prove to be an effective high yield bleaching agent. Lignin model studies show that at pH 2 - 3.5 the α-carbonyls and styrene/conniferaldehyde units are the most reactive lignin structures while free phenolics and the β-aryl ether structure are relatively inert (26).

If oxygen by itself does not bleach high yield pulps, there are good reasons to expect that combining oxygen with hydrogen peroxide will. The product of peroxide anion attack on lignin model compounds is often a catechol or hydroquinone which looses a proton under the alkaline conditions and becomes somewhat stable against further reactions with the peroxide (20 - 22). The hydroquinones and catechols however are quite sensitive to oxidation by molecular oxygen (15) and the resulting quinones react much more readily with peroxide (14,27). Fortifying a conventional peroxide bleach stage with oxygen may not only reduce the peroxide requirements but should also reduce the sensitivity of the pulp to light and heat induced reversion.

Preliminary experiments will be conducted as follows: Samples of cottonwood and loblolly pine will be refined in the Sprout Waldron atmospheric refiner to 150 ml. Canadian Standard Freeness. Oxygen bleaching and oxygen fortified peroxide bleaching experiments will be conducted at 80 deg. C, 80 psig and starting pHs of 2.0, 5.0, 8.0 and 11.0. In cases where these conditions are too mild to give a noticeable change in pulp brightness, a second reaction will be conducted at 120 deg. C. and 120 psig. Mild conditions are important to avoid extensive yield losses. The oxygen fortified peroxide bleaching experiments will be stabilized with DTPA, sodium silicate and magnesium sulfate and will be evaluated against a peroxide control conducted under a nitrogen atmosphere. Any usable bleaching response will be followed up with a additional experiments to identify optimum condition for brightness gain. All pulp samples will be second stage bleached with 1% sodium hydrosulfite and 1.5% hydrogen peroxide. Samples will be evaluated for brightness, scattering coefficient, absorption coefficient and light induced brightness reversion. Samples will also be evaluated for handsheet physical properties.

Subsequent experimentation will be planned as the results of the above preliminary experiments become available. It will include exploration of the utility of using metal ions and their complexes as catalysts in oxygen abd peroxide bleaching.

References:

1. Sharman, P. M., Pulp and Paper, "BCTMP Special Report", 63(5), pp S3-S32, (1989).

2. Simmonds, F. A., Keller, E. L. and Chester, G. H., Southern Pulp and Paper Manufacture 8: 57(1963).

3. Cockram, R., "CTMP in Fine Papers" Int. Mech. Pulping Conf. Proceedings , pp 20-24, (1989).

4. Jackson, M. and Akerlund, G., "Chemithermomechanical Pulp Production and End-Uses in Scandinavia", TAPPI 68(2): 64 (1985).

5. Aurell, R., "Prospects For Mechanical Pulps in Different Regions of the World", Int. Mech. Pulping Conf. Proceedings pp. 282-290, (1985).

6. Joachimides, T. "High Brightness Mechanical Pulps", TAPPI 1989 Pulping Conference Proceedings, p. 131 (Seattle, Oct 22-24, 1989).

7. Lougheed, M. and Presley, J. R., "The Upgrading of a Bleach Plant: Mill Experience with a Two Stage Peroxide Bleach Plant Retrofit",TAPPI 1989 Pulping Conference Proceedings, p. 261 (Seattle, Oct 22-24, 1989).

8. Hooks, J., Wallin, S. and Akerlund, G., "Optimization and Control of Two-Stage Peroxide Bleaching", TAPPI 1989 Pulping Conference Proceedings, p. 267 (Seattle, Oct 22-24, 1989).

9. Berger, M. I., Meier, J., Suss, H. U. and Schmidt, K., Two-Stage Peroxide Bleaching - Method of Choice for Mechanical Pulps", TAPPI 1989 Pulping Conference Proceedings, p. 249 (Seattle, Oct 22-24, 1989).

10. Leduc, C. Gagne, M. C., Barbe, M. C. and Daneaut, C., "Bleaching of Chemimechanical Pulps: A Comparison of Oxidizing and Reducing Multistage Sequences", TAPPI 1989 Pulping Conference Proceedings, p. 627 (Seattle, Oct 22-24).

11. Gierer, J. and Imsgard, F., "The Reactions of Lignins With Oxygen and Hydrogen Peroxide in Alkaline Media", Svensk Papperstid. 80(16):510(1977). (1989).

12. Gellerstedt, G., Pettersson, I. and Sunkin, S., "Light Induced and Heat-Induced Yellowing of Mechanical Pulps", Svenk Papperstid. 86(15): R157(1983).

13. McLellan, G., Collette, J. C., Fairbanks, M. G. and Whiting, P., "Factors Affecting Ambient Thermal Reversion of High Yield Pulps" TAPPI 1989 Wood and Pulping Chemistry Symposium Proceedings, p. 535 (Raleigh,

14. Leary, G. T., "The Yellowing of Wood by Light", TAPPI, 51(6):

15. Gellerstedt, G. and Pettersson, B., "Autoxidation of Lignin", Svensk Papperstid. 83(11): 314(1980).

16. Marton, R., Brown, A. and Granzow, S., Oxygen Pulping of Thermomechanical Fiber", TAPPI, 58(2): 64(1975). 257(1968).

17. Agnemo, R., Gellerstedt, G. and Lindfors, E.-L., "Reactions of Lignin with Alkaline Hydrogen Peroxide", 1979 Canadian Wood Chemistry Symposium Preprints, p. 13 (1979).

18. Smith, P. K. and McDonough, T. J., Transition Metal Ion Catalysis of the Reaction of a Residual Lignin Related Compound with Alkaline Hydrogen Peroxide", Svensk Papperstid., 87(12): R106(1985).

19. Sjogren, B., Zachrison, H. and Rejtberger, T., "The Importance of Radical Reactions For Brightness Increase in Hydrogen Peroxide Bleaching of Mechanical Pulps", TAPPI 1989 Wood and Pulping Chemistry Symposium Proceedings p. 161 (Raleigh 1989).

20. Gellerstedt, G., and Agnemo, R. "The Reactions of Lignin With Alkaline Hydrogen Peroxide Part III: The Oxidation of Conjugated Carbonyl Structures", Acta. Chem. Scand. B34(4): 275(1980).

21. Dakin, H. D., "The Oxidation of Hydroxy Derivatives of Benzaldehyde, Acetophenone and Related Substances", Amer. Chem J., 42(6): 477(1909).

22. Reeves, R. H. and Pearl, I. A., "Reaction Products Formed Upon the Alkaline Peroxide Oxidation of Lignin-Related Model Compounds" TAPPI, 48(2): 121(1965).

23. Lebo, S. E., Lonsky, W. F. W., McDonough, T. J. and Medvecz, P. J., TAPPI 1988 Intl. Pulp Bleaching Conf., p 247 (Orlando, 1988).

24. Mih, J. F. and Thompson, N. S., "The Effect of Liquor Composition on the Rate of Reaction of Lignin Model Compound Acetoguaiacone in Oxygen and Alkali", J. Wood Chem. and Tech., 3(2): 145(1983).

25. Abrahamsson, K and Samuelson, O. "Oxygen-Alkali Cooking of Wood Meal. Part VI: Influence of Carbon Dioxide at Different Concetrations of Active Alkali", Svensk Papperstidn. 78(11): 417(1975).

26. Gierer, J. and Nilvebrant, N.-O., "Studies on the Degredation of Lignins by Oxygen in Acidic Media", Int. Symp. Wood and Pulping Chem. Proceedings, 4 pp. 109-112(May 23-27, 1983).

27. Gellerstedt, G. Hordell, H.-L. and Lindfors, E.-L., "Reactions of Lignins With Hydrogen Peroxide. Part IV: Products From Oxidation of Quinone Model Compounds", Acta. Chem. Scan., B34: 669(1980).

PROJECT SUMMARY FORM

DATE: March 20, 1990

PROJECT NO. 3605: COMPUTER MODEL OF RECOVERY FURNACE

PROJECT LEADER: H. L. Empie

IPC GOAL:

Increase the energy efficiency and productivity of recovery boilers

OBJECTIVE:

Develop a comprehensive mathematical model of fireside processes in a recovery furnace. The model is to be based on first principles and will incorporate and integrate the results of ongoing fundamental studies of black liquor combustion.

CURRENT FISCAL YEAR BUDGET (JULY 1989 to JUNE 1990): $40,000

PRIOR RESULTS:

A three-dimensional model of a kraft recovery furnace has been developed as a result of three Ph.D. theses. Based upon data from black liquor burning in a single particle reactor, sequential models of the burning stages-drying, volatiles burning, and char burning were written. This burning model was then integrated with a computational fluid dynamics model (called FLUENT as marketed by Creare, Inc. of Hanover, NH) to fully characterize the physical and chemical unit processes occurring in the recovery furnace. One typical mill example was simulated resulting in a final, converged solution. A major drawback that was identified from this exercise was the large computational time requirement, namely over three months on a Micro VAX II.

This work was presented in the previous PAC report under Project 3473-6 because of its close connection with the DOE-funded activity on the fundamentals of black liquor combustion.

SUMMARY OF RESULTS SINCE LAST REPORT:

Simulations with the recovery furnace model have provided extraordinary insight into the nature of the black liquor combustion process. The model shows that the main mode of combustion is particle burning. Carryover is not simply determined by liquor spray size, but rather by a complex relationship between drop size, gas flow patterns, and oxygen concentrations. Gas flow patterns are determined primarily by the air inlet geometry and are not greatly modified by liquor sprays and in-flight combustion. Bed shape can have a strong effect on gas flow patterns.

The model is being applied to a Weyerhaeuser recovery furnace in Plymouth, N.C. Convergence has not been achieved, as judged by the non-convergence of carryover values. A User's Manual is being written which describes the model technology, details the actual keystrokes and prompts needed to enter data, and presents example calculations and the program code.

PLANNED ACTIVITY THROUGH FISCAL YEAR 1990:

Computation time for the model must be significantly reduced if the model is to be used as an effective tool in the improvement of recovery boiler operation. Options to be explored include speed-up of the computational fluid dynamics code, model simplification, and adaptation of the model to a faster state-of-the-art computer. The model must also be validated if it is to be used by industry. To accomplish this, a velocity probe will be developed to measure flue gas velocities in the furnace cavity of an operating recovery boiler. Results will be compared with model predictions, and if significant discrepancies exist, revisions to the model will be considered. We have hired a new faculty member, Dr. Robert Horton, to assume responsibility for model enhancements. Support funding is being solicited from OIP-DOE.

STUDENT RESEARCH:

A. Jones, Ph.D.-1988, A. Walsh, Ph.D.-1988, D. Sumnicht, Ph.D.-1989, T. Kindler, M.S.-1990.

Project 3605 STATUS REPORT

COMPUTER MODEL OF RECOVERY FURNACE

Three - Dimensional Modeling of a Kraft Recovery Furnace

(T. Grace, A. Walsh, A. Jones, D. Sumnicht & T. Farrington)

There are serious limitations to one-dimensional and two-dimensional recovery furnace models. A critical need is an ability to relate critical performance parameters (extent of carryover, gas temperatures, combustible and oxygen concentrations, bed growth or depletion, reduction efficiency, etc.) to the firing practice and furnace design. This can only be done with a three-dimensional model that can handle the complex gas flow patterns that exist in recovery furnaces.

A three-dimensional mathematical model of a kraft recovery furnace was recently developed as three Ph.D. theses at the Institute of Paper Science of Technology. This model is based on a computational fluid dynamics package (FLUENT) that is modified to incorporate in-flight black liquor particle burning and char bed burning. It is called FLUENT-RFM where RFM stands for recovery furnace model.(1)

Description of FLUENT-RFM

FLUENT-RFM is based on a finite-volume solution of the governing equations for mass, momentum, energy, and species concentration for the gas phase. In-flight burning of liquor drop/particles and bed burning are included and affect the gas phase through source-sink terms.

Gas Phase

The gas flow velocities are found by a finite-volume solution of the mass, momentum, and energy conservation equations in three-dimensional geometry. The furnace volume is divided into a large number of cells (50,000 in our case) and the difference equations are solved numerically. The interaction between the liquor phase and the gas is handled through source/sink terms using the psi-cell approach. In the psi-cell (particle source in cell) approach, the gas phase conditions (velocity, pressure, enthalpy, and chemical composition) are treated as a continuum in a fixed coordinate system. The properties of the gas are then a function of position only. The properties of the liquor phase are described in a reference frame moving with the individual drop/particle and are determined at small discrete time steps as the particle passes through the gas phase. Trajectory equations for individual drops are written in a fixed reference frame and are coupled with state equations that describe the drop properties as a function of time. The drop/particles are able to exchange mass, momentum and energy with the gas phase through source and sink terms in the gas flow equations. The position of a drop/particle at any time, t, uniquely determines which cell it is in. The change in state properties become the source and sink terms and are added to the cell which the drop/particle is in at time, t. The approach is illustrated in Figure 1. If the drop is drying as it passes through the cell, the amount of water evaporated from the drop during the interval would be a mass source of water vapor to that cell, and the amount of heat absorbed by the drop would be an energy sink.

The gas phase properties of interest are the three velocity components, pressure, temperature, density, and species concentration. The gas species considered are oxygen, water vapor, carbon monoxide, carbon dioxide, fuel (pyrolysis gases), and inerts (nitrogen). Sulfur gases are not handled in the present state of the model. Temperature is determined from enthalpy balances using temperature dependent specific heats for each of the gas species. Gas density is determined using the ideal gas law. Turbulence is handled through effective gas properties determined from the k-epsilon model of turbulence. Radiation energy fluxes are determined from a six-flux radiation model, one flux in each of the positive and negative coordinate directions. Rates of chemical reactions between gases can be controlled by either a chemical reaction rate or the degree of turbulent mixing. In practice, the rates were controlled by turbulent mixing.

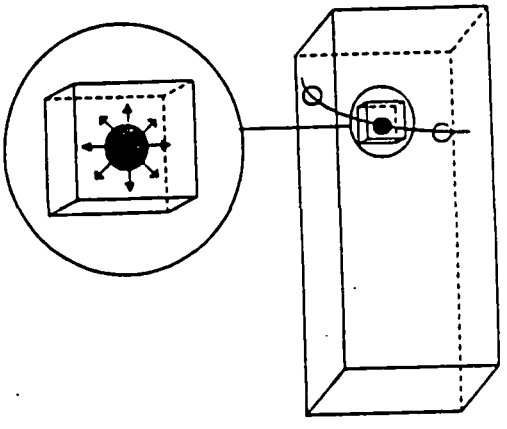

Figure 1. Illustration of PSI-cell approach.

Black Liquor Phase

The behavior of the black liquor phase was described by trajectory equations for the individual drop/particles and by a drop combustion model. The trajectory equation relates the change in particle momentum to the drag force exerted on the particle by the gas and to the force of gravity. The drag force is related to the square of the relative velocity between the particle and the gas, the particle cross-sectional area, the gas density and a drag coefficient. Standard correlations for spheres are used for the drag coefficients. At present, the number of drops used in a simulation is 10,000. Each drop represents an equal mass fraction of the spray and each drop has a unique initial position, velocity, and diameter. The diameter distribution was assumed to be log-normal. The initial speeds of all the drops were assumed to be the same, regardless of size or direction. Angular boundaries in the vertical and horizontal plane are set and the mass of the spray is assumed to be evenly distributed between the boundaries.

The combustion is modeled as four distinct stages; drying, volatiles burning, char burning and inorganic oxidation. Drying is treated as an external heat transfer controlled process. Some swelling of the drop during drying is allowed. Ignition signals the start of the volatiles burning stage. The solids content at which ignition occurs is a user-specified parameter. Volatiles burning is handled by an empirical rate equation developed by Crane (2). Swelling during volatiles burning is handled by assuming the drop diameter increases linearly during the volatiles burning period, reaching a maximum at the end of the period. The user specifies the maximum extent of swelling. Char burning is treated as an oxygen mass transfer limited process. A standard Sherwood number correlation for flow past a sphere is used to calculate the mass transfer coefficient. The volume of the char particle is allowed to decrease during char burning linearly with the mass of carbon remaining. At the end of the char burning period, the inorganic smelt drop is allowed to oxidize and convert sodium sulfide to sulfate. The rate of oxidation is treated as an oxygen mass transfer limited process. The user sets the maximum allowable mass increase, in effect setting the sulfidity and reduction state after char burning.

The species in the drop/particle are water, fuel, fixed carbon and ash (inorganic). The information on the liquor supplied by the user is summarized in Table 1. Liquor density and diameter determine the initial mass of the drop. Solids content determines water, fraction volatiles determines fuel, fraction char carbon determines fixed carbon and the amount of smelt oxidation represents the fraction of sulfur that can be oxidized. Water is transferred to the gas phase during drying, fuel is transferred during volatiles burning, fixed carbon is converted to CO and CO_2 during char burning, and inorganics are allowed to oxidize after char burning is complete. The mass exchange terms and oxygen sinks that are calculated by FLUENT/RFM are shown in Figure 2.

Table 1. User-Supplied Parameters for Liquor Phase.

Composition	Burning Characteristics
Liquor density	Solids content at ignition
Solids content	Swelling during drying
Fraction volatiles	Swelling during volatiles burning
Fraction char carbon	$CO/(CO + CO_2)$ ratio
Amt. of smelt oxid.	
Spray Parameters	
Initial diameter distribution	
Vector velocity distribution	

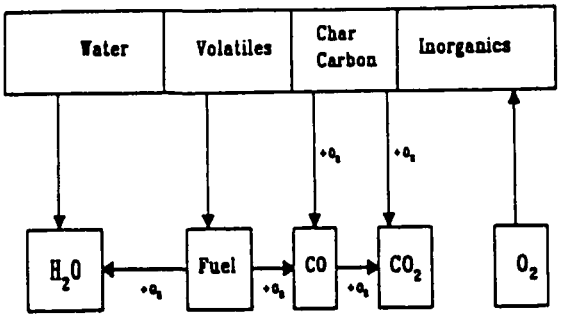

Figure 2. Mass exchange between liquor and gas phases.

Char Bed

The char bed is modeled using a special type of cell, the bed cell. Bed cells act like wall cells in that they act as a barrier to flow, but they differ in being able to exchange mass and energy with the gas phase (normal wall cells can only exchange energy). All of the bed behavior is assumed to occur at the interface between the bed and the gas phase. The bed is a sink for oxygen from the combustion air and from oxidized smelt drops landing on the bed and a source for CO and CO_2. The burnup of carbon by oxygen is assumed to occur through a sulfate-sulfide cycle. Oxygen reaching the bed is assumed to oxidize sulfide to sulfate and this rate is assumed to be controlled by the rate of oxygen mass transfer. Any sulfate present is allowed to react with carbon by a temperature dependent kinetic expression. This permits the state of reduction to be determined as a resultant of two competing rate processes. Gasification of the char carbon by reaction with CO_2 and H_2O is also allowed. Heats of reaction for the individual bed reactions are accounted for, and the bed is able to exchange heat with the gas phase above by radiation and convection. The temperature of each bed cell is determined by an enthalpy balance over the cell.

Bed cells do not operate at steady state as far as the carbon material balance is concerned. The temperature- and gas composition-dependent rate processes determine the rate at which char carbon is consumed on the bed. The rate at which carbon is supplied to any particular area of the bed (any particular bed cell) is determined by particle trajectories above the bed and the associated particle state variables. These do not normally balance on any given cell. The model simply keeps track of the rate of carbon accumulation or depletion in any given bed cell. The bed reactions per se only involve char carbon and inorganic. If the material landing on the bed is not fully dried or pyrolyzed, the residual water and/or fuel content is put directly into the neighboring gas cells.

The trajectories of some of the drop/particles may cause them to strike the wall. These are handled by assuming any liquor particle striking the wall sticks, dries, and partially pyrolyzes and then falls down to the char bed. For all material reaching the wall, all of its residual water and 1/2 of its residual fuel are transferred to the neighboring gas cells. The rest of the material is then directed to the char bed immediately below.

Overall Structure

The choice of FLUENT as the computational fluid dynamics code underlying the model was based on its versatility, applicability, and the availability of the source code for modification. Model development included writing original code for black liquor burning in flight and on the char bed, and modifying the base FLUENT code to provide for the five chemical species in the gas phase, revising the combustion model, and providing the source and sink terms needed to communicate with the bed and in-flight burning models.

Preliminary Results

The feasibility of 3-dimensional modeling of kraft recovery furnaces was demonstrated by carrying out a "base case" simulation. This "base case" used a generic recovery furnace that is shown in Figure 3.

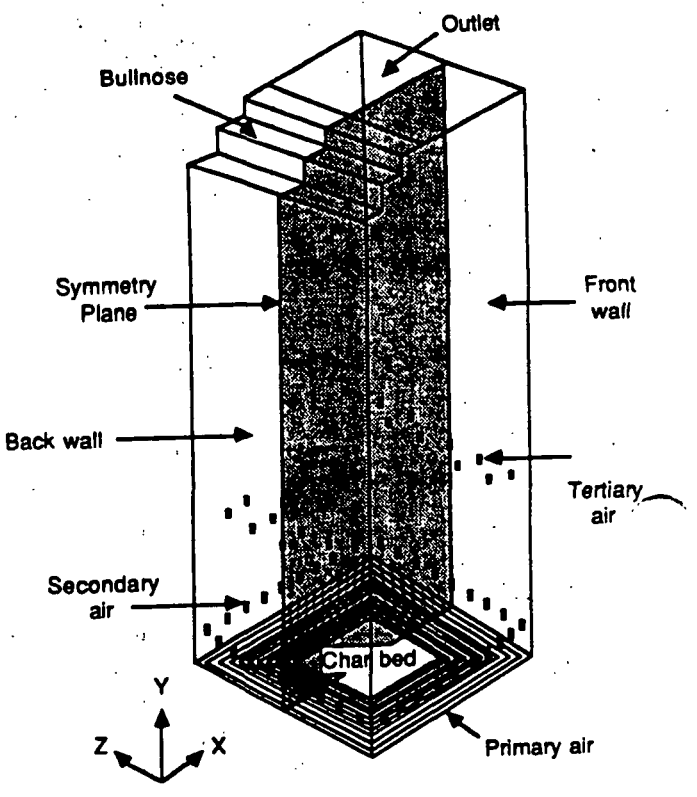

Figure 3. "Base-Case" Furnace

The furnace is 10 meters by 10 meters by 30 meters high. The bull nose, located on the back wall, occupies about one-half of the furnace cross-section. There are three basic levels of air entry. Primary air is modeled as a slot extending the entire length on all four walls. The width of the slot is chosen so that the total primary air port opening matches typical values. Secondary air is located two meters above the primary air. A total of 36 secondary air ports are used, evenly spaced on all four walls. Tertiary air is located on the front and back walls at two different elevations above the liquor gun openings. Nine ports are used on each wall and they are staggered and interlaced so that no tertiary nozzles are directly opposed to each other. The bottom row of tertiary nozzles is located 8.5 meters above the floor and the top row is 1.25 meters above the bottom row. Four liquor guns are used, located 6 meters above the floor at the midpoints on each wall. The bed shape is a truncated pyramid extended to a level just below the secondary air ports. A symmetry plane is used (only 1/2 of the furnace is actually modeled) in order to make the most effective use of the 50,000 nodes.

The black liquor solids firing rate is 11.0 kg/m^2 min (2.25 lb./ft^2 min). The solids content is 65% and the high heating value is 6600 Btu/lb. The mean drop diameter was 2.5 mm. The total air rate is 86.2 kg/sec (about 10% excess air). The primary air is 45% of the total at an entrance velocity of 43 m/sec, secondary air is 34% of the total at 39 m/sec, and the tertiary air is 21% of the total at a velocity of 95 m/sec. The air temperature was 400 K.

The model is capable of giving a great deal of information about the burning process in the furnace. At each node point the vector velocity, temperature and concentration of each species in the gas phase is found. Particle trajectories and state information are available. Thus carryover rates and bed char fluxes can be determined. In addition composite rates of drying, volatiles burning, char burning, etc., can be determined as a function of position and displayed. Heat fluxes to the walls and to the char bed can be found. Average reduction rates are also calculable.

The gas flow paths determined by the model for the base case are complex but in general agreement with expectation. The dominant feature, illustrated in Figure 4, is a central core of high upward velocity. Around the perimeter, particularly in the corners, is a region of downflow. The core is disrupted by the tertiary air jets but reforms above the tertiary air level and persists past the bullnose and out of the furnace cavity. The core is formed by the convergence of the four-wall primary and secondary air above the char bed.

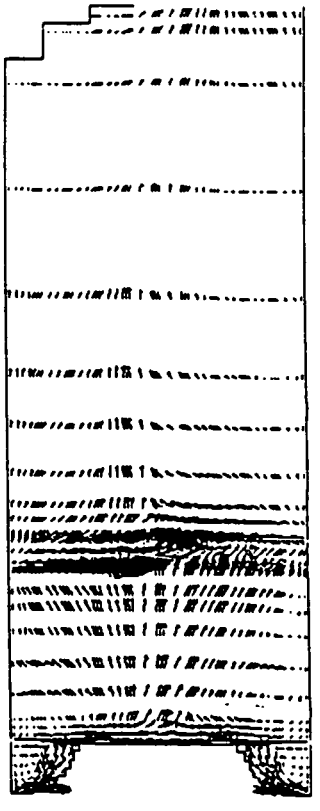

Figure 4. Gas flow pattern at center plane.

Gas temperature tends to be highest in the core, and the O_2 concentrations the lowest. Average gas temperatures as a function of height are shown in Figure 5. The general shape of the curve agrees with experience. The peak in temperature occurs slightly above the surface of the char bed where large amounts of CO and pyrolysis gas are present and able to react with secondary air. Three dimensional distribution of temperature and gas concentrations is complex and strongly coupled to details of the gas flow pattern and particle trajectories.

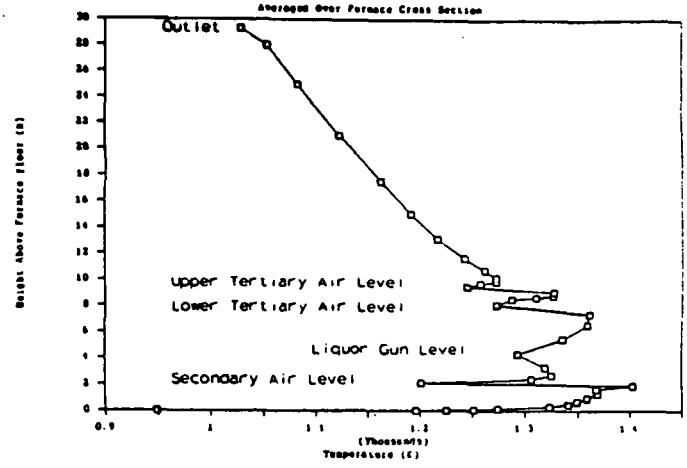

Figure 5. Average Temperature as a function of furnace height.

Black liquor burning is highly complex and dependent on the details of flow patterns, gas temperatures and O_2 concentrations as well as initial drop size and velocity. Carryover of particles out of the furnace cavity, in particular, is highly interdependent on many variables. Color raster plots of the trajectories of drops with an initial diameter of 0.5 mm are very different for the nozzles on the front, back and side walls. Thus drop size and average gas velocity are not the only determinants to carryover.

The bed model indicates that carbon gasification by reaction with CO_2 and H_2O is an important part of bed burning. Figure 6 shows bed burning data calculated from the model with and without the gasification reactions included. The addition of the gasification reactions converts the base case from one in which there is substantial buildup of carbon on the bed to one where there is a slight depletion of carbon.

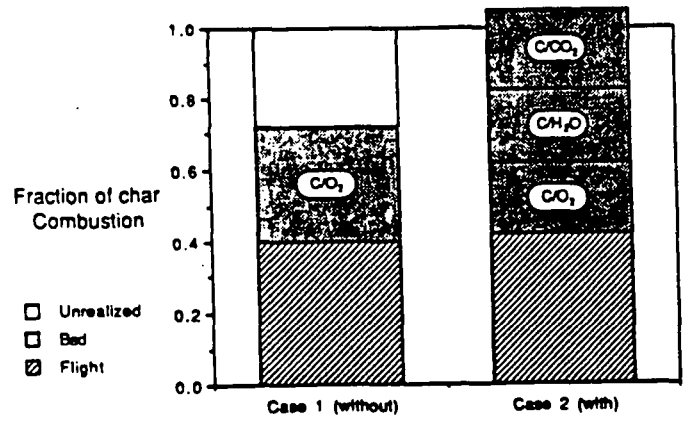

Figure 6. Comparison of char combustion without and with gasification reactions.

Process Insights

The model and the results of the base case simulation provide a great deal of insight into the processes occurring in recovery furnaces. The important role of in-flight burning is clearly evident. Burning of black liquor is primarily a process of drop/particles burning in flight and not one of burning gases produced by pyrolysis and gasification of material delivered directly to the char bed. Oxygen is consumed wherever the particles are present, and the majority of that consumption takes place above the bed. There are limits on the amount of combustion which can take place on the char bed which are imposed by limitations on the ability to transfer oxidants (primarily oxygen) to the bed.

Carryover of material out of the furnace is very complex. There are two distinct modes of carryover, and the variables which control each mode are different. One type is carryover of dense smelt drops which are small enough that their terminal velocity is less than the upward velocity of the gas stream that they are caught up in. The key variables for this mode are drop size and gas velocity, and the temperature and composition of the gas has little effect. The second type is carryover of low density partially burned particles. Black liquor can swell greatly during volatiles release and burning, and the particle only gradually densifies again during char burning. Thus the rate and extent of char burning of in-flight particles is very important, since this controls the particle density and hence the ease of carryover. The extent of carryover of unburnt particles is very strongly influenced by oxygen concentrations in the vicinity of the particle, since the char burning rate is directly proportional to the oxygen concentration. This can override the influence of gas velocities and initial drop size.

The dual nature of carryover is clearly shown in Figure 7. The extent of carryover is not a monotonic function of initial drop diameter. Carryover is high for the smallest drops (the ones that carryover as smelt drops) and then drops off. However, at intermediate sizes the carryover amount again increases and forms a local maximum. This is due to the carryover of incompletely burned liquor particles. The smaller particles require shorter burning times and densify quicker and are not carried over as easily. The biggest particles have higher terminal velocities throughout their histories and get to the bed much more easily. The data on particle in-flight residence times given in Table 2 supports this interpretation.

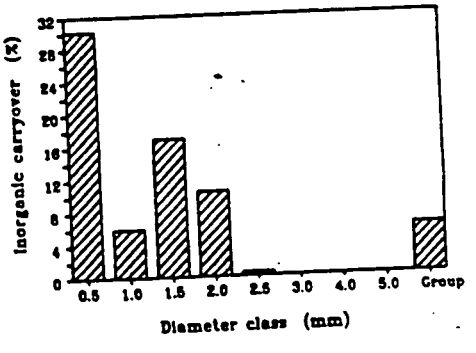

Figure 7. Inorganic carryover vs. initial drop diameter.

Table 2.

In-flight residence times of particles (in seconds).

	Initial Drop Diameter, mm								
	0.5	1.0	1.5	2.0	2.5	3.0	4.0	5.0	lognormal
	Particles Striking Bed								
Average	4.1	4.7	4.7	3.5	5.0	2.5	1.4	1.2	3.3
Max.	7.4	12.6	21.4	20.0	19.7	19.0	1.7	1.4	28.2
Min.	1.8	2.6	1.3	1.2	1.2	1.2	1.2	1.2	1.1
	Particles Carried Over								
Average	8.4	6.1	6.6	7.8	8.7	---	---	---	7.4
Max.	29.8	9.0	10.3	10.5	8.7	---	---	---	22.0
Min.	4.6	4.9	4.9	5.8	8.7	---	---	---	4.6

The model results cast some doubt on the commonly held notion that more uniform spray size distributions will result in less carryover. It was shown, for example, that the same size drops behave completely differently when introduced on the front, back and side wall nozzles. There is clearly a small drop size cutoff, below which smelt drops have a high probability of being entrained. In addition, very large drops are likely to reach the bed in a wet state which would interfere greatly with bed burning rates. However, it is not clear that uniformity inside this range is beneficial. It is possible that highly uniform sprays might cause the combustion process to be more unstable. Further simulations are needed to resolve this issue.

The gas flow patterns appear to be determined primarily by the geometry and conditions at which the air enters the furnace and only secondarily by the liquor sprays and the combustion process. The bed shape, however appears to exert a strong influence on gas flow patterns and the intensity of the central core. In a given furnace, control of the gas flow patterns would be pretty well set by the air distributions and pressures and not highly dependent on other aspects of the operations. There is an implication that some bed shapes are preferred to others and that this should be considered in selecting firing strategies and manipulating spray variables.

Breaking up the center core by momentum transfer may not be the primary function of the tertiary air. There is evidence in the base case simulation that the core was disrupted by the tertiary jets but then reformed above the tertiary elevation. Since particle burnout is a key factor in carryover, it is possible that the most crucial role of the tertiary air is to reinject oxygen into the central core to allow char carbon burnout.

Introducing gasification reactions into the char bed model had a very significant impact on bed burning rates and on the temperature and concentration distributions above the bed. Published data on the rates of char gasification by CO_2 and H_2O are very sparse and the expressions used in the model have a high degree of uncertainty. This is an area where data are urgently needed.

Model Status

A converged solution of a recovery furnace simulation using all of the features present in FLUENT/RFM has been obtained. The results are reasonable and consistent with experience. Behavior which is not in accordance with conventional wisdom is readily interpretable and provides new insight into what is truly happening inside recovery boilers.

Convergence is a major problem with FLUENT-RFM. Convergence requires a certain amount of operator interaction as it proceeds, and some 3500 iterations, involving about 12 trillion mathematical operations, are needed to get a converged solution. About 3 months of CPU time were needed for the base case simulation on a MicroVAX II. The long time needed to obtain a solution has restricted the number of cases which have been run so far. Modifications to the CFD code and use of bigger and faster machines can reduce the time needed for a solution considerably, but the problem remains very computationally intensive.

Another limitation imposed by machine constraints and the long convergence times is the use of a plane of symmetry. At present we are only able to model furnace goemetries that have side-to-side symmetry. This eliminates many cases of interest such as tangential tertiary air and side wall interlaced secondaries, since the gases do not flow across the symmetry plane. The means for overcoming this limitation are readily apparent and this is also a part of further developments. The need to limit nodes also places other, subtle restrictions on the ability to model real boilers. Compromises need to be made on laying out air ports so they lie above each other, even though this is not the case in the actual furnace. The need to "pack" nodes around air ports leads to cells with high aspect ratios and this can cause convergence problems.

Recent experience with attempts to mathematically model "cold flow" cases has shown that this is a very difficult problem with a high potential for computational artifacts. Much work needs to be done on establishing the validity of computational fluid dynamics solutions to problems of this type before the model can be used with confidence.

The model as it currently exists does not include sodium and sulfur chemistry. Ultimately, this needs to be part of a recovery furnace simulation model, since sulfur gas concentrations and dust loads are important operating parameters. S/Na chemistry is not included in the present model because the necessary rate equations for sulfur release and dust production have not yet been developed, and because these reactions have only a very minor effect on the basic combustion, flow and temperature data. Plans are underway to develop a model to handle sulfur and sodium chemistry that would use a converged solution without sulfur and sodium chemistry as a starting point.

The final issue is model validation. No attempt at modeling an actual operating recovery boiler and comparing the results with field data has been made as yet. In fact very few sensitivity tests of model parameters have been made to date because of the long convergence times. The model is based on fundamental principles and does display many of the features qualitatively known to exist in recovery furnaces. It would be premature, however, to blindly use the model for simulating an actual furnace. Model validation with actual furnace data will be done over the next two years and this should greatly increase the reliability of model predictions.

References

1. Grace, T., Welch, A., Jones, A., Sumnicht, D. and Farrington, T. "A Three-Dimensional Mathematical Model of the Kraft Recovery Furnace" presented at the 1989 International Chemical Recovery Conference in Ottawa, Ontario in April 1989.

2. Crane, K.A., "An Empirical Equation for the Volatilization of Kraft Black Liquor Droplets During Burning", AIChE Meeting, (Aug. 16-20, 1987), Minneapolis, MN.

PROJECT SUMMARY FORM

DATE: March 20, 1990

PROJECT NO. 3657-2: KRAFT BLACK LIQUOR DELIVERY SYSTEMS
(Supported by the Office of Industrial Program - U. S. Department of Energy)

PROJECT LEADERS: T. N. Adams, H. L. Empie

IPST GOAL:

Increase recovery boiler throughput and operating efficiency through improved liquor spraying technology at modest capital cost.

OBJECTIVE:

Develop new and improved black liquor spraying nozzles by understanding the characteristics of spray behavior and reducing the fraction of undersize droplets to avoid carryover and pluggage and to accommodate firing higher solids liquors.

CURRENT FISCAL YEAR BUDGET: $300,000

PRIOR RESULTS:

Spray trials carried out at the IPST spray facility in Appleton using black liquor from a local paper mill were primarily directed at increasing the data base on black liquor nozzle flow and pressure drop characteristics, as well as sheet thickness and velocity. Limited droplet size distribution data were taken using a flash x-ray imaging technique. A high-speed video camera was identified as an alternative, and initial runs with this equipment gave encouraging results.

Data were taken on two nozzles (a B&W splash plate and a CE U-type) for a black liquor solids range of 55% to 66%, liquor temperature of 200° to 225°F, and liquor flows of 7.5 to 25 gpm. Data were also taken using corn syrup as the working fluid. The flow and pressure drop characteristics for these nozzles are consistent with the specific geometry of each, allowing reasonable speculation about the flow characteristics of other nozzle designs. Neither the splashplate nor the U-type nozzle is very sensitive to normal fluctuations in liquor property variations.

Fluid sheet thickness was measured using the splashplate nozzle. Limited data indicate that sheet thickness (and likely droplet size) will increase by less than a factor of two for a ten-fold increase in viscosity.

Black liquor spray trials were carried out at the Camas Mill of James River Corp. to compare the performance of three types of black liquor nozzles under range of liquor temperature and pressure conditions. The CE recovery boiler Camas was operated at normal load conditions with one gun location using three alternative nozzle designs - a CE V-type, a CE swirl cone, and a B&W splashplate. High speed video recordings of the spray pattern were made for each condition. Due to spray geometry the video pictures for the V-type nozzle were not clear, but the recordings of the other two nozzles were good. Patterns of spray breakup could be seen for each that are very similar to the breakup observed in the spray booth facility at the Institute.

SUMMARY OF RESULTS SINCE LAST REPORT:

Analysis of spraying data has continued, leading to a number of conclusions about droplet formation mechanism, nozzle flow/pressure drop characteristics, fluid sheet thickness, and drop size distribution of black liquor sprays. Considerations of the observed mechanism of droplet formation suggest a major revision is needed in the theory of how droplets form from splashplate and similar nozzles. The standard deviation about the median droplet size for black liquor is nearly the same as for a wide variety of other fluids and nozzle types. Preliminary correlations for fluid sheet thickness on the plate of a splashplate nozzle for black liquor show the strong similarities to other fluids. The flow/ P characteristics of black liquor nozzles follow a simple two-term relationship similar to other flow devices. In routine mill operation only the fluid acceleration in the nozzle is important; viscous loses are quite small.

The Flash X-ray (FXR) shadowgraph technique originally proposed for this program was shown to be inferior to use of a high-speed video approach. This is because black liquor is a weak absorber of radiation resulting in poor image contrast for diameters under 0.5mm, and it gives an image blur of about 0.5mm, the end result being poor sensitivity for droplet diameters under one millimeter. In addition, the number of FXR images per run was limited so that droplet history could not be recorded; such is not the case with the video approach.

A summary report has been written covering the first year of activity on this program.

PLANNED ACTIVITY THROUGH FISCAL YEAR 1990:

Major activities for the present year involve reinstallation of the spraying equipment in an environmentally acceptable configuration at our new Atlanta location followed by spraying studies for conventional splash plate nozzles using simple fluids and non-flashing black liquors. A companion spraying study at one or more mill sites to examine spraying characteristics of black liquor in an operating recovery boiler will also be conducted. Comparison of results from the laboratory and mill activities should produce some interesting insights into black liquor spraying phenomena.

PROJECT SUMMARY FORM

DATE: March 20, 1990

PROJECT NO. 3661: SULFUR-FREE SELECTIVE PULPING PROCESS
(DOE FUNDED PROJECT)

PROJECT LEADER: D. R. Dimmel

IPC GOAL:

Improved process for bleached chemical pulps

OBJECTIVE:

To develop a sulfur-free pulping process based on conversion of lignin to pulping additives which will increase delignification rates and decrease the degradation of carbohydrate fibers.

CURRENT FISCAL YEAR BUDGET: $128,000

PRIOR RESULTS:

The research work of John Wozniak (Ph.D. 1988, IPC) demonstrated that pulping catalysts can be prepared from lignin and lignin-derived chemicals. The aromatic rings of lignin were oxidized to benzoquinones, which in turn were modified by Diels-Alder reactions into anthraquinone type pulping catalysts. The synthetic yields achieved by Wozniak were respectable; the Diels-Alder products had moderate to excellent pulping activity. The process (lignin--- catalysts) has potential for providing an inexpensive, selective, sulfur-free pulping process.

The oxidative procedures developed by Wozniak were reexamined in an attempt to develop accurate yield measurements when employing small sample sizes. Both peracetic acid and peroxide oxidation procedures when applied to small samples, gave inconsistent results with gas chromatography (GC) analysis. High water solubility and volatility make the product analysis difficult by GC. Therefore, liquid chromatography (LC) was turned to as a method of analysis. Derivatization and solvent changes should not be necessary for this technique. Starting materials and product components have been shown to separate well by LC. Treating the product mixtures with iron salts converts hydroquinones to quinones and simplifies the product analysis.

The Fremi salt oxidation of lignin models has also been extensively studied. The analysis of products here was also complicated, primarily because of the suspected instability of the benzoquinones and hydroquinones on the GC columns. Analysis by UV and by reduction acetylation were partially successful. After much experimentation, we were able to get reproducible GC results on small samples. Several Solar Energy Research Institute (SERI) samples have been oxidized with Fremi salt and yields determined. Supercritical fluid extracted aspen kraft black liquors and stream exploded lignin gave poorer benzoquinone yields than did EtOAc extracted liquors. However, the yields are still better than that observed with straight lignin; for example, yields close to 20% dimethoxybenzoquinone from the residue of EtOAc extracted organosolv aspen pulping liquors, but only 1-2% from kraft lignin.

According to a preliminary economic evaluation, our ability to produce low cost anthraquinone pulping catalysts from lignin is highly dependent on the chemical yields of the synthetic steps. Consequently, we have been examining better methods of converting benzoquinones (single-ring compounds) to anthraquinones (3-ring compounds). The first of two ring-forming reactions can be accomplished in high yield. If the structure of the product from the first step is not modified, the second ring-forming reaction generally does not occur. We have found that adding aluminum oxide to the benzoquinone-diene reaction promotes modification of the intermediate product and the yields of anthraquinones in the single step reaction go up. Other ring forming catalysts were also examined, but generally were less effective than aluminum oxide. The anthraquinone yields are still only modest (20%) by these procedures.

Quite high Diels-Alder yields (70%) have been demonstrated when 1-acetoxy-3-methyl-1,3-butadiene (a ring forming reagent) is used. The practicality of using this diene in a low cost commercial process is questionable; however, we have at least demonstrated that high yield synthetic yields are possible.

Mr. Patrick VanVreede, a B.S. technician at IPST, has been concentrating his research efforts on optimization of benzoquinone yields from hydrogen peroxide oxidation of lignin model compounds. Conditions have been developed for the isolation of benzoquinone after peroxide reaction. Isolated yields of 7.5% for methoxybenzoquinone from vanillin have been obtained using 1M H_2O_2.

Dr. Joseph Bozell at SERI has been examining more efficient ways to prepare benzoquinones by way of cobalt promoted oxidations, establishing procedures for performing high yield Diels-Alder products, and characterizing Diels-Alder products.

SUMMARY OF RESULTS SINCE LAST REPORT:

The isolated yields of methoxybenzoquinone from vanillin have been increased to 95% using 1.5 M H_2O_2. Several experimental conditions have been explored, such as reaction volume, reagent concentrations, slow vs fast addition, and different reaction times, in an attempt to define the optimum yield vs cost factors. A state-of-the-art liquid chromatograph has been purchased and used to help define reaction yields. Much time has been spent in becoming familiar with the instrumentation and developing a quantitative analysis procedure.

Mohammad Karim, a postdoctoral fellow, began laboratory work in November. His research has been concerned with exploring new ways of generating quinones from lignin (model) phenols and new Diels-Alder strategies. Studies with copper oxide have shown that this reagent is poor at converting lignin monomers to quinones. Both sodium chlorite and chlorine dioxide provide low yields of quinones from lignin models; conditions have not yet been optimized. On the other hand, N-hydroxysuccimide, in the presence of nitrogen dioxide, appears to give very high yields of quinones with some lignin models.

Chlorinated quinones may be present in, or be prepared from, chlorine-chlorine dioxide bleaching liquors. Therefore, we have looked into the possibility of performing Diels-Alder reactions with chlorinated quinones. Such reactions do, indeed, occur at high temperatures.

Bozell and colleagues at SERI have continued to explore colbalt-promoted oxidations, using a variety of substrates and conditions. The scope of the usefulness of such reactions has been better defined. The other major area of investigation has involved developing extraction techniques which provide a low molecular weight lignin for subsequent oxidation to quinones.

Low molecular weight lignin fractions have been obtained from kraft, soda, and soda/AQ pulping liquors of aspen. However, the yields were quite low. Recent investigations have focused on a series of organosolv lignins, derived from aspen, red oak, white oak and scarlet oak. Treatment of whole aspen lignin with selected solvents, followed by filtration, caused the dissolution of lignin in good yield a low molecular weight. Lignins from red oak, white oak and scarlet oak also gave significant amounts of low molecular weight material, although the amount was less than that observed for aspen. Not all solvents treated gave good yields. There appear to be no simple correlation of solvent properties to the selectivity of the fractionation. These observations are significant and suggest that organosolv lignins are significantly richer in the necessary low molecular weight material.

PLANNED ACTIVITY THROUGH FISCAL YEAR 1990:

Because of the significance of the organosolv lignin extraction results, many of the experiments will be repeated to determine the reproducibility of the results and to more completely characterize the extracted lignin. We will continue work aimed at optimizing oxidation yields with H_2O_2, cobalt/oxygen, and hydroxysuccimide and simple lignin model substrates. Diels-Alder reactions in water (MS student work), in supercritical solvents, and with chlorinated quinones will be further expanded.

POTENTIAL FUTURE ACTIVITY:

The following areas will be addressed:

Optimize oxidation yields for 2-3 reagents and test on low molecular weight lignin samples.

Develop analytical methods for determining quinone yields from the oxidation of lignin substrates.

Screen several lignin samples for their potential to generate quinone catalyst.

Optimize Diels-Alder reaction yields.

Decide which oxidation agent, starting lignin, diene, and quinone catalysts to pursue for commercial development.

Continue economical evaluation updates.

Project 3661 Status Report

SULFUR-FREE SELECTIVE PULPING PROCESS
(DOE FUNDED PROJECT)

Reporting period: September, 1988 - February, 1990

OBJECTIVE

To develop a sulfur-free pulping process based on conversion of lignin to pulping additives which will increase delignification rates and decrease the degradation of carbohydrate fibers.

BACKGROUND

The research described herein has its roots in two projects, one initiated at The Institute of Paper Science and Technology (IPST) and the other at The Solar Energy Research Institute (SERI). In 1985, Ph.D. student John Wozniak, under the direction of Dr. Donald Dimmel, began a study aimed at converting a wood component, lignin, to a pulping catalyst, anthraquinone. At roughly the same time, SERI was examining efficient procedures for removing lignin components from pulping liquors.

Both projects showed great promise and were combined (at least in part) to meet the objective of developing an economic procedure for converting extracted lignin to anthraquinone. The combined projects (now Project 3661 at IPST) are being financially supported by the Department of Energy (DOE); a successful implementation of the research would lessen the energy requirements for making paper. The funding began in September, 1988 and is to continue for three years. The project leaders are Dr. Joe Bozell at SERI and Dr. Don Dimmel at IPST.

INTRODUCTION

One of the most widely studied discoveries in paper chemistry in the last 12 years is Holton's report that catalytic amounts of anthraquinone (**1**) can significantly promote alkaline pulping processes.

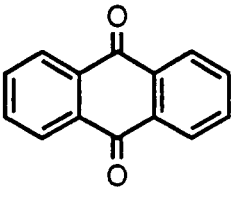

1,anthraquinone

There are a number of benefits associated with the use of anthraquinone as a pulping promoter:

- When added to a kraft cook, it generally increases the pulping rate while decreasing the amount of pulping chemicals required. The pulps obtained have qualities similar to non-catalyzed processes. The combination of these features translates into lower energy requirements and expense for running the mill.

- The lower amount of alkali required results in a savings in the chemical recovery stage of pulping as well as a decrease in the amount of makeup chemicals required.

- Anthraquinone promotes pulping at catalytic levels. Typically 0.05-0.1% based on the weight of raw wood feedstock is added.

- Importantly, the amount of carbohydrate degradation decreases in an anthraquinone promoted process, meaning higher pulp yields are possible.

Considerable mechanistic studies have been performed to determine how anthraquinone exerts these effects. While a complete mechanism has not yet been established, a general picture has emerged. Figure 1 gives a simplified description of how anthraquinone is thought to work.

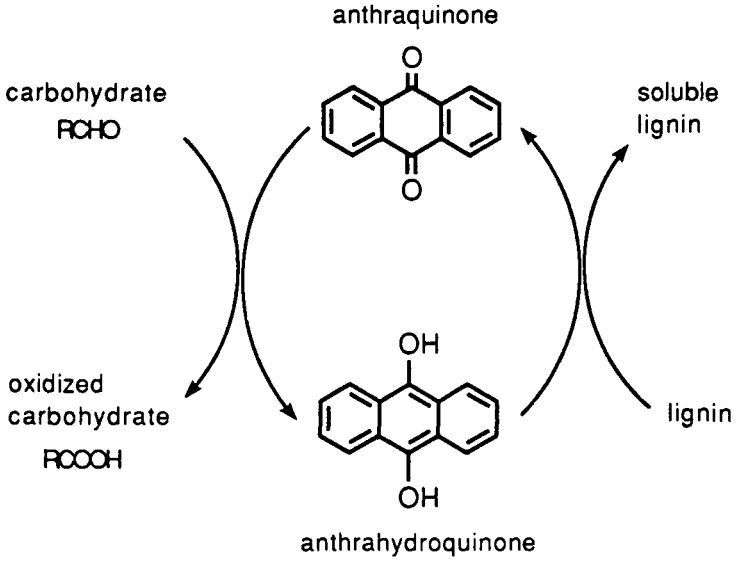

Figure 1

In the first step, anthraquinone oxidizes the aldehyde end groups of the cellulose to carboxylic acids. This oxidation lowers the reactivity of the carbohydrates (carboxylic acids being much less reactive than aldehydes) and renders them less susceptible to peeling. Lower amounts of peeling result in a higher pulp yield. At the same time, anthraquinone is reduced to anthrahydroquinone. In the second stage of the cycle, anthrahydroquinone (which exists as a dianion in alkali) reacts with the lignin and

causes its dissolution. This process reoxidizes the anthrahydroquinone to anthraquinone, which can continue the catalytic cycle.

The regeneration of the anthraquinone from a lignin adduct has been studied and a proposed mechanism is detailed in Figure 2.

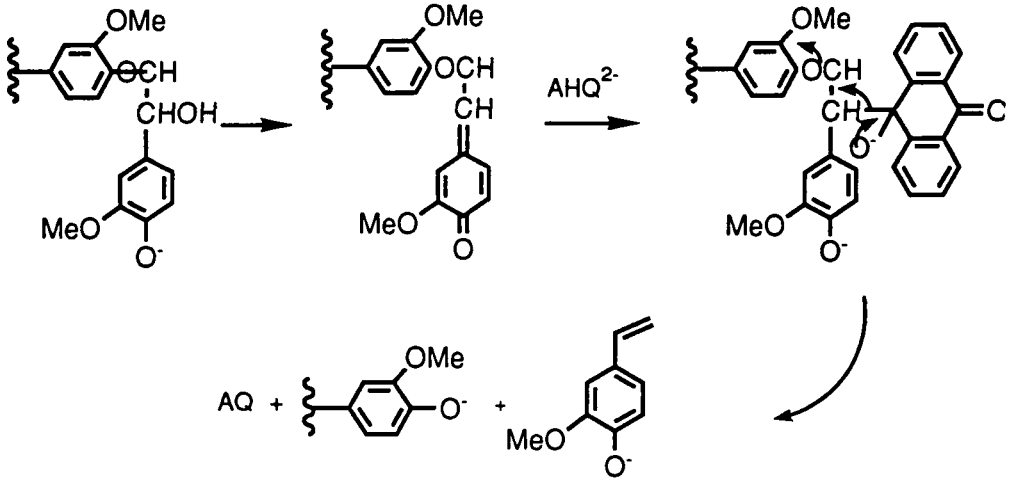

Figure 2

During pulping, free phenolic units of the lignin which contain benzylic oxygenated functional groups are converted to quinone methides. The adduct mechanism proposes that anthrahydroquinone dianions attack the quinone methides in a Michael fashion to generate a covalent bond. Fragmentation of these adducts into smaller pieces results in lignin dissolution. An alternate proposal suggests that anthrahydroquinone dianion transfers electrons, rather than bonding, to the quinone methides. The quinone methide ion radicals then fragment. Anthraquinone reactions are not completely catalytic, since some of the anthrahydroquinone is irreversibly bound to the lignin fragments during pulping.

Despite the reported advantages of anthraquinone catalyzed pulping, there has been little acceptance of this method from the paper industry, except in Japan where a most mills are using this technology. The current market cost of anthraquinone, about $3.00/lb., makes it too expensive for general use, except in areas where wood costs are high and pulping yields take on greater importance. The purpose of this project is to prepare anthraquinone at a cost which would make it attractive for general industry use.

To prepare anthraquinone, we have chosen lignin as a starting material. Lignin has a number of attractive features as a raw material for anthraquinone production. First, lignin is quite inexpensive; it is readily available as a waste product from the paper industry. Secondly, a successful synthesis of anthraquinone from lignin will give a new, higher value added product to the industry.

The structure of lignin bears little resemblance to that of anthraquinone. However, lignin is susceptible to oxidation. A number of studies on both lignin and lignin models lignin have shown that oxidation can be a highly selective reaction leading to compounds much more closely related structurally to anthraquinone. Examples of such reactions are shown in equations 1-3.

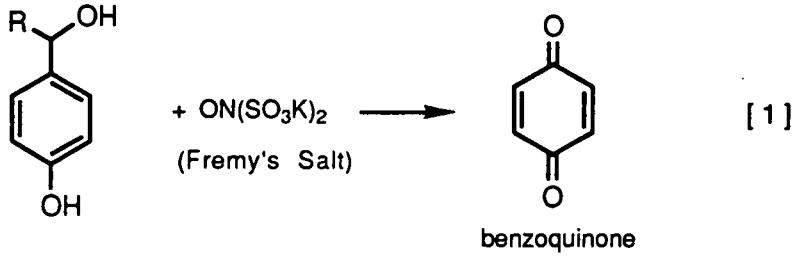

[1]

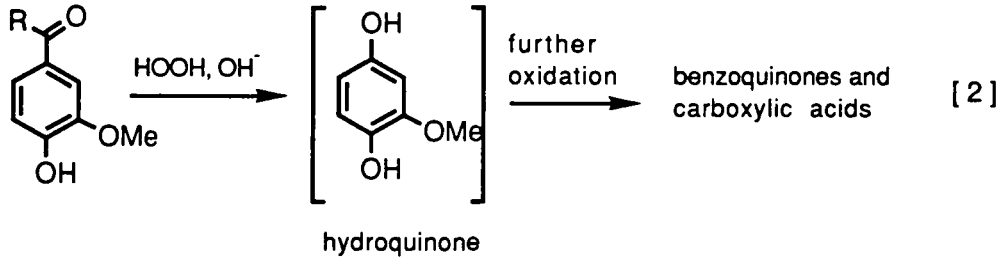

[2]

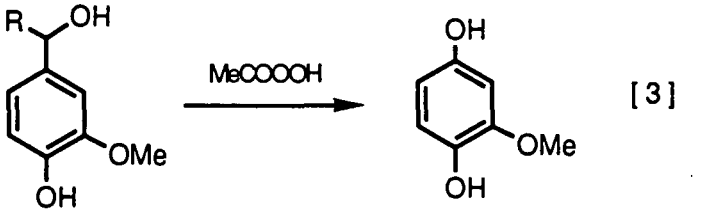

[3]

Fremy's salt (potassium nitrososulfonate), which is a stable free radical, is an excellent reagent for the conversion of lignin models to benzoquinones (equation 1). Hydrogen peroxide is also useful as an oxidizing agent for lignin models (equation 2). In contrast to Fremy's salt oxidation, the primary product from a peroxide oxidation is the corresponding hydroquinone. However, hydroquinones are readily transformed into benzoquinones by simple oxidation. Peracetic acid has been used to oxidize lignin models to give hydroquinones (equation 3). Other reagents have been reported for this oxidation, however, they are less convenient to use or more expensive than those of equations 1-3.

RESULTS

Proposed Approach to Anthraquinone from Lignin

The proposed approach for the preparation of anthraquinone from lignin is shown in Figure 3. The approach has been divided into two large stages. The first is a

lignin processing stage in which the lignin is subjected to a fractionation process in order to isolate a low molecular weight fraction from the whole lignin.

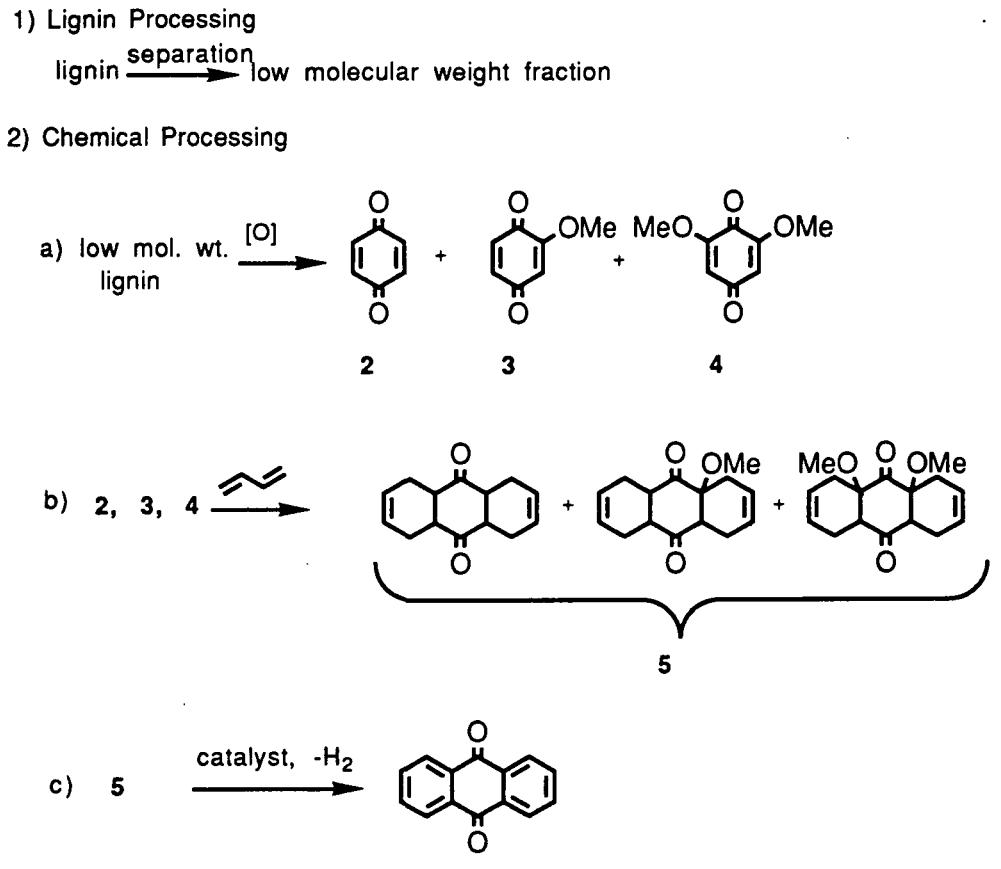

Figure 3

The first stage is the separation of a lignin material into a low molecular weight fraction. Lignin is a complex high molecular weight biopolymer, which during alkaline pulping is fragmented and converted (via condensation reactions) into a broad range of molecular weights. While the chemical processing stages could be performed on the whole unfractionated lignin, an economic evaluation has indicated this approach would be economically unattractive. In addition, chemical processing of high molecular weight material would probably be difficult.

Two methods for lignin fractionation and isolation of a low molecular weight portion are being investigated: extraction using supercritical fluids and conventional solvent extraction.

Work by Dr. David Johnson and Dr. Guiseppe Filardo of SERI has shown that extraction of kraft black liquor with supercritical carbon dioxide, in the presence of added organic entrainers (up to 20%), allows selective removal of a low molecular weight fraction. Size exclusion chromatography indicates that the apparent molecular

weight of this material is less than 2000. The actual yield of material using supercritical extraction is low and the cost is highly dependent on the conditions required.

More recent work at SERI has focused on developing an alternate method which employs a selective solvent extraction. Ms. Bonnie Hames has been looking at the extraction of a number of organosolv lignins with various organic solvents. Preliminary results from size exclusion chromatography indicate that these organosolv lignins contain significantly higher level of the necessary low molecular weight lignin than other sources. Since this material may be proprietary, further details cannot be given at this point; however, the investigation is continuing. These samples have not been examined yet for their ability to be oxidized to quinones.

The second stage of the process involves taking a low molecular weight lignin fraction through three chemical steps. In the first step, the low molecular weight lignin will be oxidized with an inexpensive oxidizing agent to give a mixture of benzoquinones (**2, 3** and **4**). The proportions in the mixture will depend on the nature of the lignin feedstock. In the second step, **2, 3** and **4** will be converted into a mixture of anthraquinone precursors (mixture **5**) by treatment with a diene under Diels-Alder reaction conditions. The final step converts mixture **5** into anthraquinone. Interestingly, the final step may not be necessary. Japanese workers have reported that dihydroanthraquinones, such as **6**, also function as pulping catalysts by conversion to anthraquinone in situ.

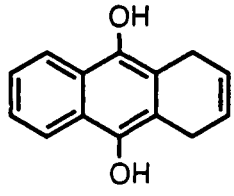

6

Economic Evaluation of the Process

A key facet of the project has been an economic evaluation of both the lignin processing and the chemical processing stages of the process. This evaluation has been carried out by Mr. Art Power, an independent engineering consultant; the results of his evaluation have been sent to the DOE for issuance as a formal report. Since the goal of the project is to develop an economically attractive anthraquinone synthesis, the evaluation was performed in order to best define the most useful routes to study from a number of differing possibilities. A summary of the parameters used for the evaluation is found in Figure 4.

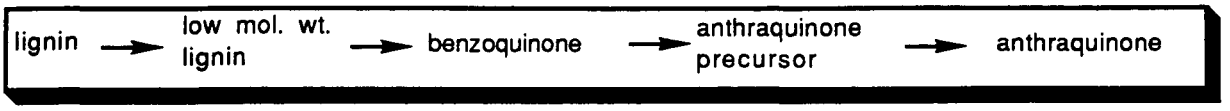

1) Lignin processing

- lignin source: kraft black liquor
- treatment of both 10% and 100% of liquor considered
- fractionation methods: CO_2 precipitation, supercritical extraction

  CO_2 precipitation, solvent extraction

  solvent extraction

2) Chemical processing

- range of overall yields for the three steps: 5-95%
- oxidizing agent for lignin: hydrogen peroxide
- preparation of anthraquinone precursor: butadiene as the diene
- dehydrogenation of precursor: catalytic, high yield reaction; disregarded

Figure 4

For the purposes of this evaluation only , kraft black liquor was considered as the source of lignin. In addition, the anthraquinone produced is considered for use as a catalyst in an existing kraft process. The effect of adding anthraquinone to a kraft process is an increase in the yield of pulp. This gain in yield is translated into a maximum allowable price per pound of anthraquinone - a breakeven price. This value is used as a benchmark above which a kraft/anthraquinone process ceases to be economical.

A kraft process was chosen for this evaluation since good engineering data, mass balances, reaction stoichiometries, plant design data, etc. are readily available. However, we are not limiting use of this technology strictly to kraft plants. A soda/anthraquinone mill is a viable possibility and will realize additional savings in capital expenditures since the chemical recovery and environmental processing portion of such a mill should be simpler. This pulping system was not evaluated since a good engineering model is unavailable to allow calculations. In addition, the process is not limited to the use of kraft black liquor derived lignin as a starting material. A number of different lignin sources are under consideration.

In the proposed process, some portion of the black liquor stream of a kraft mill is diverted, processed, and the unused portion returned to the operation. Two processing levels were examined: treatment of 10% of the black liquor stream and treatment of 100% of the black liquor stream. The evaluation considered three different fractionation methods to obtain the necessary low molecular weight lignin: (1) a CO_2 precipitation of the whole lignin followed by a supercritical fluid extraction of the remaining soluble portion, (2) a CO_2 precipitation of the whole lignin followed by a conventional solvent extraction of the remaining soluble portion, and (3) conventional solvent extraction of the whole lignin.

The chemical processing stage of the overall process was also examined. Since extensive lab data was not yet available at the time the evaluation, our approach was to evaluate costs over a range of possible yields for the chemical steps based on reasonable estimates for each step in the process.

The results of the evaluation are shown in Figure 5. The evaluation generated a large matrix of results; however, the graph is illustrative. The single most important determining factor in the final cost of anthraquinone is the overall yield of the chemical processing steps. While not shown in Figure 5, the evaluation determined that the cost of anthraquinone drops exponentially with increasing overall yield. Figure 5 shows the results assuming an overall yield of 50%. As a result of the strong dependence on chemical yield, the contribution of the preliminary lignin processing step to the overall cost is not significantly larger for supercritical fluid extraction when compared to conventional solvent extraction.

A second conclusion of this evaluation is that the anthraquinone cost drops significantly if the process can treat 100% of a lignin containing black liquor stream. Under optimum conditions, the cost of anthraquinone could be as low as $1.00/lb. More realistically, a cost between $1.25 and $1.75/lb can be expected.

This evaluation is still quite preliminary and is designed to be continually updated and revised as further lab data is obtained. The results of revisions will be used to direct research along the most profitable path. In addition, we will be continually comparing our approach to other routes for anthraquinone preparation from non-renewable sources.

Chemical Processing Results

Each of the proposed steps in the chemical processing stage outlined in Figure 3 has been investigated. This section will summarize the current results.

A. Oxidation of lignin and lignin models.

The initial step in the chemical processing of lignin is oxidation to give a benzoquinone mixture. The early work on this step by IPST involved the oxidation of

Preliminary Technoeconomic Evaluation Combined Extn and Chemical Processing

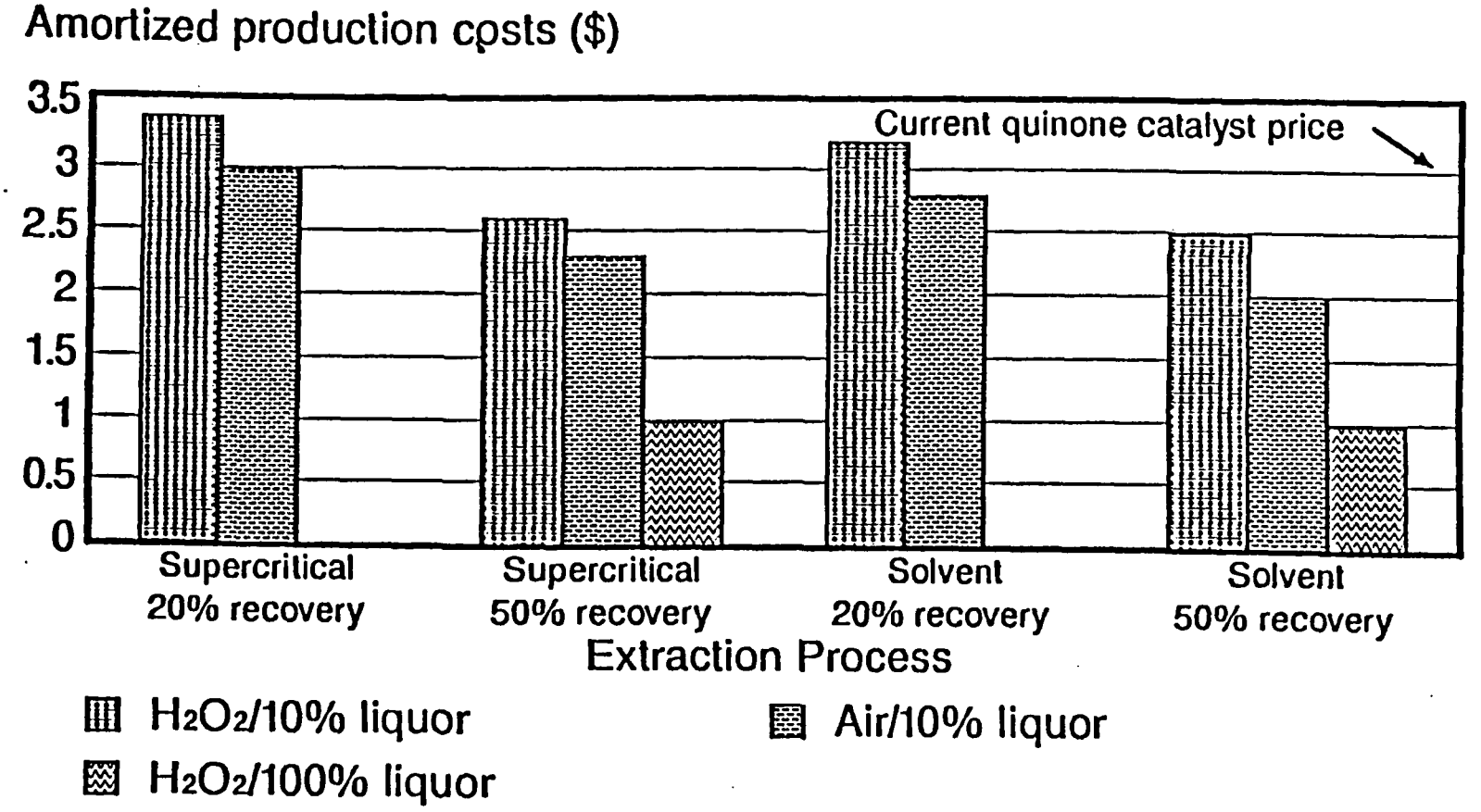

Overall yield 50%

Figure 5

both lignin and lignin models with a number of oxidizing agents. The results of the study are summarized in Figure 6.

Lignin Model	Oxidizing agent, yield (%)[1]		
	Fremy's salt[2]	hydrogen peroxide[3]	peracetic acid[4]
α-methylvanillyl alcohol	79	4	1
vanillic acid	77	NR	NR
acetovanillone	0	77	89
vanillin	0	95	21
α-methylsyringyl alcohol	79	12	30
syringic acid	77	0	3
syringaldehyde	65	96	17
acetosyringone	3	43	32
lignin samples	16 (lmw ethanol) 15-25 (SCE)	none	traces

Notes:

1-yields calculated from GC by internal standard method
2-products almost exclusively the corresponding benzoquinone
3-products almost exclusively the corresponding hydroquinone
4-products a mixture of hydroquinone and acetylated hydroquinone

Figure 6

Three oxidizing agents were investigated: Fremy's salt, hydrogen peroxide and peracetic acid. Fremy's salt proves to be an excellent and mild reagent for the conversion of both lignin models and lignin into benzoquinones. Hydrogen peroxide also worked well for the conversion of lignin models into hydroquinones. Note that the results of the Fremy's salt oxidation and the H_2O_2 oxidation are complementary; substrates that fail with Fremy's salt are readily oxidized with H_2O_2. However, authentic lignin samples fail to give detectable amounts of benzoquinone when treated with H_2O_2. Peracetic acid was also investigated, but gave results inferior to either Fremy's salt or H_2O_2.

The oxidative procedures developed by Wozniak were reexamined in an attempt to develop accurate yield measurements when employing small sample sizes. Both peracetic acid and peroxide oxidation procedures, when applied to small samples, gave inconsistent results with gas chromatography (GC) analysis. High water solubility and volatility make the product analysis difficult by GC. Therefore, liquid chromatography (LC) was turned to as a method of analysis. Derivatization and solvent changes should not be necessary for this technique. Starting materials and product components have been shown to separate well by LC. Treating the product mixtures with iron salts converts hydroquinones to quinones and simplifies the product analysis.

The Fremy salt oxidation of lignin models has also been extensively studied. The analysis of products here was complicated, primarily because of the suspected instability of the benzoquinones and hydroquinones on the GC columns. Analysis by UV and by reduction acetylation were partially successful. After much experimentation, we were able to get reproducible GC results on small samples.

The small scale analysis technique gave Fremy's salt oxidation yields of DMBQ that were consistent with previous values for selected materials: 82% for a-methyl syringyl alcohol (previously 79%), 3.3% for hardwood ethanol lignin (previously 4%), and 12% for low molecular weight ethanol lignin (previously 11%). All oxidations used a ratio of 4 g of Fremy's salt per gram of sample. This value represents a 3:1 molar ratio of Fremy's salt to lignin phenyl propanoid subunit with the subunit's weight estimated at 198 g/mole. Table 1 presents DMBQ yields at various Fremy's salt loadings for SERI lignin OSA 2. The 4 gram Fremy's salt level gave the optimal DMBQ yield.

Table 1. Effect of Fremy's salt loading on 2,6-dimethoxy-p-benzoquinone yield from Organosolv lignin 2.

Fremy's Salt Level g/g sample	2,6-Dimethoxy-p-benzoquinone Yield, %
1	2.4
2	5.7
4	10.7
6	10.4

The SERI samples were oxidized by the small scale reaction procedure. The DMBQ yields are listed in Table 2 and grouped into three categories. The lignin sources (GF 41, etc.) are not descriptive, but convenient for the simple presentation given here. The first group with yields under 5% is entries 1-5. The next group with yields of 5-12% is given by entries 6-19. The final group, which could represent the lignin sources targeted for future study, are entries 20-21 and exhibit DMBQ yields of 15.9-18.3%. These samples came from supercritical fluid extraction of a kraft black liquor after the high molecular weight lignin was precipitated with carbon dioxide.

Repetition of selected lignin oxidations were performed to examine if DMBQ yields varied between different days. Entries 10-13 indicate some yield variability. This variability may be due to nonhomogeneous samples or the analytical technique. Recent work which uses 2-methoxy-1, 4-naphthoquinone as an internal standard for determining DMBQ amounts has shown better reproducibility. The variability implies that the absolute DMBQ yield from a lignin source is somewhat uncertain, but the methods used would still give relative rankings of the lignin sources. We are presently examining the use of liquid chromatography for the DMBQ/MBQ analysis.

Table 2. 2,6-Dimethoxy-p-benzoquinone yields from select lignin sources.

Entry	Lignin Source, SERI name	2,6-Dimethoxy-p-benzoquinone Yield, %
1	GF 41	1.4
2	42 I XE	1.5
3	42 II XE	2.5
4	4 BH1-13 P/N-A	4.4
5	11	4.7
6	43 II	5.9
7	44 ES	6.8
8	43 I	7.1
9	38	8.4
10	OSA 1 (repeat)	8.5
11	OSA 1	9.3
12	SBIX-1	8.5
13	SBIX-1 (repeat)	10.2
14	44 E2	8.5
15	13	8.9
16	OSA 2	8.9
17	XVII 107 NaCl ES	10.4
18	OA Cook G	10.7
19	XVII 107 ACES	11.3
20	XVII 107 ES	15.9
21	45	16.2
22	46	18.3

Recently, Mr. Pat VanVreede of the IPST has reinvestigated the peroxide oxidation of the lignin models syringaldehyde, vanillin and acetovanillone. This reinvestigation was carried out in order to determine isolated yields for this reaction in order to compare them to the GC yields of Figure 6. In addition , it is necessary to develop an oxidation procedure which does not require an expensive oxidant such as Fremy's salt. The results of this study are given in Figure 7.

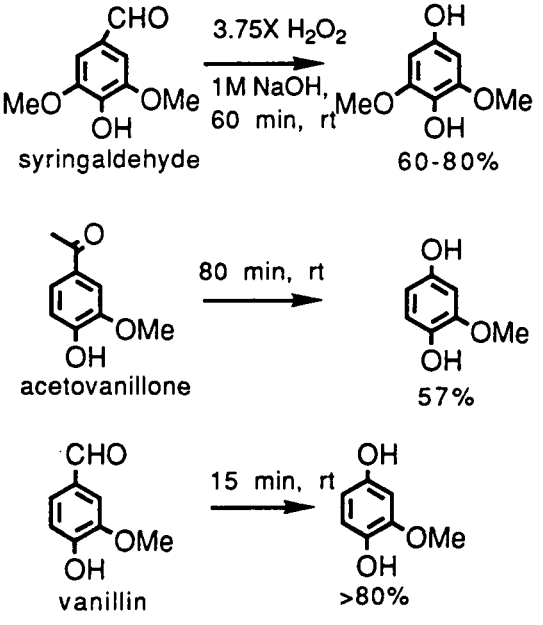

-oxidation proceeds well with some models, although the GC yields h been matched

-oxidation shows high selectivity at moderate conversions

-rate of oxidation strongly dependent on model structure

-competing nonproductive peroxide consumption exists

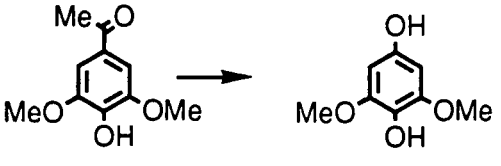

acetosyringone

2.5X excess of H_2O_2, no reaction
3.5X excess of H_2O_2, 20%

Figure 7

Optimum oxidation of the models was obtained with a 3.75-fold excess of peroxide in alkaline media. Each of the models undergoes the expected oxidation in moderate to excellent yield to give the corresponding hydroquinone. While reaction yields could be determined by directly measuring the hydroquinone produced, in practice it was easier to convert the hydroquinone product into the corresponding benzo-

quinone by oxidation with iron (III) sulfate. This oxidation proceeds almost quantitatively. The yields shown in Figure 7 are for isolated benzoquinone.

The quinone yields appear to be quite dependent on the level of peroxide employed. The yields go up 20% when changing the peroxide concentration from 1.0 to 1.5 M; this true for both vanillin and acetosyringone. The latter model fails to undergo oxidation in the presence of a 2.5-fold excess of peroxide, but increasing the peroxide level results in observable, albeit low yield, oxidation. We suspect that the increased yields are associated increasing the peroxide/model ratio, rather than a concentration effect, since doubling the model concentration at a constant high peroxide level led to lower yields.

A potential problem in the peroxide oxidations is the different reaction times required for the different lignin models. Vanillin is oxidized much more rapidly than either of the other two models. The difference between vanillin and acetovanillone is apparently due to the lower reactivity of a ketone carbonyl in comparison to an aldehyde. Syringaldehyde reacts more slowly since the electron releasing ability of a second methoxyl group lowers the reactivity of the carbonyl.

The product hydroquinones formed in the peroxide oxidation may be unstable to the reaction conditions and undergo ring opening reactions to give dicarboxylic acids products. Therefore, when subjecting a lignin sample to peroxide, some components will undergo rapid oxidation, and possibly over oxidation, while other components will be incompletely oxidized. Methods will be needed to balance these differing reactivities.

Experimental data thus far suggests that methoxyhydroquinone is relatively stable to peroxide. One of the best isolated yields (94%) of methoxybenzoquinone we have observed was in a case where the time was extended from 15 to 30 minutes in a reaction of vanillin with 1.5 M peroxide, followed by iron oxidation. A fast addition of 1.0 M H_2O_2 to vanillin routinely gives a 75% yield of quinone; a dropwise addition of 1.0 M H_2O_2 over roughly 25 minutes has given yields of 41 and 80% on two occasions.

Although the selectivity of the peroxide oxidation is high, the reaction conversion is normally 70-75%. An explanation for this incomplete conversion is the existence of a competing, non-productive reaction which consumes H_2O_2. A number of observations support this conclusion. Reactions that require a longer time generally proceed in lower yield. This reflects the greater competition of a peroxide decomposition reaction in the presence of a slow reacting substrate. At lower concentrations of H_2O_2, the reaction yields drop dramatically. If a competitive reaction is consuming peroxide, then there would be less available to drive the desired reaction.

Current work is directed at tracking the peroxide consumption using an iodometric titration as well as continuing to optimize the conditions for the oxidation. Unfortunately, it appears at this time that large excesses of peroxide will be required

to get good yields and this means added cost. Therefore, alternate methods for lignin oxidation need to be pursued.

Of the oxidizing agents studied, Fremy's salt remains as the most general reagent for the conversion of lignin models directly into benzoquinones. It is also the only reagent found that gives benzoquinones from oxidation of lignin samples (Figure 6). However, Fremy's salt is impractical for use on a large scale since it is expensive, relatively unstable and requires stoichiometric amounts. Fremy's salt is thought to oxidize phenolics via the key intermediate 7 shown in equation 4.

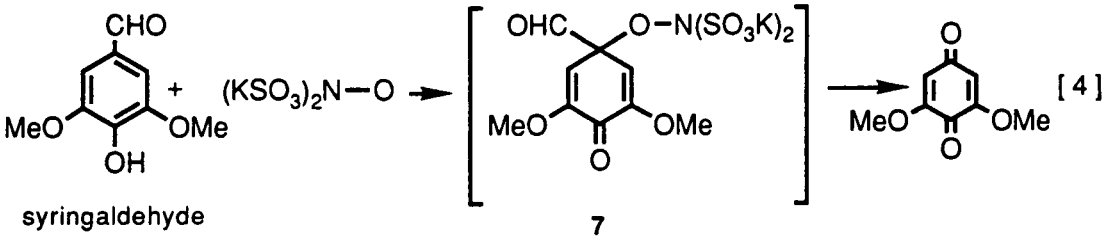

syringaldehyde

7

An area of active research at both SERI and IPST is the development of reagents that mimic the action of Fremy's salt but are either inexpensive or exhibit good activity at a catalytic level. The research attempts to produce intermediates like 7, which can fragment to quinones. An analogy to this reaction sequence is found in transition metal chemistry. A number of organometallic complexes exist which reversibly bind oxygen (Figure 8).

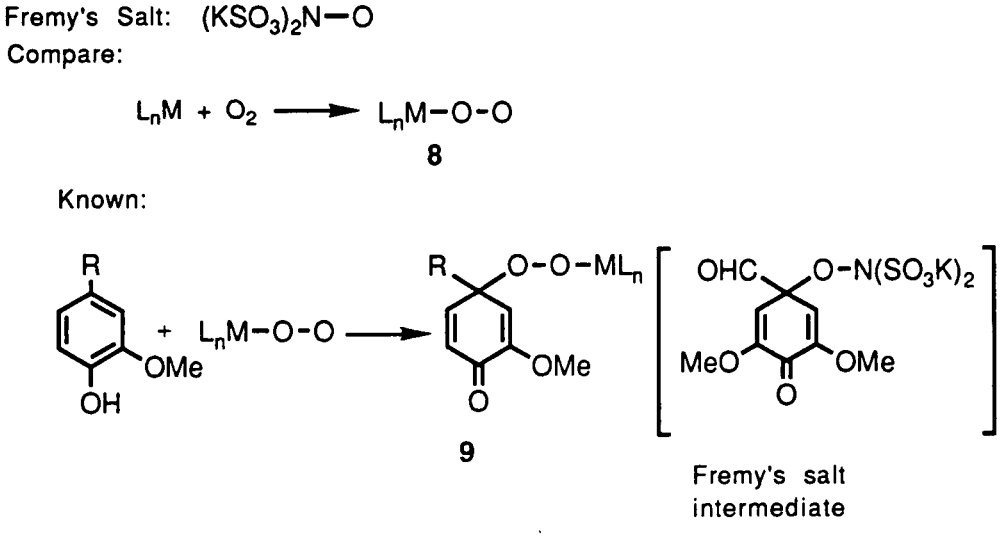

Figure 8

Some oxygen complexes adopt the superoxo structure 8, giving a species similar to Fremy's salt. While the exact location of the unpaired electron has been debated, the reactivity of these complexes can be rationalized assuming structure 8. More importantly, the oxygen complexes undergo reaction with phenolics to give the intermediate 9, structurally similar to the Fremy's salt intermediate.

A number of advantages exist for oxygen complexes. First, the reaction proceeds catalytically. Depending on the substrate chosen, as little as 1% of the metal catalyst is needed for oxidation. Secondly, the oxidations are reported to proceed in high yield. Finally, the reaction uses an inexpensive oxidizing agent, oxygen, to give quinones. Recent reports in the patent literature suggest that air could also be used for the oxidation.

Dr. Bozell at SERI has investigated the reactions of selected oxygen complexes with a number of lignin models. Since this approach could be proprietary, the nature of the catalyst cannot be disclosed, however, we find that the lignin model syringaldehyde undergoes a high yield oxidation to the corresponding benzoquinone (equation 5).

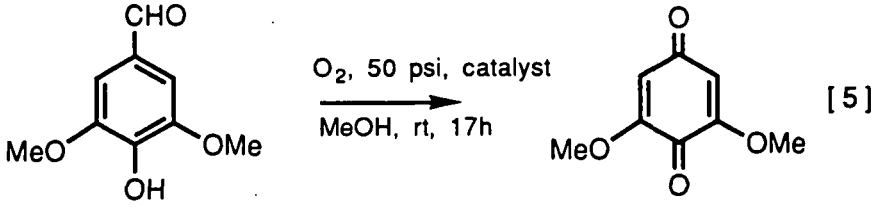

[5]

syringaldehyde

97% selectivity at
84% conversion

The reaction appears to work best with 10% of the metal catalyst. The reaction has been performed with 1% catalyst, but the conversion of starting material drops to 40-50%. Further investigation of this approach is currently underway at SERI.

Another compound which we have examined as a possible mimic of Fremy's salt is N-hydroxysuccimide (NHS). In the presence of nitrogen dioxide, NHS very effectively oxidizes vanillyl and syringyl alcohols to the corresponding quinones in 15 minutes. Syringaldehyde is not completely converted to a quinone in 15 minutes, but probably could be with longer reaction times. Vanillin, on the other hand, gives a mixture of quinone and a nitrated aromatic product. The nitro group must be coming from the nitrogen dioxide, which was added to generate phenoxy and NHS radicals. Some other radical generator may result in cleaner reactions in the vanillin case. These results are quite preliminary, but show great promise if NHS could be used in catalytic amounts with an oxidant such as peroxide.

Various metal oxides have been shown to be good oxidizing agents for the conversion of polymeric lignin compounds to its monomers. Some of these metal oxides, such as cupric oxide, have been tested under pilot plant conditions and shown to be suitable candidates for industrial use for the oxidation of aspenwood lignin, lignosulphonates, and sawdust. The products of these reactions were usually a mixture of compounds such as vanillin, acetovanillone, syringaldehyde and acetosyringone. No formation of the corresponding benzoquinone is reported in the literature. Therefore, we decided to use CuO under various conditions in order to force quinone formation.

The CuO oxidation of these lignin model compounds were studied. The compounds vanillyl and syringyl alcohols, and syringaldehyde, were added to an aqueous basic suspension of CuO and refluxed for several hours. Reactions were followed by GC analysis by taking aliquots at suitable time intervals. No formation of the desired quinone was observed by GC analysis; further tests were not conducted.

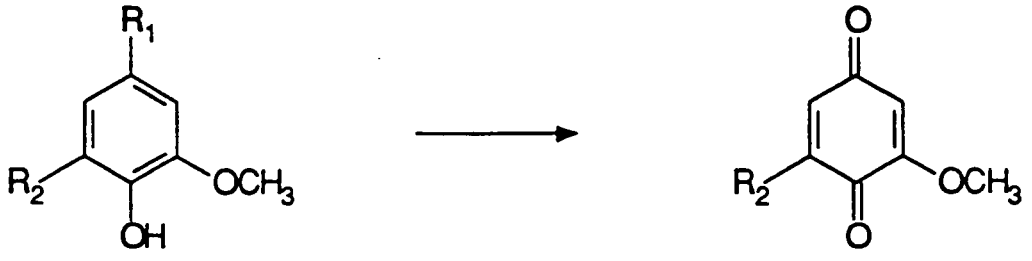

B. Diels-Alder Reactions of Benzoquinones.

The second step in the chemical processing stage is a Diels-Alder reaction of the benzoquinone mixture with an inexpensive diene to give an anthraquinone precursor. The reaction expected is shown in equation 6.

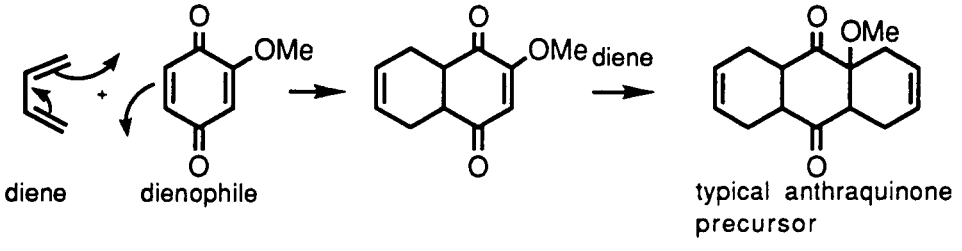

[6]

In a normal Diels-Alder reaction, a diene adds to a dienophile to form a new six membered ring. Butadiene and isoprene were chosen as the dienes because of their availability and low cost.

There are some important features about the specific Diels-Alder reaction required for synthesis of the anthraquinone precursor. First, the reaction could, theoretically, be performed in one step, using a 2:1 ratio of diene to quinone, without the isolation of a 1:1 diene-quinone intermediate. In practice, a stepwise reaction may be necessary because of the methoxyl substitution on the benzoquinones. Olefins substituted with electron releasing groups react more slowly in the Diels-Alder reaction than electron poor olefins. The Diels-Alder reaction of the three benzoquinones expected from the oxidation of a lignin sample has been examined with both butadiene and isoprene. The results are shown in Figure 9.

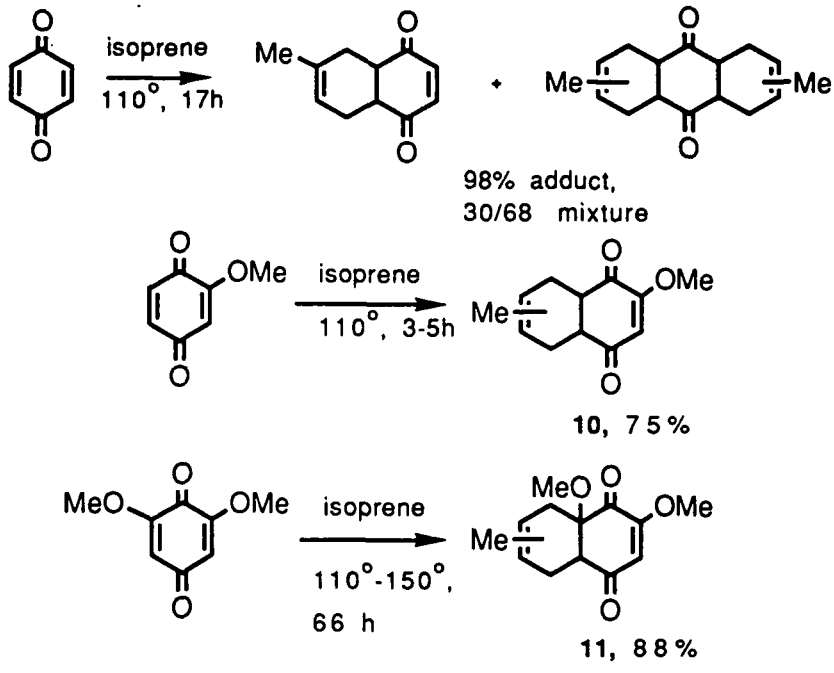

Figure 9

The simplest quinone, benzoquinone, undergoes reaction with isoprene to give a mixture of Diels-Alder adducts in excellent yield. The major product of the reaction results from the desired addition of two equivalents of diene to the quinone. The reaction can probably be driven to give exclusively the desired adduct by increasing the diene concentration or the reaction temperature. Unfortunately, lignin from woody plants contains very few non-methylated aromatic rings and, thus, the yield of unsubstituted benzoquinones from oxidation of such lignin will be extremely low.

As expected, the presence of methoxyl groups on the quinone changes the reactivity. Methoxybenzoquinone undergoes a rapid and high yield reaction with one equivalent of diene to give adduct **10**. Addition of a second equivalent of diene is not observed under moderate temperatures. Dimethoxybenzoquinone also undergoes reaction with a single equivalent of diene to give monoadduct **11**. The reaction is slower that of methoxybenzoquinone, but the yield is high.

The observed high yields of monoadducts is an important finding, since it demonstrates that the presence of a methoxyl group on a double bond does not preclude a Diels-Alder addition. Indeed, the results from the reaction of dimethoxybenzoquinone suggest that a second addition should be possible since the electronic nature of the remaining olefin should not differ significantly from the first.

An explanation for the failure to observe the addition of two equivalents of diene to a substituted quinone may be related to the three dimensional structure of the monoadducts and the geometric requirements for further reaction. Figure 10 shows

the predicted transition state conformation for the addition of a diene to dimethoxybenzoquinone.

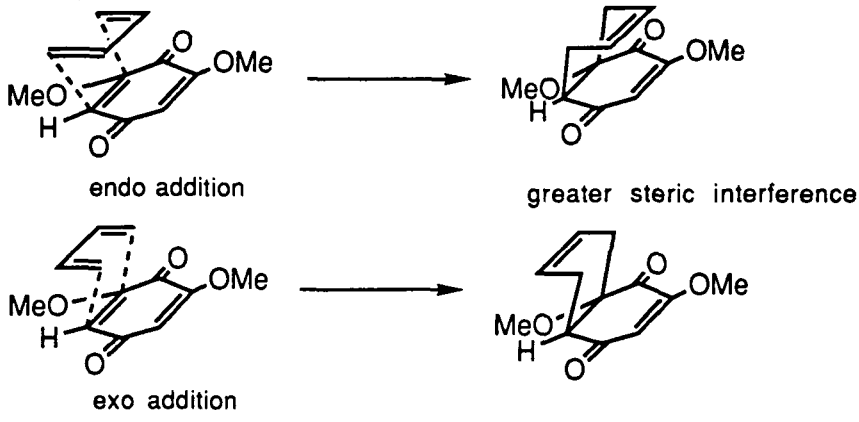

Figure 10

The incoming diene has the choice of adding in either an endo or exo mode. From a steric standpoint, the exo mode is preferred since there is less crowding. However, there exist several literature reports indicating that endo addition is preferred, despite the greater steric hindrance. This preference has been attributed to a number of factors including secondary orbital interactions in the transition state and has been formalized as the "Alder rule."

Certainly once the first addition is complete the resulting product can undergo a ring flip to the more stable exo conformation. However, some fraction of the mixture will continue to exist in the endo conformation and slow a second addition. The second diene will also attempt to adopt an endo conformation in the transition state. There will be higher steric interference to the second addition regardless of the conformation of the monoadduct. Experiments involving NMR spectroscopy are planned in order to substantiate the importance of these effects in our system.

If the first addition of diene gives a sterically hindered product, removal of the hindrance will make the second addition easier. A simple method of removing the hindrance is aromatization of the newly added ring to give methoxynaphthoquinone (Figure 11).

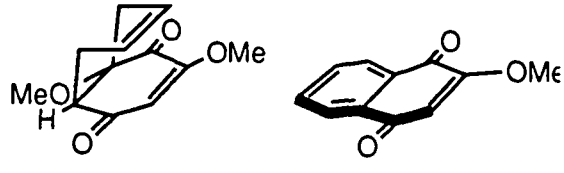

Figure 11

One approach to aromatization is shown in equation 7. The adduct formed from the Diels-Alder reaction of dimethoxybenzoquinone and butadiene has been observed by the IPST team undergo a facile aromatization when heated in the presence of alumina. This result suggests that a stepwise approach to anthraquinone is possible proceeding from benzoquinone to a monoadduct, then aromatization to a naphthoquinone, and, finally, a second Diels-Alder reaction/aromatization to anthraquinone.

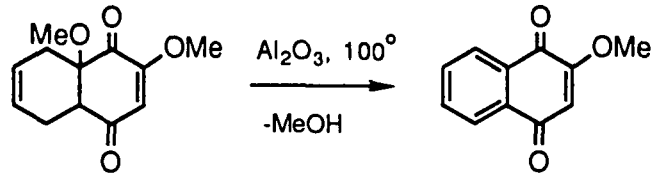

[7]

Another possible way to use alumina is to put it in the same vessel as the diene and quinone and attempt to promote aromatization of the monoadduct *in situ* . Since diene is still present, a second Diels-Alder should commence, eventually leading to an anthraquinone product (Figure 12). In fact, alumina might also function as a Lewis acid and catalyze the Diels-Alder steps.

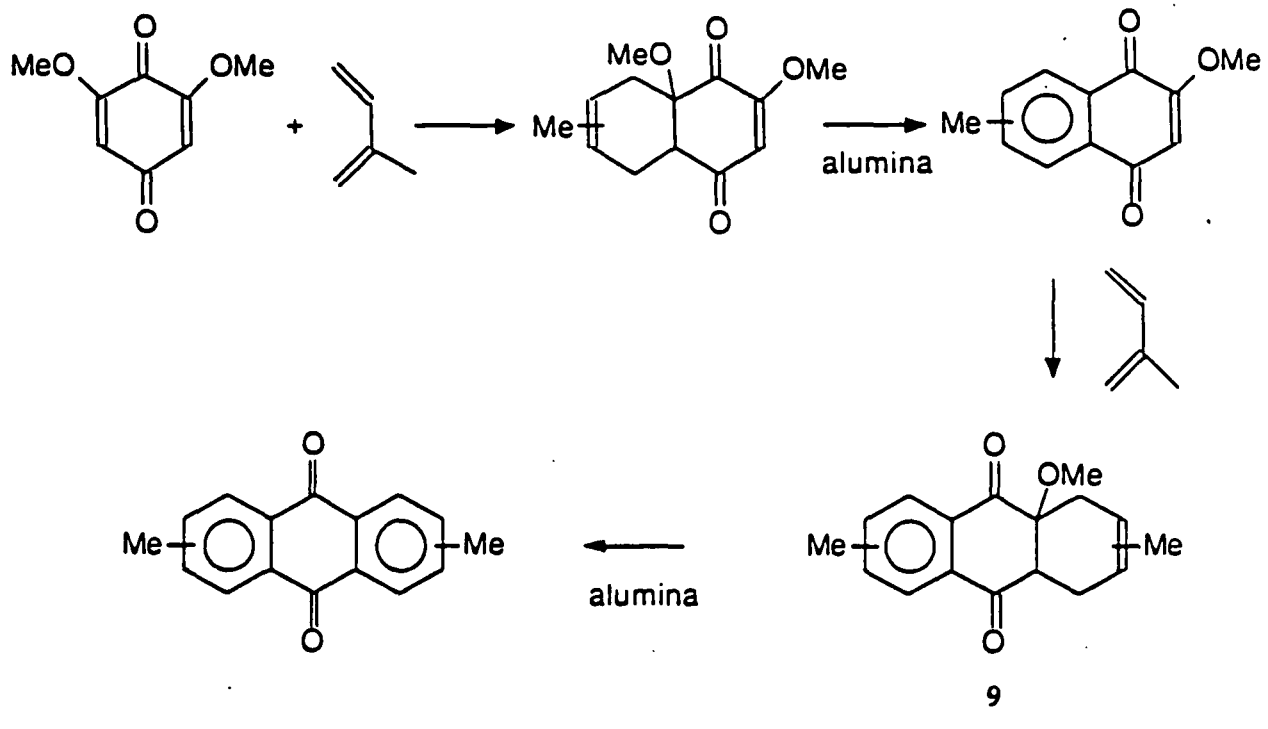

Figure 12. One pot reaction of DMBQ and isoprene with alumina added.

Table 3. MMNQ, DMAQ, and Diels-Alder adduct yields from the reaction of DMBQ and isoprene in toluene with alumina (3.4 eq. per DMBQ) at 180°C.

Time, hr	Diene/dieophile ratio, eq.	Alumina type	MMNQ, %	DMAQ, %	Diels-Alder Adduct, %
2	3.4	Woehm/O[a]	32.0	1.6	-
5	3.4	Woehm/O	31.4	2.2	-
12	3.4	Woehm/O	21.5	9.6	-
24	3.4	Woehm/O	11.3	17.9	-
24	3.4	EM Reagents/O	9.1	17.4	-
24	3.4	Camag/O	8.3	20.7	-
24	3.4	Woehm/N[b]	19.0	10.2	-
24	3.4	EM Reagents/N	10.3	15.6	-
24	3.4	Camag/N	7.9	18.8	-
24	3.4	-	12.9	0.9	-
24	3.4	-	11.0	0.5	68.6
24	5.0	-	17.1	1.6	63.7
24	3.4	EM Reagents/O	2.5	21.9	-
24	3.4	Camag/O	8.5	18.3	-
24	3.4	Camag/I[c]	5.6	20.7	-
24	4.4	Camag/O	4.3	24.0	-
24	2.4	Camag/O	11.6	15.9	-
24	3.4	Camag/O[d]	0.7	21.8	-

[a] The O represents activated alumina stored under O_2.

[b] The N represents activated alumina stored under N_2.

[c] The I represents alumina obtained from the manufacturer.

[d] This sample had double the alumina loading.

Results of reacting isoprene (the diene) with dimethoxybenzoquinone (DMBQ) in the presence of different types of aluminum oxide are given in Table 3. Two aromatized Diels-Alder products were observed in the presence of alumina: methoxymethylnaphthoquinone (MMNQ) and dimethylanthraquinone (DMAQ). The latter generally predominated. In the absence of alumina, the main product was the simple nonaromatic monoadduct.

The alumina type had some influence on DMAQ yield with the neutral alumina giving higher yields over that seen with basic alumina. An increase in alumina loading increased the DMAQ yield while the MMNQ yield was lowered. Alumina activation had little effect on the final DMAQ yields. Control experiments without alumina gave 80% product yields, compared to 30% product yields with alumina. It appears that products are being lost by unknown reaction pathways when alumina is present. This work suggests that DMAQ yields may be greater when reactions are preformed sequentially with aromatization on alumina after each Diels-Alder reaction.

Another approach taken to promote aromatization during the Diels-Alder reaction was to change the diene to 1-acetoxy-3-methyl-1,3-butadiene (AMB). An adduct formed from AMB could aromatize directly by losing both methanol and acetic acid (Figure 13).

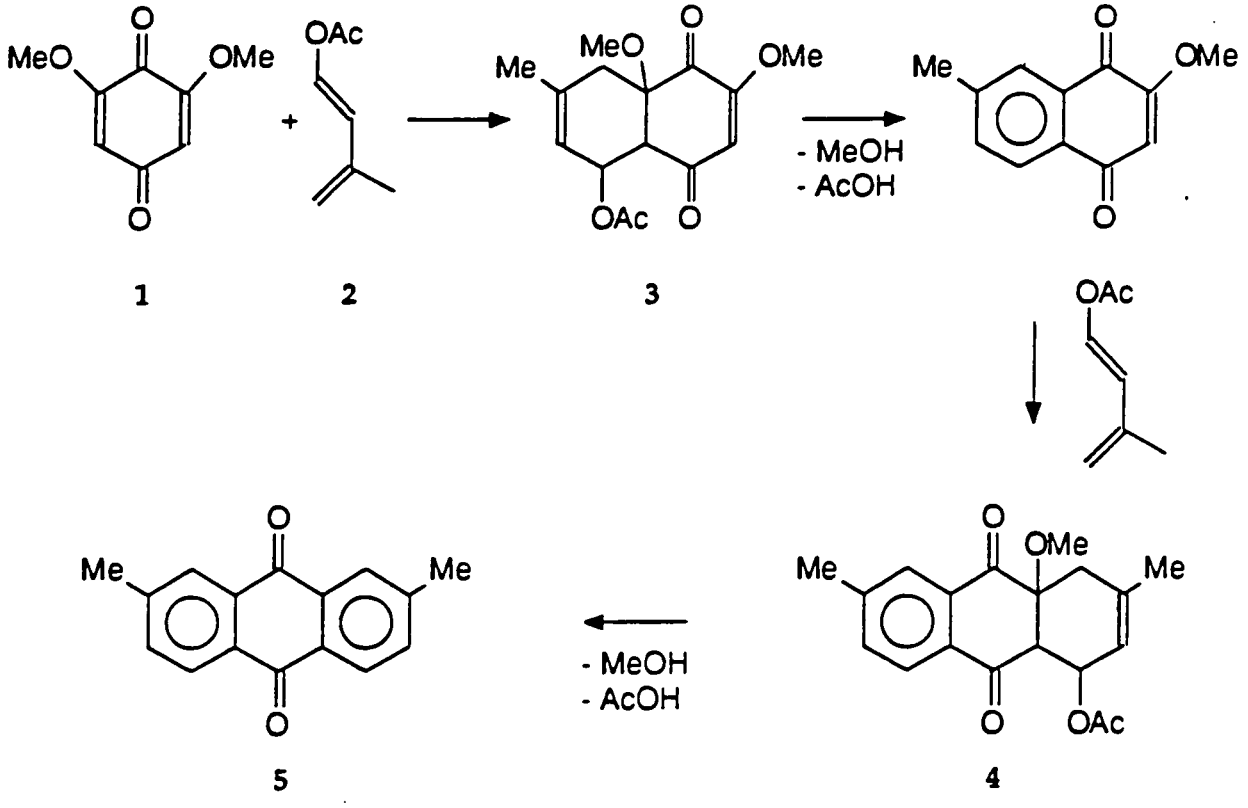

Figure 13. Diels-Alder reactions of DMBQ with 1-acetoxy-3-methyl-1,3-butadiene.

Table 4 lists DMAQ yields for selected reactions. The observed 70% DMAQ yield indicates that it is possible to design a high yield method to synthesize DMAQ. The yields exhibited a positive effect due to time and diene loading.

Table 4. DMAQ yields from the reaction of DMBQ and AMB in toluene at 180° C

Time, hr.	Diene/dieneophile ratio, eq.	DMAQ yield %
2	2.4	1.9
4	2.4	4.7
6	2.4	11.2
24	2.4	32.4
48	2.4	41.0
48	2.9	53.3
48	4.0	61.5
48	4.9	70.5

The reaction was repeated at 200°C to examine the effects temperature, time, diene loading, and DMBQ concentration. Yields (Table 5) were in the 57-63% range. Time, temperature, and concentration had surprisingly little effect on the final DMAQ yield, but diene loading had a positive effect on DMAQ yield.

Table 5. DMAQ yields from the reaction of DMBQ and AMB in toluene at 200° C

Time, hr.	DMBQ, M	Diene/dieneophile ratio, eq.	DMAQ yield %
12	0.2	4.0	58.0
12	0.4	4.0	56.9
24	0.2	4.0	57.3
24	0.4	4.0	58.2
24	0.6	4.0	58.8
24	0.2	5.7	62.4

The AMB reactions were also run in the presence of alumina to determine if the alumina acted as a Lewis acid or just facilitated aromatization. The yield/product composition data given in Table 6 shows that alumina affords more AQ-type product, but the catalytic effects were not very pronounced.

Another way to promote aromatization of an intermediate adduct is to place another leaving group, such as a chlorine atom, on the quinone along with the methoxy groups. Chlorinated quinones may be present in Cl_2/ClO_2 pulp bleaching liquors, or easily generated from such liquors. To see if chlorinated quinones are good substrates in Diels-Alder reactions, Dr. Karim has examined the reactions of

Table 6. DMAQ and MMNQ yields from the reaction of DMBQ and AMB (4.1 eq.) in toluene with alumina (3.4 eq. per DMBQ) at 180°C.

Time, hr	Alumina type	MMNQ, %	DMAQ, %
5	Camag/O[a]	35.0	20.8
24	Camag/O	14.0	52.0
24	EM Reagents/O	11.0	54.8
24	Woehm/O	8.3	37.5
24	Camag/O	10.4	54.1
24	Camag/I[b]	11.4	54.2
24	Camag/O	12.0	54.3
24	-	19.4	45.9

[a] The O represents activated alumina stored under O_2.

[b] The I represents alumina obtained from the manufacturer.

tetrachlorobenzoquinone with isoprene. Very little reaction occurred at room tem perature or 70°C in benzene solvent; however, an unaromatized monoadduct was observed in high yields at roughly 200°C. Simple base treatment of the adduct caused elimination of two molecules of HCl and the formation of a napthoquinone. Consequently, this type of approach has merit.

Several Lewis acid catalyzed, DMBQ/isoprene, Diels-Alder reactions were run at room temperature. The $TiCl_4$ catalyzed reaction gave the Diels-Alder unaromatized monoadduct product similar to what was found in the high temperature reactions. Control reactions without catalyst exhibited no reaction over the same time period. The Diels-Alder adduct yield was very dependent upon $TiCl_4$ charge as listed in Table 7. The low yield with 0.1 eq. of $TiCl_4$ indicates that there is little catalytic activity. The DMBQ that did not go to Diels-Alder adduct was not degraded.

Table 7. Diels-Alder adduct yields from the titanium tetrachloride catalyzed reaction of DMBQ and isoprene in dichloromethane at room temperature for 24 hours.

$TiCl_4$ eq.	Diels-Alder adduct, %
1.00	37
0.50	26
0.25	6
0.10	1

Research at SERI, which is very preliminary, has shown that the reaction of methoxynaphthoquinone with butadiene in the presence of a Lewis acid promoter at 100°C gives anthraquinone in 22% yield (equation 8). No intermediate Diels-Alder adduct is observed. Although the yield is low, this experiment substantiates other results in our laboratory which indicate that direct preparation of anthraquinone from a methoxy substituted quinone is possible.

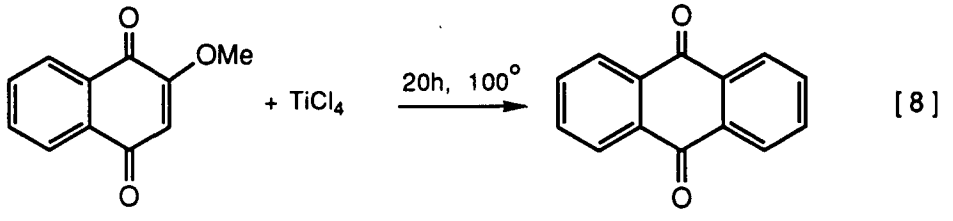

[8]

22%

We also examined $BF_3 \cdot Et_2O$ and $FeCl_3$ catalyzed reactions. The product mixtures from these reactions were similar, but different than that found in the high temperature or the $TiCl_4$ catalyzed reactions. The predominate product has a molecular mass of 238 units by GC/MS and was tentatively identified, by Joe Bozell of SERI, as the addition product of isoprene to the 3 position of 2,6-dimethoxy-p-benzohydroquinone.

Changes in solvent can often have dramatic effects on Diels-Alder reaction yields. Therefore, the results of reactions of isoprene with DMBQ in a polar (acetic acid) and nonpolar (toluene) solvent were compared at the same temperature. The reaction in toluene gave predominantly unaromatized monoadduct and was relative "clean" (see Table 5). The acetic acid reaction product mixture contained DMBQ (starting material) as the main product, along with a wide range of minor components. According to a gas chromatography-mass spectroscopy analysis, many of the minor components contained incorporated acetic acid molecules. The potential overall yield would appear to be better in the toluene case.

The literature suggests that an aqueous medium can promote Diels-Alder reactions. Micelles with the dieneophile and diene are formed and the proximity of the reactants increases the reaction rate. A DMBQ/isoprene reaction in water was run for 18 hours. Micelle formation was aided by an ultrasonic cleaner. Heat generated by the ultrasonic unit boosted the temperature to 70°C. Gas chromatographic analysis indicated mostly DMBQ, the Diels-Alder adduct (predominate product), MMNQ, and DMAQ.

The literature also suggested that ethylene glycol and formamide similarly could promote Diels-Alder reactions; however, when the aqueous reaction conditions were repeated with the other these solvents, Diels-Alder adducts were not observed. Work in this area is being continued by M.S. student Dave von Oepen. The aqueous Diels-Alder reactions show a great deal of promise.

FUTURE STUDIES

Because of the significance of the organosolv lignin extraction results, many of the experiments will be repeated to determine the reproducibility of the results and to more completely characterize the extracted lignin.

We will continue to optimize oxidation yields with peroxide, cobalt/oxygen, and hydroxysuccimide and simple lignin model substrates. Diels-Alder reactions in water (M.S. student work), in supercritical solvents, and with chlorinated quinones will be further expanded.

Long -term research areas will address:

Optimize oxidation yields for 2-3 reagents and test on low molecular weight lignin samples.

Develop analytical methods for determining quinone yields from the oxidation of lignin substrates.

Screen several lignin samples for their potential to generate quinone catalyst.

Optimize Diels-Alder reaction yields.

Decide which oxidation agent, starting lignin, diene, and quinone catalysts to pursue for commercial development.

Continue economical evaluation updates.

THE INSTITUTE OF PAPER SCIENCE AND TECHNOLOGY

D. R. Dimmel

Donald R. Dimmel
Professor and Principal Research Scientist

PROJECT SUMMARY FORM

DATE: March 20, 1990

PROJECT NO. 3664: Precursors and Variables in Dioxins Formation (API/NCASI funded)

PROJECT LEADERS: T.J. McDonough (IPST); L. LaFleur (NCASI)

IPST GOAL:

To minimize the environmental impact of bleached kraft pulp production.

OBJECTIVE:

Assess the significance and determine the source of precursors for chlorinated dioxins, and understand the effects of process variables on their conversion.

CURRENT FISCAL YEAR BUDGET: $150,000

PRIOR RESULTS:

Since this project was initiated subsequent to preparation of the last set of status reports in fall, 1988, no results have been reported in that form. Results were presented at both the Spring, 1989 and Fall, 1989 meetings of the Pulping Processes Project Advisory Committee, and at "Dioxins '89" in Toronto in September. The current report summarizes all of these data.

SUMMARY OF RESULTS SINCE LAST REPORT:

Bleaching experiments have been done to (1) assess the significance of dibenzodioxin (DBD) and dibenzofuran (DBF) as precursors for the chlorinated dioxins and furans formed in kraft pulp bleaching; (2) determine whether DBD and DBF are present in wood and whether they are formed or destroyed during pulping; (3) determine whether chlorine dioxide can effectively destroy precursors for chlorinated dioxins; and (4) evaluate the effects of changes in chlorination stage variables, alone and in various combinations.

The experiments aimed at objective (1) in this list have been completed and are being published. The main conclusion was that nonextractable precursors, different from DBD and DBF are present. Objective (2) experiments have met with analytical difficulties and are incomplete. Objective (3) experiments have shown that chlorine dioxide is ineffective in destroying precursors. Objective (4) experiments, with the exception of mixing and consistency studies, are complete and analysis of the resulting samples is in progress.

PLANNED ACTIVITY THROUGH FISCAL YEAR 1990:

We plan additional experiments to confirm and extend the conclusions of effects of chlorine dioxide [objective (3) above]. Mixing and consistency effects will be studied and a proposal for studying the possibility of destruction of dioxins in the extraction stage will be prepared. These plans will be confirmed with the research oversight committee of API.

Project 3664 Status Report

PRECURSORS AND VARIABLES IN DIOXINS FORMATION
(API/NCASI Funded)

INTRODUCTION

Work proposed under this project encompasses three areas: the source of the known precursors, dibenzodioxin (DBD) and dibenzofuran (DBF); the significance of DBD and DBF relative to other, unidentified precursors; and the effects of chlorination stage variables.

In the first part, wood shavings were manually prepared from jack pine logs and pulped in the laboratory under controlled conditions. Samples of the unpulped wood, the pulp, the spent pulping liquor, and solvent rinsates of the laboratory equipment were submitted for analysis for DBD and DBF. A second batch of wood shavings was exhaustively extracted with known solvents for DBD and DBF, and pulped. Samples of the resulting wood, pulp, liquor and rinsates were similarly submitted for DBD and DBF analyses. Difficulties were subsequently encountered with the analysis of these samples, due to unknown interferences. Completion of this part of the work must await resolution of the analytical difficulties by NCASI staff; it will not be discussed further in the present report.

Work on the significance of DBD and DBF as precursors centered around bleaching experiments in which a control pulp was compared with samples of the same pulp after (a) spiking with DBD and DBF and (b) exhaustively extracting and steam distilling . All three pulps were bleached in chlorination and caustic extraction stages, and the resulting pulps, effluents and solvent rinsates were analyzed for 2,3,7,8-tetrachlorodibenzodioxin (2378-TCDD) and 2,3,7,8-tetrachlorodibenzofuran (2378-TCDF). This part is complete, and a paper has been submitted for publication. A summary is presented below and the journal article is appended.

That part of the project dealing with the effects of chlorination stage variables was subdivided into three parts: (a) ability of chlorine dioxide to destroy precursors; (b) effects of timing of chlorine dioxide addition, temperature, oxygen delignification, spent liquor carryover to the chlorination stage and recycle of chlorination effluent; and (c) effects of mixing and consistency.

SIGNIFICANCE OF DBD AND DBF AS PRECURSORS

Table 2 of the appended article shows that virtually all of the 2378-TCDD and 2378-TCDF emerging from the chlorination stage was found in the pulp, the amounts in the filtrate being negligibly small. After the extraction stage, the amounts found in the filtrate were roughly comparable to those found in the pulp (Figure 1). Most importantly, it was observed that significant amounts of 2378-TCDD/F were formed even when the level of DBD in the brownstock had been reduced to less than 1 ppt and the level of DBF had been reduced to that of the laboratory blank (Table 1). This shows that other, nonextractable precursors are important. It was also shown that the amounts of TCDD/F entering the extraction stage were not significantly different from those leaving it (Table 2).

Project 3664 Status Report

TEST OF ABILITY OF CHLORINE DIOXIDE TO DESTROY PRECURSORS

Substitution of chlorine dioxide for chlorine in the chlorination stage is known to decrease the amounts of chlorinated dioxins formed in that stage. Learning more about the mechanism by which this occurs may enable further reductions to be made. Accordingly, we have done experiments to determine whether dioxin precursors are destroyed by chlorine dioxide.

In principle, this can be determined by chlorinating pulps which have been pretreated with chlorine dioxide and comparing dioxin levels to those of control chlorinations. However, the results of such an experiment would not be conclusive, because the precursors are probably less reactive toward chlorine dioxide than lignin. It is thus likely that, even if chlorine dioxide is capable of destroying the precursors, it would be consumed by lignin before having an opportunity to do so. To minimize the chance of this occurring, a preliminary chlorination was employed to satisfy most of the lignin's oxidant demand, while at the same time keeping the amount of chlorine applied small enough to preclude dioxin formation at this stage. The preliminary chlorination was followed by application of chlorine dioxide and then by another chlorine charge. The purpose of the final application of chlorine was to generate chlorinated dioxins from precursors surviving the chlorine dioxide treatment. Determination of the amount formed would then serve as an indicator of the amount of surviving precursor.

Table 1 contains the results of experiments of this kind for various levels of application of chlorine in the final stage. They were conducted in a Quantum Technologies high-shear laboratory mixer, the preliminary chlorination being run at 5.5% consistency. After 30 minutes reaction at 40 degrees C, chlorine dioxide solution was injected, reducing the consistency to 4.5%. At the end of a further 30-minute reaction period, chlorine solution was injected, the consistency being further decreased to 3.5%. For comparison, the table includes the results of a series of experiments in which the chlorine dioxide solution injected for the second stage was replaced by an equal volume of pure water. Also included are the results of two earlier chlorinations conducted in a single stage at 3.5% consistency, without chlorine dioxide, in a glass vessel stirred by an ordinary glass impeller.

TABLE 1 THREE STAGE CHLORINATION DATA

Chemical Charges as Multiples of Unbleached Kappa Number					Concentration (ppt)		
Stg 1 (Cl_2)	Stg 2 (ClO_2)*	Stg 3 (Cl_2)	Total Cl_2	Total Active Cl	2378-TCDD	2378-TCDF	1278-TCDF
0.12	0.08	0.00	0.12	0.20	ND(0.3)	0.6	0.5
0.12	0.08	0.06	0.18	0.26	0.6	3.1	2.9
0.12	0.08	0.08	0.20	0.28	13.9	50.3	24.6
0.12	0.08	0.12	0.24	0.32	21.3	105.5	49.9
0.12	0.08	0.16	0.28	0.36	40.4	331.9	152.2
0.12	0.00	0.00	0.12	0.12	ND(0.3)	1.7	1.5
0.12	0.00	0.06	0.18	0.18	0.8	3.5	2.8
0.12	0.00	0.08	0.20	0.20	1	8.7	6.8
0.12	0.00	0.12	0.24	0.24	10.1	30.3	14.5
0.12	0.00	0.16	0.28	0.28	15.1	64.2	28.0
0.25	0.00	0.00	0.25	0.25	32.8	231.4	112.7
0.25	0.00	0.00	0.25	0.25	41.5	333.3	161.5

*As active chlorine

The observed trends were very similar for 2378-TCDD, 2378-TCDF and 1278-TCDF. At a molecular chlorine multiple (chlorine factor, the sum of Cl2 charges in stages 1 and 3 divided by unbleached kappa number) of 0.18 or less, the amounts of dioxins produced were small or nondetectable, while at higher molecular chlorine multiples they increased sharply. This parallels similar observations in the literature for conventional chlorinations. More importantly, treatment with chlorine dioxide in the second stage increased the amounts produced in the final stage. Since precursor destruction by chlorine dioxide would have resulted in a decrease, it may be concluded that such destruction does not occur. In view of the known beneficial effect of chlorine dioxide substitution, it is likely that the observed increase resulted from a higher average chlorine concentration during the final stage. Alternatively, it may be hypothesized that chlorine dioxide generates precursors.

Comparison with the data from the earlier single stage chlorinations shows that the multistage experiments gave lower levels of dioxins. This supports similar observations by Westvaco researchers of beneficial efects of adding a given amount of chlorine in two or more separate doses. There were other differences between the two sets of experiments (consistency and reactor type) but these are not expected to have large effects.

Project 3664 Status Report

EFFECTS OF CHLORINATION STAGE VARIABLES

An understanding of the effects of chlorination stage process variables on dioxin formation is important as a source of mechanistic information and also may be expected to suggest control strategies. Accordingly, experimental work is in progress to study the effects of the following: (1) timing of chlorine dioxide addition relative to chlorine addition; (2) temperature; (3) recycle of chlorination stage filtrate; (4) oxygen delignification before the chlorination stage; (5) amount of black liquor left in the unbleached pulp; (6) degree of mixing; and (7) consistency.

To study interactions, the first 5 variables in this list were studied together, in a fractional factorial experiment. The experiment was replicated, to increase precision and guard against spurious observations. The variable levels and combinations used are shown in Table 2. These experiments are complete and analysis of the resulting samples is in progress. AOX results will be discussed at the March PAC meeting.

TABLE 2 CHLORINATION STAGE VARIABLES AND LEVELS

VAR LEVL COMB	ClO_2 SEC AFTR Cl_2	TEMP DEG C	C-ST FILT RCYC %	OXGN DLIG %	WASH LOSS L/KG
1	-15	30	0	0	6
2	15	30	0	0	0
3	-15	60	0	0	0
4	15	60	0	0	6
5	-15	30	30	0	0
6	15	30	30	0	6
7	-15	60	30	0	6
8	15	60	30	0	0
9	-15	30	0	50	0
10	15	30	0	50	6
11	-15	60	0	50	6
12	15	60	0	50	0
13	-15	30	30	50	6
14	15	30	30	50	0
15	-15	60	30	50	0
16	15	60	30	50	6

CONCLUSION

The existence of nonextractable precursors has been established, and chlorine dioxide treatment under normal conditions has been shown to be ineffective in destroying dioxin precursors. Data will soon be available on the effects of chlorination stage variables and their interactions.

Paper Presented at '89
The 9th International Symposium on Chlorinated Dioxins
and Related Compounds, September 17-22, 1989, Toronto Canada
Submitted for publication in
Special DIOXIN '89 Edition of Chemosphere

STUDIES ON THE MECHANISM OF PCDD/PCDF FORMATION DURING THE BLEACHING OF PULP

L. LaFleur*[1], B. Brunck[1], T. McDonough[2], K. Ramage[1],
W. Gillespie[1] and E. Malcolm[2]

[1]National Council of the Paper Industry for Air and Stream Improvement
P.O. Box 458 Corvallis, OR 97339 USA

[2]Institute of Paper Science and Technology
575 14th Street, NW Atlanta, GA 30318 USA

ABSTRACT

Laboratory bleaching experiments were performed to investigate PCDD/PCDF formation mechanisms. The results indicated that there were two (or more) mechanisms; direct chlorination of DBD/DBF and formation from precursors which are not extractable. In general, PCDDs/PCDFs are formed in the C stage but some minor isomers were found to be formed in the E stage.

KEYWORDS

Dibenzo-p-dioxin, Dibenzofuran, 2378-TCDD, 2378-TCDF, pulp bleaching

INTRODUCTION

It was recently reported that oil based defoamers were implicated in TCDD/TCDF production in the pulp bleaching process and that one possible precursor was dibenzofuran (DBF) (Allen et al. 1989). Further studies have supported these findings and have implicated dibenzo-p-dioxin (DBD) as another possible precursor (Voss et al., 1988, and Berry et al. 1989). The objectives of the present study were to (a) determine to what extent that PCDD/PCDF are formed from DBD/DBF present in unbleached brownstock (b) seek evidence of other formation mechanisms and (c) determined if PCDDs/PCDFs are formed in the E stage.

The experimental approach taken was to thoroughly wash all traces of DBD/DBF from a mill brownstock pulp, bleach the washed pulp, and analyze C and E stage pulps and filtrates for PCDD/PCDF. If PCDDs/PCDFs were detected, it could be inferred that they were produced from other precursors. To evaluate conversion efficiency and to establish the isomer profile of DBD/DBF derived PCDD/PCDF, a sample of the mill pulp was spiked with elevated levels of DBD/DBF, bleached and analyzed. The mill brownstock was bleached without pretreatment and the resulting pulps and filtrates analyzed to serve as a control.

METHODS

Brownstock Preparation Procedures. Brownstock pulp with 31.8 kappa number was obtained from a mill pulping northern softwoods. A portion was first soxhlet extracted with methanol. In order to displace the methanol and replace it with water and to further remove DBD/DBF, the pulp was placed in a round bottomed flask, reagent grade water was added and distilled off until a constant boiling point was achieved. The results relating to this pulp will be referred to as the extracted experiment. A separate portion of brownstock was diluted in reagent grade water that had been spiked with a methanol solution of DBD/DBF and was allowed to equilibrate for two days. The pulp suspension was then chilled and the consistency was reduced through filtration. The results relating to this pulp will be referred to as the spiked experiment.

Bleaching conditions. All pulps were bleached in a two stage CE bleaching sequence. The C stage bleaches were conducted in an all glass apparatus equipped with a glass impeller. The E stage was conducted using a stainless steel vessel with a horizontal shaft pin mixer. A kappa factor of 0.25 at 3.5% consistency, 40° C for 45 minutes was used for the C stage. A 4.4% caustic charge at 10% consistency, 70° C for 60 minutes was used for the E stage. Pulps and filtrates from each bleaching stage, along with ethanol and toluene rinsates from the bleaching equipment were analyzed. Each experiment was conducted in duplicate.

DBD/DBF and PCDD/PCDF Analyses The methods for the determination of DBD/DBF will be described elsewhere (NCASI, 1989a). The PCDD/PCDF determinations were made using an adaptation of procedures previously reported (NCASI, 1988). The adaptations included incorporation of additional labelled PCDD/PCDF internal standards and modifications of the cleanup procedure and will be described in more detail (NCASI, 1989b). Wherever possible, isomer identifications were made based on comparison of the relative retention times from a mixture of commercially available native standards which were run on the same day as the samples. Other peaks were tentatively identified based upon relative retention times published in the literature.

RESULTS

Table 1 summarizes the average quantities (expressed as ng/kg) of DBD/DBF and 2378-TCDD, 2378-TCDF and 1278-TCDF detected on the unbleached brownstocks and the corresponding C stage pulps. The concentrations of DBD/DBF fall within the range of values NCASI has measured in 23 different pulp mill brownstocks. There were no detectable levels of DBD and no significant levels of DBF in any of the bleached pulps or filtrates.

Table 1. Summary of Brownstock and C Stage Pulp Analysis Results

	Concentration (ng/kg)				
Sample	DBD in Brownstock	2378-TCDD	DBF in Brownstock	2378-TCDF	1278-TCDF
Extracted	ND (0.6)	19.7	49	41.2	26.1
Brownstock	ND (0.6)	20.8	NQ (26)	33.9	20.8
Control	34.0	32.8	2030	231	113
Brownstock		41.5		333	162
Spiked	1740	1011	61700	10000	4570
Brownstock	1750	1150	60100	8540	4080

Table 2 summarizes the average of the results obtained for other PCDD/PCDF isomers for the duplicate experiments expressed in ng/kg. Due to space limitations, if no sample showed more than 1 ng/kg of a given isomer, it was deleted from Table 2. Also, HpCDDs and OCDD data were deleted due to laboratory blank problems.

DISCUSSION

The results were first used to look at the C stage pulp and any change that might occur in the E stage. The direct chlorination of DBD/DBF does not require the presence of base and therefore, formation of additional PCDD/PCDF was not expected in the E stage. The total PCDD/PCDF observed in C stage pulp was compared with that found in the sum of the E stage pulp, filtrate and equipment rinsates. Fig. 1 illustrates the results of the this comparison for 2378-TCDD and 2378-TCDF. Note that there is no consistent trend toward increase or decrease for these two analytes. Other major PCDDs/PCDFs displayed similar results. Based upon these observations, it is reasonable to focus attention on the C stage samples alone.

Comparison of the total 2378-TCDD and 2378-TCDF detected on the C stage pulp verses that detected in the C stage filtrate (the quantities in the rinsates were negligible in the C stage) indicated that 98% to 99% of the analytes were present on the pulp. This greatly simplifies the evaluation of the data, since meaningful comparisons can be made using the C stage pulp data. It should be emphasized, however, that this was observed in the context of a laboratory bleaching experiment where care was taken to minimize the passage of pulp fines into the filtrate and therefore, should not necessarily be considered generally applicable to mill survey data.

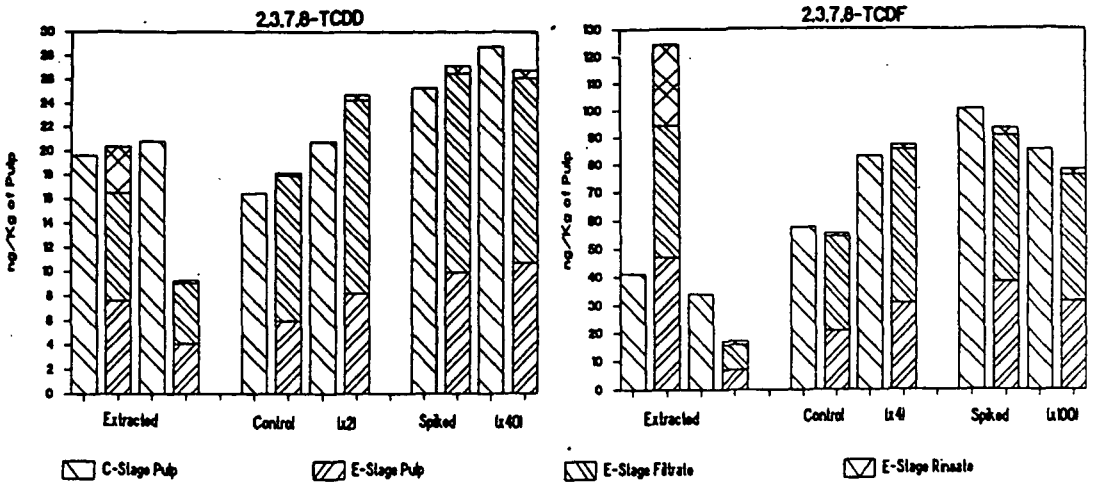

Fig. 1 Comparison of C Stage Pulp PCDD/PCDF with Total Detected in E Stage

With the exception of some minor isomers (2367-TCDF, 2468-TCDF, 12378-PeCDF and 123478/67-HxCDF), the fingerprints of all three experiments were similar. The most important observation that can be made from the data is that 2378-TCDD and 2378-TCDF/1278-TCDF are still formed even when the DBD levels are non-detect or the DBF levels are essentially at the level of the laboratory blank. The concentrations of 2378-TCDD, 2378-TCDF and 1278-TCDF all increase in the control and spiked bleaching experiments proportional to the increased levels of DBD/DBF in the brownstock pulp. A plot of the 2378-TCDD produced verses the DBD levels in the brownstock showed a linear relationship with the intercept essentially at the concentration of 2378-TCDD detected in the extracted pulp experiment.

These observations lead to the conclusion that there are two (or more) independent mechanisms for the formation of PCDD/PCDF in the bleaching process. The first is direct chlorination of DBD/DBF in the C stage which has been previously discussed (Allen et al. 1989, Voss et al. 1988, and Berry et al. 1989). The second, indicated from the results reported here, involves formation from other precursors. It can be further stated that, since even thorough washing failed to remove these precursors, they can be characterized as "non-extractable." Fig. 2 shows the lower end of a plot of DBD in brownstock versus 2378-TCDD formed and illustrates the relative contributions of the proposed mechanisms.

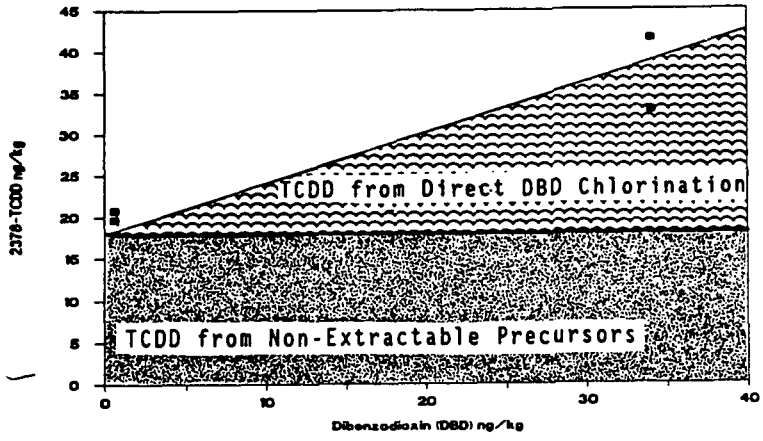

Fig. 2 Illustration of Relative Contribution of Proposed 2378-TCDD Precursors

Table 2. Summary of PCDD/PCDF Analysis Results

Analyte	Extracted Experiment (ng/kg)				Control Experiment (ng/kg)				Spiked Experiment (ng/kg)			
	C-Stage		E-Stage		C-Stage		E-Stage		C-Stage		E-Stage	
	Pulp	Filtrate	Pulp	Filtrate	Pulp	Filtrate	Pulp	Filtrate	Pulp	Filtrate	Pulp	Filtrate
PCDDs												
1237/1238	ND	ND	0.2	0.1	0.1	ND	0.2	ND	2.9	ND	0.2	1.7
2378	20.2	0.1	5.9	6.9	37.2	0.9	14.1	28.0	1080	12.7	410	642
1278	0.4	ND	0.2	0.3	1.8	ND	0.4	1.3	63.3	0.4	25.0	36.8
12468/12479	ND	ND	1.7	ND	ND	ND	1.5	ND	ND	ND	0.8	ND
12469	ND	ND	0.6	0.3	0.1	ND	1.1	0.6	0.2	ND	1.0	0.3
12378	1.2	ND	0.3	0.5	1.4	ND	0.4	1.3	20.6	0.1	8.6	13.1
123468	ND	ND	2.1	0.6	ND	ND	1.7	0.8	ND	ND	0.0	0.9
123467/123789	0.4	0.2	0.7	0.5	0.4	0.1	0.8	0.5	0.6	0.1	1.1	1.0
PCDFs												
1378	ND	ND	ND	ND	0.5	ND	0.2	0.1	9.6	ND	4.0	4.8
1347/1379	ND	ND	ND	ND	0.1	ND	0.1	ND	2.1	ND	ND	1.6
1247/1468	0.3	ND	0.2	0.2	1.6	ND	0.4	0.5	27.9	0.2	14.7	10.1
1348	ND	ND	0.1	0.1	0.9	ND	0.4	0.9	23.1	0.1	8.8	10.5
1248/1346	3.5	ND	1.1	1.4	16.1	0.2	5.7	11.5	329	1.8	117	150
1268/1478	ND	ND	ND	ND	ND	ND	ND	ND	ND	2.0	ND	114
1369	1.9	ND	1.3	1.3	14.2	0.1	6.3	12.7	387	2.1	177	104
2468	9.8	0.1	4.1	4.3	9.2	0.2	8.8	15.2	ND	0.1	6.4	4.6
1238/1467	1.3	ND	1.2	1.2	16.4	0.1	6.2	10.6	382	1.9	136	166
1278	23.5	0.3	14.1	13.5	137	2.2	49.0	88.7	4320	57.5	1550	2200
2368	1.2	0.1	1.3	1.2	3.2	0.1	3.9	6.4	108	0.6	110	129
1267/1279/1469	0.3	ND	0.4	0.3	3.9	ND	1.5	0.9	153	0.8	55.9	69.7
2467	0.1	ND	ND	ND	ND	ND	0.1	0.1	ND	ND	ND	1.7
2347	ND	ND	0.1	0.1	1.8	ND	ND	1.2	50.7	0.3	19.8	17.6
2378	37.5	0.6	27.1	28.1	282	4.2	104	177	9300	108	3470	4860
1239/2348	3.5	ND	2.0	2.2	21.1	0.3	4.2	13.1	616	7.3	226	320
2346	ND	ND	ND	0.1	2.2	ND	0.3	0.5	50.8	0.3	18.4	15.5
2367	0.5	ND	1.0	1.1	13.2	0.1	5.8	8.5	604	6.1	218	247
1289	5.3	ND	1.9	2.0	18.9	0.2	6.7	11.8	294	5.5	107	148
12468/13468	2.4	ND	1.6	2.5	2.4	ND	3.4	5.8	4.4	ND	5.0	5.5
13479/23469	ND	ND	0.5	0.3	1.8	ND	1.3	0.6	33.2	0.5	16.6	25.7
12479	ND	ND	ND	ND	ND	ND	ND	ND	1.4	ND	0.7	0.5
12346/47/12469/ 13469/23468	2.9	0.1	2.2	2.3	3.6	0.1	3.2	6.3	14.3	0.1	9.0	13.7
12348	0.3	ND	0.1	ND	1.1	ND	0.5	0.9	23.5	0.3	9.6	14.3
12378	2.5	ND	0.9	0.8	4.3	ND	1.7	3.2	77.4	1.1	30.2	47.6
12367	ND	ND	ND	ND	0.1	ND	ND	ND	2.4	ND	0.4	0.5
12379/23489	0.6	ND	0.3	0.1	1.2	ND	0.6	0.8	27.4	ND	11.5	17.4
12369/12489/ 13489/23478	1.0	ND	0.6	0.5	3.9	0.1	1.5	2.9	125	1.5	51.8	73.5
23467	1.3	ND	0.3	ND	3.8	ND	1.4	3.0	19.0	0.2	8.6	13.3
12389	0.4	ND	0.1	0.1	0.3	ND	0.2	0.6	8.7	0.1	3.4	6.2
123468	0.7	ND	0.3	0.5	0.8	ND	0.5	0.9	1.1	ND	0.7	0.5
124678/134678/ 134679	1.1	ND	0.4	0.2	1.2	0.1	0.6	0.8	2.6	ND	1.2	0.5
124689	1.2	ND	0.5	0.5	1.9	ND	0.8	1.3	1.9	ND	0.6	1.1
123467/123478	7.0	0.2	2.5	2.8	9.9	0.3	3.6	7.4	14.7	0.5	6.3	9.9
123479/123678	0.8	ND	0.4	0.3	0.6	ND	0.5	0.5	1.6	ND	0.6	1.4
234678	0.9	0.3	0.3	0.4	1.0	0.2	0.3	0.4	2.0	0.2	1.2	0.4
123489	1.6	ND	0.7	0.3	2.1	0.1	0.7	1.6	3.2	ND	0.8	2.0
1234678/1234689	0.8	0.1	0.4	1.1	ND	ND	ND	1.2	1.2	ND	ND	0.7
1234679	1.5	0.1	0.4	0.9	4.1	0.2	1.0	3.1	2.5	0.1	0.6	0.5
1234789	1.8	ND	0.5	0.9	3.7	0.1	0.8	2.6	2.8	0.1	0.8	2.9
Octa-CDF	3.2	0.2	0.5	1.7	6.5	0.2	2.3	5.8	3.3	0.4	1.5	2.9

[a]Isomers are identified by listing the positions occupied by chlorine.

An estimate of the relative contribution of the two mechanisms in the control experiment was obtained by (a) assuming that the contribution of the direct DBD chlorination can be approximated by calculating the DBD (or DBF) to PCDD (or PCDF) conversion efficiency for the spiked experiment results (since the non-extractable contribution would be negligible) and that (b) the average concentration detected in the extracted pulp experiment represents the contribution attributable to non-extractable precursors. These assumptions, can be used to predict the concentration of PCDD/PCDF which would be accounted for by the hypothesis of two mechanisms as follows:

Contribution from non-extractable precursors
+ (DBD/DBF level in unbleached pulp x Direct chlorination factor) =
PCDD/PCDF Predicted in C stage Control Pulp

The results of this calculation for 2378-TCDD, 2378-TCDF and 1278-TCDF are summarized in Table 3 and the results for other isomers are illustrated in Fig.3.

Table 3. Predicted Versus Observed Concentrations in the Control Experiment

	ng/kg in C Stage Pulp			
	Expt. #1	Expt. #2	Conversion Factor	Predicted
2378-TCDD	32.8	41.5	0.607	40.8
2378-TCDF	231	333	0.152	345
1278-TCDF	113	162	0.071	167

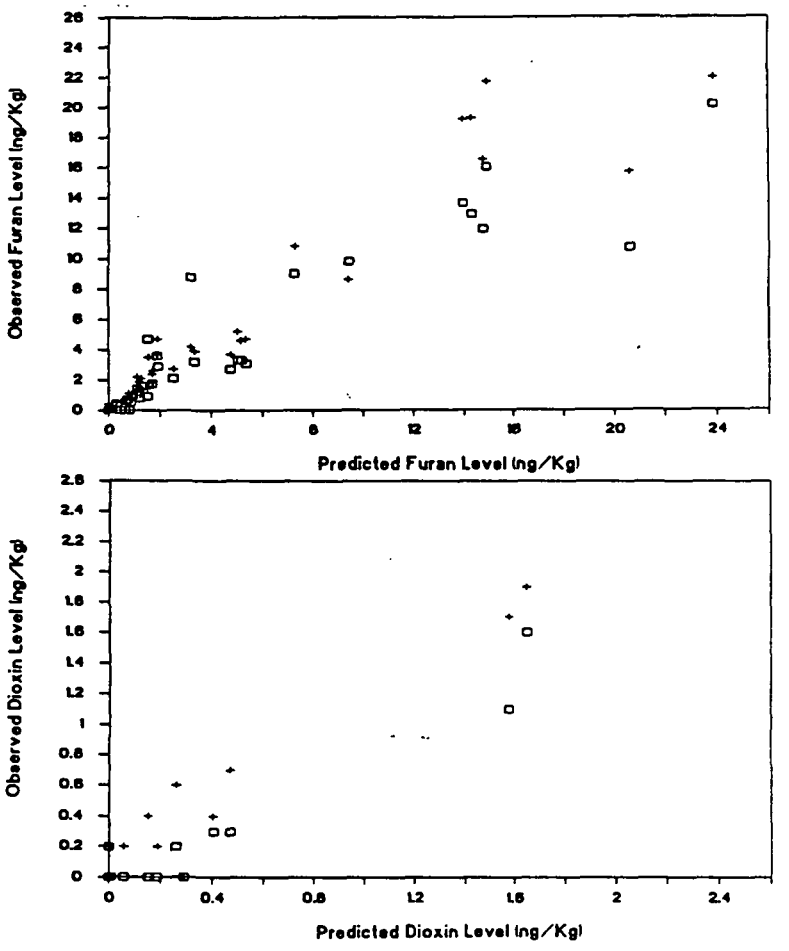

Fig. 3 Predicted vs Observed PCDD/PCDF in C Stage Pulp

In general, the predicted values were very close to the observed values. This indicates that all the material detected can be accounted for by the two proposed mechanisms. It also suggests that the major PCDD/PCDF precursors extracted from the pulp are DBD and DBF. The relative contribution of the two proposed mechanisms are essentially equal for 2378-TCDD. However, the "non-extractable" precursors account for only 13% of the 2378-TCDF formed in the control experiment indicating that the direct chlorination mechanism is clearly the dominant source of 2378-TCDF (and 1278-TCDF). It is also interesting that under the conditions used for this experiment, the conversion of DBD to 2378-TCDD was about 4 times greater than the conversion of DBF to 2378-TCDF and 8 times greater than DBF to 1278-TCDF.

Although the initial comparison of 2378-TCDD and 2378-TCDF in C stage pulp verses E stage pulp plus filtrate indicated no substantial increase in the E stage, there were some minor PCDF isomers for which this was not true. These include 2368-TCDF, 2468-TCDF, the co-eluting isomers 12468/13468-PeCDF and 12346/12347/12469/13469/23468-PeCDF. Of these, only 2368-TCDF showed a significant dependance on the DBF level. The others showed some DBF dependance but the yield factors were very poor.

No evidence of PCDD isomer formation in the E stage was found in the data. It has been reported that 12378-PeCDD is formed in the E stage (de Sousa, 1989). Review of the data generated in this experiment showed that the overall levels of 12378-PeCDD increased with increasing brownstock DBD but there was no evidence of substantial formation in the E stage within our experimental error.

CONCLUSIONS

These experiments demonstrate that there are two (or more) mechanisms for the formation of PCDD/PCDF in the pulp bleaching process. The first is the direct chlorination of DBD/DBF present on the brownstock. The second involves formation from precursors which are not extractable from the unbleached pulp. In the control experiment, the relative contribution of the two proposed mechanisms were about equal for 2378-TCDD but the direct chlorination mechanism accounted for the majority of the 2378-TCDF formation.

Generally, most of the PCDD/PCDF formation occurs in the C stage. However, there are several minor PCDF isomers which do increase in the E stage.

REFERENCES

Allen, L.H., R.M. Berry, B.I. Fleming, C.E. Luthe and R.H. Voss (1989). "Evidence that Oil-Based Additives are an Indirect Source of the TCDD and TCDF Produced in Kraft Bleach Plants," Chemosphere, 19, Nos.1-6, 741-744.

Berry, R.M., B.I. Fleming, R.H. Voss, C.E. Luthe and P.E. Wrist (1989). "Preventing the Formation of Dioxins During Chemical Pulp Bleaching," paper presented at the 75th Annual Meeting of the CPPA Technical Section, Montreal, Jan. 31- Feb. 3.

NCASI Technical Bulletin No. 551 (1988). "NCASI Procedures for the Isomer Specific Analysis of Pulp and Paper Industry Samples for 2,3,7,8-TCDD and 2,3,7,8-TCDF." New York, NY.

NCASI Technical Bulletin (1989) "DBD/DBF Analytical Protocol," in preparation

NCASI Technical Bulletin (1989) Full Congener PCDD/PCDF Analytical Protocol", in preparation

de Sousa, F., M-C. Kolar, K.P. Kringstad, S.E. Swanson, C. Rappe and B. Glas (1989). "Influence of Chlorine Ratio and Oxygen Bleaching on the Formation of PCDDs and PCDFs in Pulp Bleaching." Tappi, 147-153.

Voss, R.H., C.E. Luthe, B.I. Fleming, R.M. Berry and L.R. Allen (1988). "Some New Insights into the Origins of Dioxins Formed during Chemical Pulp Bleaching," Pulp and Paper Can., 89, No. 12, 151.

PROJECT SUMMARY FORM

DATE: March 20, 1990

PROJECT NO. 3671: A STUDY OF THE FEASIBILITY OF THERMAL DESTRUCTION OF CHLORINE-CONTAINING CONCENTRATED STREAMS FROM CLOSED CYCLE PROCESSES
(NCASI FUNDED, part of the 301(m) Research and Development program)

PROJECT LEADER: K.M. Nichols

IPST GOAL:

Part of overall IPST program goal to improve pulping and bleaching technology, with emphasis on environmental impact.

OBJECTIVE:

Evaluate potential technologies for thermal destruction of concentrated streams from closed cycle processes in a device other than a kraft recovery furnace.

CURRENT FISCAL YEAR BUDGET: $75,000

PRIOR RESULTS:

No significant results prior to October 1989. (Project was initiated in August 1989).

SUMMARY OF RESULTS SINCE LAST REPORT:

Characterization of the Closed Cycle Streams

In order to conduct laboratory testing here at IPST for the characterization of concentrates, it is necessary to have samples of these concentrates. Since applications of closed cycle technologies, such as ultrafiltration and reverse osmosis, are not presently found in the pulp and paper industry, it has not been possible to obtain samples of concentrates from industry. To overcome this problem, the decision was made to obtain bleach plant effluents (C/D and E1) from a kraft pulp mill, and treat these effluents at IPST using closed cycle technologies for the purpose of producing enough concentrates for characterization and combustion testing.

After consideration of various mills located in the Southeastern section of the U.S., a mill site was selected, arrangements were made with the mill, and IPST received the necessary quantities of effluent from both the C/D first bleach stage and the first-stage caustic extraction. These samples are currently being analyzed at IPST for total solids, total organics, organic chlorine (as AOX), elemental composition (C, H, O, S, Cl, Na, K), and heating value of the dried solids.

Two closed cycle treatment technologies were selected for the laboratory treatment of these bleach plant effluents: ultrafiltration and reverse osmosis. Laboratory-scale filtering equipment has been leased from Niro Atomizer in Hudson, Wisconsin. Niro Atomizer is a U.S. marketer of DDS (De Danske Sukkerfabrikker of Danish Sugar Company, Nakskov, Denmark) filtration equipment. The DDS equipment was selected because of availability and because DDS equipment has been used in prior pilot scale ultrafiltration studies.

The DDS LAB-20 unit being leased for filtering at IPST is of a scale appropriate for research and development. It can be used for both ultrafiltration and reverse osmosis. It has 0.72 m2 (7.8 ft_2) of membrane area, can operate with pressures up to 8 MPa, pH from 0 to 14, and temperatures up to 100°C. The average filtration capacity of the LAB-20 is approximately 35 liters of filtrate per hour.

Combustion Behavior of the Streams

Various experimental methods are being considered for measuring the time-temperature destruction behavior of specific chemical compounds. These include TGA (Thermal Gravimetric Analysis), DSC (Differential Scanning Calorimetry), and a method similar to that developed by Rubey & Carnes (1985) which uses a high-temperature tubular reactor for conducting gas-phase thermal decomposition studies of organic substances. This thermal reactor uses a counterflow heat exchanger in conjunction with a narrow-bore quartz tubular reactor to obtain precise control over physical factors, such as exposure temperature and mean residence time. Gaseous species are subjected to essentially a square-wave thermal pulse as they pass through the thermal reactor. This thermal reactor has been used by Dellinger, et al. (1984) to measure thermal decomposition profiles and kinetic data on nearly 100 different hazardous organic compounds.

Rubey W.A., and Carnes, R.A., "Design of a Tubular Reactor Instrumentation Assembly for Conducting Thermal Decomposition Studies," Rev. Sci. Instrum. 56(9), September 1985.

Dellinger, B., et al., "Determination of the Thermal Stability of Selected Hazardous Organic Compounds," Hazardous Waste, Vol. 1, No. 2, 1984.

PLANNED ACTIVITY THROUGH FISCAL YEAR 1990:

The immediate goal is to obtain concentrates from ultrafiltration and reverse osmosis of C/D and E1 bleach plant effluents according to the matrix shown below. The untreated effluents have been obtained. The UF treated and RO treated samples will be obtained once the filtration device is successfully operated. Once these 6 samples are obtained, determination of the chemical compositions, physical properties, and combustion behavior of the concentrates will proceed.

	C/D	E1
Untreated	x1	x2
UF treated	x3	x4
RO treated	x5	x6

PROJECT SUMMARY FORM

DATE: March 20, 1990

PROJECT NO. 3684: MECHANISMS OF DIOXIN FORMATION IN PULP PRODUCTION. PART I: PRECURSOR FORMATION AND REACTIVITY
(API/NCASI FUNDED PROJECT)

PROJECT LEADER: L.B. Sonnenberg

IPST GOAL:

Eliminate or minimize chlorinated dioxins and chlorinated furans in bleached pulp production.

OBJECTIVE:

The proposed research will develop a fundamental understanding of the chemistries associated with the production and destruction of polychlorinated dioxins and polychlorinated furans (PCDD/Fs) during wood pulping and bleaching operations. The levels of PCDD/F appear to be related to the levels of dibenzo-p-dioxane (DBD) and dibenzofuran (DBF) in pulp and liquors. Therefore, understanding the reactivities of the DBD/F compounds appears critical. One goal is to find a method to chemically modify precursors in order to prevent their conversion to PCDD/Fs. The second set of goals is to determine if a specific wood component is responsible for precursor formation, to identity it, to further define what structural features are necessary for precursor formation and, from these data, to postulate mechanisms of precursor formation.

CURRENT FISCAL YEAR BUDGET: $143,000

PRIOR RESULTS:

Funding was approved by API/NCASI in June. Specific research goals were planned and experimental strategies were developed to attain these goals. Laboratory work began in early December.

SUMMARY OF RESULTS SINCE LAST REPORT:

In the initial phase of the project several electrophilic reagents are being examined and the one(s) most reactive with DBD/F will be determined. Analytical methods have been developed and evaluated for use in the initial phase of the project. Methods for spiking cotton linters with DBD/F, extracting them and analyzing them were examined. Duplicate injections of a five-point standard curve are used to generate the full regression equation used for quantitation with an internal standard. The cleanliness of the

experimental system and the chromatographic resolution have eliminated the need for clean-up procedures thus far. Detection limits are in the ppb range. For each electrophilic reagent examined at least four samples are analyzed; a blank, a control and duplicate experimental samples. The control sample consists of spiked linters which undergo all of the procedures as the experimental samples except for the actual application of the reagent. A recovery standard is added to the concentrated control extract in order to determine the recovery of DBD/F from the linters after treatment.

Dry, spiked linters have been treated with nitrogen dioxide for approximately 10 minutes. The NO_2 doses of 2% (on a dry linters basis) represents a large excess for the reactions with the adsorbed dioxin and furan. The results indicate that dibenzodioxin is considerably more reactive to NO_2 than is dibenzofuran. There is a loss of 99% of the DBD as compared to 33% of the DBF. A single experiment in which the reaction time was quadrupled indicated that the time of reaction was not a limiting factor; the dioxin reacted almost completely and $\leq$ 30% of the furan reacted. Once the major reaction product(s) are determined by GC/MS, the reasons for the difference in reactivity between DBD and DBF may be postulated. Chromatograms from the GC/FID analyses suggest that there is one major product with a high molecular weight that results from DBD reacting with NO_2.

A preliminary experiment in which DBD/F in solution were subjected to concentrated nitric/phosphoric acid in solution showed that the precursors are also susceptible to reaction under these stringent conditions.

PLANNED ACTIVITY THROUGH FISCAL YEAR 1990:

Screening of six different reagents for reactivity with DBD/F will mostly be completed. The reactivities of DBD/F to nitric acid will be completed and studies evaluating the effects of sulfuric acid, ozone, oxygen and peroxides will be conducted.

POTENTIAL FUTURE ACTIVITY:

Once the effective reagent(s) are determined, the procedure(s) will be applied to DBD/F-spiked pulp under varying conditions to determine the applicability of the procedure to DBD/F destruction under realistic industrial conditions. The sequence of experiments will elucidate the wood components that are potential competitors to the DBD/F reactions. The relative selectivities of the reagent(s) for the wood components and DBD/F will be evaluated.

Experiments will be conducted to determine the wood component responsible for DBD/F formation. The investigation will also consider precursors other than DBD/F (should they exist). Methods for inhibiting precursor formation could then be researched.

Project 3684 Status Report

MECHANISMS OF DIOXIN FORMATION IN PULP PRODUCTION.

PART 1: PRECURSOR FORMATION AND REACTIVITY

Reporting Period: September 1989 - February 1990

OBJECTIVE

Chlorination of pulp has been associated with the formation of potentially harmful chlorinated dibenzodioxins and chlorinated dibenzofurans in paper and effluent.[1-2] Research has shown that the unchlorinated compounds, dibenzodioxin and dibenzofuran, are likely to be major precursors to the chlorinated compounds.[3-4] Understanding the reactivities and the sources of these compounds is necessary to eliminate their production in the chlorine bleaching of pulp. One goal of this research is to investigate chemical methods of modifying the precursors in order to prevent their conversion to the chlorinated analogs. A second set of goals is to 1) identify any specific wood component (i.e. lignin, carbohydrates, extractives) that may be responsible for precursor formation, 2) to further define what structural features are necessary for precursor formation and 3) to postulate mechanisms of precursor formation.

INTRODUCTION

The chlorination of wood pulp to improve its brightness appears to lead to low levels of chlorinated dibenzodioxins and chlorinated dibenzofurans (PCDD/F) which are very toxic to some species and possibly harmful to humans.[5-6] The most toxic congener of the PCDD/Fs is 2,3,7,8-tetrachlorodibenzodioxin (2378-TCDD); 2,3,7,8-tetrachlorodibenzofuran (2378-TCDF) is one-tenth as toxic as 2378-TCDD.[6] In general, the most prevalent congener found in pulp is 2378-TCDF followed by 2378-TCDD.[1,3] Structures for these compounds are shown below:

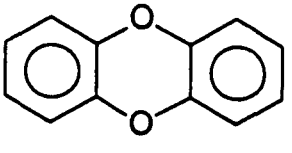

DBD

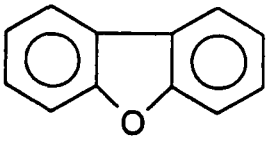

DBF

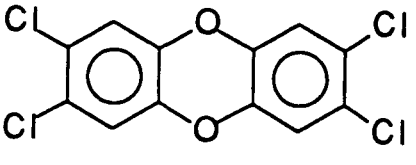

2378-TCDD

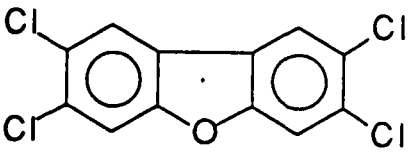

2378-TCDF

The typical levels of the 2378-TCDD and 2378-TCDF are parts per trillion (ppt) in bleached pulps and parts per quadrillion (ppq) in effluents from chlorine bleaching. These are quite low relative to other dioxin sources[7]. Even so, the paper industry is concerned over the public's reaction to dioxins and meeting limits imposed by state and federal regulations. Consequently, ways to reduce the levels dioxins in paper products and mill discharges has been a recent major research thrust.

Dibenzodioxin (DBD) and dibenzofuran (DBF) are present in pulp [3,8] and there is strong evidence that chlorination of these compounds is leads to a significant portion of the observed PCDD/Fs. Under proper conditions, DBD and DBF can be chlorinated to give 2378-TCDD and 2378-TCDF.[3,8-11] The pattern of chlorine isomers obtained after chlorinating pulp spiked with DBD/F is very similar to the PCDD/Fs that are observed with chlorination of unspiked pulps.[8-9] (The isomer distribution is somewhat dependent on the conditions of the chlorination; chlorination of DBD/F in water, in the absence of pulp, gives a different distribution of isomers).[4,8] The levels of DBD in the pulp are of the same order as the levels observed for TCDD after chlorine bleaching, however the levels of DBF detected in brownstock cannot account for all of the TCDF formed.[8] While DBD/F may not be the only precursors to PCDD/Fs, based on the available published literature, they are probably the most important precursors.

Control of PCDD/F formation will be greatly aided if there is an improved understanding of the fundamental chemistry of the precursors. An important consideration is the reactivities of dibenzodioxins and dibenzofurans in comparison to that of wood components. The rates and extents of reactions are dependent on the stabilities of the reaction intermediates and of the products. Charged intermediates are produced when electrophiles (E+) add to DBD/F compounds (Schemes 1 and 2). The charge delocalization in the DBD/F - E+ intermediates is quite good and could contribute to a high reactivity of DBD/F towards electrophiles. The same stabilization through delocalization would occur for charged radical intermediates.

The fact that extremely trace quantities of DBD/F in pulp are chlorinated in the presence of lignin, which is present in percentage levels, suggests that electrophilic reagents may be selective for DBD/F. A possibile reason for the potential selectivity is that the stabilities of the intermediates formed in the electrophilic addition of chlorine (E+ = Cl+) to DBD/F are better than those for lignin. Electrophilic reagents, other than chlorine, are potentially useful for selectively reacting with DBD/F in the presence of lignin so that the precursors cannot subsequently become chlorinated to form PCDD/Fs.

EXPERIMENTAL PLAN

The strategy for finding an effective chemical modifier of DBD/F in pulp is outlined in Scheme 3. In the initial phase of the project several charged and radical electrophiles will be applied to DBD/F-spiked cotton linters under opti-

Scheme 1
Electrophile Addition to Dibenzodioxin

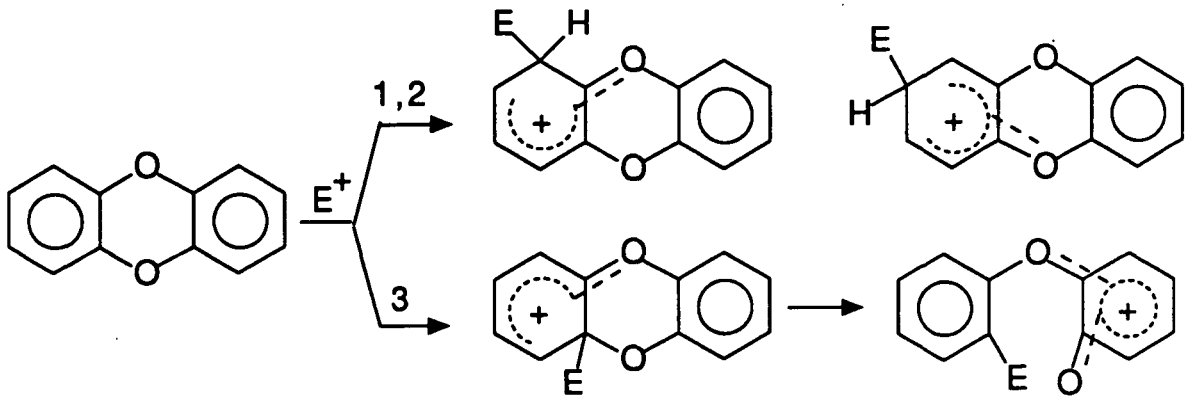

Scheme 2
Electrophile Addition to Dibenzofuran

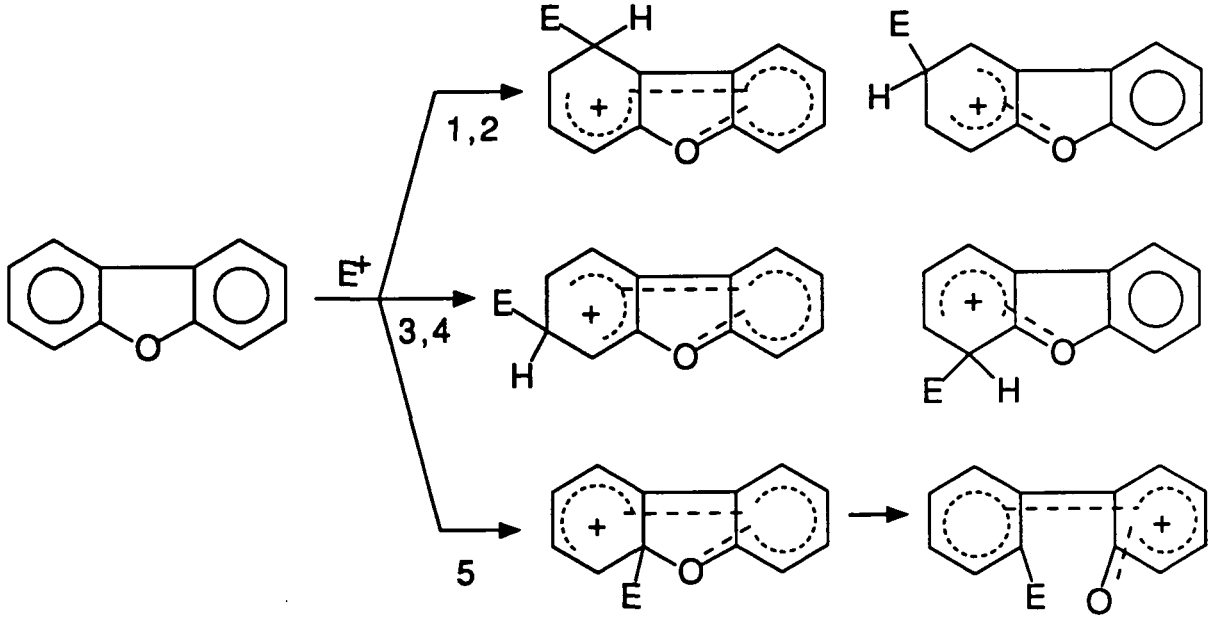

Scheme 3

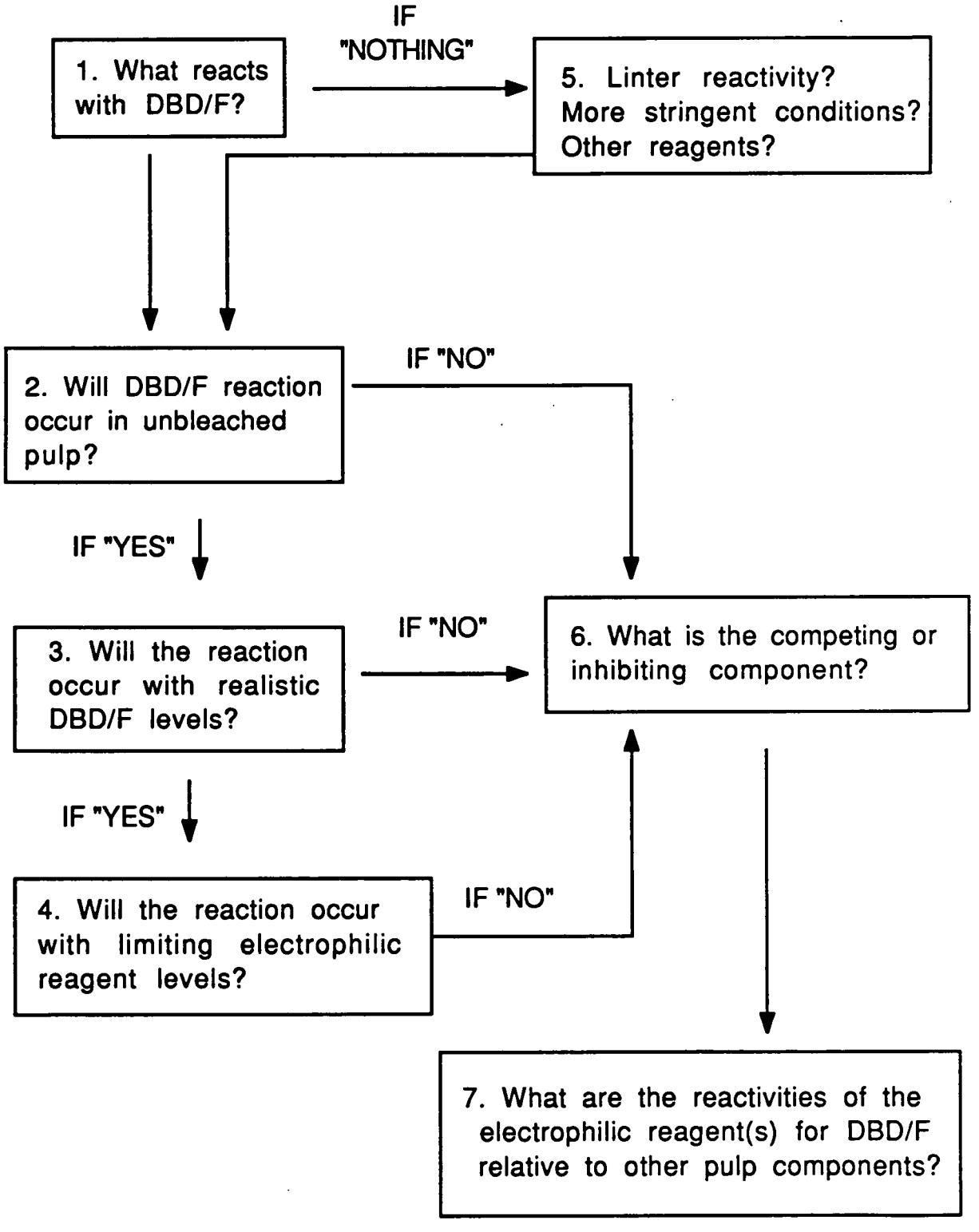
1. What reacts with DBD/F?
IF "NOTHING"
5. Linter reactivity? More stringent conditions? Other reagents?
2. Will DBD/F reaction occur in unbleached pulp?
IF "NO"
IF "YES"
3. Will the reaction occur with realistic DBD/F levels?
IF "NO"
6. What is the competing or inhibiting component?
IF "YES"
4. Will the reaction occur with limiting electrophilic reagent levels?
IF "NO"
7. What are the reactivities of the electrophilic reagent(s) for DBD/F relative to other pulp components?

mal conditions to determine which reagents react most effectively with the precursors. The reagents to be examined include nitric acid, nitrogen dioxide, sulfuric acid, disodium peroxide, ozone and oxygen under ultraviolet light.

Once the effective reagent(s) is determined, the procedure(s) will be applied to DBD/F-spiked pulp under varying conditions to determine the applicability of the procedure to DBD/F reactions under realistic industrial conditions. The sequence of experiments will elucidate the wood components that are potential competitors to the DBD/F reactions. The relative selectivities of the reagent(s) for the wood components and DBD/F will be evaluated utilizing model compounds.

Experiments will also be conducted to determine the wood component responsible for DBD/F formation. Experimental details will develop as information regarding precursor production with different reaction variables becomes available (Project 3664). The investigation will also consider precursors other than DBD/F (should they exist). Methods for inhibiting precursor formation could then be researched.

METHODS

Methods have been developed and evaluated for use in the initial phase of the project. Methods for spiking cotton linters with DBD/F, extracting them and analyzing them have been examined. Soxhlet-extracted linters (10 g) were soaked in a methylene chloride solution of DBD/F to yield a maximum initial concentration of the precursors in the linters of 500-900 ppm. The solvent was evaporated off using rotary evaporation. After treatment with an electrophilic reagent, the linters were spiked with about 100 ug of internal standard, 2-methoxybiphenyl. The dry linters were wetted in hexane, placed in a soxhlet extraction apparatus and extracted overnight. The extract was evaporated to approximately one mL using a rotary evaporator.

One to two microliters of concentrated extract was injected into a GC/FID fitted with a high resolution HP-5 capillary column. Duplicate injections of a five-point standard curve were used to generate the full regression equation used for quantitation. Detection limits are in the ppb range. The cleanliness of the experimental system and the chromatographic resolution have eliminated the need for clean-up procedures.

For each electrophilic reagent examined at least four samples were analyzed; a blank, a control and duplicate experimental samples. The control sample consisted of spiked linters which underwent all of the procedures as the experimental samples except for the actual application of the reagent. The DBD/F values obtained in these samples were used as the initial concentration since loss of the precursors through volatilization is possible during the sample handling. In addition, approximately 100 ug of a recovery standard, diphenyl ether, was added to the concentrated control extract in order to determine the recovery of DBD/F from the linters after treatment.

RESULTS AND DISCUSSION

Dry, spiked linters have been treated with nitrogen dioxide for approximately 10 minutes. The NO_2 doses of 2% (on a dry linter basis) represents a large excess

for the reactions with the adsorbed dioxin and the furan. The NO_2 remaining after 10 minutes was removed by repeated application of vacuum and N_2 purging. The results are shown in Table 1.

Only 61% of the original furan spike and 64% of the original dioxin spike was actually applied to the linters. Volatilization during the spiking procedure probably accounts for the loss. Once the spike has been applied, 99% and 101% of the furan and dioxin, respectively, were recovered (based on the control sample from the point of internal standard application). The control values were used as initial concentrations in subsequent calculations.

Table 1. Dibenzodioxin and Dibenzofuran Concentrations After Treatment with Nitrogen Dioxide

	Original Spike	Control	Exp. 1	Exp. 2
DBF (ppm)	60.0	36.5	24.2	24.5
% DBF Reacted[1]	-	-	34	33
DBD (ppm)	90.0	57.9	ND[2]	0.4
% DBD Reacted[1]	-	-	$\geq$ 99	99

[1] Percent reacted is based on the initial concentration determined from the control sample.

[2] The detection limit was about 240 ppb for this sample.

It is quite clear from these results that dibenzodioxin is considerably more reactive to NO_2 than is dibenzofuran. Once the major reaction product(s) are determined by GC/MS the reasons for this difference may be postulated. Chromatograms from the FID suggest one major product with a high molecular weight resulted from DBD reaction with NO_2. A single experiment in which the reaction time was quadrupled indicated that the time of reaction was not a limiting factor; the dioxin reacted almost completely and $\leq$ 30% of the furan reacted.

A preliminary experiment in which DBD/F in solution were subjected to concentrated nitric/phosphoric acid suggested that the precursors also reacted under these stringent conditions.

SUMMARY

The reactivities of the precursors to polychlorinated dibenzodioxins and furans, dibenzodioxin and dibenzofuran, are currently being examined. Nitrogen dioxide effectively reacts with DBD adsorbed onto dry cotton linters, however DBF appears to be less reactive toward the reagent. Preliminary experiments suggest nitric acid may be an effective reagent for DBD/F chemical modification.

REFERENCES

1. S. E. Swanson, C. Rappe, J. Malmstrom, K. P. Kringstad, Chemosphere, 1988, 17(4), 681.

2. G. Amendola, D. Barna, R. Blosser, L. LaFleur, A. McBride, F. Thomas, T. Tiernan, R. Whittemore, International Symposium on Chlorinated Dioxins and Related Compounds, Las Vegas, Nevada, October 1987.

3. R. H. Voss, B. I. Luthe, B. I. Fleming, R. M. Berry, and L. H. Allen, 1988 CPPA Environment Conference, Vancouver, B. C., October, 25-26, 1988.

4. C. Rappe, S. E. Swanson, B. Glas, K. P. Kringstad, F. de Sousa, L. Johansson, and Z. Abe, Pulp Paper Can., 1989, 90(8), T273.

5. D. G. Barnes, J. Bellin, D. Cleverly, Chemosphere, 1986, 15(9-12), 1895.

6. R.D. Kimbrough, H. Falk, P. Stehr, G. Fries, J. Toxicology and Environmental Health, 1984, 14, 47.

7. K. P. Kringstad and A. B. McKague, 1988 International Pulp Bleaching Conference, Orlando, Florida, June 5-9, 1988, abstract p.63. K. P. Kringstad, F. de Sousa, L. Johansson, M.-C. Kolar, S. E. Swanson, C. Rappe, and B. Glas, Addendum to the above paper.

8. L. E. LaFluer, R. Brunck, K. Ramage, T. J. McDonough, and E. W. Malcolm, DIOXIN '89, Toronto, Ontario, Sept. 21, 1989.

9. R. M. Berry, B. I. Fleming, R. H. Voss, C. E. Luthe, and P. E. Wrist, 75th Annual Mtg. CPPA Tech. Sect., Montreal, Quebec Jan. 31-Feb. 3, 1989.

10. A. P. Gray, V. M. Dipinto, and I. J. Solomon, J. Org. Chem., 1976, 41, 2428.

11. A. P. Gray, S. P. Cepa, I. J. Solomon, and O. Aniline, J. Org. Chem., 1976, 41, 2435.

PROJECT SUMMARY FORM

DATE: March 20, 1990

PROJECT NO. 3685: MECHANISMS OF DIOXIN FORMATION IN PULP PRODUCTION
PART II: CHLORINATION AND DIOXIN REACTIONS
(CHLORINE INSTITUTE FUNDED)

PROJECT LEADER: D. R. Dimmel

IPST GOAL:

Eliminate or minimize chlorinated dioxins and chlorinated furans in bleached pulp production.

OBJECTIVE:

The production of dioxins during chlorine bleaching is a major concern to the paper industry. The objective of this project research is to develop a fundamental understanding of chemistry which leads to dioxins in bleached pulp, the reactions of dioxins with selected bleaching reagents, and ways to chlorinate pulps without dioxin production. Conditions will be sought that will (a) define the relative importance of different dioxin precursors, (b) determine the reactivity of chlorine with functionalized precursors, (c) selectively chlorinate lignin and not the dioxin precursors, and (d) destroy dioxins in partially bleached pulps. The principle difference between the research of Project 3685 and that of Project 3684 is that chlorination and dioxins will be the focus of the 3685 study. A laboratory (Battelle) that is specifically equipped to handle toxic materials and is capable of performing ultratrace analyses will be involved.

CURRENT FISCAL YEAR BUDGET: $180,000

PRIOR RESULTS: New project.

SUMMARY OF RESULTS SINCE LAST REPORT: New project.

PLANNED ACTIVITY THROUGH FISCAL YEAR 1990:

Most of the planned experiments will involve a very clean system, namely, substrate absorbed onto cotton linters and, hopefully, will provide valuable fundamental information about reactivities without possible by-product problems. The absorbed substrates are dibenzodioxane (DBD), dibenzofuran (DBF), and lignin models. Spiking with a simple substrate onto a "pure" polymer simplifies the analytical procedures and allows a greater number of experiments to be performed at a reasonable cost. However, a selected number of experiments will compare

the reactions of unbleached pulps with the model systems to determine the validity of the model systems. Control experiments will (1) compare tetrachloro dioxin isomer patterns at several different absorbed levels of DBD/F on cotton linters and (2) use radioactive tracers to address the validity of comparing reactions of spiked samples with natural samples.

One set of experiments will address the issue of the source of the dioxin precursors. The distribution of mono-, di-, tri-, and tetrachlorodioxins (DBD/F-Cl_x) as a function of chlorination time will be compared for a DBD/F spiked cotton linters sample and an unspiked pulp sample. If the time development profile of the DBD/F-Cl_x components for the two substrates differ substantially, precursors other than DBD/F will be indicated. The profile of tetrachloro isomers for the two samples will also indicate possible sources of precursors and provide an estimate of the relative importance of different precursors.

Another set of experiments will provide rate data for the disappearance of DBD/F-Cl_x (x=0-4) on a lignin-like substrate. Done at different temperatures, the chlorination rate data should provide energies of activation (Ea) for the substrates and, thus, allow one to better control the chlorination process to give greater selectivity for lignin vs DBD/F. A follow up competitive experiment will verify the expected selectivities under different chlorination conditions. We will also examine how the selectivity changes with the addition of chlorine dioxide to the chlorination reactions. DBD/F spiked cotton linters, which have been treated with NO_2 or O_2, will be chlorinated to show if substituted precursors will still give rise to dioxins upon chlorination.

Finally, we will treat bleached pulp (which contains trace levels of dioxins) with ozone, peroxide, oxygen, and other possible commercial electrophilic reagents to test the stability of dioxins to various post-chlorine bleaching stages.

POTENTIAL FUTURE ACTIVITY:

This is a one-year funded project.

Project 3685 Status Report

MECHANISMS OF DIOXIN FORMATION IN PULP PRODUCTION

PART II: CHLORINATION AND DIOXIN REACTIONS

Reporting Period: October, 1989 -- February, 1990

OBJECTIVES

The proposed research will develop a fundamental understanding of chemistry which leads to dioxins in bleached pulp, the reactions of dioxins with selected bleaching reagents, and ways to chlorinate pulps without dioxin production. Conditions will be sought that will (a) define the relative importance of DBD/F dioxin precursors, (b) determine the reactivity of chlorine with functionalized precursors, (c) selectively chlorinate lignin and not DBD/F components, and (d) destroy dioxins in partially bleached pulps. The principle difference between this proposed research and that of PART I is that chlorination and dioxins will be the focus of the study and a laboratory that is specifically equipped to handle toxic materials will be involved.

INTRODUCTION

This project was approved for funding by the Chlorine Institute in mid-January 1990 and contracts are now being worked out, with a possible starting date of mid-March. The discussion which follows outlines the probable direction of the research. The research is to be completed and reported within a one-year time frame.

EXPERIMENTAL PLAN

Initially, control experiments will examine the validity of comparing reactions of spiked samples with natural samples. Will the chemistry of samples containing parts per billion DBD/F be comparable to "natural" pulp samples which may have parts per trillion DBD/F? Will the partitioning the DBD/F between the fiber surface and a contacted liquid phase be similar at the ppb and ppt levels? The combination of comparing tetrachloro isomer pattern at several different absorbed levels and performing appropriate radioactive tracer experiments should provide answers to these questions.

The accompanying table details the experimental plan. The first set of experiments (1 and 2) address the issue of the source of the dioxin precursors. The distribution of mono-, di-, tri-, and tetrachlorodioxins (DBD/F-Cl_x) as a function of chlorination time will be compared for a DBD/F spiked cotton linters

Table I

EXPERIMENTAL PLAN

Exp	Substrate	Rx	Observe	Information
1	(A) DBD/F spiked linters	Cl_2	rx rate	rate law, Ea
			DBD/F-Clx yield with time	reaction course
			TCDD/F isomer distribution	Cl_2-ation pattern
2	(B) DBD/F-free unbleached pulp	Cl_2	DBD/F-Clx yield	reaction course dioxin source
			TCDD/F isomer distribution	Cl_2-ation pattern dioxin source
3	(C) lignin model spiked linters	Cl_2	rx rate	rate law, Ea
4	(A) + (C)	Cl_2	rel. rates	selectivity
5	(A) + (C)	Cl_2/ClO_2	rel. rates	selectivity
6	(A)	NO_2	rx rate	precursor react.
7	(A)	O_2	rx rate	precursor react.
8	(A)-NO_2 product	Cl_2	TCDD/F prod.	modified precursor reactivity
9	(A)-O_2 product	Cl_2	TCDD/F prod.	modified precursor reactivity
10	unbleached pulp	$NO_2 + Cl_2$	TCDD/F prod.	possible control measure
11	unbleached pulp	$O_2 + Cl_2$	TCDD/F prod.	possible control measure
12	bleached pulp	O_3	dioxin decrease	possible control measure
		H_2O_2	dioxin decrease	possible control measure
		O_2	dioxin decrease	possible control measure

sample and an unspiked pulp sample. If the time development profile of the DBD/F-Clx components for the two substrates differ substantially, precursors other than DBD/F will be indicated. The profile of tetrachloro isomers for the two samples will also indicate possible sources precursors. The dioxin isomer distribution in DBD/F spiked linters and unspiked pulp samples should be identical, if DBD/F are the only precursors in the pulp. Semiquantitative results would provide estimates of importance for different sets of precursors.

Project 3685 Status Report

The combination of experiments 1 and 3 will provide rate data for the disappearance of DBD/F-Clx (x=0-4) and a lignin-like substrate. Done at different temperatures, the chlorination rate data should provide energies of activation (Ea) for the substrates and, thus, allow one to better control the chlorination pro-cess to give greater selectivity for lignin vs DBD/F. The competitive experiment # 4 will verify the expected selectivities under different chlorination conditions. Experiment #5 will examine how the selectivity differences change with the addition of chlorine dioxide to the chlorination reactions. Both experiments #4 and 5 may be able to be simplified in terms of only looking at TCDD/F levels, rather than the whole spectrum of congeners (mono-, di-, ... chloro products).

Experiments #6 and 7 will probably be performed in the activities of PART I of this proposed research; however, the products of the reactions of DBD/F spiked cotton linters, which have been treated with NO2 or O2, will be chlorinated in experiments #8 and 9. The experiments are intended to show whether or not precursors which have been altered by selective treatments will still give rise to dioxins upon chlorination. For example, if nitrogen dioxide selectively attacks DBD/F to give a nitrogen derivatized product, what will the latter do upon chlor-ination?

Except for #2, the experiments suggested so far involve a very clean system, namely, substrate adsorded onto cotton linters. The experiments provide valuable fundamental information about reactivities without possible by-product problems. The combination of spiking and a clean substrate simplifies the analytical procedures and allows a greater number of experiments to be performed at a reasonable cost. Experiments #10 and 11, however, examine the reactions of unbleached pulps as a follow-up to the model system conclusions (assuming that model system results are positive in the direction of lowering dioxin levels).

Finally, experiment #12 involves treating bleached pulp, which contains trace levels of dioxins, with ozone, peroxide, oxygen, and other possible commercial electrophilic reagents to test the stability of dioxins to various post-chlorine bleaching stages.

BUDGET

The budget for the proposed research is based on completion of the proposed work in a one year time period. Should the research suggest new, exciting areas of investigation, the project could (subject to approval by the financing organization) be redirected into these areas. Additional funding will be sought if the redirection means expansion of the originally proposed work.

Project 3685 Status Report

PROPOSED BUDGET

	Dollars
Dr. Donald Dimmel, Project coordinator	$20,000
IPST personnel[a]	5,000
Equipment and Supplies[b]	10,000
Travel[c]	8,000
Battelle	137,000
TOTAL	$180,000

[a]Includes other IPST professionals and secretarial services
[b]Related to experiments to be performed at IPST, document mailing costs, etc.
[c]Between IPST and Battelle, Chlorine Institute meetings, and an international meeting (such as DIOXIN 90)